

CATACLASTIC FAULT ROCKS IN UNDERGROUND EXCAVATIONS - A GEOLOGICAL CHARACTERISATION

THÈSE N° 1975 (1999)

PRÉSENTÉE AU DÉPARTEMENT DE GÉNIE CIVIL

ÉCOLE POLYTECHNIQUE FÉDÉRALE DE LAUSANNE

POUR L'OBTENTION DU GRADE DE DOCTEUR ÈS SCIENCES

PAR

Christoph BÜRGI

géologue diplômé EPF

de nationalité suisse et originaire d' Aarberg (BE)

acceptée sur proposition du jury:

Prof. A. Parriaux, directeur de thèse

Prof. M. Burkhard, rapporteur

Prof. F. Descoedres, rapporteur

Prof. S. Löw, rapporteur

Dr P. Méan, rapporteur

Prof. S. Pelizza, rapporteur

Lausanne, EPFL

1999

To my parents

ABSTRACT

The present study makes part of a research project on the geological and geomechanical characterisation of weak cataclastic fault rocks encountered in underground excavation sites in the Alps. The project is composed of a geological and a geomechanical part, split up in two PhD thesis and realised in parallel at the Laboratory of Geology (GEOLEP) and the Laboratory of Rock Mechanics (LMR) at the Swiss Federal Institute of Technology Lausanne.

By their very contrasting and unfavourable mechanical behaviour in underground excavations, weak cataclastic fault zones influence directly the excavation method, the safety of the working site, the choice of tunnel support, the long-term behaviour and the costs of the infrastructure. The construction of galleries across cataclastic fault zones bears furthermore the potential risk to modify the local and regional hydrogeological regime.

Weak cataclastic fault rocks show a large scatter of geological and geomechanical properties. Due to their low cohesion, they alter rapidly when exposed to weathering. They can hence be studied and sampled in natural outcrops and exploratory boreholes only with great difficulty. Analyses and laboratory tests are laborious and require special sample preparation techniques and equipments. For these reasons still little is known about their geological, hydrogeological and geomechanical behaviour.

The purpose of this study is to develop a detailed and objective differentiation and characterisation method for weak cataclastic fault rocks. Classifications and terminologies of (weak) cataclastic fault rocks are in fact still controversial.

After a review of fault rock definitions and rock deformation mechanisms, the term *kakirite* has been retained in agreement with Heitzmann (1985) and Wyder (1997) as a general designation for weak, cohesionless cataclastic fault rocks. This term has been approved recently by the Swiss Society of Engineers and Architects (SIA) to designate fault zones made up of "loose, structureless material" (SIA Norm 199, 1998).

Cataclastic fault zones have been studied and sampled in galleries currently under construction in different geological and tectonic contexts in the Alps. Research has been concentrated mainly on fault zones occurring in quartzo-phylitic host rocks. For comparison, fault rocks from greenstones and serpentinite have been analysed too.

To improve the understanding of the geomechanical and hydrogeological behaviour of weak cataclastic fault rocks, a new quantitative characterisation method has been developed. In a simplified approach, the geomechanical behaviour of (fault) rocks is considered to be controlled by two factors, namely the:

- *mineralogical composition* (mwVh), and
- *rock fabric* (TC, MC)

The proposed mineralogical and structural characterisation of cataclastic fault rocks is referring to the meso- to microscopic scale, respectively to a scale comparable with common geomechanical laboratory tests.

Mineralogy is expressed quantitatively by means of the *mean weighted Vickers hardness*, mwVh (Calembert et al., 1980a). The relative proportions of the principal rock forming minerals have been determined by semi-quantitative XRD-analyses.

The mineralogical composition of kakirites, adjacent host rock samples and sieved kakirite grainsize fractions has been determined. Comparing the composition of the different grainsize fractions a clear dependency of grainsize on mineralogical composition has been found in kakirites. Quartz content is in general considerably higher in the clast than in the matrix fraction. The later is in fact composed mainly of phyllosilicates. This mineralogical grainsize fractionation

is interpreted to be controlled by the original host rock fabric, the strength contrast between the involved mineral phases and alteration processes. Except kaolinite (Varzo), no other alteration mineral phases have been identified. The presence of (swelling) clay-minerals in very low proportions which can not be detected by the performed whole rock XRD-analyses can not be excluded however.

Kakirite samples sieved for XRD-analyses show an extended grainsize distributions with in general high proportions of silt/clay grainsize fraction (mean 45%). This may explain the often observed very low permeability of kakirite zones. Their hydrogeological role is illustrated in the last part of this work by the means of a case history of a fault zone crossed by the gallery of Cleuson-Dixence. It demonstrates the often observed groundwater flow barrier-effect of cataclastic fault zones and its impact on the excavation work and the local hydrogeological regime.

Rock fabric of kakirites has been characterised by thin section analyses with subsequent semi-automatic image analysis. It is based on a two-phase "clast-matrix" model, considering kakirites to be composed of varying proportions of "hard" clasts and "weak", fine-grained matrix. Clast properties (density, shape and relative orientation) are quantified by the *texture coefficient* (TC) of Howarth & Rowlands (1987). Pre-existing discontinuities in the matrix are characterised by a newly developed *matrix coefficient* (MC), involving the discontinuity density, roughness, mean length and relative orientation.

The combined structural approach involving the MC and TC has shown to be appropriate to characterise and differentiate a wide range of weak cataclastic fault rocks by their microscopic rock fabric. Two opposite kakirite fabric types can be distinguished: first, a granular fabric, characterised by clasts taken in a fine-grained, isotropic matrix. Second, a discontinuity dominant, often schistose fabric wherein no clasts can be identified. A gradual transition is observed in-between these two end-member types.

In order to assess the validity of the developed characterisation method, a first attempt of correlation has been made between the mineralogical-structural parameters and corresponding rock strength of kakirites tested by Habimana (1999). The found correlation is a strong motivation to continue the started research on cataclastic fault rocks with the presented mineralogical and structural approach.

RESUME

La présente étude géologique s'inscrit dans le cadre d'un projet de recherche sur le comportement des roches cataclastiques dans les ouvrages souterrains. Ce projet est divisé en un volet géologique et un volet géomécanique réalisés en parallèle aux Laboratoires de Géologie (GEOLEP) et de Mécanique des roches (LMR) de l'École Polytechnique Fédérale de Lausanne.

Par leurs propriétés géomécaniques très défavorables, les roches cataclastiques issues d'une déformation tectonique essentiellement cassante, influencent fortement la réalisation d'ouvrages souterrains. Elles peuvent avoir notamment une répercussion directe sur la méthode d'excavation, la sécurité du site de travail, le choix du type de soutènement ainsi que sur le comportement à long terme et les coûts de l'ouvrage. Leur rôle hydrogéologique étant souvent celui d'un panneau étanche dans un massif fissuré, la traversée de ces zones peut avoir des impacts sur les conditions hydrogéologiques environnantes et les ressources en eau à l'échelle locale ou régionales.

L'objectif de ce travail était de développer une caractérisation et différenciation plus détaillée des roches cataclastiques. En effet, en raison des difficultés liées à leur étude en surface, l'échantillonnage et la réalisation d'analyses et d'essais en laboratoire, ces roches souffrent jusqu'à présent d'un déficit de connaissance. Les roches cataclastiques, dont la terminologie et classification sont encore soumises à discussion, sont souvent regroupées sous le terme de "roches broyées" et montrent une vaste dispersion de propriétés géologique et géomécanique.

Après le passage en revue des définitions actuelles des roches de faille et des mécanismes de déformation tectoniques, le terme *kakirite* a été retenu pour désigner les roches cataclastiques à cohésion faible ou nulle. Son application suit la proposition de Heitzmann (1985) et Wyder (1997) et est en accord avec la nouvelle recommandation de la Société Suisse des Ingénieurs et Architectes (SIA No 199, 1998).

L'opportunité offerte par la réalisation de différents grands ouvrages souterrains dans les Alpes a été saisie pour étudier et échantillonner des zones de kakirite dans des contextes géologiques très variés. L'étude porte principalement sur de kakirites formées dans des lithologies quartzo-phylitiques complété par l'analyses de kakirites formées dans des roches vertes ainsi que dans des serpentinites.

Pour améliorer les connaissances des propriétés géologiques, hydrogéologiques et géomécaniques des roches cataclastiques, une nouvelle méthode de caractérisation de ces roches a été développée. Elle se base sur l'approche simplifiée selon laquelle le comportement mécanique d'une roche (de faille) s'explique principalement par sa *composition minéralogique* et sa *structure* (microscopique). La méthode proposée se réfère à l'échelle des essais géomécaniques en laboratoire, respectivement à l'échelle meso- et microscopique des échantillons et de lame minces.

La minéralogie des kakirites a été déterminée de façon semi-quantitative par des analyses aux rayons-X. Elle est exprimée par le biais de la dureté moyenne pondérée de Vickers (mwVh) (Calembert et al. 1980,a).

Par la comparaison des compositions minéralogiques des différentes fractions granulométriques des kakirites nous avons démontré et quantifié la dépendance de la granulométrie de la composition minéralogique. La teneur en quartz et en générale nettement plus élevée dans la fraction des clastes que dans la matrice. Cette dernière est composé essentiellement de phyllosilicates. Ce fractionnement minéralogique est interprété comme résultant d'une part de la structure originale de la roche mère, de la résistance différée à la cataclase des minéraux impliqués et d'autre part de altération. A l'exception de la kaolinite (Varzo) aucun autre type de minéral issue de l'altération n'a été identifié. La présence de minéraux argileux (gonflants) en quantités très mineures, et ainsi non-détectée dans les analyses XRD de roche totale, ne peut cependant pas être exclue complètement.

Les kakirites, tamisées pour les analyses XRD, montrent des distributions granulométriques étendues et en générale des teneurs élevées en matière fine (moyenne 45%). Ceci peut expliquer la perméabilité souvent très faible des zones de kakirite. Leur rôle hydrogéologique est illustré à la fin de ce travail à l'aide d'un exemple d'une zone de kakirite rencontrée dans la galerie de Cleuson-Dixence. Il expose le rôle d'écran étanche que jouent ces zones et leur impact sur les travaux d'excavation et sur le régime hydrogéologique du milieu environnant.

La caractérisation de la structure microscopique des kakirites se fait à l'aide d'analyses sur lame mince, suivies par une analyse d'image semi-automatique. Elle se base sur un modèle "deux-phases", considérant les kakirites comme composées de proportions variables de *clastes* dures dans une *matrice* tendre. Les propriétés des clastes (densité, forme et orientation relative) sont quantifiées en appliquant le *coefficient de texture* (TC) de Howarth & Rowlands (1987). Pour caractériser les propriétés des discontinuités préexistantes dans la matrice un nouveau *coefficient de matrice* (MC) a été développé. Il tient compte de la densité, de la longueur moyenne, de la rugosité et de l'orientation relative des discontinuités.

En combinant les deux paramètres TC et MC, la méthode proposée s'est avérée appropriée pour caractériser et distinguer une vaste gamme de kakirites. Deux types de kakirites opposés sont distingués: 1: les kakirites granulaires composées de clastes dans une matrice fine et isotrope; 2: les kakirites à structure dominée par les discontinuités et souvent schisteuse mais sans clastes identifiables. Le passage entre ces deux extrêmes est graduel.

Pour évaluer la validité de l'approche choisie et de la méthode de caractérisation développée, une première tentative de corrélation a été réalisée entre les paramètres minéralo-structuraux (mwV, MC, TC) et le comportement géomécanique des kakirites (voir Habimana, 1999). La corrélation trouvée est fortement encourageante pour continuer la recherche sur les roches cataclastiques avec l'approche présentée.

ACKNOWLEDGEMENTS

I am grateful to my thesis director Prof. A. Parriaux who proposed me this research project on cataclastic fault rocks almost four years ago. My thanks go also to Prof. R. Favre (presidency), Prof. M. Burkhard, Prof. F. Descoedres, Prof. S. Löw, Dr P. Méan and Prof. S. Pelizza to have accepted to make part of my thesis jury.

I enjoyed a lot the cheerful ambience at GEOLEP and the scientific (and less-scientific) discussions with my colleagues and friends. A *grand merci* goes to all the members of GEOLEP who supported me during all these years and contributed in one way or another to the success of my work.

My most grateful thanks go to Alina Tomaniak for spending many laborious hours preparing my "very special" kakirite samples for the analyses and for all the other little and big things she made with great reliability.

I am much indebted to Giuseppe Franciosi for his everlasting optimistic attitude towards my work, his untiring help and many many XRD-analyses he performed with great proficiency. I always enjoyed the stimulating discussions we had and I rarely left his office without new ideas.

Jean-Philippe Rey I owe special thanks, he supported me from the beginning and never lost interest in the progress of this project. I have appreciated much his competent feedbacks and his critical review of the manuscript.

Thanks also to Laurent Tacher and Stefan Zenhäusern for their precious help in statistics and rock mechanics.

Last but not least, an enormous *merci* to my office mate Nicole Schaffter. She patiently endured my (bad) moods for the last four years and ceaselessly cheered me up and encouraged me to go further in my work.

The collaboration with Jean Habimana, with whom I spent many hours sampling kakirites in dark and moist galleries, had a great impact on my work and I learned a lot about rock mechanics and civil engineering.

Many other people working in the studied underground sites have contributed to the success of this work, they shall all be acknowledged here for their generous help. Special thanks go to A. Pralong, R. Marclay, H. Détraz, G. Schaeren, G. Cerveraz, H.-J. Ziegler, H. Zeltner, P. Grasso, L. Soldo, G. Scotti and M. Sapigni.

The Swiss National Science Foundation (No. 21-42390.94), EOS Cleuson-Dixence SA and BLS AlpTransit - Lötschberg AG are sincerely acknowledged for their financial support of this project.

TABLE OF CONTENTS

1 INTRODUCTION	1
1.1 ORGANISATION AND FINANCIAL SUPPORT OF THE PROJECT "CATACLASTIC FAULT ROCKS"	2
2 FAULT ROCKS - GENERAL REVIEW	3
2.1 DEFORMATION MECHANISMS	3
2.1.1 Cataclastic flow (cataclasis)	4
2.1.2 Crystal plasticity	4
2.1.3 Pressure-solution and diffusion creep	5
2.2 TERMINOLOGY AND CLASSIFICATIONS OF FAULT ROCK	5
2.2.1 Mylonites	6
2.2.2 Cataclasites	6
2.2.3 Kakirites	7
2.2.3.1 Fault breccia and fault gouge	7
2.2.4 Retained terminology of fault rocks	7
2.3 PARAMETERS CONTROLLING ROCK DEFORMATION MECHANISMS	8
2.3.1 Lithology external controls	8
2.3.2 Lithology internal controls	9
2.3.2.1 Mineralogy	11
2.4 GEOTECHNICAL ROCK MASS CLASSIFICATION SYSTEMS	12
3 THE STUDY SITES	15
3.1 EOS CLEUSON-DIXENCE, SWITZERLAND	15
3.1.1 The hydraulic gallery of Cleuson-Dixence	15
3.1.2 Regional and geological settings	16
3.1.3 Studied cataclastic fault zones	18
3.1.3.1 Unit B, le Chargeur - Tortin	18
3.1.3.2 Unit C Tortin - Tracouet (c)	18
3.1.3.3 Unit D, access gallery F5 - Zerjona (d1)	20
3.1.3.4 Unit D, "Verrucano" (d2)	21
3.2 BLS - ALPTRANSIT, SWITZERLAND	22
3.2.1 The Löttschberg pilot gallery	22
3.2.2 Regional and geological settings	23
3.2.3 Studied cataclastic fault zones	25
3.2.3.1 Löttschberg pilot gallery	25
3.2.3.2 Borehole Goltschried (95/23)	26
3.3 FS - GENOA, ITALY	27
3.3.1 The project	27
3.3.2 Regional and geological settings	27
3.3.3 Studied cataclastic fault zones	29
3.4 ENEL - VARZO, ITALY	30
3.4.1 The project	30
3.4.2 Regional and geological settings	30
3.4.3 Studied cataclastic fault zones	32
4 THE INVESTIGATION METHODS	33
4.1 GENERAL CONSIDERATIONS	33
4.1.1 Observation and sampling opportunities in galleries under construction	33
4.1.1.1 Excavation by drill & blast (or backhoe machine)	33
4.1.1.2 Excavation by full-face tunnel boring machines (TBM)	34
4.1.1.3 Sampling fault rocks from cored boreholes	35

4.2 SAMPLING TECHNIQUES	35
4.2.1 Sample orientation	35
4.2.2 Correspondence of samples for geological and geomechanical analyses	36
4.3 LABORATORY TESTS AND ANALYSES	36
4.3.1 Thin section analyses	36
4.3.2 Grainsize analysis	37
4.3.3 X-ray diffraction analysis	37
4.4 THE GEOLOGICAL CHARACTERISATION METHOD	37
4.4.1 The clasts - matrix model	38
4.4.2 The rock fabric characterisation	38
4.4.2.1 The Texture Coefficient TC	39
4.4.2.2 The matrix coefficient MC	43
4.4.3 The mineralogical characterisation	51
4.4.3.1 The Vickers hardness	52
5 PRESENTATION OF RESULTS	55
5.1 FAULT ROCKS IN QUARTZO-PHYLLITIC SERIES	55
5.1.1 Cleuson-Dixence, unit B (TM 2780-2900)	55
5.1.2 Cleuson-Dixence, unit C (TM 5180 and 5597)	56
5.1.3 Cleuson-Dixence, unit D (Zerjona)	60
5.1.4 Borehole Goltschried	69
5.1.5 Gallery Varzo	74
5.2 FAULT ROCKS IN GREENSTONES (CLEUSON-DIXENCE, UNIT B)	76
5.3 FAULT ROCKS IN SERPENTINITE (GENOA, ITALY)	77
5.3.1 Massif serpentinite	77
5.3.2 Schistose serpentinite	78
5.4 FAULT ROCKS IN CARBONATE ROCKS (CLEUSON-DIXENCE, UNIT D)	80
5.5 SYNTHESIS	81
5.5.1 Conceptual rock fabric - mineralogy diagram	83
5.5.2 Critical discussion of the proposed characterisation method	85
6 CORRELATION OF GEOLOGICAL AND GEOMECHANICAL PROPERTIES	87
7 THE HYDROGEOLOGICAL ROLE OF CATACLASTIC FAULT ZONES	93
7.1 CASE HISTORY: CLEUSON-DIXENCE LOT C (PM 5597)	93
8 SUMMARY AND CONCLUSIONS	97
8.1 GEOLOGICAL CHARACTERISATION	97
8.1.1 Mineralogy	97
8.1.2 Rock fabric	98
8.2 HYDROGEOLOGICAL ASPECT	99
8.3 SUGGESTED FURTHER RESEARCH	99
8.3.1 Practical recommendations	99
REFERENCES	101
ANNEXES	

LIST OF SYMBOLS

clast parameters

TC	<u>T</u> exture <u>C</u> oefficient	[-]
AF	<u>A</u> ngular <u>F</u> actor	[-]
AF ₁	<u>A</u> ngular <u>F</u> actor of elongated clasts	[-]
AR	<u>A</u> spect <u>R</u> atio	[-]
\overline{AR}_1	mean <u>A</u> spect <u>R</u> atio of elongated clasts	[-]
CD	<u>C</u> last <u>D</u> ensity	[%]
FF	<u>F</u> orm <u>F</u> actor	[-]
\overline{FF}_0	mean <u>F</u> orm <u>F</u> actor of non-elongated clasts	[-]
N ₀	number of isometric clasts (AR < 2.0)	[-]
N ₁	number of elongated clasts (AR > 2.0)	[-]
i	weighting factor, class number	[-]

matrix parameters

MC	<u>M</u> atrix <u>C</u> oefficient	[-]
β	angle of discontinuity orientation	[°degree]
$\Delta\beta_i$	angle between sets of discontinuities	[°degree]
δ	discontinuity orientation factor	[-]
L'	projected trace <u>L</u> ine	[mm]
L _{RL}	<u>L</u> inear <u>R</u> egression <u>L</u> ine	[-]
n	number of discontinuity sets	[-]
R _L	<u>L</u> inear <u>R</u> oughness	[mm/mm]
T _L	<u>T</u> race <u>L</u> ine	[-]
T _{LL}	<u>T</u> race <u>L</u> ine <u>L</u> ength	[mm]
\overline{T}_{LL}	mean <u>T</u> race <u>L</u> ine <u>L</u> ength	[mm]
T _{Ld}	<u>T</u> race <u>L</u> ine <u>d</u> ensity	[mm/mm ²]
tT _{LL}	<u>t</u> otal <u>T</u> race <u>L</u> ine <u>L</u> ength	[mm]

mineralogy

mwVh	<u>m</u> ean <u>w</u> eighted <u>V</u> ickers <u>h</u> ardness	[Pa]
Vh _i	<u>V</u> ickers <u>h</u> ardness of mineral phase i	[Pa]
v _i	weight proportion of mineral phase i	[%]

stress & strain

σ	normal stress	[Pa]
σ_1	principal major stress	[Pa]
σ_3	principal minor stress	[Pa]
$\sigma_1(5)$	principal major stress for $\sigma_3 = 5$ MPa	[Pa]
ϵ	linear strain	[-]

1 INTRODUCTION

By the increasing demand of underground infrastructures, tunnels and galleries are built in more and more difficult geological conditions. They often have to be constructed in intensely tectonically deformed rock, bearing a great number of (large) cataclastic fault zones. Due to their very contrasting mechanical properties the crossing of such zones, especially when excavated by full face tunnel boring machines, is often coupled with serious technical problems and safety risks for miners and equipment. Cataclastic fault zones may act as highly conductive groundwater channels or, more commonly, as natural flow barriers. High water pressures can develop behind or inside of them and when crossed by a gallery, there is a considerable risk of a sudden outburst of water and crushed rock material under high pressure. Hence, the construction of galleries through such natural flow barriers may also have great impacts on the local and/or regional hydrogeological regime.

Due to their geomechanical and hydrogeological behaviour, cataclastic fault rocks influence directly the choice of excavation method (traditional excavation vs. Tunnel Boring Machine, choice of TBM type), the tunnel support, the safety on the working site, the duration of the works, the long-term behaviour and finally the cost of the construction. In the case of the hydraulic gallery of Cleuson-Dixence e.g., the summed up length of crossed cataclastic fault zones represented only about 2% of the total length of excavation. The working time spent to pass these zones, however made up 30% of the duration of excavation works (Botte et al., 1996). This example illustrates the interest to take into account the occurrence and properties of cataclastic fault rocks at a very early stage of a planned underground construction.

Weak cataclastic fault rock alter very rapidly when exposed to weathering, they can therefore rarely be studied in natural outcrops and can be sampled and prepared for analyses and tests only with great difficulties. In fact, little is presently known about their geological, hydrogeological and geomechanical properties. This lack of knowledge hinders an effective progress in getting over the geotechnical difficulties they cause in underground constructions.

In many underground works cataclastic fault zones are suddenly encountered but without sufficient time to study their properties in detail. For tunnel design purposes they are classified on the basis of field observations, receptively on "a visual impression of the rock structure" (Hoek et al. 1998). Characterisation of (fault) rocks is therefore quite subjective and depends largely on the experience of the geotechnician or geologist. The actual approach in practice is in fact a purely mechanical one: weak cataclastic rocks, regardless of origin, lithological, textural or mineralogical differences are regrouped under the general labels of "mylonites", "crushed rocks" or "weak rocks". Their only common characteristic is a poor geomechanical behaviour. Performed geomechanical tests hence show often a broad scattering of results, making them difficult to be interpreted for engineering purposes. The great variability of geomechanical properties of tested samples can be explained by their differing geological properties, such as mineralogical composition, rock fabric, degree of alteration, porosity, etc.. Benefit and significance of geomechanical tests and geological previsions can hence be improved by a more detailed differentiation of cataclastic fault rocks.

In geological studies, fault rocks have been of major interest since the earliest beginnings. A great variety of definitions and many different classification systems can be found in literature. Most of the attention however has been paid to ductile deformed fault rocks as they reveal more easily informations about their geological and tectonic history. In fact, the often "chaotic" rock fabric of cataclastic fault rocks, together with the mentioned sampling and preparation difficulties, makes them a stale bread for structural geologists.

In the last few years, research on cataclastic fault rocks has been intensified, motivated by the realisation of large underground constructions in the Alps. Interesting data about their structural aspects, genesis and geomechanical properties have been presented recently by Wyder & Mullis (1998), Wyder (1997), respectively Habimana (1999). The geological classification of weak, cohesionless cataclastic fault rocks however is still summary and controversial. A general differentiation is commonly made between coarse-grained fault breccias and fine-grained fault

gouges (e.g. Schmid & Handy, 1991, Heitzmann, 1985, Higgins, 1971). Wyder (1997) proposes a mesoscopic distinction of *kakirite type I* and *type II* depending on the host rock fabric being preserved respectively erased during cataclasis.

The present research project aims to improve the fundamental knowledge about the geological, hydrogeological and geomechanical properties of cataclastic fault rocks. With regard to the initially mentioned scattering of mechanical (and geological) parameters of cataclastic fault rocks, a more detailed and objective differentiation of "crushed rocks" is required. Furthermore, research aims to determine in parallel the geological and geomechanical characteristics of analysed fault rocks in order to seek a more appropriate correlation between structural, mineralogical and geomechanical properties. This knowledge is decisive when making geological prognosis about cataclastic fault zones, interpretations of geomechanical tests and decisions about the measures to take when crossing such zones in underground works.

In this context and in order to develop an objective (and quantitative) method to differentiate sub-types of weak cataclastic fault rocks, fault zones in different geological contexts crossed in underground excavation site have been analysed. It was not a prime objective to determine their genesis or tectonic history, but to analyse the general characteristics of cataclastic fault rocks. In this first phase of the project, mainly fault zones occurring in quartzo-phyllitic series have been studied. Results are compared with observations made of fault zones in other geological contexts, namely in serpentinite and in greenstones.

The chosen geological characterisation involves analyses from the macro- to microscopic scale. Macroscopic studies and sampling of cataclastic fault zones were performed in different excavation sites in the Alps during the period of may 1994 to october 1997. Own in situ observations were completed with the tunnel profile mappings and hydrogeological data put to our disposal by the geological investigation bureaux engaged by the owners of the constructions.

With regard to the sought correlation between geological and geomechanical properties, the geological analyses have been performed at similar scales as common geomechanical laboratory tests. Characterisation is based principally on structural and mineralogical analyses performed on hand specimens and thin sections.

The hydrogeological aspects of cataclastic fault zones have been studied with regard to their impacts on the realisation of underground works and on local and regional groundwater situation. In fact, major impacts on the realisation of galleries are due to the presence of high water pressure behind impermeable fault zones (chap. 7). Hydrogeological data from the site of Cleuson-Dixence where put to our disposal and used to assess indirectly the lateral extension and continuity of the cataclastic fault zones.

The influence of cataclastic fault zones on the groundwater regime in crystalline massifs and the interaction with underground infrastructures has been treated recently by Maréchal (1998) and is currently the subject of several ongoing research projects at ETH-Zürich.

1.1 Organisation and financial support of the project "Cataclastic Fault Rocks"

The research project has been split up in a geological and a geomechanical part, realised in parallel at the Laboratory of Geology (GEOLEP) and the Laboratory of Rock Mechanics (LMR) at EPF-Lausanne. Research has been supported financially by the Swiss National Science Foundation (project "Cataclasites", subside No. 21-42390.94) and by EOS SA - Cleuson-Dixence and BLS AlpTransit AG - Lötschberg. Further collaborations have been engaged with GEODATA S.p.A. (Turin - Italy) and ENEL S.p.A. (Venice -Italy).

2 FAULT ROCKS - GENERAL REVIEW

The manner how rocks accommodate tectonic strain during faulting controls their later geomechanical properties. Two major types of competitive deformation processes can be distinguished: brittle deformation (cataclastic flow), which may reduce the primary cohesion of rocks, and ductile deformation processes (crystalplastic flow) which preserve or even increase cohesion. The principal deformation mechanisms are reviewed below with regard to the corresponding microstructural features in thin section analyses. Classification and terminology of cataclastic fault rocks are still the subject of discussions in geological and engineering domain (e.g. Hoek et al., 1998, SIA 199, 1998, Wyder, 1997, Manatschal, 1995, Schmid & Handy, 1991, Heitzmann, 1985, etc.). Ambiguities arise mainly from the application and mixing of genetic and descriptive criteria, respectively by the application of terms with obsolete genetic connotations (e.g. mylonite). The retained terms and definitions for this study are presented in chap. 2.2.4.

2.1 Deformation mechanisms

The terms of *brittle* and *ductile* deformation are used corresponding to their signification in rock mechanics. However, they are referring in the following discussion to the rock behaviour at the time of tectonic faulting and not to the one observed today in underground works or in performed geomechanical tests (Figure 2-1). The term *brittle* is applied to rocks whose ability to resist (tectonic) stress decreases with increasing strain, whereas *ductile* is referring to rocks which accommodate permanent deformation without losing their ability to resist stress (Hoek & Brown, 1997a).

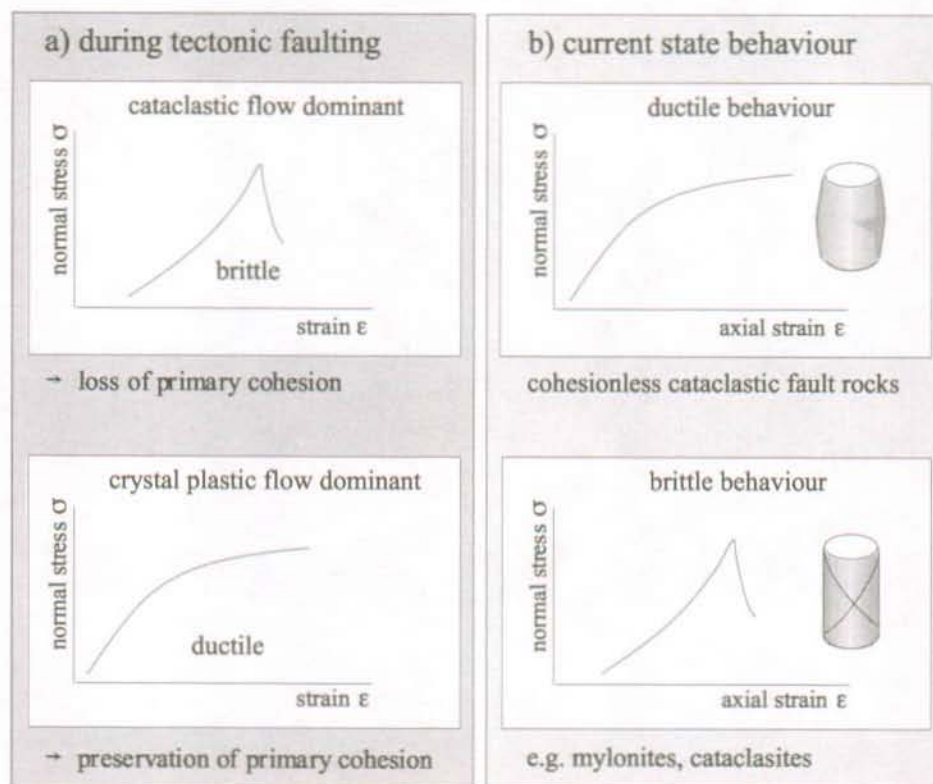


Figure 2-1: Schematic behaviour of rocks during tectonic faulting (a) and current state behaviour of resulting fault rocks (b). Cataclastic fault rocks show, in function of the intensity of endured tectonic strain, geomechanical properties in-between the brittle and ductile behaviour.

The involved deformation mechanisms are controlled by a large number of factors of which temperature, pressure and strain rate are the most important ones (chap. 2.3). Below are

presented in a brief review the two principal groups of competitive deformation mechanisms: *cataclastic flow* and *crystal plasticity*. In a general way the processes of the former group can be considered to be predominant under low temperature - high strain rate conditions, whereas the later are predominant during high temperature - low strain rate deformation. The predominance of one of these competitive deformation processes is critical for the geomechanical properties of the resulting fault rocks. Detailed reviews and discussions of deformation processes are given in Passchier & Trouw, 1996, Schmid & Handy, 1991 and Knipe, 1989, 1986.

2.1.1 Cataclastic flow (*cataclasis*)

The term *cataclastic flow* (*cataclasis*) is referring to purely mechanical deformation processes involving brittle fragmentation of grains by microcracking, frictional grain-boundary sliding, dilatancy and rigid-body rotation of crystal and grain fragments (Passchier & Trouw, 1996, Schmid & Handy, 1991, Sibson, 1977). Fracturing takes place by nucleation, propagation and displacement along newly formed cracks. It is accompanied by frictional grain-boundary sliding, the individual grains and crystals endure in general no intracrystalline deformation (Knipe, 1989). Because of dilatancy, strength of cataclastic fault rocks strongly depends on effective stress, it is hence favoured by low confining pressure and high fluid pressure. Temperature and strain rate are of lesser importance (Schmid & Handy, 1991). Cataclastic flow is the dominant deformation process at non- to low-grade metamorphic conditions and at relatively high strain rates. It is favoured by high fluid pressures (increase of differential stress).

Typical cataclastic rock fabrics (Figure 2-2) show fractured, angular rock and grain fragments of a large grain size range. Open spaces are subsequently healed by quartz or carbonate and refractured by further cataclasis.

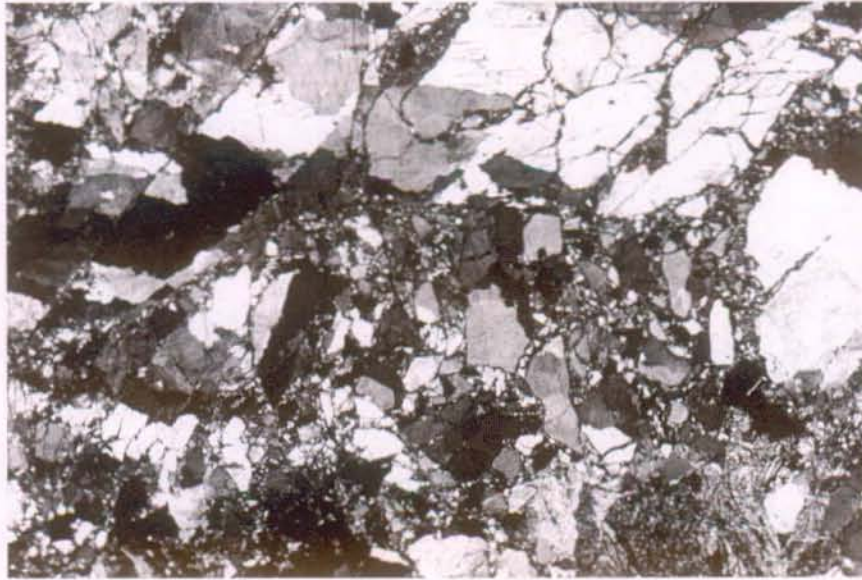


Figure 2-2: Cataclastic rock fabric illustrating the fracturing and granulation of quartz. Thin section image, crossed polarised light, width of view 9mm. (Sample Zr 29.1b, Cleuson-Dixence)

2.1.2 Crystal plasticity

By *crystal plasticity*, permanent strain is accommodated in crystals without loss of cohesion by intracrystalline deformation processes based on the movement of lattice defects (Grshong, 1988, Knipe, 1989). It is a general term for the group of intracrystalline deformation mechanisms based on lattice defect migration, such as dislocation glide, dislocation creep, twinning, all of which are accompanied by dynamic recovery and recrystallisation. All these processes are controlled mainly by temperature, strain rate and grain size, whereas effective pressure is of minor importance.

In thin sections the effects of intracrystalline deformation can be observed as undulose extinction, formation of subgrains, deformation lamellae and tapered twins. Partially recrystallised rock fabrics show a bimodal grainsize distribution, with small, dynamically recrystallised grains between large ones of undulose extinction (Passchier & Trouw, 1996).

2.1.3 Pressure-solution and diffusion creep

Deformation is achieved by mass transfer through an intergranular fluid by dissolution-precipitation processes, respectively by solid-state diffusion (e.g. Schmid & Handy, 1991, Knipe, 1989). Pressure solution is localised at grain contacts where crystal lattices are under higher stress and solubility of minerals in aqueous fluids is increased. The dissolved material is redeposited at the grain boundaries adjacent to pore spaces where stress in the crystal lattice is lower. Pressure solution processes are important under low-grade metamorphic conditions in porous materials with abundant pore fluids. Solid-state diffusion creep in contrast becomes important at relatively high temperatures with respect to the melting temperature of the involved minerals. Crystals deform by diffusion of vacancies through the crystal lattice, respectively along the grain boundaries (Passchier & Trouw, 1996).

2.2 Terminology and classifications of fault rock

A great number of fault rock classification systems is found in literature, a brief review, with regard to studied cataclastic fault rocks, is presented below (see also Bürgi, 1995). Reviews of descriptive fault rock classifications and terminology have been published by Higgins (1971) and Heitzmann (1985), genetic classification systems by Schmid & Handy (1991) and Wise et al. (1984). As will be shown in the following, the evolution of terminology and definitions of (cataclastic) fault rocks in function of achieved progress in understanding rock deformation mechanisms is at the origin of some (persistent) confusion between geologists and practitioners in engineering geology. The definitions of *mylonite*, *cataclasite* and *kakirite* have been tracked back to their origins.

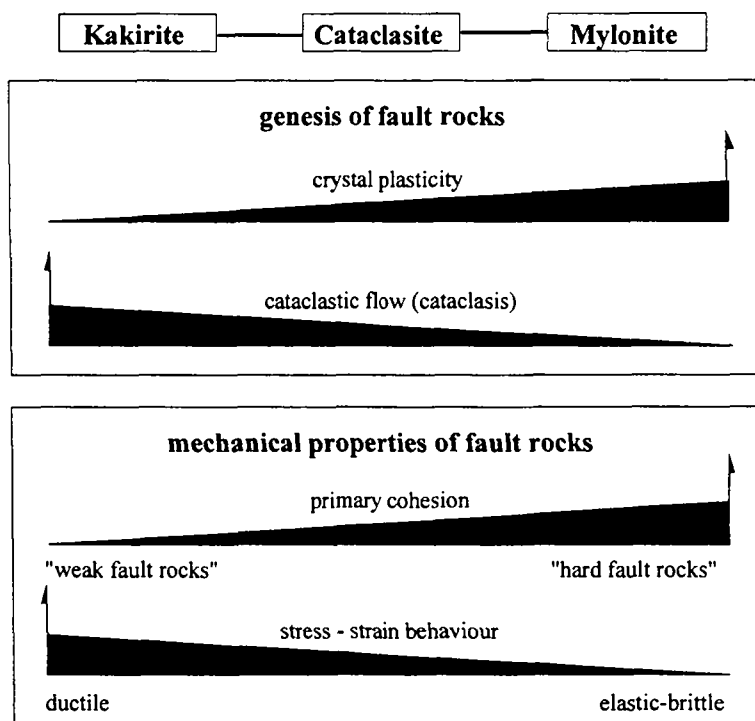


Figure 2-3: Competitive deformation mechanisms during tectonic faulting and resulting geomechanical properties. The term "cataclastic fault rocks" is referring to fault rocks formed by dominant cataclastic deformation processes (kakirites and cataclasites).

2.2.1 Mylonites

The term *mylonite* was introduced by Lapworth in 1885 considering fine-grained schistose fault rocks related to the Moine Thrust Zone, Scotland. At his time, and until about 1973, the dominant deformation mechanism leading to the typical rock fabric of mylonites was thought to be cataclasis, respectively intense "crushing", "dragging" and "grinding" of the host rock along fault planes (Lapworth, 1885). The similarity of the (supposed) mechanical metamorphism with the process of grinding flour in a mill inspired Lapworth to call these fault rocks *mylonites* (Greek *μύλη*, mylon; mill.). The observed microscopic rock fabric is characterised by an important grain size reduction (in comparison with the host rock) and by a manifest lamination structure.

Although the different definitions of *mylonite* and its various sub-types are based on principally descriptive criteria (Lapworth, 1885, Staub, 1915, Quensel, 1916, Termier & Maury, 1928, Waters & Campbell, 1935, Christie, 1960, Higgins, 1971, White, 1982, Heitzmann, 1985), they include since the very first definition the genetic connotation of mechanical "crushing, dragging and grinding". By progresses achieved in understanding rock deformation mechanisms, this connotation has started to change (Bell & Etheridge, 1973). They made evident that ductile deformation processes can give rise to grain size reduction just as cataclasis does. In particular they showed that grain size reduction in mylonites is achieved mainly by dynamic recrystallisation processes and not by cataclasis as supposed before. This was the beginning of the troubling disharmony between the used term *mylonite*, with its original genetic connotation (cataclasis), and the actually involved deformation mechanisms (crystal plasticity). While structural geologists easily accepted the modified perception of *mylonites*, in engineering domains the old connotation is still popular (e.g. Hoek et al. 1998). *Mylonites* in the sense of miners are (still) referring to weak, cohesionless cataclastic fault rocks, which cause important difficulties in underground works. This is in fact in great contrast to the sense of the term given by geologists, for whom *mylonites* do not have a priori poor mechanical properties but who distinguish them from ordinary schists only by their higher strains and association with fault zones (White, 1982).

Based on the preceding it is strongly recommended to abandon the use of the term *mylonite* to describe weak, cohesionless cataclastic fault rocks in engineering domain. Attempts are presently in progress to clarify and harmonise its meaning for the two groups of professionals (e.g. Schaeren, 1998, SIA, Norm 199, 1998, Bürgi, 1995, Heitzmann, 1985).

2.2.2 Cataclasites

Grubenmann & Niggli (1924) have introduced the term *cataclasite* in order to differentiate unfoliated, structureless cataclastic fault rocks from schistose mylonites (in the sense of Lapworth, 1885). The term is derived from the Greek word *cataclase* (*κατακλάω*, *katakláo*) referring to purely mechanical deformation processes as described in chap. 2.1.1. Higgins (1971) defined cataclasites as "aphanitic, structureless cohesive cataclastic rocks,... essentially like mylonite but lacking fluxion structure". The term is still controversial as it includes descriptive and genetic criteria too. It is generally agreed that *cataclasites* are the result of a combination of cataclastic *and* (minor) crystal plastic deformation processes and that they are cohesive fault rocks (White, 1984, Heitzmann, 1985, Schmid & Handy, 1991).

Although cataclasis is a purely brittle deformation process, it does not necessarily imply the loss of (primary) cohesion to the fault rock. Schmid & Handy (1991) pointed out that during "cohesive cataclasis" the loss of cohesion is limited to small but constantly changing populations of grains at a given time. As simultaneously crystal plasticity and pressure-solution processes are acting, the fault rock (*cataclasite*) as a whole maintains cohesion during faulting. In contrast, "cohesionless cataclasis" involves the loss of cohesion at a larger proportion of grains at the same time and hence the rock as a whole loses cohesion (see *kakirite*).

In disagreement to the original descriptive definition of Grubenmann & Niggli (1924), the notion of *cataclasite* has been modified to include "foliated cataclasites" (Chester et al., 1985). It has been shown that purely cataclastic flow can produce foliated fault-related rocks just the same way as intracrystalline deformation does. Without contesting the prime importance of the made observation, the author prefers to maintain restriction of the term *cataclasites* to structureless cataclastic fault rocks corresponding to the original definition. It is agreed that genetic

connotations of descriptive classification criteria have to harmonise with improved understanding of rock deformation mechanisms. It is however troubling to see changed not only the evolved genetic connotation of well established terms but also their descriptive criteria. The inclusion of "foliated cataclasites" reinforces furthermore the trend towards purely genetic classification systems which are based on highly sophisticated analysing methods and are inaccessible for most non-specialists.

2.2.3 *Kakirites*

The term *kakirite* (in ref. to Lake Kakir, Sweden) was first defined in 1910 by Holmquist (in Quensel, 1916), referring to cataclastically deformed fault rocks without parallel structure. Quensel emphasised the occurrence of dense networks of shear planes and gliding surfaces along which intense mechanical granulation is observed, whereas the grains in-between show only minor evidence of deformation. Grubenmann & Niggli (1924) considered *kakirites* as equivalents of (low cohesive) fault breccias.

Heitzmann (1985) has redefined the term *kakirite* as a general term for cohesionless, intensely cataclastically deformed fault rocks characterised by dense networks of shear planes and gliding surfaces. Grain size of *kakirites* is varying between coarse-grained (fault breccias) and very fine-grained (fault gouges). This definition of *kakirite* becomes more and more accepted in the geological as well as in the engineering geological domain in Switzerland (Kellerhals & Isler, 1998, Schaeren, 1998, SIA - Norm 199, 1998, Wyder, 1997, Schneider, 1992).

2.2.3.1 Fault breccia and fault gouge

In english written literature *fault breccias* and *fault gouges* are considered as cohesionless equivalents of cataclasites (Groshong 1988, Sibson, 1977, Higgins, 1971). Distinction is made on the proportion of rocks fragments large enough to be visible by the naked eye, it is > 30% of the rock mass for *fault breccias*, respectively < 30% for *fault gouges*. The term *kakirite* is proposed as collective term for both type of cohesionless cataclastic fault rocks.

According to descriptive fault rock classification systems (Wyder, 1997, Groshong, 1988, Heitzmann, 1985, Sibson, 1977, Higgins, 1971, a. o.) cohesiveness is referring to the state of the fault rock when exposed in outcrops. This is in disagreement with most genetic classifications, in which cohesiveness is referring to the cohesive state of fault rocks during faulting (Manatschal, 1995, Schmid & Handy, 1991). Distinction becomes important inasmuch as *kakirites* may regain a secondary cohesion by substantial post tectonic cementation. In fact, they have to be considered as cataclasites when applying descriptive classification criteria, but are still *kakirites*, respectively *fault breccias* or *fault gouges*, when classified in a genetic classification system. With regard to the study of cataclastic fault rocks in underground works, it is obviously their current state of cohesiveness in the outcrop that is referring to the term *cohesion(-less)*.

2.2.4 *Retained terminology of fault rocks*

As mentioned above, terminology of fault rocks is still controversial mainly because descriptive and genetic criteria are incorporated in the various definitions. Purely genetic classification systems are preferred when interested in the understanding of deformation mechanisms during tectonic faulting. The identification of these mechanisms is based on detailed microstructural analyses, often performed by Transmission Electron Microscopy, and hence in general reserved for specialists. Descriptive classification systems are in contrast more easily applied and more useful, e.g. for engineering geology purposes. Attention has to be paid however to maintain up to date the genetic connotations of the descriptive criteria. Otherwise, as shown by the example of mylonite, communication between specialists and non-specialists becomes rapidly ambiguous.

Based on the preceding review the following definitions of three major types of fault rocks have been retained:

cataclastic fault rocks			
cohesionless cataclastic fault rocks		cohesive fault rocks	
Kakirites		Cataclasites	Mylonites
Fault breccia	Fault gouge		

Figure 2-4: Retained fault rock classification.

Kakirites are cohesionless (weak) cataclastic fault rocks generated by purely brittle deformation processes. They show intense micro- and macrofracturing across and within grains. Distinction is made between coarse-grained *fault breccias* and fine-grained *fault gouges*.

Cataclasites are cohesive, structureless fault rocks showing evidence of intense cataclastic and crystal plastic deformation.

Mylonites are fine-grained, cohesive fault rocks characterised by a strongly developed penetrative foliation and often with stretching lineations. They are formed by dominant crystal plastic deformation processes.

For field classification, cataclastic fault rocks which are easily crushed by hand down to a grain size of < 1cm are considered, according to Wyder (1997), as cohesionless and classified as kakirites. Fault rocks analysed in this study are essentially kakirites and in minor proportion cataclasites, they are referred to collectively as *cataclastic fault rocks*.

2.3 Parameters controlling rock deformation mechanisms

Tectonic rock deformation processes are controlled by a large number of lithological internal and external parameters. As internal controls are considered: mineralogical composition, rock fabric, grain-size, composition of intragranular fluids, porosity, permeability, etc.. Strain rate, confining pressure, fluid pressure, applied stress and temperature are external controls. The exact identification of the involved lithology internal and external controls during faulting of the analysed fault zones is beyond the scope of the project. They are discussed in a general way below insofar as they influence the present day geomechanical behaviour of cataclastic fault rocks.

2.3.1 Lithology external controls

The determination of the effective P-T conditions during faulting needs detailed microstructural, mineralogical and microthermometric analyses for each studied fault zone. This is beyond the chosen approach of this study. Weak cataclastic fault rocks out of different geological and tectonic contexts have been analysed considering their geological and geomechanical properties as observed during excavation works. However, it is evident that the knowledge about faulting conditions and regional tectonics is of great importance in regards of geological previsions for underground excavation projects.

The generation of weak cataclastic fault rock is commonly thought to occur in shallow depth. Under near-surface conditions rocks show a mainly elastic-frictional behaviour, whereas with increasing depth, respectively increasing temperature and pressure conditions, rock behaviour becomes more ductile. The depth of this gradual transition between predominantly cataclastic and

predominantly crystal plastic deformation processes depends on mineralogical composition, rock fabric, geothermal gradient, strain rate, fluid pressure, a.o.. The critical temperature in the transition zone is commonly assumed to lie around 300°C (Mancktelow, 1985, Sibson et al., 1979, Sibson, 1977). The formation of fault rocks in function of depth is shown schematically by Passchier & Trouw (1996), Mancktelow (1985), Sibson (1977) and others (Figure 2-5).

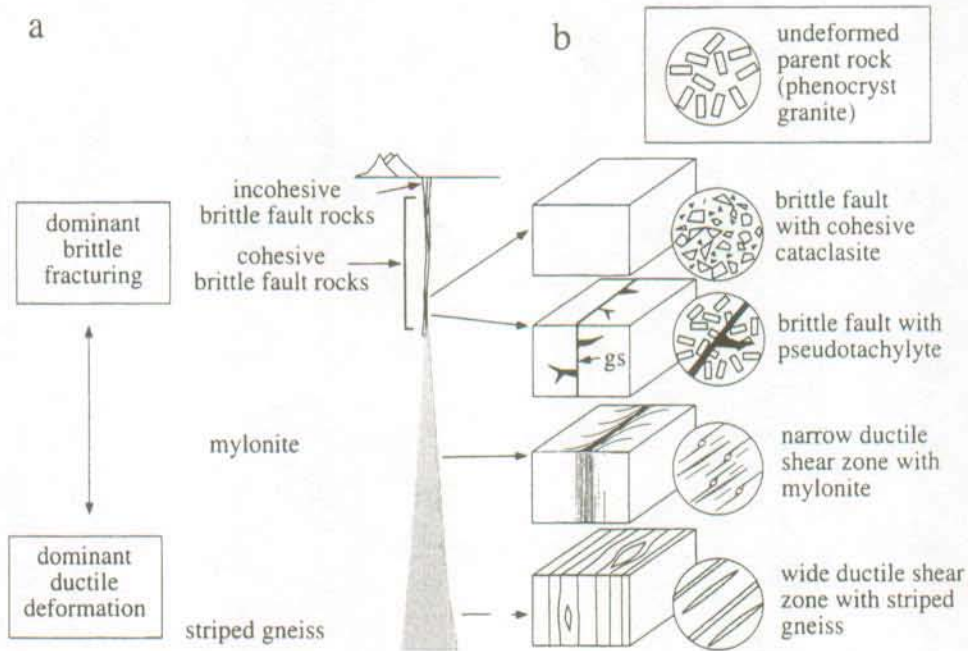


Figure 2-5: Conceptual model showing the distribution of main fault rock types with depth. At the right are presented schematically four typical fault rocks and the corresponding shear zone geometries at a metric scale. The generation of cohesionless cataclastic fault rocks is restricted to a narrow zone near the surface. (Passchier & Trouw, 1996, Fig. 5.1).

Wyder (1998a, 1997) has evaluated the p-T conditions during faulting of the Tavetsch massif by the means of microthermometric analyses on related fluid inclusions. Formation of the Tavetsch kakirites is reported to have occurred at depths between 6 to 9 km and temperatures between 280 to 190°C. This study furthermore shows that brittle faulting involving loss of cohesion was associated with a drop in fluid pressure from lithostatic to hydrostatic values.

According to the preceding the formation of kakirites can be assessed to take place generally in the uppermost ~10 km of earth-crust.

2.3.2 Lithology internal controls

At given extern controls, faulting mechanisms depend on mineralogical composition, rock fabric and intragranular fluid properties. The influence of grain size on rock strength e.g. has been analysed amongst others by Onodera & Kumara (1980), Hugman & Friedman (1979) and Olsson (1974). A negative correlation is reported between grain size and rock strength. Influence of mineralogy on rock strength has been discussed amongst many others by Tugrul & Zarif (1999), Gunsallus & Kulhawy (1984), Calembert et al. (1980a), Bell (1978), a.o.. Conflicting relationship between quartz content and rock strength are reported. Tugrul & Zarif (1999) and Schroeder (1972) found positive correlations between the quartz/feldspar ratio, respectively quartz content and uniaxial compressive strength for granites. The complex influence of mineralogical composition on rock behaviour is briefly discussed below.

Mineral phase	low-grade metamorphic conditions	medium-grade metamorphic conditions	high-grade metamorphic conditions	dominant extern controls
Quartz	<p>brittle fracturing, pressure solution and solution transfer predominant</p> <p>dislocation glide and creep</p> <p>fractured grains, undulose extinction, pressure solution phenomena, deformation lamellae, veins</p>	<p>dislocation creep dominant (pressure solution)</p> <p>strongly flattened crystals recovery and recrystallisation structures</p>	<p>recrystallisation, recovery</p> <p>strain-free apparent recrystallised grains of irregular shape, relatively uniform grain size</p>	<p>essentially temperature, strain rate, differential stress, presence of pore and lattice water</p>
Plagioclase/ K-feldspar	<p>brittle fracturing, cataclastic flow</p> <p>dislocation glide</p> <p>angular grain fragments showing strong intracrystalline deformation (undulose extinction, subgrains), wide range of grain size,</p> <p>tapering deformation twins, deformation bands, kink bands</p>	<p>dislocation climb, recrystallisation, microkinking,</p> <p>core-mantle structure formed by fine-grained feldspar around cores of old grains</p>	<p>myrmekit growth, dislocation climb, recovery, subgrain and,</p> <p>subgrains of similar size, irregularly shaped, strain free grains, isolated micro-kink bands,</p>	<p>metamorphic conditions</p>
Calcite/ Dolomite	<p>pressure solution, deformation twinning (recrystallisation)</p> <p>deformation twins, pressure solution phenomena</p>	<p>dislocation glide, deformation twinning, grain boundary migration recrystallisation</p> <p>deformation twins, irregular grain shape</p>	<p>grain boundary migration recrystallisation, grain boundary sliding,</p>	<p>presence of water, temperature</p>
Mica	<p>pressure solution, fracturing, crude kinking, folding, dislocation glide</p> <p>undulose extinction, kinked, folded and fish-shaped boudinaged grains</p>	<p>grain boundary migration recrystallisation</p> <p>mica fish</p>		<p>temperature</p>

Table 2-1: Deformation properties of common rock forming minerals and diagnostic features in thin sections. After Passchier & Trouw, 1996.

2.3.2.1 Mineralogy

Mineral phases react differently to external controls such as temperature, pressure, fluids etc. in function of their specific physical and chemical properties. Hence it is common to observe microstructures resulting of brittle and crystal plastic deformation mechanisms in fault rocks. In Table 2-1 are summarised some specific deformation properties of a few common rock forming minerals.

Behaviour of polymineralic rocks depends in a complex way on the stress-strain behaviour, the proportions, shape and spatial distribution of the rock forming minerals. After Handy (1990) polymineralic rocks show three end-member types of microstructural and mechanical behaviour (Figure 2-6): In domain 1, the strong mineral phase forms a load bearing framework (grain-supported); rock strength is controlled by the strength of the strong mineral and by the size, shape and distribution of the weak phase. In domain 2, rock fabric is characterised by elongated boudins of the strong phase in a weaker matrix. Rock strength is controlled by the properties of both mineral phases. In domain 3, rocks show a veritable clast-matrix fabric, composed of relatively undeformed clasts caught in weak matrix. Strength of the aggregate is controlled by the properties of the weak mineral phase.

Strength of a polymineralic rock does not behave linearly with the proportion of the hard, respectively weak mineral phase. In fact, it changes abruptly when packing density of the strong mineral becomes so high, that grains start to touch. This discontinuity resulting of the geometrical transition from matrix-supported to grain-supported rock fabric is indicated in Figure 2-6 by a heavy line.

During tectonic faulting rock fabrics continuously change. It may shift in fact from matrix-supported to grain-supported if accumulated strain is high enough. Strength behaviour of polymineralic rocks during faulting is hence very complex (e.g. Passchier & Trouw, 1996, Schmid & Handy, 1991, Handy, 1990, Wise et al., 1984).

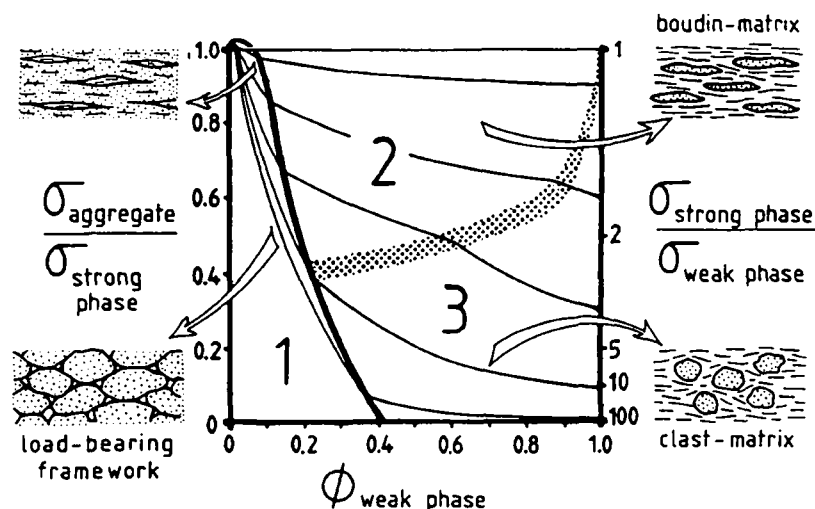


Figure 2-6: Conceptual diagram showing the normalised strength (left-hand axis) of a biphasic rock aggregate as a function of the volume proportion of the weak phase (ϕ_w). The right-hand axis indicates the strength contrast between the strong (set to be 1) and the weak mineral phase. Strength of the aggregate in function of the mineral strength contrast are indicated by thin lines. Note the strength discontinuity at the transition between grain-supported and matrix-supported rock fabric. (Handy, 1990, Fig. 1).

Handy (1990) suggests mineral strength contrast in domain 3 to be at least 10:1, whereas it is supposed to be less in domain 2. As will be shown later, most of studied cataclastic fault rock fabrics are located in domain 3 and 1.

2.4 Geotechnical rock mass classification systems

As summarised by Takacs & Clay (1997), rock mass classification systems (r. m. c. systems) have been developed as a support for tunnel design and contractual purposes, respectively to "transform tunnelling from an art into science". Widely used in underground works, they are mainly based on experiences achieved in hard rock tunnelling, their applicability to weak (cataclastic fault) rocks has shown to be very limited. An integral review and discussion of existing r. m. c. systems is given in Bieniawski (1989). Their aptitude to characterise weak rocks is discussed in Russo (1994), Clerici (1992) and Ünal et al. (1992).

Before discussing more in detail the applicability of r. m. c. systems to *weak rocks*, one has to specify what is commonly conceived by this expression: weak rocks are basically characterised by a low mechanical strength situated somewhere between that of rocks and soils. Expressed in terms of uniaxial compressive strength, the range of weak rocks is varying between ~1 MPa (transition to soils) and ~25 MPa (transition to strong rocks), depending on the different authors (Bieniawski, 1989). According to Sciotti (1990, in Russo, 1994), weak rocks are characterised additionally by high deformability, strong strength dependence on water saturation and temperature, and by their susceptibility to weathering.

R. m. c. systems are based on the division of a rock mass formation into geotechnical units, whose characteristics can be considered to be uniform with regard to the requirements of the project. Considering the traditional classification systems, two different approaches can be distinguished: The first one is based on a "rock - discontinuity" model, in which rock masses are characterised as an assemblage of blocks of intact rock material separated by discontinuities. The geomechanical characteristics of this assemblage are determined by taking into account the properties of the intact rock (e.g. uniaxial compressive strength) and of the discontinuities (e.g. spacing, friction angle, alteration, etc.). The overall rock mass quality can then be expressed in a quantitative way and is often related to recommendations for tunnel support design (e.g. Bieniawski, 1979, Barton et al., 1974, Cording & Deere, 1972).

With regard to their possible largeness and macroscopic structures, cataclastic fault zones can hardly be conceived as discontinuities. The latter are by definition surfaces where a specific material property brusquely changes. In contrast, cataclastic fault zones can be up to several decametres wide and, in comparison with the scale of underground constructions, have to be considered as true 3-dimensional structures forming geotechnical units of their own.

The applicability of common r. m. c. systems to weak cataclastic fault rocks is very limited, mainly because it is often impossible to determine correctly the required classification parameters, such as intact rock strength, discontinuity orientation, roughness, spacing, effect of water, etc. (e.g. Russo, 1994, Ünal et al., 1992). In fact, as stated by Russo (1994), the reliability of rock mass classification systems decreases in a general way, the more the considered rock mass resembles a weak continuous medium compared to the size of the cavity. Cataclastic fault rocks are hence often "classified", together with any other kind of weak rocks, in the "worst category" of existing rock mass classifications. In consequence the variance of geological and geomechanical properties of weak rocks is quite large. Several attempts are presently in progress to improve the geomechanical characterisation and classification of weak (cataclastic fault) rocks (Habimana, 1999, Hoek et al., 1998, Russo, 1994).

R. m. c. systems of the second type are based on a more global approach; the entire rock mass is qualified with regard to its geomechanical behaviour and tunnel support requirements (e.g. Hoek et al. 1998, NATM in Bieniawski, 1989, Lauffer, 1958). Rock mass quality is appreciated as a whole, without considering separately the properties of the intact rock material or discontinuities. The "input data" for these classification systems are hence more subjective and principally based on acquired experiences. The Geological Strength Index (GSI), introduced by Hoek (1994), characterises rock masses qualitatively with regard to their interlocking and state of alteration of discontinuity surfaces. It is essentially based on field observations, respectively on a "visual impression of the rock structure" (Hoek et al. 1998). By a recent modification its application has been extended to weak rocks (Hoek et al. 1998).

A similar approach has been proposed by the Associazione Geotecnica Italiana (AGI, 1979 in Russo, 1994): Rocks are defined as "complex rocks" when they show pronounced lithological, structural and geotechnical inhomogeneity at macroscopic scale (1 to 10m). Different types of complexity are distinguished visually. The terms *weak rocks* and *complex rocks* are interesting inasmuch as together they summarises the essential characteristics of weak cataclastic fault rocks.

The principal deficiency of classification systems based on "visual rock impression" is in fact their elevated degree of subjectivity and dependence on experience. The appreciation of rock mass quality in weak rocks hence still resembles more an "art than a science".

The existing r. m. c. systems are referring to the rock mass characteristics at the macroscopic scale, whereas common geomechanical laboratory test are performed on hand specimens measuring some centimetres at most. With regard to the seeked correlation between geological and geomechanical properties, it is important to characterise and classify studied fault rocks at similar scales. A geological characterisation method referring to the meso- to microscopic scale is presented in this work.

3 THE STUDY SITES

For the development of a site independent characterisation of cataclastic fault rocks, different owners and contractors of currently active underground excavation sites in the Alps have been contacted. The sites have been chosen in function of their geological context and the "positive" prognosis about the opportunities to cross cataclastic fault zones. Two underground construction projects are associated to the research, namely the hydraulic gallery of EOS Cleuson-Dixence and the pilot gallery of BLS AlpTransit - Löttschberg. The gallery of Cleuson-Dixence is build mainly in schists, gneisses and green stones, the pilot gallery of Löttschberg in sedimentary rocks of the Helvetic nappes. During the ongoing project, research was enlarged to two other underground sites in Italy where important fault zones occur in serpentinites (Genoa) and in gneiss (Varzo).

3.1 EOS Cleuson-Dixence, Switzerland

3.1.1 The hydraulic gallery of Cleuson-Dixence

The hydroelectric complex of Grande Dixence is located in the south-western part of Switzerland, near the city of Sion in the valley of Rhone (Figure 3-1). The complex includes the gravity dam of Grande Dixence, hundreds of kilometres of galleries, four pumping stations and three power plants. The vocation of this complex is to assure the supply of energy during winter and working day peak demand hours. In order to increase its capacity from 800MW to 2000MW, the construction of an additional power plant and hydraulic supply gallery started in 1993. The excavation works started in 1994 were finished at the beginning of 1996, the new power plant (Bieudron) is operational since winter 98/99.

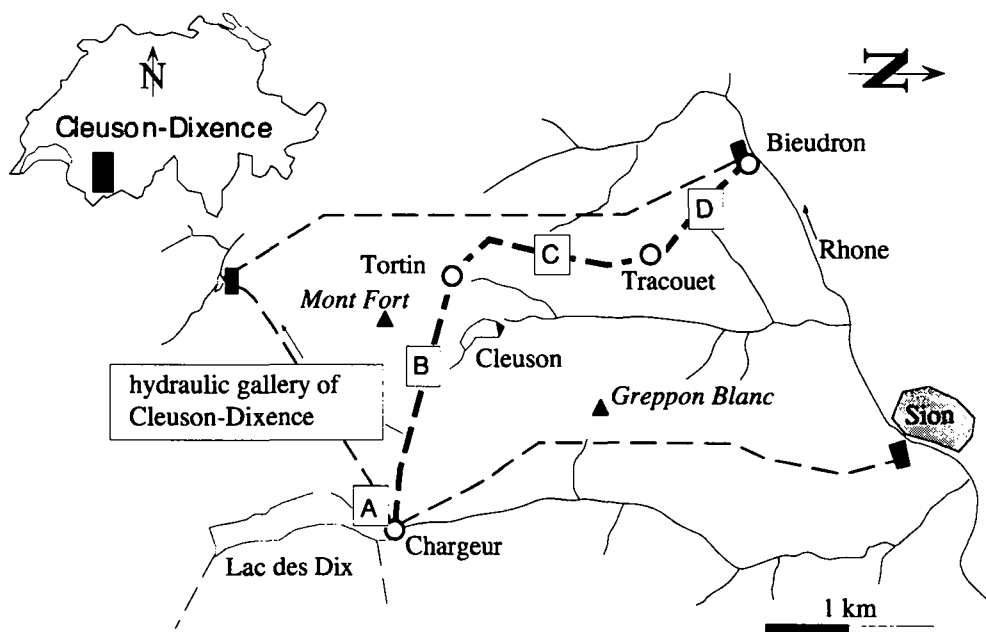


Figure 3-1: Geographic situation of the hydroelectric complex of Grand Dixence with the newly constructed gallery and the power plant at Bieudron. Geotechnical units are indicated by letters A to D. Modified after Méan (1994).

The 20 km long new hydraulic supply gallery is connecting the reservoir of Lac des Dix at 2364 m m.s.l. with the new power plant at Bieudron in the valley of Rhone (480 m m.s.l.). The excavation works were subdivided in five construction units (Figure 3-1) and have started simultaneously. The construction units concerning the gallery are named B, C and D whereas the units A and E comprise the connection work at the barrage of Lac des Dix and the power plant

cavern, respectively. The galleries were excavated mainly by full face tunnel boring machines with diameters varying between 4.80m and 5.80m (Botte et al., 1997, 1996). Excavation in the units A and B has been made by open hard rock TBM's with local installation of rockbolts, shotcrete and steel sets. For the units C and D several shielded TBM's with installation of precast concrete segments immediately behind the TBM-head were chosen. Several access galleries and partially the high pressure shaft (D), were carried out by traditional excavation methods.

3.1.2 Regional and geological settings

The study site is located in the "super" nappe of Grand Saint-Bernard. After Escher (1988) it can be subdivided in four units, all of which are crossed by the hydraulic gallery of Cleuson-Dixence. The four units are from external to internal: the Zone Houillère, the Pontis, Siviez-Mischabel and the Mont Fort nappe (Figure 3-2). The Zone Houillères and Mont Fort nappe comprise only monometamorphic units while the two other nappes include polymetamorphic units¹ as well (Thélin et al., 1994). A recent overview of the nappes cited above is given in Gouffon & Burri, 1997).

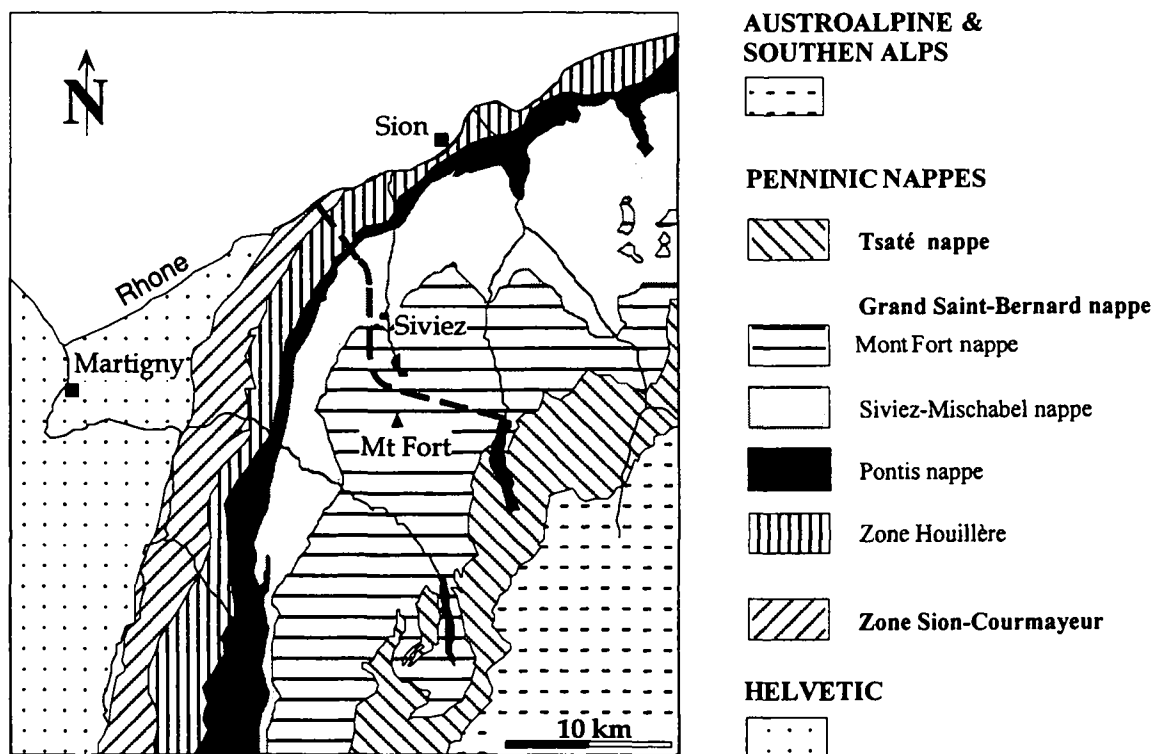


Figure 3-2: Sketch of the tectonic situation of the gallery of Cleuson-Dixence. Modified after Thélin et al. (1994).

The Permo-Carboniferous rocks of the Zone Houillère are divided in two parts by a discontinuous strip of Triassic gypsum and cornieule. The external part includes a chaotic Carboniferous series of sandstones, quartzites, shales and schists, as well as important bodies of Triassic quartzites and limestones. The internal part consists mainly of Permo-Carboniferous shales, graphitic schists and sandstones (Burri, 1983a).

¹ After Thélin et al. (1994): The term "polymetamorphic basement" is applied to a unit which has been affected successively by pre-Alpine metamorphisms and Alpine metamorphism. A "monometamorphic basement" has been subjected in contrast only to the Alpine metamorphism.

The Pontis nappe is composed of polymetamorphic and monometamorphic basement rocks together with fragments of its Triassic sedimentary cover. Only the two latest are crossed by the gallery of Cleuson-Dixence, they consist mainly of sandstones, conglomerates, quartzites, marbles and dolomites.

The Siviez-Mischabel forms a large fold nappe making up the main part of the nappe of Grand Saint-Bernard. The existence of a normal limb, a frontal zone and inverted limb has been stated by different authors (e.g. Thélin et al., 1994, Escher, 1988). The fold nappe comprises poly- and monometamorphic basements and a Mesozoic cover. The core of the nappe is formed mainly by homogeneous paragneisses with an envelope of micaschists, prasinites, amphibolites and Permo-Triassic quartzites. The Siviez-Mischabel nappe has been studied in detail by Escher et al. 1992, Thélin, 1987, Sartori, 1990, Marthaler, 1984, a. o..

The monometamorphic basement of the Mont Fort nappe is composed of paragneisses and micaschists and intercalated greenstone. Within the Mont Fort nappe distinction is furthermore made between the Greppon Blanc and the Métailler units. The later is principally composed of greenstones, with intercalated micaschists and paragneisses, the former is made up mainly of micaschists, paragneisses some greenstone lenses and quartzites.

The Mont Fort and Siviez-Mischabel nappes are separated from each other by a tectonic contact. It is marked by the "Synclinal des Chèques", a thin strip of Mesozoic rocks formed of quartzites, gypsum, anhydrite, dolomitic limestone and cornieule (Schaer, 1959).

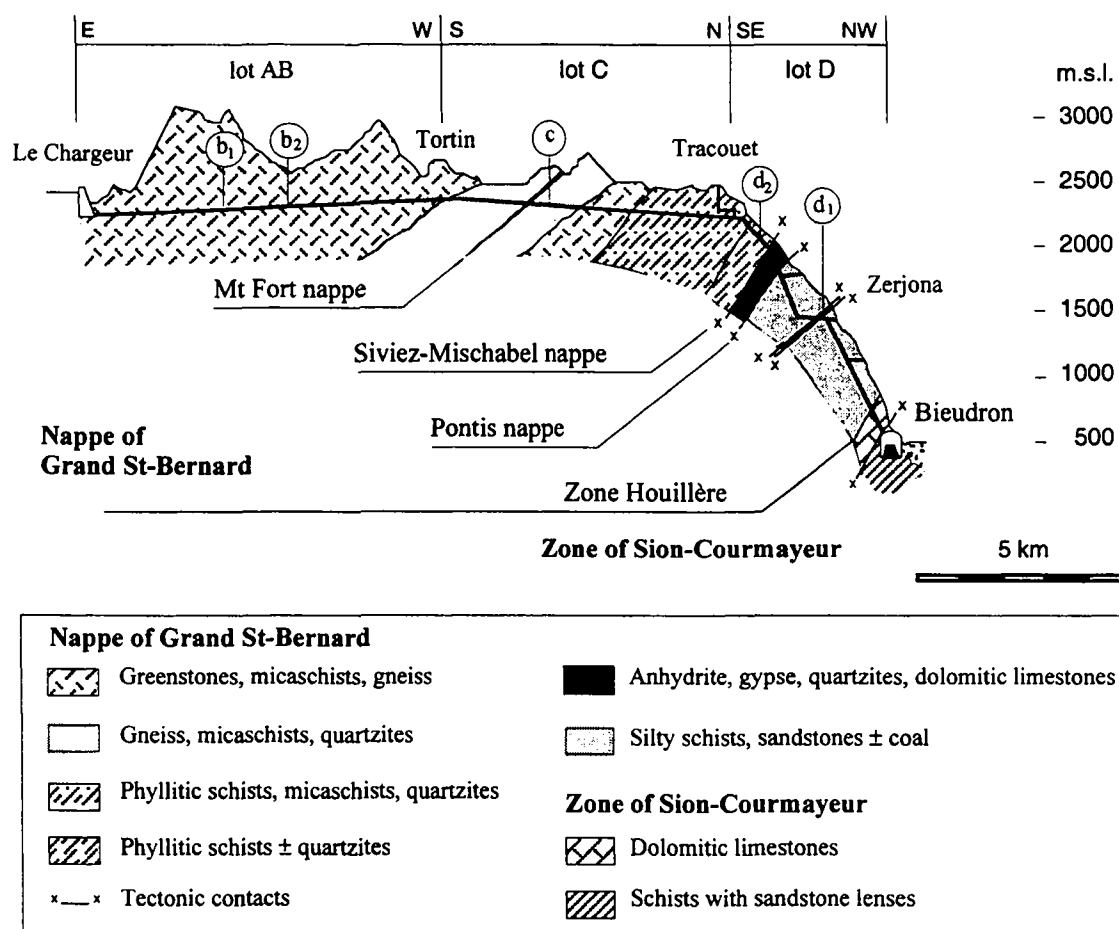


Figure 3-3: Geological profile through the "super" nappe of Grand Saint-Bernard along the hydraulic gallery of Cleuson-Dixence. Letters b₁ to d₂ indicate the location of studied fault zones. Modified after Schaeren (1994).

3.1.3 Studied cataclastic fault zones

3.1.3.1 Unit B, le Chargeur - Tortin

The gallery of unit B with a length of 7.6 km has been excavated by an open hard rock TBM. Installed temporary tunnel support has offered in general good sampling opportunities.

In its whole length the gallery is located in the Métailler unit of the Mont Fort nappe. It is composed of frequently alternating intercalations of greenstones, mica schists, gneisses and phyllites with occasionally some lenses of carbonaceous schists. Transition between these lithologies is in general gradual. A great number of smaller and larger cataclastic fault zones have been crossed, some with important impact on excavation work (Botte et al. 1996). Below are described two examples of fault zones occurred in mica schist, respectively greenstone. Their locations (b_1), respectively (b_2) are indicated in Figure 3-3.

(1) Kakirite zone in chlorito-sericitic schist (b_1)

Between TM 2780 and TM 2900 the gallery has crossed a fault zone orientated sub-parallel to the axis of the gallery (Figure 3-4). Steeply dipping to the NNE it intersected the gallery on a length of 120 metres. The fault zone of varying thickness between a few decimetres and metres has caused a dome-like overbreak of about 100 m³ in front of the TBM head. It was passed after infilling of the cavity with grout and organo-mineralic foam and the injection of a ring-like pre-vault (Botte et al. 1996).

Host rock consists of poorly fractured, greenish-grey chlorito-sericitic schists, characterised by a fine lamination of dark and light greyish layers of a few mm thickness. Transition between mica schist and darker coloured, chlorite rich schist is gradual. Both bear abundant, intensely broken quartz veins. Schistosity is transversal to the gallery and dipping at 30-40° to the NW. Its orientation is quite variable at large scale.

The fault zone is made up of a light greenish to grey schistose kakirite bearing abundant shearzones crosscutting the schistosity. Due to the high content of fine-grained mica it has a soapy touch, especially in presence of water.

(2) Kakirite zone in greenstone (b_2)

Between TM 4280 and 4300 the TBM has crossed two transversally orientated kakirite zones of 10, respectively 2 metres large (Figure 3-4). Detected in pilot boreholes, they have been passed after the injection of pre-vaults. The zones occurred in variably fractured greenstone (ovardite) of the Métailler unit, showing macroscopically small (≤ 1 mm) white feldspar spots in a dark-green coloured matrix. It is composed mainly of albite and chlorite, and lesser amount of carbonate, epidote and opaque minerals.

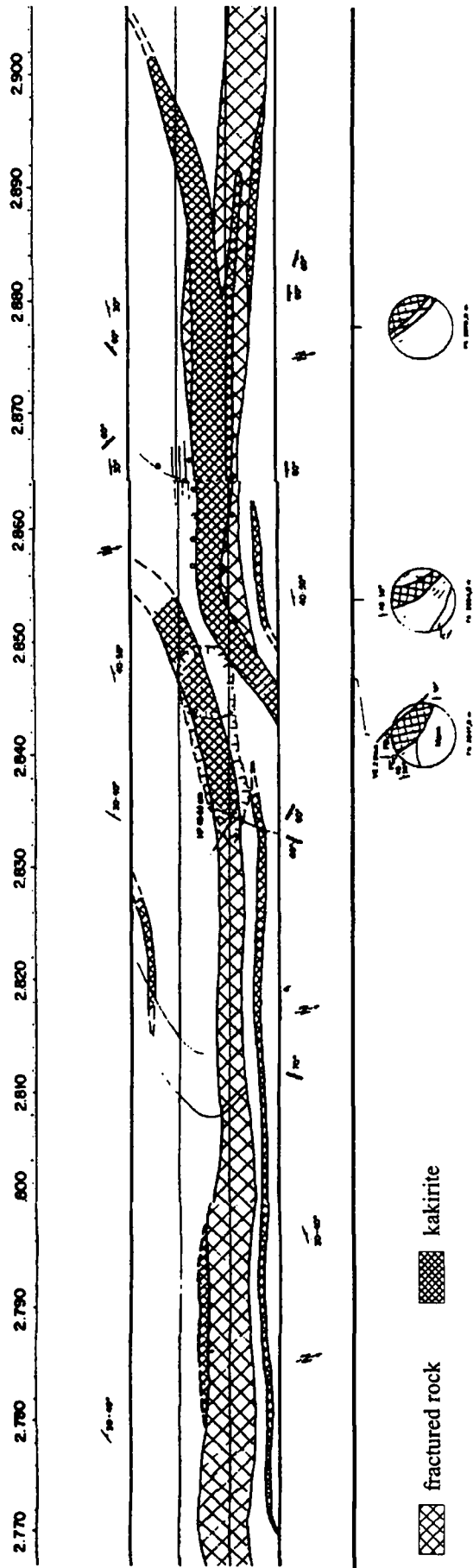
3.1.3.2 Unit C Tortin - Tracouet (c)

As mentioned earlier, excavation in this unit has been made by a telescopic shielded TBM with installation of precast concrete segments immediately behind (Botte et al., 1996). Available geological observations are in consequence rather scarce.

Several kakirite zones have been crossed occasioning variable impact on the excavation work (Botte et al., 1996, Schaeren & Cervera, 1995, 1998). The crossing of two major kakirite zones near the tectonic contact between the Siviez-Mischabel and the Mont Fort nappe, offered the opportunity to take samples in the head of the TBM, respectively in a cored borehole. The fault zones occurred at TM 5180 and TM 5597 caused the interruption of excavation work for two, respectively ten weeks. Both zones occurred in quartz rich gneisses and mica schists of the Siviez-Mischabel nappe. The schistosity is dipping at 20°-40° in drive direction.

The first of the studied kakirite zones was crossed at TM 5180, after advancing for more than 500 meters in poorly fractured gneisses and mica schists. The dry fault zone, dipping at 60-70° from the tunnel face, measured 7 to 8 m large and intersected the gallery transversally at an angle of about 60°. Trying to force the passage, the head of the TBM was filled progressively with the

b1) Fault zones in Chlorito-sericitic schists, Métailler unit (TM 2700 - 2900)



b2) Fault zones in greenstone, Métailler unit (TM 4280 - 4300)

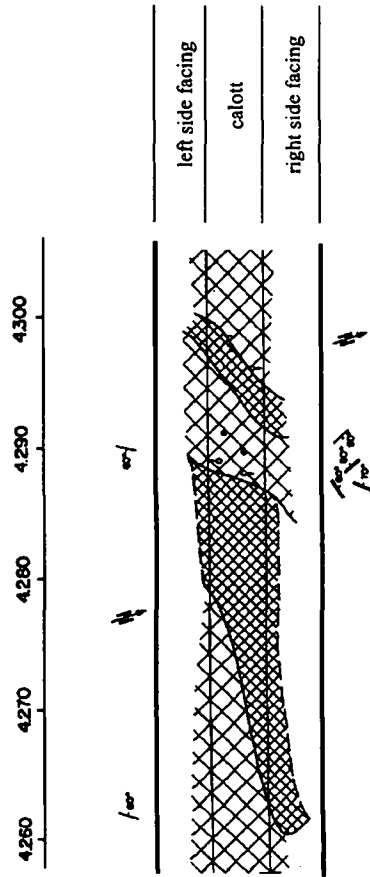


Figure 3-4: Géologique mapping of studied fault zones in the gallery of Cleuson-Dixence, unit B. Simplified after Bureau Technique Norbert SA, Lausanne.

paste-like kakirite material. The zone was passed after it has been reinforced by a pre-vault, injected from a ring-like cavity built around the TBM at the position of the telescopic shield.

The fault zone at TM 5597 represented the most important geological incident in unit C. Similar to the former, it consisted of a sub-vertically orientated, 8 - 12 m large zone composed of past-like kakirite. Two important mudflows (up to 100 m³) accompanied by water inflows of about 10 l/s have occurred as the TBM started to enter this zone. In contrast to the dry fault zone of TM 5180, the present one formed an impermeable panel hiding a high water pressure of 15 bar behind (see chap. 7). To drain the upstream compartment, 20-30 boreholes have been drilled from a small heading gallery built above the TBM. Again, a pre-vault made up of polyurethane resin and cement grout was injected.

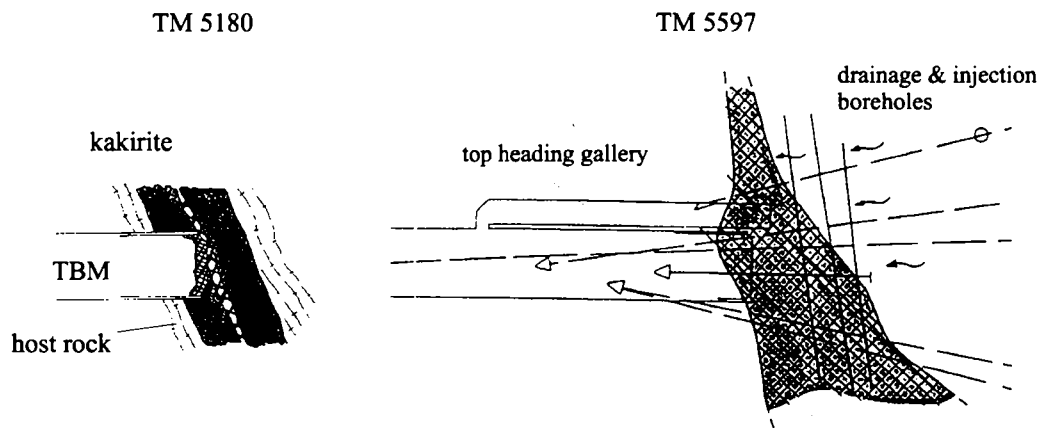


Figure 3-5: Schematic sketch of the crossed fault zone in the gallery Cleuson-Dixence, unit C. Modified after Bureau Technique Norbert SA, Lausanne.

3.1.3.3 Unit D, access gallery F5 - Zerjona (d₁)

The TBM cavern in the access gallery of Zerjona (Figure 3-6) was excavated mainly by backhoe machine. In a first run, a 40 meters long small top heading gallery was built, whereas enlargement of the cavern has been made in opposite, downward direction. The site offered an excellent opportunity to follow the excavation through a large zone of cataclastically deformed rocks.

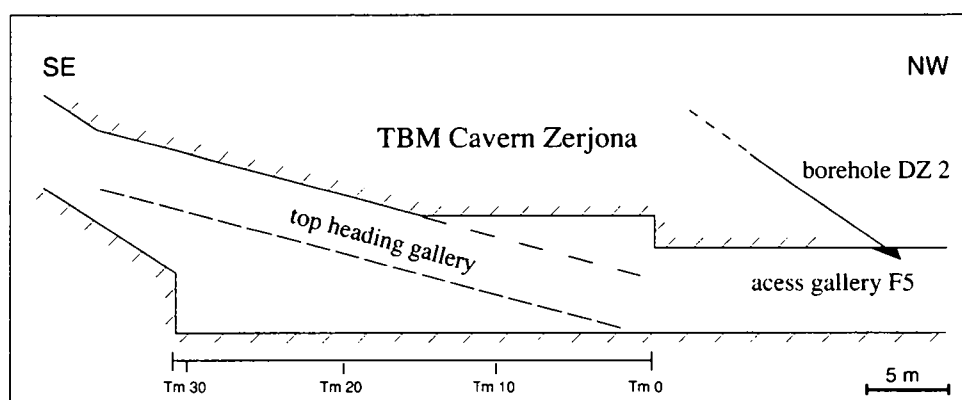


Figure 3-6: Profile of the TBM cavern excavated at the end of the access gallery F5. Samples have been taken in the top heading gallery and the inclined borehole DZ2. After Bureau Technique Norbert SA, Lausanne, intern documents.

The gallery is located in more or less sandy, carbonaceous and locally anthracite bearing schists, schistose meta-sandstones and quartzite of the Zone Houillère (Escher, 1988, Burri, 1983a, b). The schistosity is dipping at 40-50° in NW direction, however as shown in Figure 3-7, the overall structure of the crossed zone is very heterogeneous at the scale of the underground work. Frequent alternations and lateral changes of the present lithologies together with intense tectonic deformation are at the origin of this "complex rock" structure. Transition between quartzites, meta-sandstones and very fine-grained, black phyllite is gradual or abrupt if tectonic. It is marked by a change of colour from light grey to black. Quartz veins measuring a few centimetres are very abundant. Their macroscopic shape being preserved, quartz inside is mostly broken down in a veritable quartz flour, especially in the black schists.

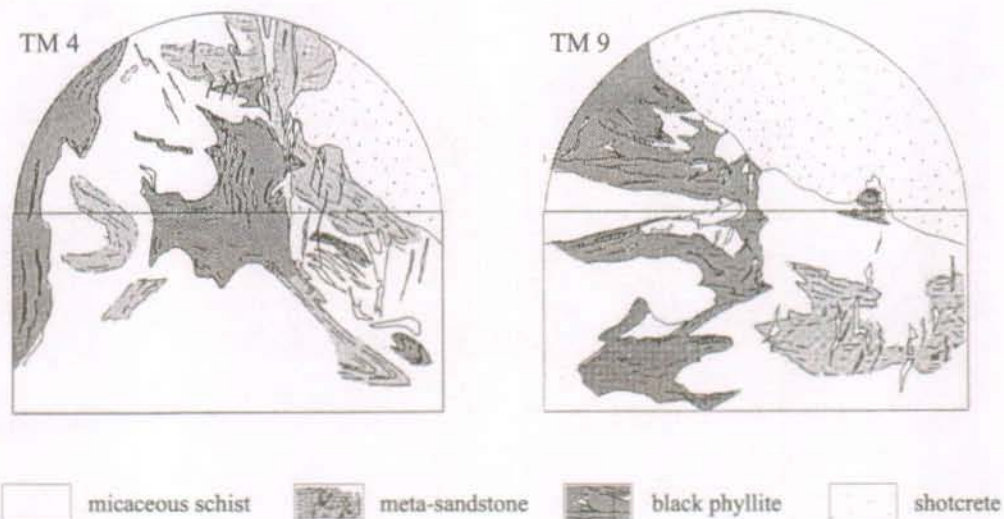


Figure 3-7: Tunnel face of top heading gallery showing complex rock structure issue of intense tectonic deformation. Shotcrete in the top heading (upper right) is installed immediately before the bench is excavated. (Cleuson-Dixence, Zerjona)

Sampled fault rocks can roughly be separated macroscopically in four groups, in function of their host rock lithology:

- Light grey, coarse grained quartzites showing a rough, anastomosing foliation defined by elongated quartz grains. It is easily broken parallel to the foliation.
- Quartz rich meta-sandstones differ from quartzite by a smaller average grainsize, a smoother and closer spaced foliation and a slightly darker colour.
- Graphite bearing micaceous schists distinguish from the former by a fine-grained slaty cleavage and black colour. It is strongly folded at the centimetric to decimetric scale. A high amount of quartz veins is observed.
- Carbonaceous black phyllite is extremely fine-grained, only a few small, spherical to eye-shaped quartz and carbonate grains are visible to the naked eye.

3.1.3.4 Unit D, "Verrucano" (d₂)

From Tracouet downwards in direction of Bieudron (Figure 3-3), the gallery has been excavated by traditional method to meet the TBM advancing upwards (see access gallery F5). The host rock is composed of phyllitic schists with intercalated quartz-rich meta-sandstones and lenses of weak, sericite-quartzitic carbonate breccia. The later are strikingly brownish - orange coloured and have shown very poor mechanical properties, particularly in the presence of water. It is composed mainly of light greyish, commonly rounded clasts (≤ 2 cm large) taken in a fine-grained, yellow

to orange coloured matrix. Based on this macroscopic observation, it has often been named "dolomitic breccia".

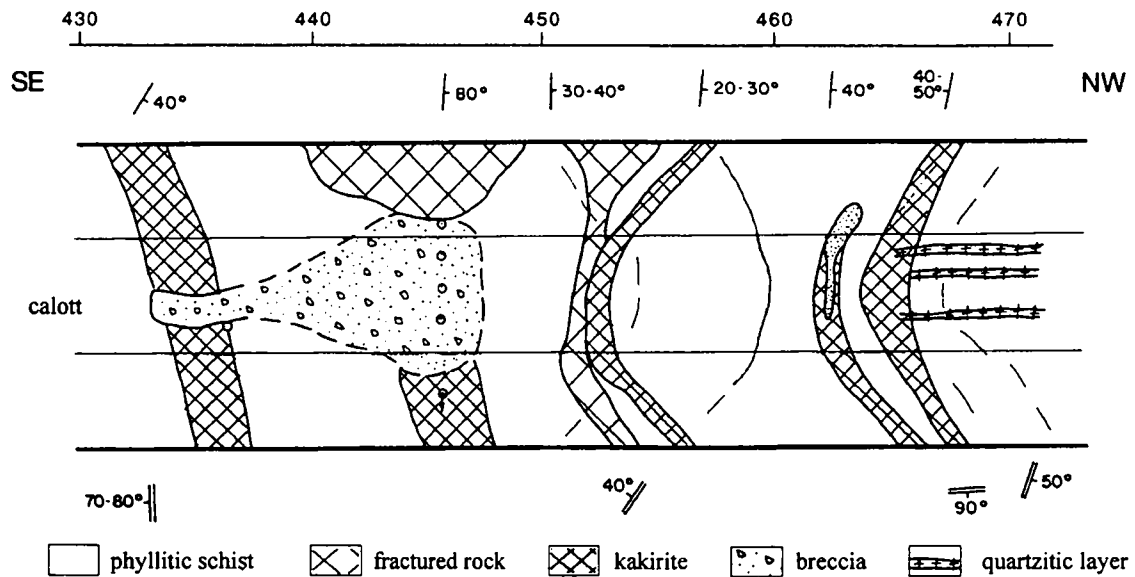


Figure 3-8: Geological mapping of the fault zone in the "Verrucano", TM 445. Simplified after Bureau Technique Norbert SA, Lausanne.

3.2 BLS - AlpTransit, Switzerland

3.2.1 The Lötschberg pilot gallery

Responding to an increasing merchandise traffic in Europe, the enlargement and modernisation of the Swiss railway net has been decided in 1992. Key element of the project is the construction of two new, N-S orientated, railway base tunnels at Gotthard (Gehriger, 1992) and at Lötschberg (Teuscher, 1992).

The project of the Lötschberg axis consists of a 35 km long railway tunnel connecting the Kandertal in the Bernese Oberland with the Rhone valley near Visp. The north portal of the tunnel will be located near Frutigen at about 800 m m.s.l.. The tunnel will be carried out in the western flank of the valley until south of Kandersteg, where it will cross under Kandertal and Gasteretal. The Bernese and Valais Alps have to be crossed under an overburden of between 600 and 2000 m. The south portal is planned near Visp, in the upper part of the Valais (Figure 3-9).

The preceding geological studies (Kellerhals, 1992) for the Lötschberg railway tunnel include geological mapping, seismic analyses, boreholes drilled from the surface and borehole logging, the excavation of a 9'540 m long pilot gallery between Frutigen and Kandersteg (Figure 3-9). Complex geological structures inside the Helvetic thrust nappes and an insufficiently known hydrogeological situation with the risk of important water inflows due to karstification were the main arguments for its construction. The pilot gallery (Teuscher, 1997) starts at Tellenburg south of Frutigen and crosses several units of Ultra- and Helvetic nappes from N to S. The gallery was drilled by an open hard rock tunnel boring machine with a diameter of 5.0 m at a lateral distance of 30 m eastern to the future railway tunnel. A second access gallery, starting from Mitholz and excavated by traditional blasting method, joins the pilot gallery at TM 7200. Excavation work started in January 1995 and was completed in February 1997.

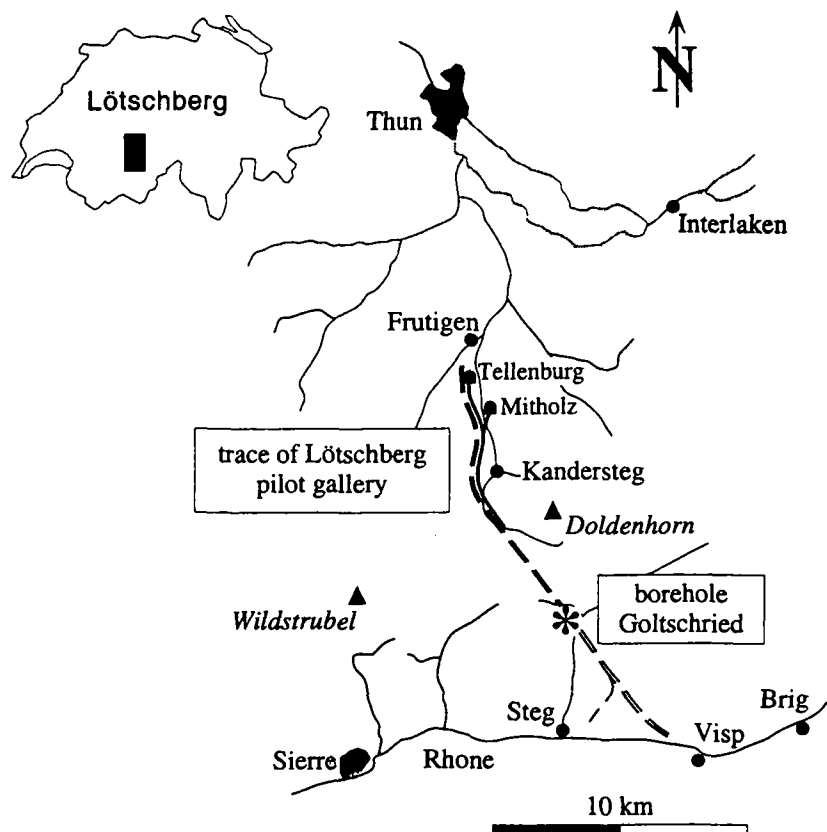


Figure 3-9: Geographic situation of the planned railway base-tunnel at Löttschberg, the pilot gallery and the position of borehole "Goltschried".

Tunnel lining consists of systematically installed shotcrete all along the excavated pilot gallery and locally additional of rockbolts, wire meshes and steel sets. Shotcrete was installed 30 m behind the TBM head.

During investigation campaign deep boreholes were drilled along the trace of the future Löttschberg tunnel to explore the position and nature of the basal thrust-planes between the Helvetic nappes, the tectonic contact with the Aar massif, major fault zones and sediment troughs inside of the Aar massif. For the scope of research on cataclastic fault rocks geological data and rock samples of the borehole "Goltschried" were put to our disposal (Figure 3-9).

3.2.2 Regional and geological settings

The new railway tunnel of Löttschberg is crossing from N to S the Ultrahelvetic and Helvetic nappes as well as the Aar massif and its northern and southern (par-) autochthonous sediment cover. The following brief description is given for the nappes crossed by the pilot gallery and the part of Aar massif concerned by the borehole of Goltschried (for a more detailed and complete description of the tectonic units to be crossed by the Löttschberg railway tunnel see Kellerhals & Isler, 1998, Ziegler, 1997, Burkhard, 1988).

The northern portal of the pilot gallery is located in undefined flysch deposits forming the basis for the overlying Wildhorn nappe. After excavation of about 4.5 km of Flysch and intercalated sandstones of the Taveyannaz series, the gallery passes through the basal thrust-plane of Wildhorn nappe. As shown in Figure 3-11, this major thrust-plane, and the Helvetic nappes, are in general orientated subhorizontally and the gallery is driven at first beneath and later closely above this tectonic contact. The pilot gallery ends just after entering the basal flysch of the Doldenhorn nappe.

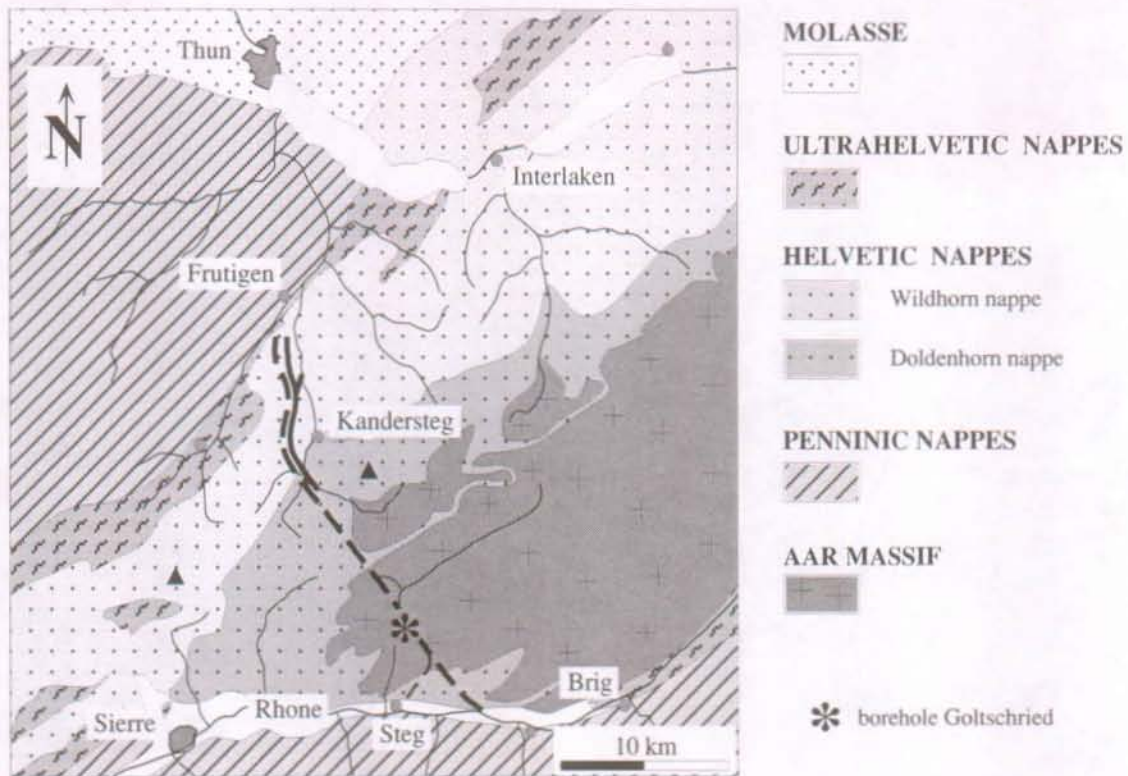


Figure 3-10: Tectonic situation of the Lötschberg railway base-tunnel. The pilot gallery crosses principally the Wildhorn nappe. "*" marks the position of the borehole "Goltschried". Simplified after Tektonische Karte der Schweiz (1980).

The undefined flysch (undefined with respect to its sedimentation realm) consists mainly of clayey to sandy marls and shales with some intercalated sandstone layers of the Taveyannaz series (Kellerhals & Isler, 1998). Due to the proximity to the basal thrust-plane of the Wildhorn nappe, a profound schistosity and intensely folded and faulted thrust slices have developed within the flysch unit and the interbedded shale and sandstone sequences.

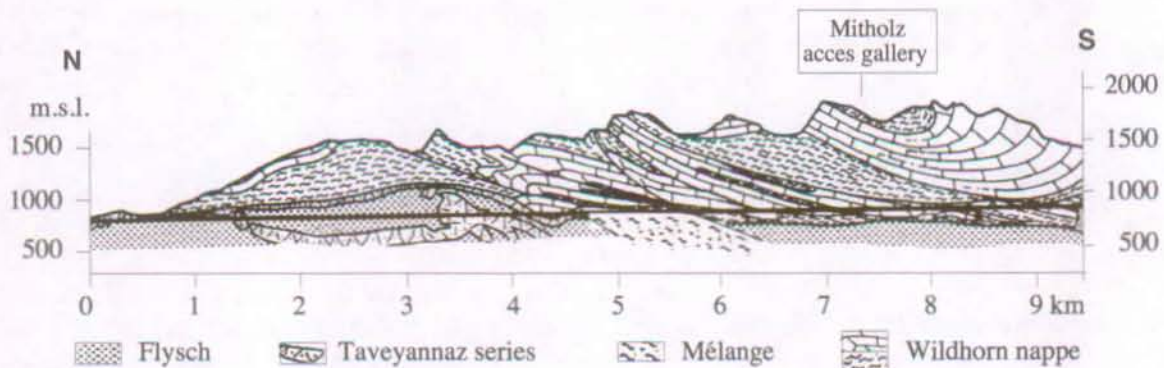


Figure 3-11: Geological profile of the pilot gallery for the Lötschberg railway tunnel after excavation. Modified after Kellerhals & Isler (1998).

The main part of the pilot gallery is located in the basal part of the Wildhorn nappe, composed principally of calcareous schists and sandstones. The nappe is divided in two levels or "stockwerk"; a underlying intensely faulted "schuppen-zone" and an overlying, open folded level. The two levels are separated from each other by weak marly (Palfries) shales, which acted as

detachment plane. Only the lower "schuppen-zone" is crossed by the gallery. Within this "schuppen-zone" several major thrust sheets can be distinguished, each of which overthrusts along the Palfries shales.

A very heterogeneous "Mélange zone" of intensely faulted and sheared schuppen was crossed below the basal thrust-plane of the Wildhorn nappe. The zone of 1 km length is composed of sheared elements of the hanging- and footwall, respectively of the Wildhorn nappe, the undefined flysch and the Taveyannaz series.

The end of the pilot gallery was defined to coincide with the tectonic contact between the Wildhorn and the flysch of the Doldenhorn nappe (Teuscher, 1997). This flysch consists mainly of irregularly alternating layers of marly to clayey schists and sandstones.

In the crystalline basement of the Aar massif, several deep boreholes were drilled to determine the persistence and nature of important tectonic shear zones on the level of the future railway tunnel. Rock samples and geological data were put at our disposal of the borehole Goltschried, drilled essentially to explore the phyllitic shear zone of Dornbach (Figure 3-10). The NE-SW striking and steeply to the SE dipping Dornbach phyllite zone is taken within chlorite-sericitic schists and gneisses of the Aar massif basement. At the level of the future tunnel the zone is some 100 m large and has shown to be ramified in two branches, with a 50 m thick wedge of intensely sheared sericitic gneisses in-between (Kellerhals & Isler, 1998).

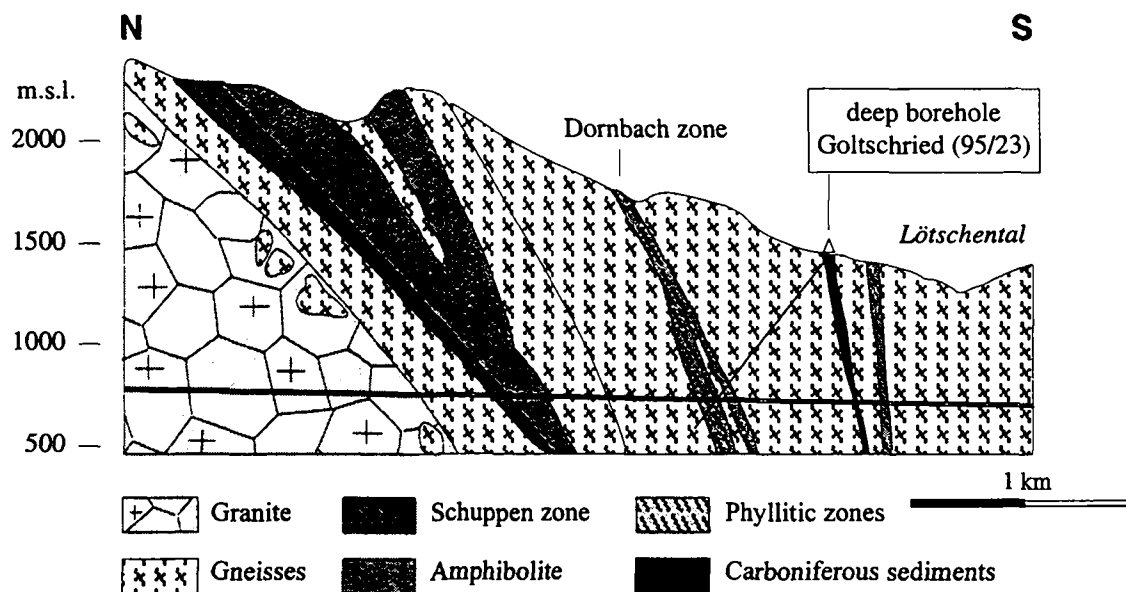


Figure 3-12: Geological profile through the Aar massif at the location of the borehole Goltschried. Simplified after Kellerhals & Isler (1998).

The southern branch of the Dornbach zone has been drilled by a triple, the northern by a double core barrel of 101 mm diameter.

3.2.3 Studied cataclastic fault zones

3.2.3.1 Lötschberg pilot gallery

Regarding the presented tectonic structure of the Helvetic nappes, important cataclastic fault zones were expected especially in proximity to the basal thrust-planes of Wildhorn and Doldenhorn nappe and along the numerous smaller thrust faults.

In contrast to these expectations, only a few minor and in general very thin kakirite zones were observed in the pilot gallery. In fact, only one kakirite bearing fault zone in the undefined flysch had an impact on the excavation of the gallery. The subhorizontal fault zone, comprising

several smaller kakirites zones of at maximum 10 cm thickness, was crossed on a length of 100 m. The rock strata of the hanging wall were gliding inside the tunnel interior which made necessary the installation of steel sets (Teuscher et al., 1998).

No important kakirites zones occurred however neither on the basal thrust-plane nor within the Wildhorn nappe. This is contrasting with the observations made in boreholes in the Gasteretal, where a 3 m thick kakirite zone was drilled on the basal thrust-plane of the Doldenhorn nappe (thrust faulted over the autochthonous sediments of the Aar massif). Along this thrust-plane still ongoing minor movements have been observed in the existing Lötschberg tunnel (Kellerhals & Isler, 1998). The pilot gallery did unfortunately not cross this basal thrust-plane as it ends at the tectonic contact between the Wildhorn and Doldenhorn nappe.

3.2.3.2 Borehole Goltschried (95/23)

The drilled gneisses of Aar massif basement in the borehole Goltschried are light grey to greenish coloured bearing small (< 3 mm) quartz grains. Foliation consist of alternating, 1 to 3 mm thick quartz/feldspar and chlorito-sericitic layers. Breaking along the foliation, the surfaces are very rough and bearing 1 to 2 mm large, dark green spots. In the Dornbach zone the schistosity surfaces are smooth and often of a soapy touch or black, polished metallic glint.

Cataclastic fault rocks have been sampled within the Aar massif basement, and in the southern and northern branch of the Dornbach Zone (Figure 3-12).

(1) Fault zone in the gneiss of Aar massif

The studied kakirite zone is 10 cm large and crosscutting the host rock foliation with a sharp contact to the host rock. It is composed of very angular, tabular rock fragments measuring up to several centimetres in a fine-grained matrix.

(2) Fault zone in the phyllitic Dornbach Zone

Kakirite zones crossed by the borhole are orientated parallel to the foliation of the host rock with an abrupt transition in-between. Small kakirites zones of 5 to 10 cm thickness have been sampled together with the host rock. The fault walls are sharp-cut and often marked by a thin, black (graphitic) layer (Figure 3-13).

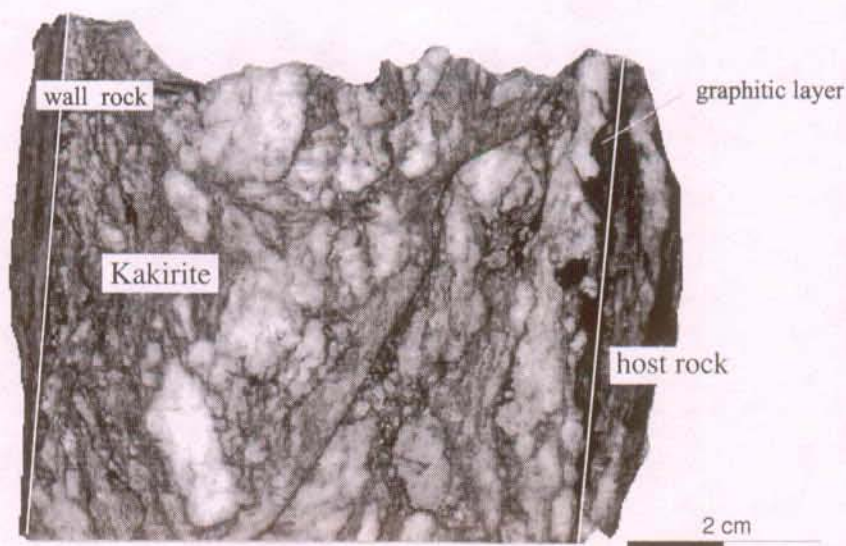


Figure 3-13: Kakirite zone from the northern branch of Dornbach zone. Note the small shear zone orientated from upper right to lower left and the schistosity-parallel abrupt transition from the host rock to the kakirite. (Polished section, sample G 8, Borehole Goltschried, 727.6 m)

3.3 FS - Genoa, Italy

3.3.1 The project

The Italian high-speed railway network is currently in planning and under construction. It comprises namely the carrying out of a N-S orientated axis between Milan and Naples, respectively a E-W axis between Venice, Milan and Turin (Figure 3-14). It is planned to connect directly the industrial centre of Milan with the harbour of Genoa-Voltri by the construction of a new high-speed railway line.

Near the city of Genoa this railway line is built mainly in the underground. In detail it involves the excavation of an about 6 km long double track tunnel (Doria and Monte Gazzo tunnel), between the harbour station Voltri and the railway station Genoa-Borzoli (Figure 3-14). The excavated cross-section of the tunnel measures about 115 m² with an inner radius of 5.2m. Connection to the existing railway network is made in three large caverns of which the largest one, the Borzoli cavern, has a maximum cross-section of 318 m². Excavation work is done by drill & blast, roadheader and hydraulic hammer. It started at the end of 1992 (Pelizza et al. 1994).

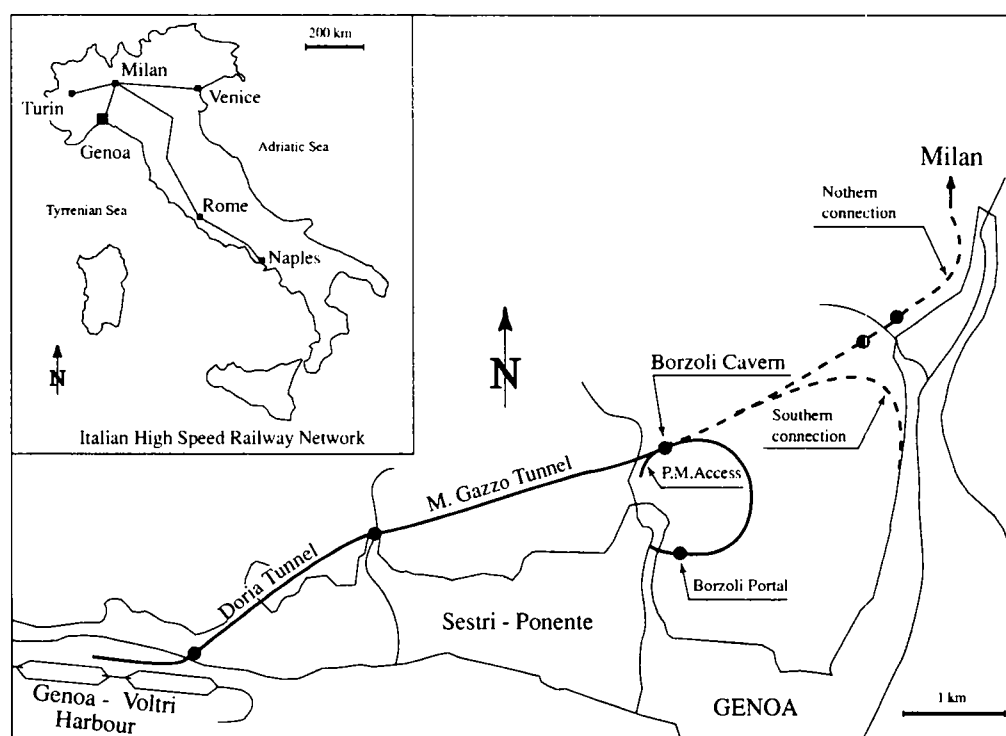


Figure 3-14: Geographic situation of the railway line connecting the new harbour of Genoa-Voltri to the high speed railway line Genoa - Milan. Fault zones have been studied in the Monte Gazzo tunnel and the Borzoli cavern. Simplified after Pelizza et al. (1994).

3.3.2 Regional and geological settings

The railway tunnel is located in a complex geological and tectonic context containing various types of lithology of different metamorphic grade. As shown in Figure 3-15, the gallery crosses the Sestri-Voltaggio fault, considered by some authors to be the tectonic contact between the different orogenic domains of the Alpine and African plates (e.g. Vanossi et al., 1984). This sub-vertical major fault zone is separating the so called *Sestri-Voltaggio Zone* in the E from the *Voltri Group* in the W. In the following only the geological units related to the studied fault rocks near the Sestri-Voltaggio fault are considered (Figure 3-15 and Figure 3-16). Geological and tectonic details are presented in Vanossi et al., 1984, Cortesogno & Haccard, 1979, Galli et al., 1979, Haccard & Lorenz, 1979.

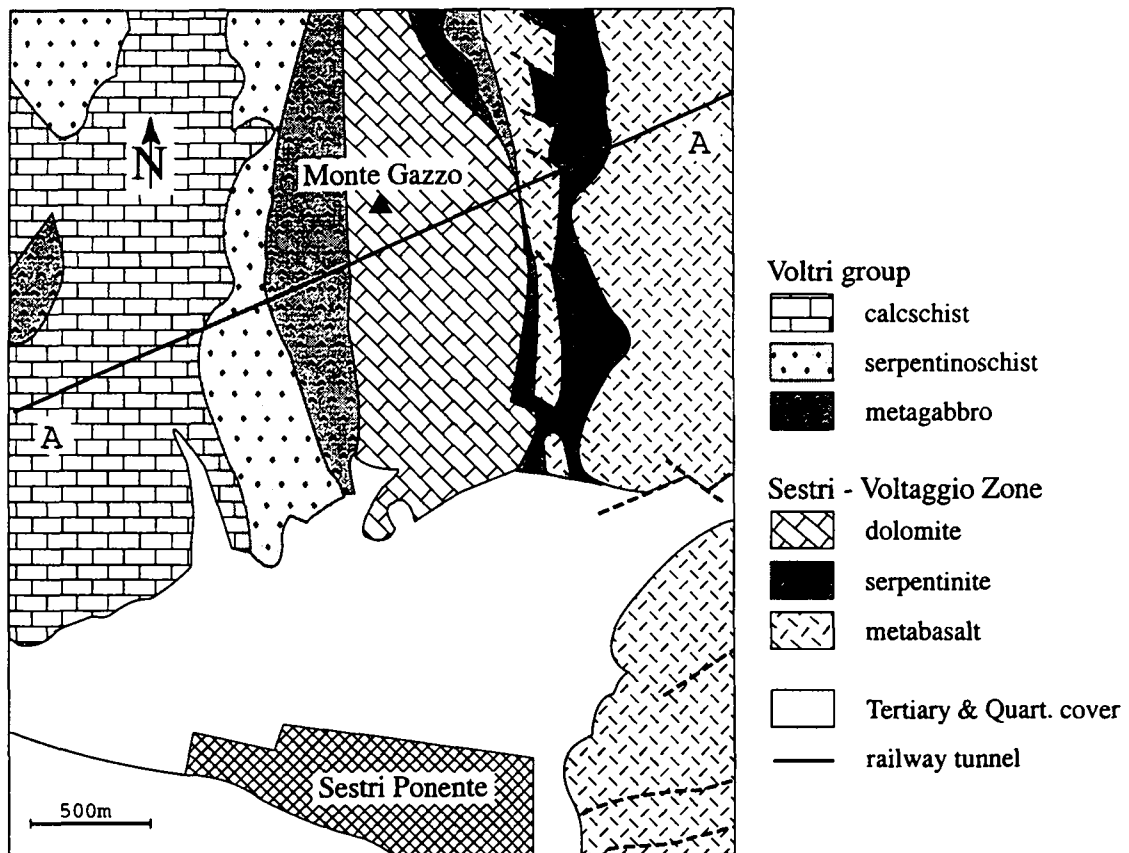


Figure 3-15: Simplified tectonic situation of the Genoa-Voltri railway tunnel. Geological profile along the tunnel (A-A) see Figure 3-16. Simplified after Cortesogno & Haccard (1985).

In the W of the Sestri-Voltaggio fault, the railway tunnel crosses the Voltri Group consisting of a large metamorphic ophiolite complex. It is composed mainly of calcschists, metagabbros and serpentinoschists. On the E of the Sestri-Voltaggio fault the gallery crosses first the Triassic Unit and enters subsequently the M. Figogna unit of the Sestri-Voltaggio Zone. The M. Figogna unit is an other metamorphic ophiolite complex, starting with metabasalt and serpentinites as shown in the geological profile below.

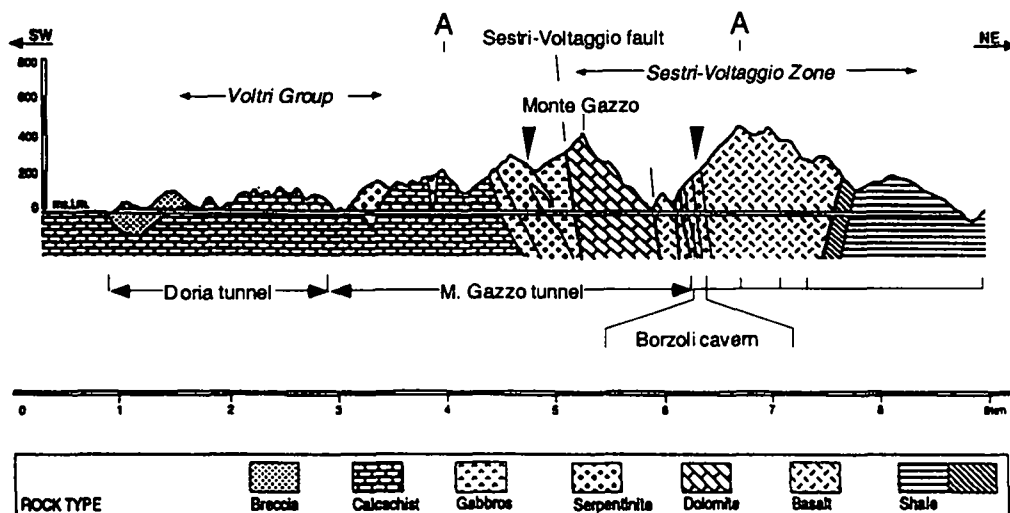


Figure 3-16: Geological profile of the Genoa-Voltri railway tunnel. Studied fault zones occurred in the Monte Gazzo tunnel and Borzoli cavern (vertical arrows). Modified after Pelizza et al. (1994).

3.3.3 Studied cataclastic fault zones

(1) Borzoli cavern

The Borzoli cavern, determined by railway alignment constraints, is located in strongly cataclastically deformed massif serpentinites and serpentinoschists near the Sestri-Voltaggio fault. Host rock at the sampling location is massif serpentinite and in minor proportions serpentinoschist. This site represents in fact the only location of the study where kakirites formed in massif host rocks could be analysed.

As shown in Figure 3-17, the kakirite zone of Borzoli cavern strikes by its structural and geomechanical heterogeneity. It is characterised by large, relatively less deformed blocks surrounded by a dense but irregularly spaced fracture network. For laboratory analyses samples of the fine-grained, respectively the weakest part of the fault zone have been taken. The observed "complex rock" structure, respectively "clast and matrix" structure is similar to that observed in kakirites at the microscopic scale (see also definition of *kakirite*, chap. 2.2.3).



Figure 3-17: Cataclastic rock fabric composed of large, relatively intact blocks of serpentinite surrounded by a crosscutting network of fine-grained kakirites. (Borzoli cavern)

The dark green coloured kakirite samples show extremely dense (spacing < 1mm), penetrative and crosscutting discontinuity networks. They are very easily crushed down by hand to homogeneously fine-grained sand fraction. Small light greenish-grey coloured veins are observed, composed mainly of recrystallised serpentine. No carbonate cementation is observed in this part of the underground site.

(2) Monte Gazzo Tunnel

Amongst other lithologies the Monte Gazzo tunnel crosses serpentinites and serpentinoschists of the Voltri Group. In contrast to the Borzoli cavern, the host rock at the sampling location is made up of schistose serpentinite comprising hard serpentinite lenses of different size, varying from macroscopic to the microscopic scale. These lenses show commonly very smooth surfaces and a great hardness contrast in comparison with the schistose matrix in-between. The schistosity is in fact formed by the preferred orientation of these lenses.

Kakirite samples from TM 5020 and 4978 are light green-greyish coloured in cleavage domains with dark green-black hard lenses with a metallic glint. Due to their structural heterogeneity, undisturbed kakirite samples were difficult to sample and prepare for analyses.

3.4 ENEL - Varzo, Italy

3.4.1 The project

The Diveria river has been exploited to produce hydroelectric energy for many decades in the Swiss and Italian part of its area. A new river power plant (Varzo II) is presently under construction in the upper part of the Val Diveria (see Figure 3-18) near the Swiss borderline. The objective of the Italian electric power company ENEL (Energia Elettrica S.p.A. Italy) is to increase the exploitation of the hydroelectric power potential of the Diveria river. The power plant Varzo II, with a net head of 250 m and a capacity of 32 MW, will replace partially the existing power stations of Iselle (net head 171m, 5.4 MW) and Varzo I (net head 36m, 4 MW). A deviation gallery for the river Diveria is presently under construction between the bordervillage Gondo and the location of the new power plant near Varzo.

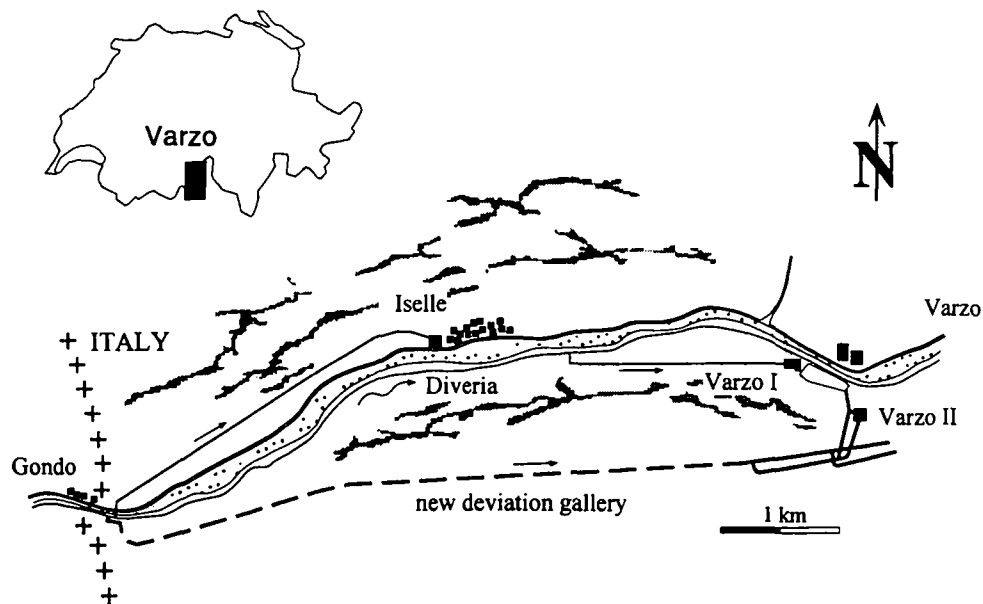


Figure 3-18: Situation of the new (Varzo II) and the existing river power plants (Varzo I, Iselle) exploiting the river Diveria. Modified after ENEL S.p.A. (1991).

The about 5.5 km long deviation gallery with a diameter of 3.9 m is excavated by a TBM in the southern slope of the Diveria valley. Excavation work started in summer 1993 with a open hard rock TBM advancing in the Antigorio gneiss at an average rate of 10 to 12 m per day. Excavation was interrupted abruptly in april 1994 after only 770 m due to major difficulties caused by the crossing of a weak cataclastic fault zone.

The installed temporary tunnel support, consisting of steel sets and locally of shotcrete, offered an exceptionally good opportunity to study the exposed rock over large parts of the tunnel. At the present time, excavation work has restarted with a new TBM.

3.4.2 Regional and geological settings

The region of Diveria valley is a highly mountainous region characterised by vertical rock faces and steeply dipping mountain slopes. It is situated in the geological context of the Lower Penninic nappes, namely from top to base the Monte Leone, Lebendun and Antigorio nappe, and of the Simplon Fault (Maurer et al., 1997, Mancktelow, 1990, 1985).

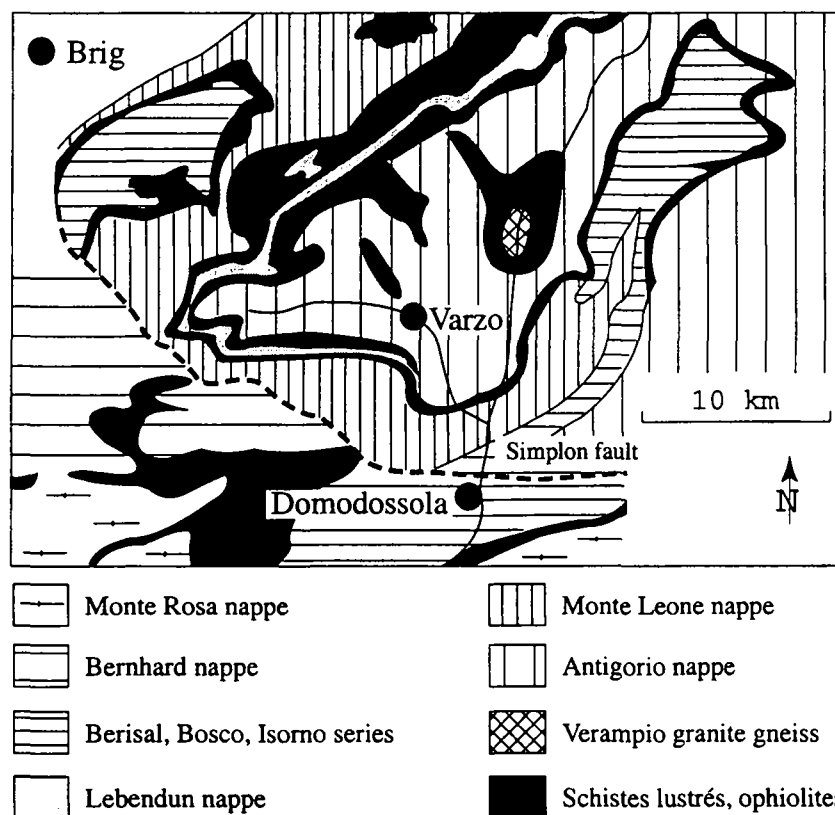


Figure 3-19: Tectonic situation of the Val Diveria region. Simplified after Laubscher & Bernoulli (1980).

The Monte Leone nappe is made up principally of a paragneissic core bearing some amphibolite and metaperidotite bodies, and its Mesozoic metasedimentary cover (Spring et al. 1992, Trümpy, 1980). It is overlaying the Lebendun nappe, which forms only a thin slice composed mainly of paragneisses and its metasedimentary cover. The lowermost nappes, the Antigorio nappe consists of a large, mainly homogeneous gneissic body of coarse to medium grained orthogneiss bearing some meta-aplite dykes and quartz or metabasic veins. Intensity of foliation is observed to increase from top to the base of the gneissic body. Three structural facies have been distinguished by the geologists of ENEL (1991), namely from top to base an almost granitic facies overlaying a typically gneissic one and finally a strongly foliated one at the base the nappe. The hydraulic gallery of Varzo II is entirely carried out in the gneisses of the Antigorio nappe.

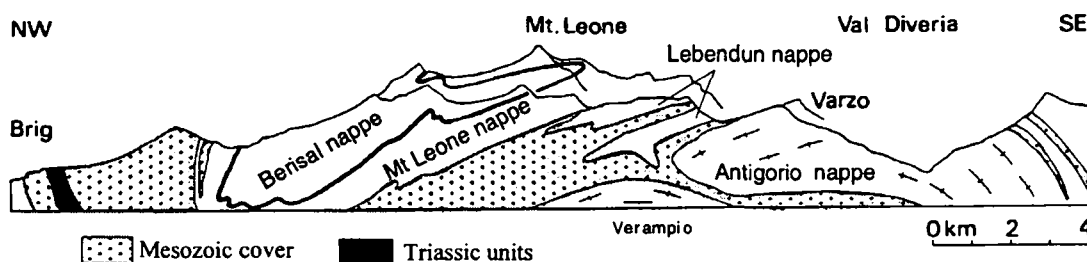


Figure 3-20: Schematic geological profile through the Simplon area. Simplified after Laubscher & Bernoulli (1980).

3.4.3 Studied cataclastic fault zones

The studied fault zone at TM 750 caused the interruption of excavation work as mentioned above. The zone is striking E-W with a dip of 55° to the S and intersecting with the gallery over a length of 20 metres at a low angle of about 15° . The passage from the intact rock into the weak, almost soil like fault zone is very sharp, no transition zone has been observed (see below). The fault zone is composed of a white-greyish granular kakirite with a ~ 1 cm thin, clay-like layer at the contact to the host rock. The thickness of the fault zone is varying between 0.5 and 1 meter at maximum.

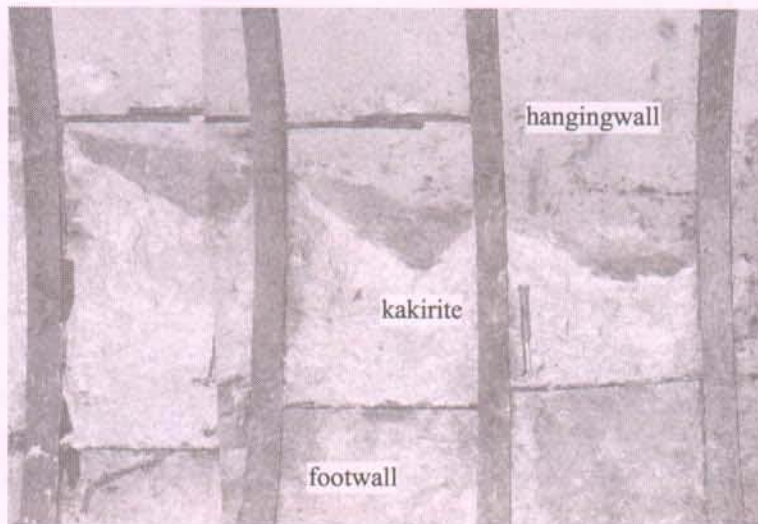


Figure 3-21: Weak, sandy kakirite zone with a very sharp contact to the host rock. Slickensides on the dark coloured, upper rock wall indicate a normal fault with downwards movement of the hangingwall in southern direction. (Gallery Varzo, TM 755)

4 THE INVESTIGATION METHODS

Cataclastic fault zones may show a very heterogeneous structural, granulometric and mineralogical composition (and hence geomechanical behaviour) on a macroscopic scale. Large blocs of intact rock can be juxtaposed to very weak, fine-grained shearzones. Such large scale heterogeneities are difficult to be represented correctly in small specimens for laboratory tests. In such cases, sampling was focused on the fine-grained shearzones, the weakest parts of fault zones respectively.

Weak cataclastic fault rocks are considered a priori to be composed of hard blocs or clasts of intact rock taken in a finer-grained, intensely ground matrix (Heitzmann, 1985). This model is valid independently of scale and can be applied for observations in the gallery as well as for microstructural analyses in thin sections. The geological and geomechanical properties of fault zones are considered to be controlled by the specific properties of the clasts (blocs), the matrix and their relative proportions and spatial distribution. As will be shown later, the proposed geological characterisation is set up mainly on the base of this two-phase "clasts - matrix" model.

4.1 General considerations

Weak cataclastic fault rocks alter very rapidly when exposed to weathering, they can be studied in general only in fresh, manmade outcrops. As weathering may affect the rock up to important depths, only underground excavations offer the opportunity to study their original geological (and geomechanical) characteristics as well as their hydrogeological behaviour under natural conditions.

For the geological characterisation, a field approach based on observations and analyses of fault zones from different underground excavation sites in the Alps has been chosen. The study of fault rocks stemming from different geological contexts and tectonic events, enables the development of a more widely applicable classification. With this objective, collaborations have been engaged with owners and contractors of different underground excavation projects.

Usual geological investigations (e.g. field observations, boreholes) for underground constructions give general prognosis about crossing fault zones. Quantity and quality of observations and sampling opportunities depend hence on the "luck" to really cross them in the chosen sites (see Löttschberg gallery).

An other limiting parameter for the study of fault zones, is excavation method and technique in unstable zones in galleries. In situ observations and rock sampling have to be organised in close collaboration with the main contractor and in function of the excavation method, available infrastructures (e.g. water, electricity, transport possibilities) and security measures.

4.1.1 Observation and sampling opportunities in galleries under construction

Rapidity of modern excavation methods and techniques at a high degree of "industrialisation", has considerably reduce the possibilities to study (fault) rocks in underground excavations. Tunnel lining is often installed mechanically and in unstable zones directly behind the tunnel face. Rock exposure, especially in the case of fault zones, is strongly limited locally and in time. Sampling of cataclastic fault zones is hence a question of being at "the right moment at the right place".

As described in chap. 3, the studied underground sites where excavated by mainly two different excavation methods: full-face tunnel boring machines and traditional method of drill & blast. Limitations of sampling opportunities offered by the two methods are briefly described below.

4.1.1.1 Excavation by drill & blast (or backhoe machine)

Excavation by blasting or backhoe machine offers quite good observation and sampling possibilities. Between the working phases of blasting (or cutting) and mucking, blocs of relatively undisturbed fault rocks can be taken in the broken material. Due to a considerable risk of instability and rockfall, it is commonly not possible to take measurements or samples directly at

the tunnel face. Newly exposed rock surfaces are furthermore rapidly covered with shotcrete for stability and safety reasons.

In earlier excavated parts of the gallery, blocs can be cut out directly of the tunnel wall by the mean of closely spaced boreholes. This requires to know exactly the position of searched fault zones and to break off the shotcrete at these locations. The method enables sampling of undisturbed rock specimens, but macroscopic structures and orientation of fault zones can rarely be observed.

4.1.1.2 Excavation by full-face tunnel boring machines (TBM)

Depending on the type of TBM and tunnel-lining, study and sampling of fault rocks is possible at different locations on the TBM, the backup train or further behind in the gallery.

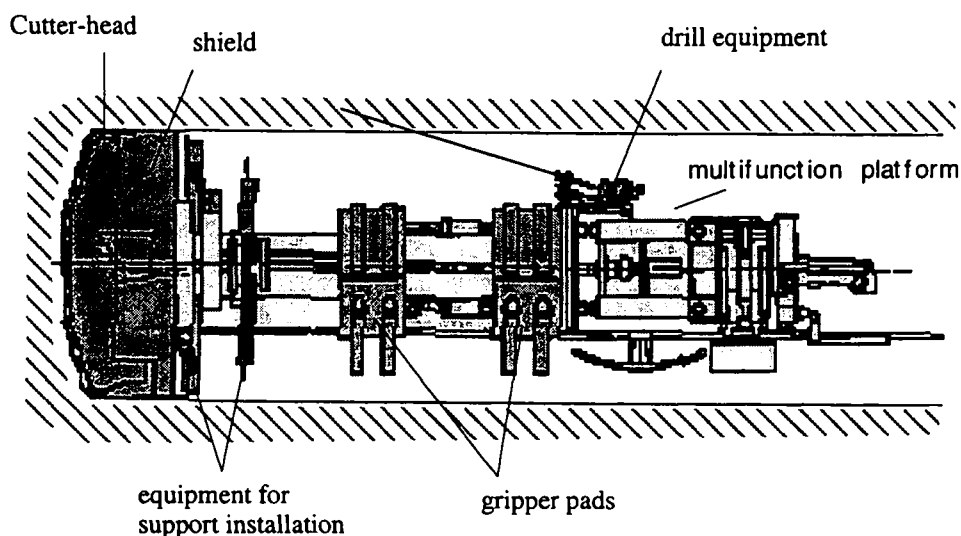


Figure 4-1: Simplified scheme of a shielded hard rock tunnel boring machine. Depending on rock quality, the tunnel lining (e.g. steel sets, shotcrete, precast concrete segments) is installed directly behind the TBM-head (see e.g. Cleuson-Dixence - unit C) or further behind on the working platform (Cleuson-Dixence - unit B).

Best opportunities are offered in underground sites where at first only a temporary tunnel support is installed, e.g. composed of rockbolts, wire meshes, steel sets, and shotcrete. Depending on the local rock quality, the different elements are built in separately or in combination. In exception of very unstable zones, tunnel support is installed on the multifunction platform on the TBM and hence samples can be taken between the TBM head and installation of support. Where the installation of loosely spaced steel sets and wire meshes in the tunnel crown is sufficient to assure the stability of smaller fault zones, sampling is possible as well on the backup train and in earlier excavated parts of the tunnel. Attention has to be paid not to take samples at the positions where the fault rock properties have been modified by the impact of the gripper pads.

When precast concrete segments are installed directly behind the head of TBM (e.g. gallery of Cleuson-Dixence - unit C), no rock surfaces are exposed during normal advancing of excavation, except in a small opening in the TBM shield. In practice, rock sampling is possible only directly in the head of the TBM, during regular or irregular stops. Based on the results of exploration boreholes (destructive drilling) in advance, maintenance stops are when ever possible planed to take place in sections of good rock quality. They are hence in general of minor interest for the study of fault rocks.

During irregular stops, when the TBM is blocked in a fault zone (Botte et al, 1996), samples can be taken in the TBM-head, in cored boreholes, behind the TBM shield, etc.. Sampling

opportunities and data about the macroscopic structures of the fault zone increase with the duration of excavation interruption and the taken measures to cross it.

4.1.1.3 Sampling fault rocks from cored boreholes

Sampling with a light core drill equipment was tested in the gallery of Cleuson-Dixence. Drilling with a single core barrel of 56 mm diameter, the effect of the rotating boring crown and the cooling water completely destroyed the weak samples and no cores were recovered. To protect the weak fault rocks from destruction, a double or even a triple core barrel would be needed. This necessitates however a much larger and heavier drill equipment, which can not be transported and installed in galleries under construction without important hindrances for ongoing excavation works.

The drilling of cored exploration boreholes (single core barrel) in advance is often considered to be too time consuming and too expensive with regard to the needed informations. In the studied excavation sites and during normal advancing, only destructive exploration boreholes were made in ahead of the TBM. Zones of poor geomechanical properties could be detected in advance by a careful evaluation of recorded drill-parameters (Detraz & Monthonnex, 1996).

4.2 Sampling techniques

Fault zones have been sampled in galleries under construction and in some core borehole samples. Corresponding samples have been taken for geological and geomechanical studies. Several sampling techniques have been used to obtain non-disturbed samples: for geological analyses, samples were cut out of weak fault zones using geological hammer and thin metal plates or a U-shaped, metallic sampler. In sites excavated by traditional methods, samples in form of blocks of several decimetre cube were taken.

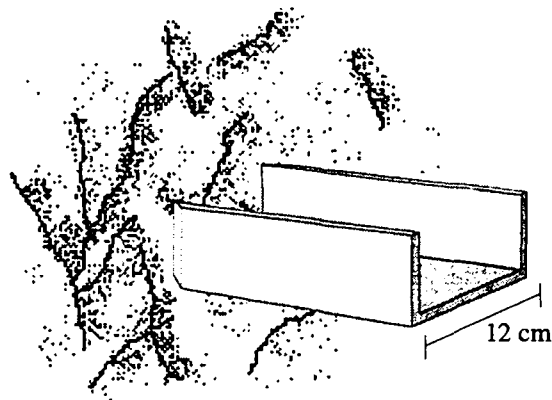


Figure 4-2: U-shaped sampler to take undisturbed material of very weak fault rocks. The sampler consists of three aluminium plates which are welded together and sharpened at one end. It is pushed into the fault rock by hand or light hammer strikes.

Samples for geomechanical tests have been taken with a specially developed portable hydraulic sampler (Habimana, 1999, Russo et al., 1998) pushing a cylindrical metallic tube into the fault rocks. This technique is specially adapted to take samples on the TBM, the backup train and in small galleries. In galleries excavated by blasting or backhoe machines, blocks measuring up to several decimetre cube were taken and redrilled in the laboratory.

4.2.1 Sample orientation

For the purposes of geomechanical tests, samples have been taken as often as possible orientated in regards of an eventually preserved local main schistosity in the fault rocks. Fault zone and

sample orientations are not put into correlation with regional structural features or tectonic events. As mentioned earlier, it is not the aim of the project to analyse the tectonic history of the studied fault zones, but to identify different types of cataclastic fault rocks and their structural characteristics. The study of tectonic history necessitate detailed regional geological studies which are beyond the bounds of the chosen approach.

4.2.2 Correspondence of samples for geological and geomechanical analyses

Geological (and especially structural) analyses and geomechanical tests could not be performed on exactly the same specimen for technical reasons. That's why corresponding samples for both parts of the study had to be taken. Although the samples were taken side by side in the studied fault zones, mineralogical and structural differences are possible due to small scale heterogeneities (e.g. presence of quartz veins, local differences in granulometry, folded schistosity, etc.).

Sampled blocks were described in the laboratory before they were sealed in concrete and resampled by drilling for geomechanical tests (Habimana, 1999). Specimens taken in the gallery with the hydraulic sampler could not be studied before they were subjected to the geomechanical tests, as they were pushed out from the sampling tube directly into the testing cell. After execution of the tests, rock fabric of the samples is in general completely destroyed. On these samples only mineralogical and, with some restrictions, granulometric analyses were still possible (see recommendations for further research, chap. 8.3).

Most geological descriptions are hence referring to the "corresponding sample", and not exactly to the one subjected to the geomechanical test.

4.3 Laboratory tests and analyses

4.3.1 Thin section analyses

Thin section analyses, using a petrographic polarising light microscope, are performed to study the fabric of cataclastic fault rocks such as, clast and matrix distribution, development of shearzones and fractures, clast morphology, textural anisotropies, etc.. Thin section scale (2.5 x 4.5 cm) is similar to common geomechanical laboratory tests. This makes the analyses appropriate for correlations between geological and geomechanical properties.

Mineralogical studies on thin sections are often limited to coarser grained fault rocks and larger clasts.

Manufacturing of thin sections of weak fault rocks necessitates previously a careful impregnation of the samples. Due to their in general very low permeability, samples can only be impregnated by special resins of extreme low viscosity. An improved impregnation technique for these rocks has been developed at GEOLEP: after drying the samples for at least 24 hours at 50°C, they are placed in a desiccator under a weak vacuum and impregnated by the force of capillarity, adding a two-component resin "drop by drop". In the case of extremely fine-grained or phyllitic fault rocks, a second impregnation (generally realised by the thin section manufacturer itself) is often necessary.

Thin sections of schistose kakirites have been orientated in a plane perpendicular to textural anisotropies, which means in general in a parallel direction to the applied load of geomechanical tests. One has however to keep in mind, that a preserved old schistosity is a priori in no direct relation with the tectonic stress orientation which gave rise to the formation of the cataclastic fault rocks. Schistosity and fault rocks may in fact have been formed during different tectonic events. Thin sections of macroscopically isotropic fault rocks are random orientated.

To enable the comparison of structural fabrics of different fault rocks, thin sections have to be analysed always at the same analytical conditions to minimise scale effects. Clasts and matrix have been analysed on the light microscope at 8x magnification. Scanned and digitalised thin section images have a resolution of 300 dpi.

4.3.2 Grainsize analysis

Samples of weak fault rocks are sieved to compare the mineralogical compositions of the different grainsize fractions and to study the clast morphology. The comparison of clast mineralogy and very fine grained matrix is of special interest. Samples are separated into the following five grainsize fractions:

- > 2 mm (gravel)
- 2 - 0.63 mm (coarse sand)
- 0.63 - 0.2 mm (medium sand) => "clast fraction"
- 0.2 - 0.063 mm (fine sand)
- > 0.063 mm (silt and clay fraction) => "matrix fraction"

The weight of the sieved samples is not always in correspondence to the quantity requested for standardised geotechnical tests (e.g. Swiss Norm SN 670800c). The analyses are therefore considered to give indications rather than the exact grainsize distribution of the fault rocks.

The air-dried samples are disaggregated first by immersion in water and treated with ultrasound before they are washed through the sieves. In order to avoid further artificial granulation of already fissured clasts, sieving is done without mechanical shaking.

4.3.3 X-ray diffraction analysis

Fault rocks are often too fine grained to permit a clear identification of their mineralogy using a normal petrographic light microscope. Thin section studies have therefore been completed with X-ray diffraction (XRD) analyses. Bulk rock analyses of fault rocks and adjacent non-deformed host rocks have been performed in order to compare their mineralogical compositions. Sieved grainsize fractions of fault rocks have been analysed to identify mineralogical differences between the clast (0.2 - 0.63 mm) and matrix fractions (< 0.063 mm). Additionally the gravel fraction (> 2 mm) has been analysed in some cases.

XRD-analyses were done at GEOLEP on a Philips Diffractometer PW 3710 mounted on a generator PW 1130 and equipped with a C-Tech Cu X-ray tube (LFF). The samples were analysed with 2θ ranging from 1 to 70° $\text{CuK}\alpha_1$. Measurement recording and treatment is done using Philips X'Pert Data Collection and X'Pert Graphics & Identify software. Phases are identified by comparing measurements with reference patterns of the ICDD PDF1 reference database.

To assure the mineralogical homogeneity of analysed fault rocks, samples of at least 200g or more were manually broken and then ground down mechanically to a grainsize of about 10 μm . Samples were prepared following the method of McCreery (1949) and the suggestions of Klug & Alexander (1974) for the preparation of random-orientated rock powders.

10 weight-% Lithium Fluoride (Griceite) was used as internal standard (Klug & Alexander, 1974). The intensity of a components pattern being proportional to its amount present in the sample (postulate of Hull), XRD-analyses permit quantitative interpretation for major rock components. The contents of quartz, plagioclase, K-feldspar, calcite and dolomite have been determined semi-quantitatively by the means of defined peak-intensity calibration diagrams.

Based on XRD and thin section analyses the non-quantified mineralogical parts have been identified to be composed mainly of phyllosilicates (see chap. 5).

4.4 The geological characterisation method

As discussed in Chap. 2, the rock mass classification systems developed for engineering purposes do not permit the required distinction of weak cataclastic fault rocks. The common "intact rock - discontinuity" approach is not appropriate to describe fault zones, which are in most cases too

large to be considered as 2-dimensional discontinuities but often too small to be distinguished as separate geotechnical units at the scale of the excavation.

For the purposes of this project, cataclastic fault zones have to be considered as distinct geological and geotechnical units. They have been studied at the macroscopic to microscopic scales: first, as regards the geomechanical and hydrogeological behaviour of cataclastic fault zones in underground sites and second, as regards their geological and geomechanical properties at the scale of hand specimens.

The macroscopic features of the studied fault zones (orientation, thickness, form, permeability, etc.) have been described in chap. 3. They depend mainly on regional tectonics and have not been included in the development of a site independent characterisation method. The presented method below is referring to the fault rock material and its geological properties at the meso- to microscopic scale. The rock fabric has been analysed on thin sections of 2.5 x 4.5 cm size, which is a similar scale as performed geomechanical laboratory tests.

To characterise weak cataclastic fault rocks two geological factors have been analysed, considering them to be the principal intern controls of mechanical properties; namely the rock fabric and the mineralogical composition.

$$\text{geomechanical properties} = f(\text{rock fabric, mineralogical composition})$$

The *rocks fabric* is defined as the spatial and geometrical configuration of all components making up a rock (Hobbs et al., 1976) which are penetrative and repeatedly developed throughout the studied rock volume. It covers the *texture* (referring to the geometrical aspects of grains composing the rock, e.g. size, shape, arrangement), and the *structure* (referring to mineralogical layering, foliation, schistosity, respectively to discontinuities s.l.).

The *mineralogical composition* is obviously one of the most important parameters influencing the properties of (fault) rocks. In order to restrain its variability, lithologies of similar mineralogical composition have been regrouped. In a first part of the project, the study has been focalised on fault zones occurred in quartzo-phyllitic series. A conceptual method, applicable to any lithology, has been tested to quantify the mineralogical compositions and its influence on mechanical properties. An interesting option has been introduced by Calembert et al. (1980a) on the basis of the Vickers hardness.

4.4.1 The clasts - matrix model

Proceeding from the definition by which weak cataclastic fault rocks are composed of rock and crystal fragments caught in a fine-grained matrix (see chap. 2), their characterisation has been based on a "*clast - matrix*" model. The mechanical properties are supposed to be controlled by the combined properties of the remaining intact rock fragments and the finely ground matrix material respectively. Applying this model, weak cataclastic fault rocks can be classified between two opposite sub-types: on the one side the kakirites of which the behaviour is controlled uniquely by the properties of the clasts ("*clast controlled*") and on the other side the kakirites of which the behaviour is solely controlled by the properties of the matrix ("*matrix controlled*").

The chosen approach enables to identify and quantify independently from each other the textural, structural and mineralogical properties of the clasts and the matrix. The developed method is described in detail below.

4.4.2 The rock fabric characterisation

The influences of texture elements on mechanical properties have been studied by different authors: negative linear correlations have been reported to exist between grain size and rock strength, respectively positive ones between grain packing density and rock strength (Onodera & Kumara, 1980, Hugman & Friedman, 1979, Bell, 1978, Olsson, 1974). Howarth & Rowlands

(1986) have developed a method by which several rock texture elements are characterised and assembled in a quantitative way (chap 4.4.2.1) in order to assess the rock strength of intact rocks.

The second type of fabric elements, the structural discontinuities, are not taken into consideration by the texture coefficient of Howarth & Rowlands (1986). Especially as regards cataclastic fault rocks in schistose rocks, pre-existing discontinuities s.l. control considerably the rock strength and behaviour. In analogy to the texture coefficient of Howarth & Rowlands (1986), a matrix coefficient (MC) has been developed in order to quantify the discontinuity properties (chap. 4.4.2.2). The matrix coefficient involves the density, roughness, mean length and orientation of the discontinuities.

4.4.2.1 The Texture Coefficient TC

The *Texture Coefficient (TC)* of Howarth & Rowlands (1986) has been developed in order to assess the geomechanical properties of intact rocks by quantitative analyses of rock the texture. The coefficient is defined on the basis of three grain parameters: the grain-shape (elongation and circularity), the grain-orientation and the grain-density, respectively the relative proportion of grains and matrix. Correlations of various significance have been reported with rock strength, percussion and diamond drilling rates for magmatic, metamorphic and sedimentary rocks (Ersoy & Waller, 1995, Azzoni et al., 1992, Howarth & Rowlands, 1987, 1986). For these rocks the TC values are varying between 0.5 and 3.0, corresponding to a low, respectively a high rock strength.

The uniaxial compressive strength is not an appropriate parameter to characterise the mechanical properties of weak cataclastic rocks. The TC has been used in this study to evaluate their mechanical performance in a larger sense.

The TC as defined by Howarth & Rowlands (1986) is:

$$TC = CD \left[\left(\frac{N_0}{N_0 + N_1} \cdot \frac{1}{FF_0} \right) + \left(\frac{N_1}{N_0 + N_1} \cdot \overline{AR}_1 \cdot AF_1 \right) \right] \quad (\text{Eq. 4-1})$$

where

- TC: Texture Coefficient, dimensionless
- CD: Clast Density
- N_0 : number of isometric clasts (aspect ratio < 2.0)
- N_1 : number of elongated clasts (aspect ratio > 2.0)
- FF_0 : mean Form Factor of isometric clasts
- \overline{AR}_1 : mean Aspect Ratio of elongated clasts
- AF_1 : Angular Factor of elongated clasts

The first term of Eq. 4-1 deals with the elongation of *non-elongated* or isometric clasts, whereas the second one takes into account the elongation of *elongated* clasts and their preferred orientation respectively.

Attempt has been made to enlarge the application of the texture coefficient to weak cataclastic fault rocks. Definition and calculation of clast length and breadth (involved in the calculation of the aspect ratio and form factor) and clast density are slightly differing from the original propositions of Howarth & Rowlands (1986). The modifications where necessary in order to improve the accuracy and objectivity of measurements when dealing with the texture of weak cataclastic fault rocks.

(1) The clast shape

Clasts have been defined as fragments of rock or minerals which by their grain size can clearly be distinguished from the surrounding, finer-grained matrix. They have been identified visually on thin sections using a light microscope at a standardised magnification (8x). Keeping their correct spatial distribution, their contours are manually outlined and copied on paper. After scanning the copy into a computer, the clasts are measured automatically using the NIH Image™ 1.61 image analysing software.

The automatically measured clast parameters are:

- the clast area
- the clast perimeter,
- the lengths of major and minor axes of best fitting ellipse,
- the angular orientation (α) of major axis to a chosen reference line
- the total clast area per reference area.

Areas and perimeters are measured directly on the clasts, whereas axes lengths and orientation are properties of the best fitting ellipses (see explanations below). Measurements are made in pixels and are recalibrated by real length measures (in mm) made directly on thin sections. The clast shape parameters in Eq. 4-1 are provided with an index in function of whether they concern only the elongated (index = 1) or only the isometric grains (index = 0).

Many different means are proposed in literature to characterise the shape of particles. The methods are in general based on measurements of Feret's diameters (Fernelund, 1997, Howarth & Rowlands 1987, a. o.), Fourier's series (Beddow et al., 1980), dynamic shape parameters (Medalia, 1970), or combinations of the former (Pirard, 1994). A variant of the ellipse¹ of inertia (Medalia, 1970), has been chosen to characterise the shape of clasts. The "best fitting ellipse" is defined to have the same centroid and moments of inertia as the given clast. The ellipse size is furthermore adjusted in order to have the same area. Length and breadth of clasts are determined indirectly by measuring the principal axes of the best fitting ellipses. When visually controlling the clast shapes and fitted ellipses, the method proves to give, in general, highly consistent results. The physical significance of ellipse axes, as well as that of Feret's diameter, is however obviously less evident for complex clast shapes, e. g. in the case of strongly re-entrant contours (see Figure 4-3). It is this a common difficulty of shape characterisations dealing with terms like particle "length" and "breadth".

Compared with the Feret's diameter, the physical signification of the axes of the best fitting ellipse are judged to be more meaningful parameters to characterise the clast length and breadth. The orientation of the major ellipse axis is furthermore clearly in a better correspondence with the (visually determined) clast orientation as shown below (see also Pirard, 1994).

¹ As mentioned earlier, schistose rocks and cataclastic fault rocks are formed under different tectonic conditions. Schistosity is issue of a ductile, dynamo-metamorphic deformation, of which the strain and strain orientation can be expressed by the means of a strain ellipsoid. The studied form and orientation of clasts in cataclastic fault rocks, and their corresponding best fitting ellipses, must however not be confused with a strain ellipsoid. Besides strain orientation and intensity, the form and elongation of the clasts is influenced by many other parameters such as mineral-properties and mineralogical layering, schistosity, etc.. There is a priori no simple correlation between the observed clast form and the hypothetical strain ellipsoid of the cataclastic event.

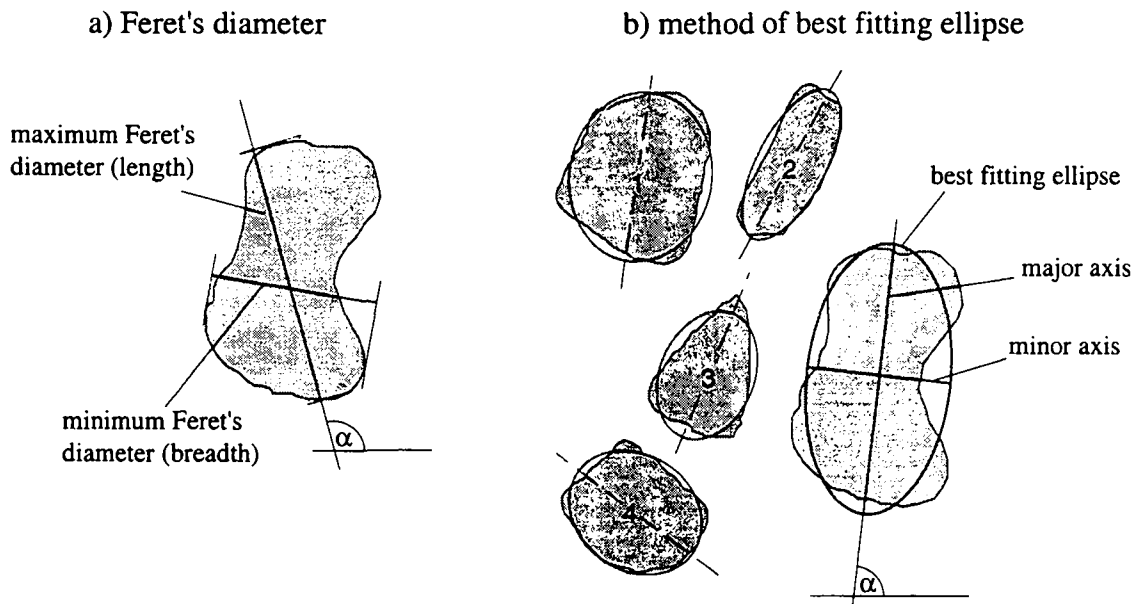


Figure 4-3: Measuring clast parameters by the means of Feret's diameter (a) and best fitting ellipse (b). The measured parameters are mainly differing with regard to the clast orientation (α).

The *Aspect Ratio (AR)* is defined as the ratio of major to minor axis of the best fitting ellipse. Elongated grains have an aspect ratio larger than 2.0. The mean aspect ratio (\overline{AR}_1) of Eq. 4-1 is calculated only for elongated grains. The AR is a dimensionless parameter varying between 1.0 and ∞ .

$$AR = \frac{\text{major axis}}{\text{minor axis}} \quad (\text{Eq. 4-2})$$

The *Form Factor (FF)* is a measure of a grain's deviation from circularity (by elongation and roughness) and defined as the ratio of the grain area to its perimeter square. It is multiplied by 4π to be equal to unity for a perfect circular particle. The mean form factor (FF_0) is calculated only for "non-elongated" grains of an AR smaller than 2.0.

$$FF = 4\pi \frac{\text{clast area}}{(\text{clast perimeter})^2} \quad (\text{Eq. 4-3})$$

Considering smooth particles of perfect circular or elliptic shape ($1 \leq AR \leq 2.0$), the FF_0^2 is varying between 1.0 and 0.8, respectively between 1.0 and 1.2 for the inverse term.

² For: ellipse area = $\pi a b$, ellipse perimeter $\approx \frac{\pi}{2} \cdot [3(a+b) - 2\sqrt{a \cdot b}]$ and $a = 2$, $b = 1$.

(2) The clast orientation

The *Angle Factor (AF)* is a quantitative assessment of the (preferred) orientation of clasts. For its calculation only elongated clasts with an aspect ratio > 2.0 are taken into account. The angular difference of major axis orientation is calculated between each and every elongated clast. The differences are sorted in nine orientation classes with interval widths of 10° and ranging from 0° to 90°. Each class is weighted by a factor *i* varying from 1 for the first class (0°-10°) to 9 for the last class (80°-90°). The angle factor is then calculated as:

$$AF = \sum_{i=1}^9 \left[\frac{X_i}{\frac{N_1(N_1-1)}{2}} \right] \cdot i \quad (\text{Eq. 4-4})$$

where

- X_i : number of angular differences in the class *i*.
- N_1 : number of elongated clasts with an aspect ratio > 2.0
- i*: weighting factor and class number

AF is a dimensionless parameter varying between 1.0 for perfectly parallel and 5.0 for completely randomly orientated grains. In order to have a similar weight as the other texture parameters, the value of AF is divided by five ($AF_1 = AF/5$) before introduced in Eq. 4-1. It is hence varying between 0.2 for parallel and 1.0 for randomly orientated clasts. After Howarth & Rowlands (1987) a minimum of 30 to 50 clasts have to be analysed in order to get a non-biased AF.

(3) The clast density

The *Clast Density (CD)*, or degree of clast packing, is defined as the total clast area per unit area and expressed in percentages.

$$CD = \emptyset \left\{ \sum_{n=1}^{10} \frac{\text{total clast area } (n)}{\text{ref. area } (n)} \right\} \quad (\text{Eq. 4-5})$$

The definition of the reference area was adapted in order to increase the objectivity and accuracy of the clast density measurements. In practice, the definition of the reference area by contouring the clasts as proposed by Howarth & Rowlands (1986), has proved to be quite ambiguous, especially in the case of loosely dispersed clasts in fault rocks. In these cases, the reference area boundary can not be defined in an unequivocal way (see Figure 4-4a). As the CD is directly introduced in Eq. 4-1 as weighting factor, it is important to determine this parameter in an accurate, unambiguous and reproducible way. The clast density is therefore measured in a "sliding reference area" of unit area, which is placed randomly within the image boundary for repeated measurements. The CD of Eq. 4-1 is calculated as the mean value of the individual density measurements.

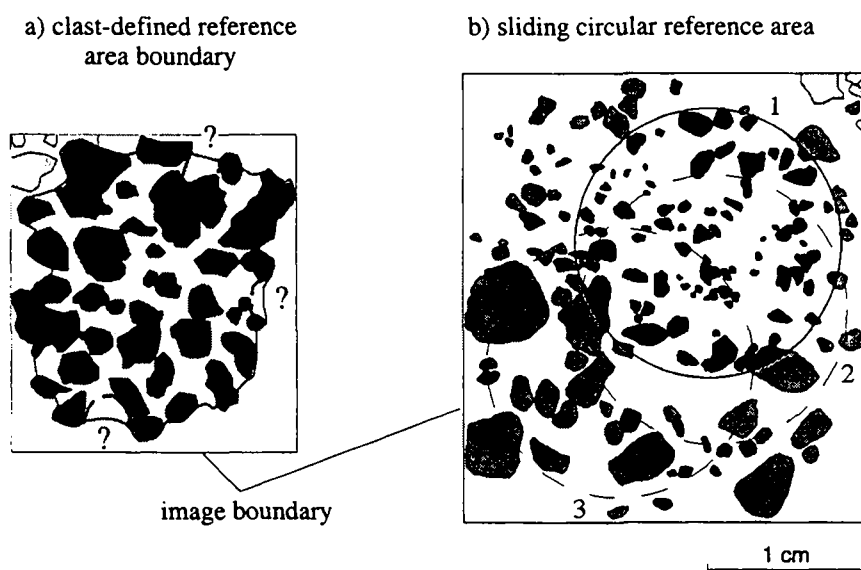


Figure 4-4: Clast density measurements: a) The reference area boundary as proposed by Howarth & Rowlands (1986) is defined by contouring the clasts. b) A circular reference area of 1 cm² is displaced randomly within the image boundary to determine an average clast density. In both methods, the clasts touching the image boundary (light grey shaded) are not taken into consideration for the measurement.

The influence of the four clast shape parameters on rock strength and the TC (Eq. 4-1) can be summarised as follows:

clast parameter	rock strength	TC	
$\overline{AR}_1 \cdot AF_1$ ↗	↗	↗	(i)
FF_0 ↗	↘	↘	(ii)
CD ↗	↗	↗	(iii)

(i) and (iii): Rock strength increases when clasts form a kind of "reinforcement". This becomes obviously more important with increasing clast density, respectively the more the clasts are elongated (\overline{AR}_1) and the more the angular differences (AF) they form are high.

(ii): The effect on rock strength is exactly the same but less important as clasts are more isometric. By its definition the FF_0 decreases as the clasts become more elongated ($AR_{max} < 2.0$) hence, in order to maintain the continuity of the TC its inverse is introduced in Eq. 4-1.

4.4.2.2 The matrix coefficient MC

Analysis of matrix is focused on the identification of structural discontinuities, e.g. preserved old schistosity, foliation, fissures, joints, etc., which represent pre-existing, potential shearzones diminishing further the mechanical strength of cataclastic fault rocks. As a general rule, the length of discontinuities to be considered has to exceed a single grain boundary, with exception for isotropic cataclastic fault rocks. In the given context, crystal - grain boundaries in intact (host) rocks are hence not considered as discontinuities.

The traces (*trace lines*, T_L) of the identified discontinuities are copied from thin sections to paper and digitalized for further treatment. The following parameters are determined: the

discontinuity-length, -roughness, -density and -orientation. These parameters have been assembled in a *matrix coefficient (MC)* as follows:

$$MC = \frac{R_L}{T_{Ld} \cdot \bar{T}_{LL}} \cdot \frac{1}{\delta} \quad (\text{Eq. 4-6})$$

where

- MC: Matrix Coefficient [-]
- R_L : linear roughness [mm/mm]
- \bar{T}_{LL} : mean trace line length [mm]
- T_{Ld} : trace line density [mm/mm²]
- δ : orientation factor [-]

The matrix coefficient is defined in correspondence with the TC (Eq. 4-1) in order to show increasing MC-values for samples of increasing rock strength. Below are presented the four involved discontinuity parameters in more detail. The assembling of Eq. 4-6 and the weighting of the individual parameters is discussed in chap. 4.4.2.2(4).

(1) The discontinuity roughness

The *linear roughness (R_L)* (Pickens & Gurland, 1976) is defined as the ratio of the *trace line length (T_{LL})* to the *projected length (L')* (Figure 4-5). L' is defined as the straight line connecting the end-points A-B of the trace line. R_L is expressed in [mm/mm].

$$R_L = \frac{\text{length of trace line}}{\text{length of projected trace line}} \quad (\text{Eq. 4-7})$$

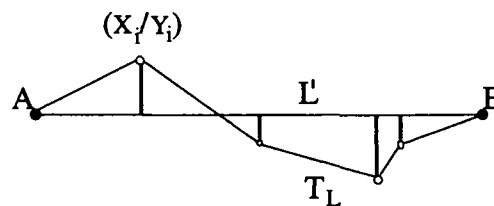


Figure 4-5: The discontinuity trace lines are digitalized in discrete segments. The linear roughness is calculated as ratio of the true trace line length (T_{LL}) to the length of the projected trace line (L').

(2) The trace line density

The *trace line density (T_{Ld})* is defined as the mean total trace line length (T_{LL}) per unit area. In analogy to the clast density (see Figure 4-4) it is determined as the mean value of several measurements performed in different reference areas of one centimetre square. In fact, it is determined by measuring pixels (black) in the reference area (white). By calibration, the number of black pixels is transformed into the total trace line length (T_{LL}). This proceeding is obviously

only appropriate if all the digitalized trace lines are of a homogeneous and consistent thickness. The samples have therefore been analysed at a standardised image resolution (300dpi) and discontinuity thickness of 1 pixel. The T_{Ld} is expressed in [mm/mm²].

$$T_{Ld} = \varnothing \left\{ \sum_{j=1}^{10} \frac{tT_{LL(j)}}{\text{ref. area } (j)} \right\} \quad (\text{Eq. 4-8})$$

where

T_{Ld} : mean trace line density [mm/mm²]

$tT_{LL(j)}$: total trace line length in the reference area j [mm]

(3) The orientation of trace lines and structural (an-) isotropy

The *orientation* (β) of the trace lines has been measured as the angle between a chosen reference line and the linear regression line (L_{RL}). The later is calculated for each trace line by the method of the least squares. As shown in Figure 4-6, the orientation of the regression line L_{RL} and of the projected line L' may be differing from each other. The angle (β) has finally be retained as it represents more accurately the general orientation of the trace line.

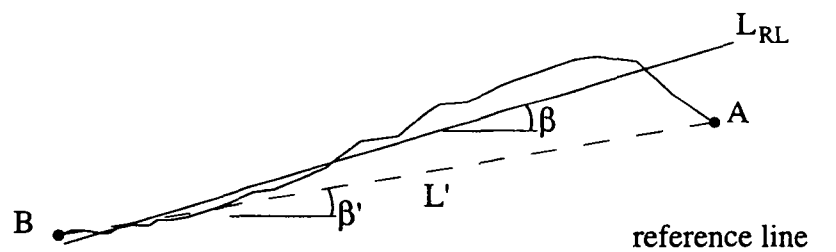


Figure 4-6: The orientation of the trace line is measured as the angle (β) between a chosen reference line and the regression line L_{RL} . As the orientation of L' is determined only by the position of the end-points, it does often not represent correctly the orientation of the trace line.

The rock strength reducing effects of structural anisotropies have been treated recently by Hoek & Brown (1997a). They show that if the number of discontinuity sets increases, the overall rock strength reduction tends to become more and more isotropic. The (theoretical) superposition of four discontinuity sets orientated at 45° to each other e.g. reduces the compressive strength of a sample nearly independently of the σ_1 -orientation relative to the discontinuity sets (Figure 4-7). For engineering design purposes in underground constructions Hoek & Brown (1997a) suggest to consider rock masses with four or more discontinuity sets to have an isotropic rock strength behaviour.

The theoretical effects of superposed multiple discontinuity sets on uniaxial compressive strength have been confirmed by Al-Harhi (1998) testing sandstones with two perpendicular discontinuity sets (bedding planes and microfissures).

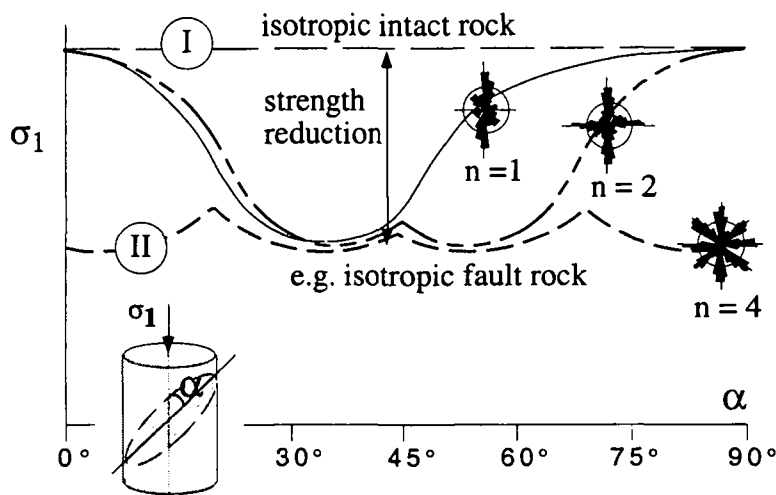


Figure 4-7: Rock strength reducing effect of multiple discontinuity sets. In the case of four discontinuity sets ($n=4$), rock strength reduction is nearly independent (isotropic) of the σ_1 -orientation with regard to that of the discontinuity sets. In the context of this research one can consider (I) to represent the strength level of intact, isotropic host rocks, whereas (II) represents the one of isotropic cataclastic fault rocks. Modified after Hoek & Brown (1997a).

To characterise accurately the structural anisotropy of a rock sample one has to take into consideration not only the orientation but also the variable lengths of the single discontinuities (Figure 4-8).

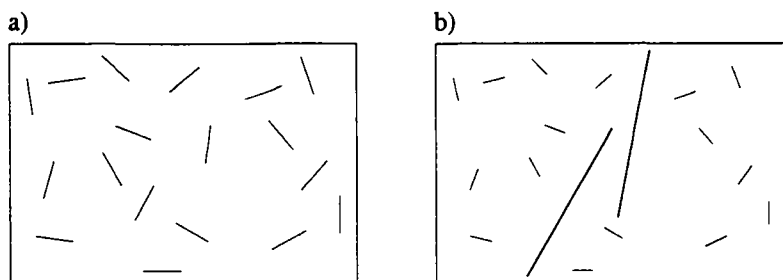


Figure 4-8: Both rock fabrics (a, b) are equal by the number of trace lines, the total trace line length and the (random) orientation of the trace lines.

By the following approach, an attempt has been made to define and express the structural (an-) isotropy of a rock by means of a single parameter taking into account the number of discontinuities, their individual length and (preferred) orientation. In a first step the orientations of the discontinuities have been measured in respect to a reference line ($\pm 90^\circ$) as shown in Figure 4-6. Discontinuities have then been sorted by their orientation in 18 classes of 10° wide and the trace line lengths have summed up in each class. The cumulative trace line lengths are plotted in a rose diagram once the 18 classes are completed symmetrically in order to have 36 classes of 10° wide (Figure 4-9). The individual discontinuity sets and their orientation are determined visually.

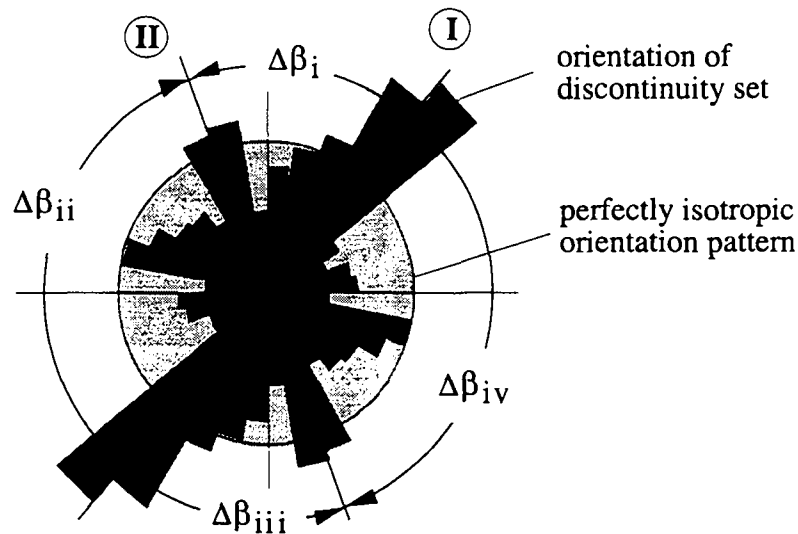


Figure 4-9: Rose diagram presenting the cumulative trace line length in each class of 10° wide in percentages of the total trace line length of the sample. The angles $\Delta\beta_i$ and $\Delta\beta_{ii}$, respectively $\Delta\beta_{iii}$ and $\Delta\beta_{iv}$ are measured in-between the two visually determined discontinuity sets (I, II).

In the case of a perfectly isotropic discontinuity distribution, the cumulative trace line length in each class is equal to 1/36th, respectively to 2.8% of the total trace line length. The resulting rose diagram is a plain circle with a radius corresponding to 2.8% as shown in Figure 4-9. In practice, discontinuity sets have been taken into consideration if the largest petal(s) exceeds the theoretical isotropic pattern, respectively the circle of 2.8%. Exceeding this limit, the influence of the different discontinuity sets on rock strength is considered to be equal, regardless of their intensity (petal size).

Identification of discontinuity sets as presented above takes into consideration the orientation and length of the individual discontinuities. In the next step the orientation of the discontinuity sets relative to each other is to take into account by measuring the angles $\Delta\beta_i$ (Figure 4-9). As the petals of the rose diagram are 10° wide, discontinuity sets with angle differences of $\Delta\beta_i \geq 20^\circ$ can be distinguished. A consistent method to transform the relative orientation of discontinuity sets in a scalar value has been found by forming the product of the measured angles $\Delta\beta_i$ as follows:

$$\delta = \frac{\log(\Delta\beta_i \cdot \Delta\beta_{ii} \cdot \Delta\beta_{iii} \cdot \dots \cdot \Delta\beta_{2n})}{\log(360)}, \quad \text{for } \sum_i^{2n} \Delta\beta_i = 360^\circ \quad (\text{Eq. 4-9})$$

where

δ : orientation factor [-]

$\Delta\beta_i$: angle measured between discontinuity sets [°degrees]

n : number of discontinuity sets.

The product of $\Delta\beta_i$ is divided by the $\log(360)$ in order to normalise δ for a perfectly isotropic discontinuity distribution ($\Delta\beta_i = 360^\circ$, $\delta = 1.0$). The variability of δ in function of the number of discontinuity sets and their relative orientation is presented in Table 4-1. It can be shown that δ increases monotonously with increasing angle(s) $\Delta\beta_i$ and that the range of δ for a given number (n) of discontinuity sets does not overlap with the ranges of $(n+1)$ or $(n-1)$.

number of disc. sets (n)	orientation factor δ
0	1.0
1	1.8
2	2.7 - 3.1
3	3.7 - 4.2
4	4.7 - 5.2
5	5.6 - 6.9

Table 4-1: Calculated range of orientation factor δ in function of the number of discontinuity sets and the angle(s) formed by the discontinuity sets ($\Delta\beta_i$). Discontinuity sets of a minimum angle difference of $\Delta\beta_i \geq 20^\circ$ are distinguished. For a given number (n) δ increases monotonously with $\Delta\beta_i$.

As shown above, the major "steps" of the orientation factor δ depend on the number of discontinuity sets. Within the range of a given number n, δ increases monotonously but in a less important way.

(4) The combination of the MC parameters

$$MC = \frac{R_L}{T_{Ld} \cdot \bar{T}_{LL}} \cdot \frac{1}{\delta} \quad (\text{Eq. 4-6})$$

The discontinuity parameters presented above have been put together with the conception to define, in analogy to the texture coefficient of Eq. 4-1, an increasing matrix coefficient (MC) for samples of increasing rock strength. The following theoretical considerations have lead to the definition of Eq. 4-6: In a general way, the rock strength is reduced the more the density of pre-existing discontinuities in a rock sample is high and the more the individual discontinuities are persistent. Rock strength is reduced further (homogeneously) as the number of discontinuity sets forming high angles ($\Delta\beta_i$) increases (see Figure 4-7). In contrast, shear strength reduction is less important the more the discontinuity surfaces are irregular. Based on the preceding reflections, the discontinuity roughness (R_L) has been placed in the numerator of Eq. 4-6 and the trace line density (T_{Ld}), the mean trace line length (\bar{T}_{LL}) and the orientation factor (δ) in the denominator.

The influence of R_L , T_{Ld} , \bar{T}_{LL} , δ and the number of the discontinuity sets on rock strength and the MC can be summarised as follows:

discontinuity parameter		rock strength		MC
R_L	↗		↗	↗
T_{Ld}	↗		↘	↘
\bar{T}_{LL}	↗		↘	↘
δ	↗		↘	↘

The influence of the individual discontinuity parameters on the MC is shown in a quantitative way in the following schematic discontinuity patterns. Every single parameter has been varied separately, keeping the other three fixed.

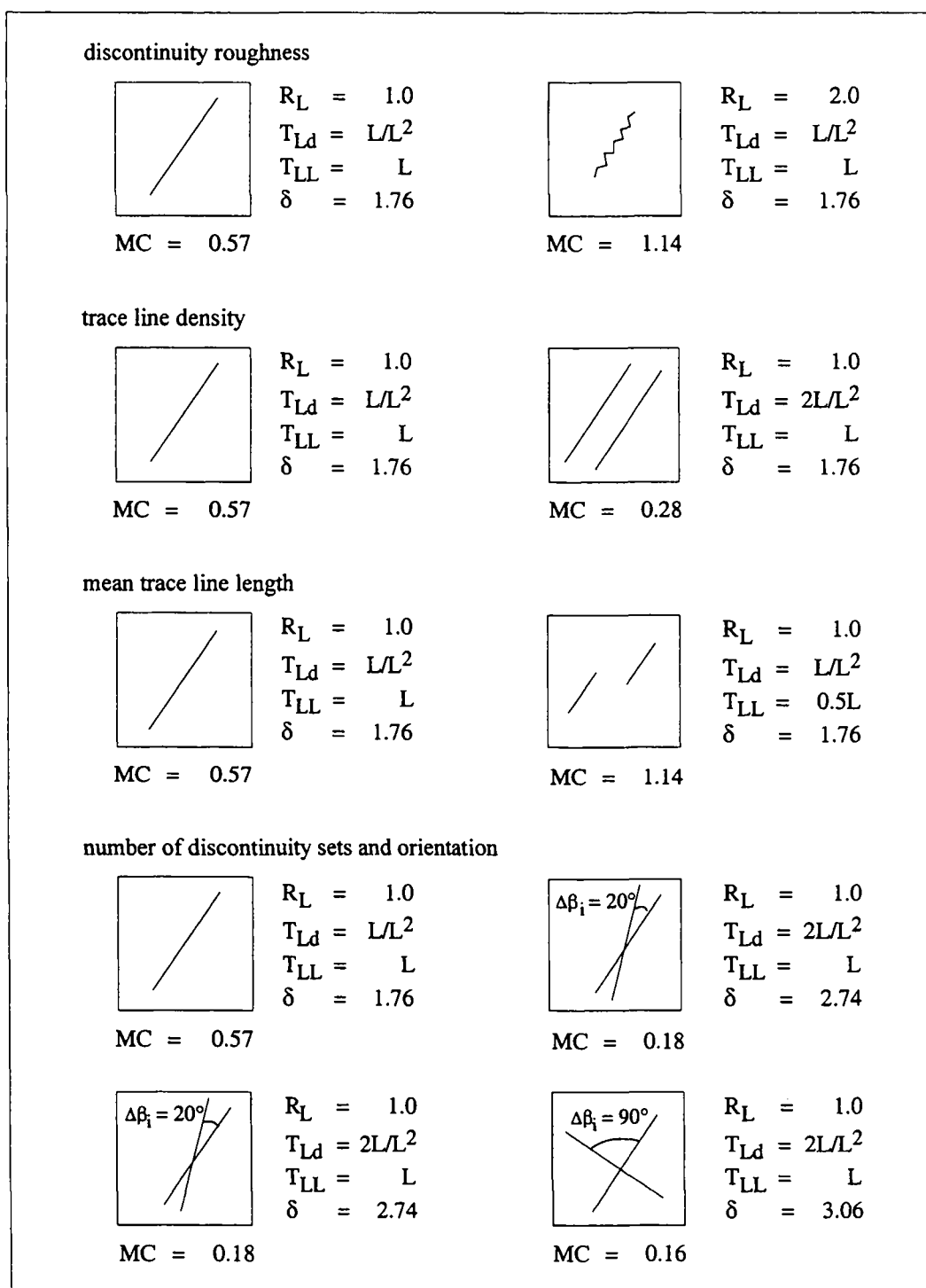


Figure 4-10: Schematic discontinuity patterns illustrating the influence of the involved discontinuity parameters on the MC.

With regard to the observed rock fabrics of analysed fault rock samples, the definition of the MC at the transition between anisotropic and isotropic cataclastic fault rocks has to be discussed more in detail. As shown in Figure 4-7 there exist two "levels" of isotropy: rock fabrics (respectively

strength behaviour) are isotropic in samples without any discontinuities, as e.g. in the case of some intact host rocks. Rock fabrics are most anisotropic in rocks with one dominant discontinuity set and become isotropic again with an increasing number of discontinuity sets. These two "kinds of isotropies" correspond to the two isotropic strength levels (I), respectively (II) presented schematically in Figure 4-7.

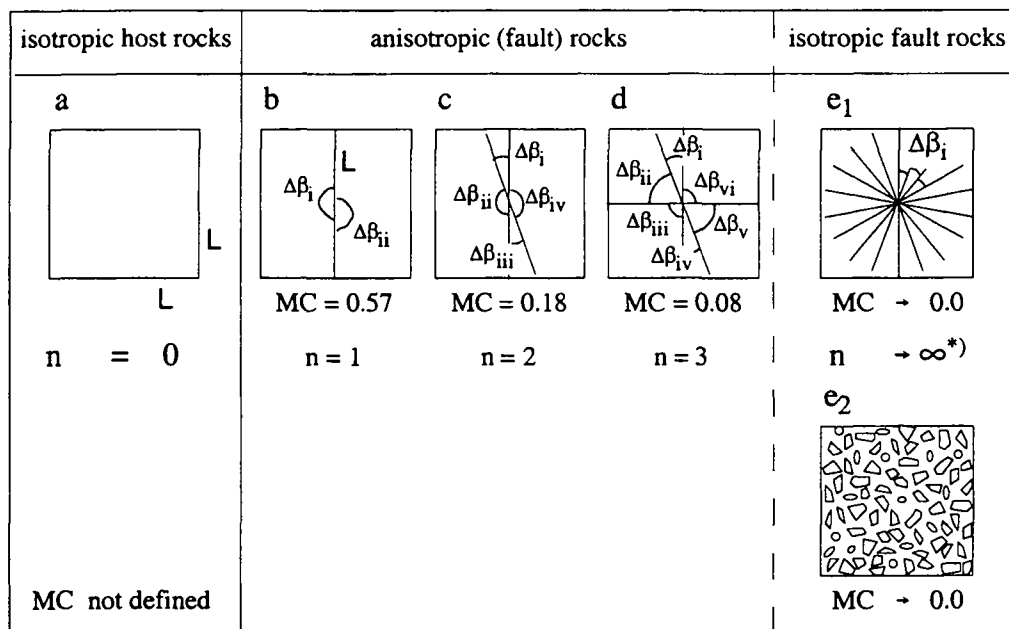


Figure 4-11: Schematic discontinuity patterns showing the evolution of the MC in function of an increasing number of discontinuity sets and related increase of isotropy. The letters (a) and (e₁) refer to the case of isotropic host rock, respectively isotropic fault rock as shown in Figure 4-7. *) In practice the number of discontinuity sets is limited at max. to $n = 9$, since only sets with $D_{bi} \geq 20^\circ$ can be distinguished. In the case of isotropic cataclastic fault rocks (e₂) the clast boundaries are considered as discontinuities of random orientation.

	isotropic host rock	anisotropic fault rock			isotropic fault rock	
	a	b	c	d	e ₁	e ₂
n	0	1	2	3	→ ∞ (9)	→ ∞
R _L	not defined	1.00	1.00	1.00	1.00	clast perimeter roughness
T _{Ld}	not defined	L/L ²	2L/L ²	3L/L ²	→ ∞ (9L/L ²)	→ ∞
T _{LL}	not defined	L	L	L	L	mean clast perimeter
δ		1.76	2.74	3.94	→ ∞ (9.2)	1.0
MC	not defined	0.57	0.18	0.08	→ 0 (0.01)	→ 0

Table 4-2: Discontinuity parameters and MC of the patterns shown in Figure 4-11. The applicability of the MC and its parameters is limited to anisotropic (fault) rocks and isotropic cataclastic fault rocks. Values in brackets in column (e₁) correspond to the case of $n = 9$. In (e₂) the discontinuity parameters refer to the clast boundaries of which the properties are clearly defined (see explication in text below). The MC of isotropic cataclastic fault rocks is mathematically defined, tending towards zero.

The MC has been developed to characterise cataclastic fault rocks. By an increasing number of discontinuity sets and increasing shear movements their structures become more and more isotropic. It is shown in Table 4-2 that for $n \rightarrow \infty$ the MC tends towards zero. By very intense

cataclasis, isotropic rock fabrics as shown in (e₂) - Figure 4-11 are formed. In these cases the clast boundaries can be considered as (relics of former) discontinuities with random orientation (Figure 4-12). Making this assumption, the R_L , T_{Ld} , T_{LL} and MC of isotropic cataclastic fault rock is mathematically defined (e.g. by calculating the roughness of the clast contours, the ratio of the Σ clast perimeters to the reference area and the mean length of the clast perimeters). The MC tends towards zero as the number of clasts per reference area tends towards ∞ . For isotropic cataclastic fault rocks it has been set equal to zero, based on the preceding considerations. A MC = 0.0 does hence not mean an intact rock fabric with no discontinuities.

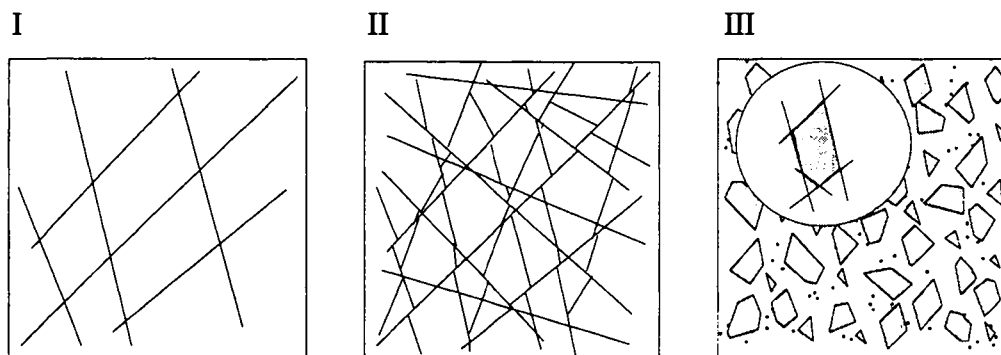


Figure 4-12: Schematic generation of isotropic cataclastic fault rocks by increasing number of discontinuities and shear movements. The clast boundaries (III) are considered as discontinuities.

The MC by itself does not enable the distinction between intact and cataclastic fault rocks. It can furthermore not be applied to intact isotropic rocks (e.g. granite) as the MC is mathematically not defined for rock fabrics without any discontinuities (crystal boundaries are not considered as discontinuities in contrast to clast boundaries). The application of the MC is hence limited to cataclastic fault rocks.

By the presented matrix coefficient only four discontinuity properties have been taken into consideration. As regards the mechanical and hydrogeological behaviour of rock samples, other parameters such as e.g. the connectivity or intersection of discontinuities, play an important role. These parameters will have to be taken into consideration in a future work.

An other difficulty is founded in the transformation of the structural anisotropy, which is by definition a tensor, in a scalar value. The author is conscious that the proposed orientation factor (δ) looks "somewhat complicated" and will have to be improved. One ambiguity is namely the strong dependency of δ on the number of discontinuity sets, whereas the influence of their orientation is undervaluated. Research has to be directed to a tensorial definition of δ , respectively of the MC and TC in order to enable a more accurate correlation with mechanical and/or hydrogeological tensorial parameters such as compressive strength, Young modulus, permeability, etc..

4.4.3 The mineralogical characterisation

The third parameter considered to control the rock mechanical properties aside from structural and textural features is mineralogical composition. It has been determined by thin section and X-ray diffraction (XRD) analyses and comprises the following three aspects:

- Identification of the fault rock mineralogy,
- Comparison of the fault rock and adjacent host rock mineralogy,
- Comparison of the mineralogy of the clast- and matrix-fraction.

The mineralogy of fault rocks

The influence of mineralogy on rock mechanical properties has been studied by different approaches by Calembert et al. (1980a, b, 1982), Schroeder (1972), Tourenq (1966) a. o.. Aleksandrov et al. (1967) have calculated the theoretical elastic modulus of rocks on the basis of the weighted elastic properties of the rock forming minerals. They have found good correlations between the calculated and experimentally determined modulus. By the same approach Calembert et al. (1980a, b, 1982) have determined the mean weighted Vickers hardness of rock samples.

As regards the mechanical properties of cataclastic fault rocks only the principal mineralogical components are supposed to be important and it seems furthermore justified to regroup minerals of similar mechanical properties, e.g. muscovite, biotite and chlorite. The contents of the mineral phases quartz, plagioclase, K-feldspar, calcite and dolomite have been determined semi-quantitatively by XRD-analyses and defined XRD peak-intensity calibration diagrams. The presence of minerals in only minor quantities is estimated to be negligible, with two important exception, namely the presence of swelling clay minerals and of graphite. Special attention has been paid to identify these mineral groups.

The mineralogy of fault rocks and host rocks

The mineralogical composition of rocks is not supposed to be changed during faulting by cataclastic deformation processes (chap. 2). However, the mineralogy of fault rocks and adjacent host rocks may be differing for the following reasons: first, the emplacement and development of a fault zone may have been triggered by small mineralogical differences in the host rock (see e.g. Dornbach zone, chap. 3.2). Such minor lithological differences are not easily identified macroscopically, especially in underground constructions. Second, the mineralogy of fault rocks may have changed as an indirect consequence of cataclasis. In fact, groundwater circulation (hydrothermal) is supposed to be enhanced directly after cataclastic deformation and to cause important alteration processes (chap. 5.1.5). To identify possible primary or secondary mineralogical differences, semi-quantitative XRD analyses have been performed on samples of fault rocks and adjacent host rocks.

The mineralogy of the clast and matrix fractions

In correspondence to the characterisation method based on the clast-matrix model, the sieved grainsize fractions 0.2 - 0.63 mm (clasts) and < 0.06 mm (matrix) have been analysed separately. Mineralogical variance between clast and matrix fractions has been expected for two reasons: first, cataclasis affects grains in function of their mineralogy and original rock fabric and can lead to a mineralogical grainsize fractionation. Second, alteration processes mainly take place at the mineral - fluid interface and are hence more likely to take place in the fine-grained matrix than in the clast fraction. Alteration products can be identified more easily when the fractions are analysed separately.

4.4.3.1 The Vickers hardness

The conceptual method of Aleksandrov et al. (1967) and Calembert et al. (1980a) is judged a promising approach to study the relationship between mineralogical composition and mechanical properties of cataclastic fault rocks.

The Vickers hardness (Vh) is a parameter originally developed to characterise the properties of ore minerals. Its application has been extended to rock forming minerals by Tourenq (1966). In contrast to the Mohs hardness it is a more precisely defined parameter and determined by measuring the impact of a small diamond pyramid on the polished surface of the tested mineral. It is defined as the ratio of the applied load to the square of the measured indentation diameter. The Vh of some rock forming minerals are presented in Table 4-3.

Mineral phase	Vickers hardness [MPa]
Talc	200
Gyps	690
Muscovite *	850
Biotite	900
Calcite *	1'100
Dolomite *	2'180
Microcline	6'900
Orthoclase *	7'200
green Hornblende *	7'300
Quartz *	12'800

Table 4-3: Vickers hardness in [MPa] after Tourenq (1966). The Vh used to quantify the mineralogy of cataclastic fault rocks are indicated with a *. The Vh of orthoclase is taken as reference for feldspars s.l., green hornblende for amphiboles s.l. and the one of muscovite for the non-quantified mineralogical part of XRD-analyses.

Calembert et al. (1980a, b, 1982) have calculated the *mean weighted Vickers hardness (mwVh)* of rocks by weighting the hardness of the mineral phases with their volumetric proportions. They report good correlation between the calculated mwVh and the uniaxial compressive strength. The mean weighted Vickers hardness is defined as:

$$mwVh = \sum_i v_i \cdot Vh_i \quad (\text{Eq. 4-10})$$

where

- mwVh: mean weighted Vickers hardness [MPa]
- v_i : weight proportion of the mineral phase i
- Vh_i : Vickers hardness of the mineral phase i [MPa]

With regard to the correlation between geological and geomechanical properties the mwVh has been chosen to quantify the mineralogical composition of cataclastic fault rocks. It is considered to be a weighting factor for the proportions of the different mineral phases rather than to have a direct physical signification. This quantification is important however with regard to the following two aspects: first, with the mwVh, the TC, and the MC all three considered geological parameters of cataclastic fault rocks can be quantified in an objective way. Second, this complete quantitative characterisation enables in the future the comparison between fault rocks from different lithologies.

To calculate the mwVh of the analysed fault rocks the relative proportions of the minerals have been determined by semi-quantitative XRD analyses. Based on the XRD-patterns and thin section analyses the non-quantified mineralogical part can be considered to be composed mainly of phyllosilicates, namely mica and chlorite, and the Vh of muscovite (850 MPa) is taken as reference. As mentioned above, the presence of minor proportion of common minerals such as e.g. sphene, turmaline, opaque minerals, etc. is not supposed to influence the mechanical behaviour of fault rocks significantly.

5 PRESENTATION OF RESULTS

Rock fabrics of the studied cataclastic fault rocks are described qualitatively and quantitatively by means of the methods developed above. Results are presented sorted by host rock lithologies and sites. As mentioned earlier, interest has been focused in a first time on fault rocks occurring in quartzo-phylitic series, namely the ones of the gallery of Cleuson-Dixence (unit C and D), the borehole Goltschried and the gallery of Varzo (chap. 3). Additionally, fault zones in greenstones (Cleuson-Dixence, unit B), serpentinites (Genoa) and carbonate rocks (Cleuson-Dixence, unit D) have been studied. The results of these analyses are presented for comparison and with regard to the future extension of the developed characterisation method to fault rocks in other lithologies. A synthesis and general discussion of results of all analysed fault rock types is given in chap.5.5.

5.1 Fault rocks in quartzo-phylitic series

5.1.1 Cleuson-Dixence, unit B (TM 2780-2900)

The kakirites sampled in the chlorito-sericitic schist of Métailler unit bear mainly quartz, white mica and chlorite, carbonate, feldspar and accessory minerals. The mineralogical composition and proportions are shown in Figure 5-1 and Append. II-a. With exception of the sample CD22, the quartz content is varying between 10 and 20%, whereas the one of chlorite and white mica varies between 60 and 80%. The original schistosity, with a gradual transition between cleavage domains and microlithons, is formed by relatively coarse grained white mica and chlorite, locally a crenulation cleavage is observed. Elongated quartz grains of granoblastic shape show deformation lamellae and undulose extinction.

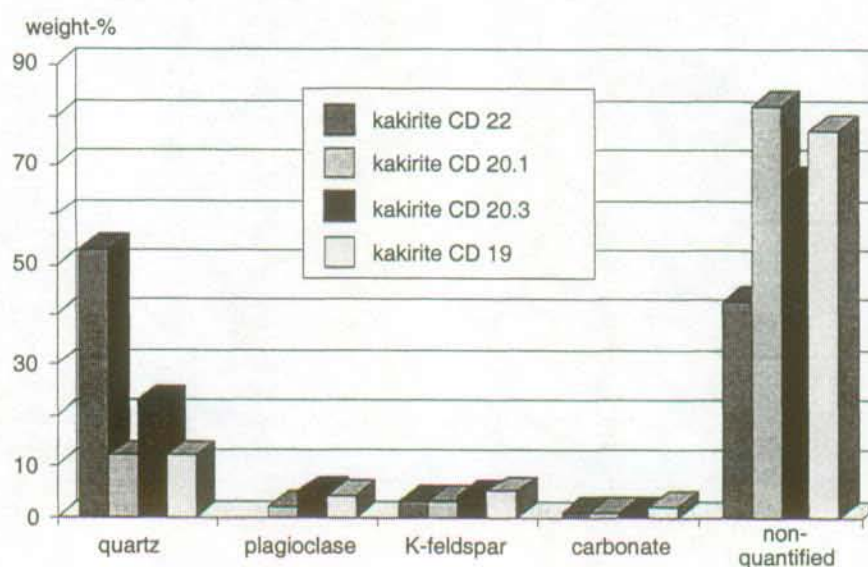


Figure 5-1: Mineralogical composition of kakirite samples from Cleuson-Dixence, unit B.

In less cataclastically deformed samples, deformation is concentrated along small shear zones orientated sub-parallel to the crenulation cleavage, respectively to the limbs of the older schistosity. These microscopic cataclastic zones distinguish from the rest by a considerably smaller grain size and the lack of large chlorite and muscovite grains which have recrystallised in fine sericite. Quartz grains are often fractured in a plane normal to the schistosity.

In intensely deformed kakirite samples, the original schistosity is only locally preserved and rock fabric shows typically a homogeneous, fine-grained matrix of very small, flaky grains of white mica and chlorite with a few larger quartz grains. The later show evidence of intense brittle fracturing with crystallisation of carbonate in the fractures.

The microfabrics of two kakirite samples (CD22, CD23) have been analysed for quantification. The determined discontinuity parameters are presented in Figure 5-5. Three, respectively two discontinuity sets have been identified, for which an orientation factor δ of 3.9 and 2.9 has been calculated. Mean discontinuity length is about 2mm and density 0.83 respectively 0.75mm/mm². The calculated MC is 0.14 and 0.23. No clasts were discernible at the standardised magnification in the analysed samples.

The kakirite sample CD20.3 has been sieved for XRD analyses. It shows an extended granulometry with about 10 weight-% gravel (max. Ø 40mm) and 45 weight-% silt-clay grainsize fraction. Clasts and gravel-size fragments are blade-shaped, very angular and consist mainly of chlorito-schist and quartz. The mineralogy of the different grainsize fractions is shown in Figure 5-6. It is noted that quartz is considerably less abundant in the finer-grained fractions, whereas in parallel the content of sheet-silicates (non-quantified) increases with decreasing grainsize. Quartz and sheet-silicate content is intermediate in the entire kakirite sample.

5.1.2 Cleuson-Dixence, unit C (TM 5180 and 5597)

The quartzo-sericitic schist of the Siviez-Mischabel nappe adjacent to the studied fault zones is characterised by a strongly developed, macroscopically recognisable crenulation cleavage. The intact rock is easily broken along these 5 to 10mm spaced cleavage domains.



Figure 5-2: Microfabric of the host rock adjacent to the fault zone. Characteristic crenulation cleavage (S2) from upper right to lower left, old schistosity (S1) horizontal. Thin section image, plane polarised light, width of view 20mm. (Sample Tr1.2, Lot C - TM 5180, Cleuson-Dixence)

At the microscopic scale, the crenulation cleavage is composed of white mica and minor proportions of chlorite. Cleavage domains are up to 0.5mm thick. Grainsize in the microlithon is bi-modal with dominantly small grains (Ø 0.3mm) and fewer blasts mainly of quartz and calcite measuring up to 2mm. Both, small and large quartz grains show only weak undulose extinction. The host rock is composed mainly of quartz, white mica and chlorite and lesser amounts of plagioclase, K-feldspar and calcite. The exact mineralogical proportions are given in Figure 5-3 and Append. II-b.

Macroscopically the kakirites in the fault zones at TM 5180 and TM 5597 consist of a white-greyish, structureless, mica-rich material, bearing some rock fragments of up to a few centimetres large. The later are in general angular to slightly rounded and of tabular shape. Clast boundaries are often recognised to have formed along crenulation cleavage domains.

Kakirites and host rock samples show an almost equiproportional, bi-phase mineralogical composition of quartz and white mica (Figure 5-3). Compared with the samples of unit B, feldspar, and especially quartz contents are higher (40-50%). The non-quantified mineralogical part in contrast comprises principally white mica. Chlorite is present only in minor proportions. Quartz and feldspar content of the host rock is slightly higher than in the kakirite samples. Mineralogically the two fault zones of unit C differ only slightly, namely in feldspar and phyllosilicate contents.

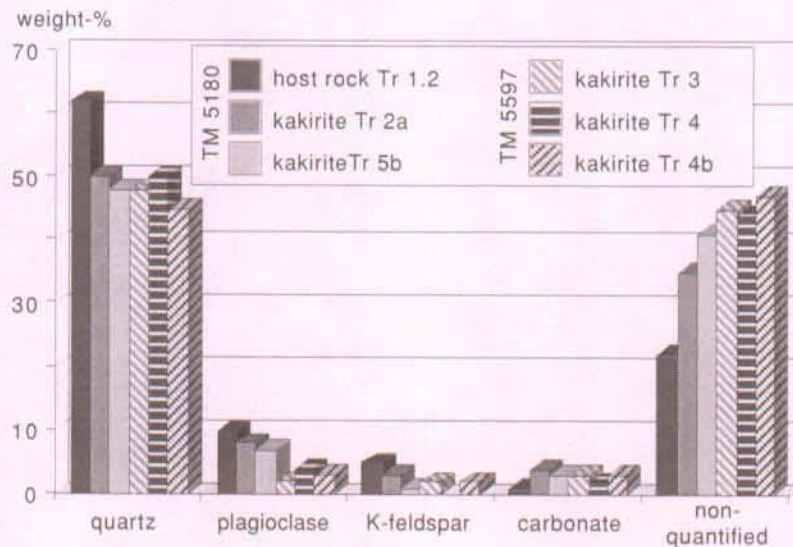


Figure 5-3: Mineralogical composition of kakirite and host rock samples from Cleuson-Dixence, unit C.

At the microscopic scale the kakirites of the two fault zones show identical rock fabrics. They are characterised by an isotropic granular fabric composed of angular, polymineralic rock fragments in a fine- to medium-grained matrix (Figure 5-4). Larger clasts often show the old folded schistosity as observed in the microlithons of the intact host rock. Intact cleavage domains in clasts are in contrast rarely observed. Shape and size of the clasts, and more in general the overall microfabric of the kakirites is controlled partially by the original host rock fabric (Figure 5-7).



Figure 5-4: Granular, isotropic kakirite rock fabric. Thin section image, plane polarised light, width of view 20mm. (Sample Tr5b, TM 5180)

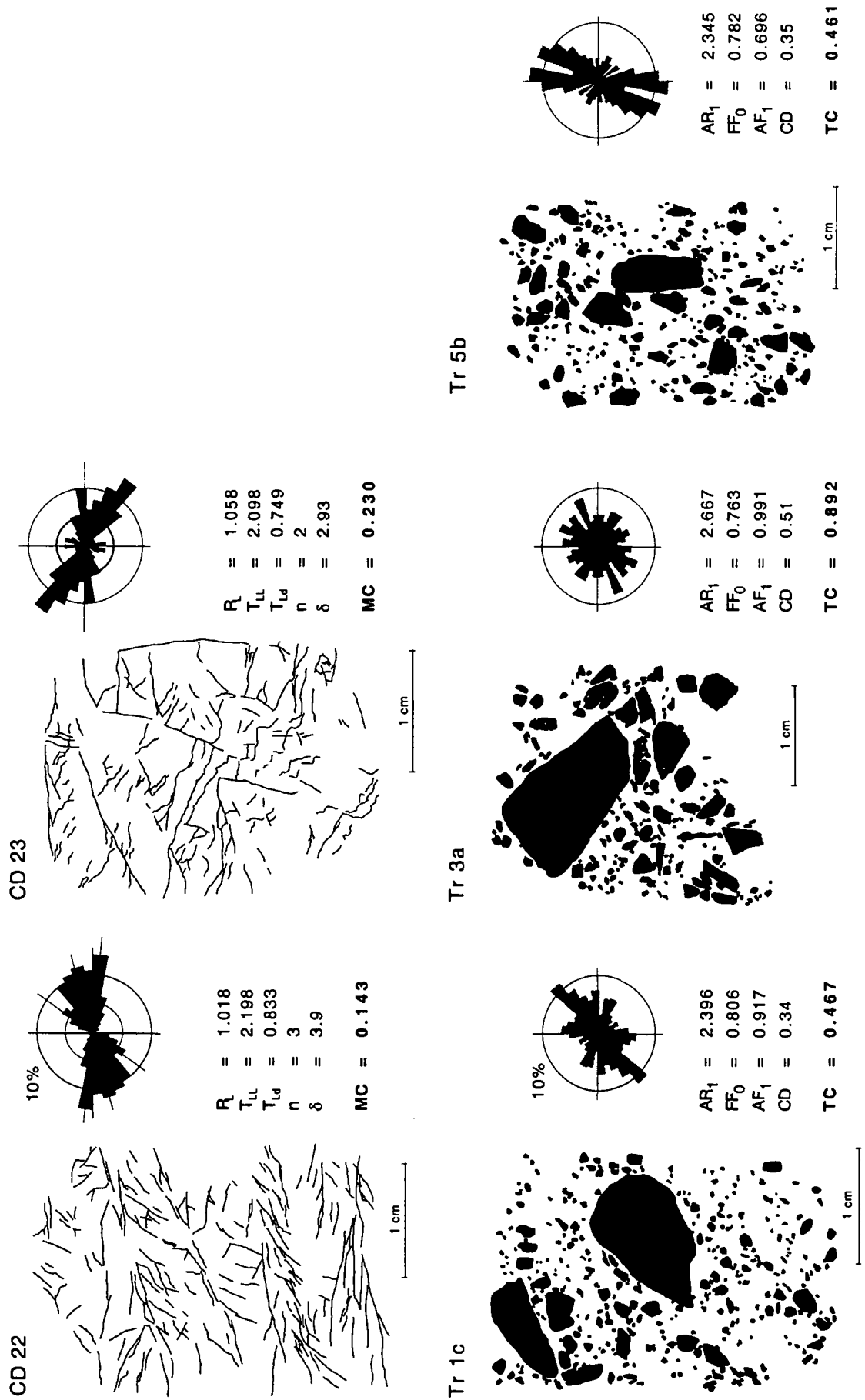


Figure 5-5: Quantified rock fabric of kakirite samples from Cleuson-Dixence, unit B (CD22, CD 23) and C (Tr1.c, Tr3a, Tr5b).

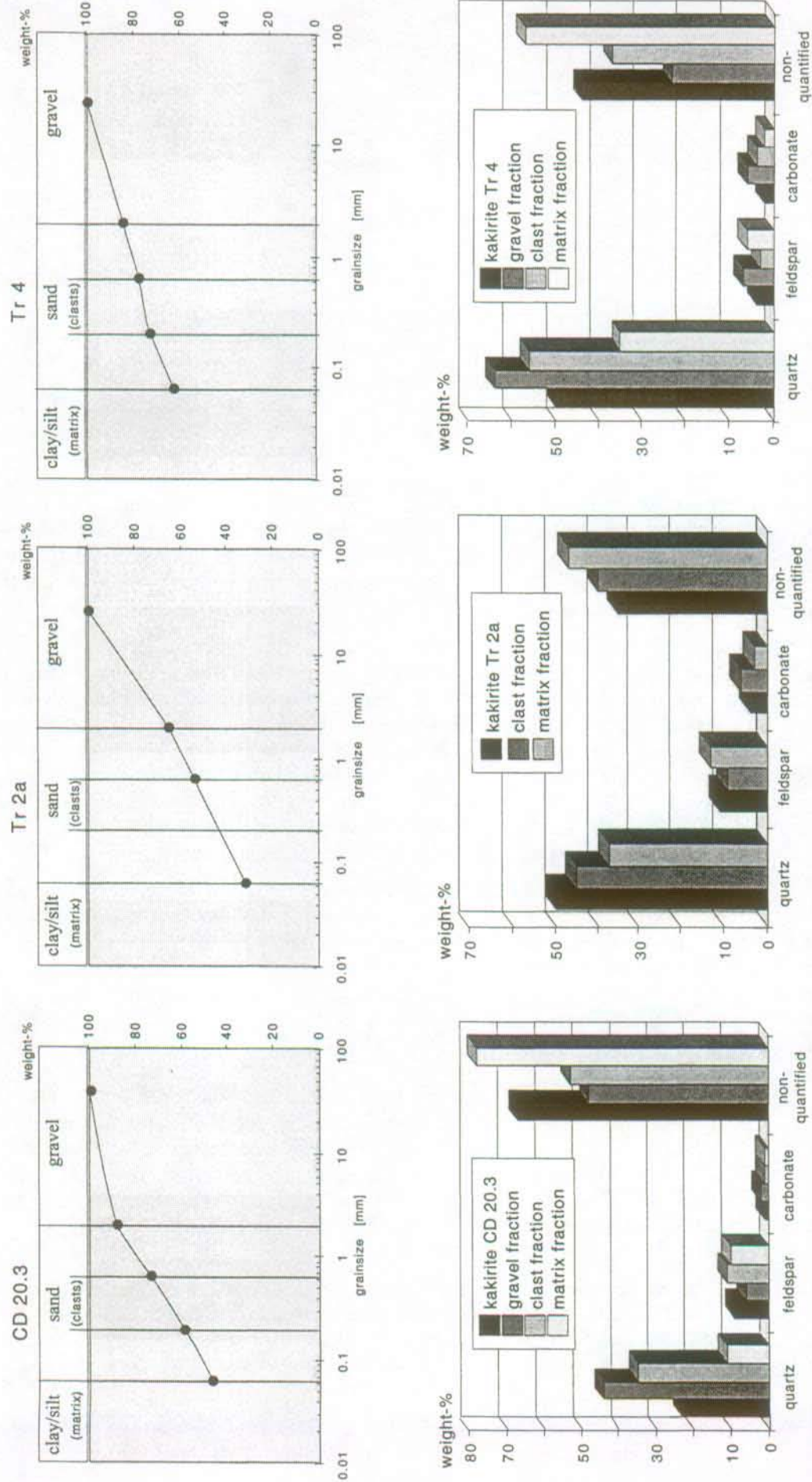


Figure 5-6: Granulometry and mineralogy of sieved kakirite samples from Cleuson-Dixence, quarto-phyllitic series. CD 20.3 unit B, Tr 2a, Tr 4 unit C.

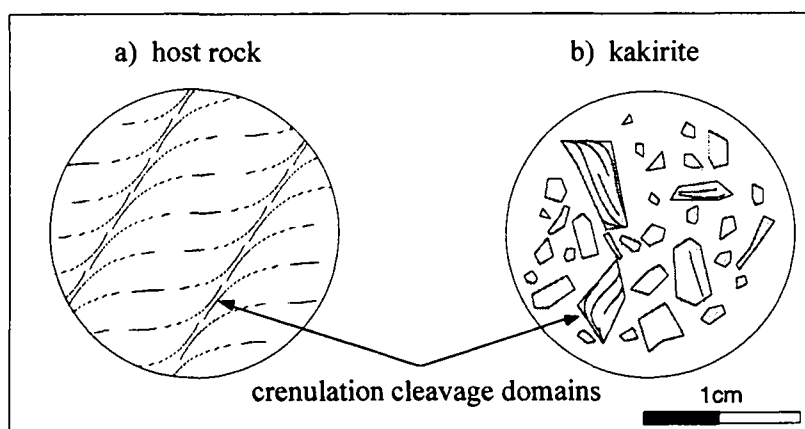


Figure 5-7: Schematic microstructure of host rock and kakirite samples. Larger clasts often have broken along the original crenulation cleavage domains.

As the host rock easily breaks along the mica rich cleavage domains, the spacing of the later controls mainly the "thickness" of larger, tabular clasts during faulting. During further frictional flow and rigid body rotation, the cleavage domains are easily detached from the clasts and split off in fine-grained sheets. Smaller clasts in the fine-grained matrix are in general monomineralic. Quartz, feldspar and, more abundant, very small, flaky mica and chlorite grains have been identified.

The granular rock fabric (Figure 5-4) is strongly differing from that of the kakirites of unit B. The original schistose rock fabric of the host rock is completely obliterated. No discontinuities are discernible in the (visually) isotropic matrix, hence the MC is equal to zero. The rock fabrics, calculated TC's and clast parameters of three samples are shown in Figure 5-5. The rose diagrams (Tr1c to Tr5b), representing the orientation of all (!) clasts, show low anisotropies. The calculated angle factors (AF_1) of only the elongated clasts are varying between 0.7 and 0.9. The clast density of 30 and 50% is strongly influenced by the relatively large grains contained in Tr1.c and Tr3a. The observed clast size is varying largely with a maximum clast diameter of 15mm.

Two samples (Tr2a, Tr4) have been sieved for XRD analyses. Both show a very extended grainsize distribution and high proportions of silt/clay grainsize fractions between 40 and 60 weight-% (Figure 5-6). XRD-analyses confirm the observations made for the sample of unit B: quartz becomes less abundant with decreasing grainsize fraction, whereas the sheet silicate contents increases. Feldspar content does not show a clear relation with grainsize.

5.1.3 Cleuson-Dixence, unit D (Zerjona)

As mentioned in chap. 3.1, four sub-types of host rocks, respectively cataclastic fault rocks are distinguished by their macroscopic structure and colour: quartzite, quartz rich meta-sandstone, micaceous schist and black carbonaceous phyllite. Considering their mineralogical composition, a gradual transition of quartz and phyllosilicate proportions is observed between the four rock types: quartz content is ranging from 70 in the quartzite, to 10% in the carbonaceous phyllite. The phyllosilicate proportion shows the inverse tendency. The mineralogical composition of the analysed samples is presented in Figure 5-8 and Figure 5-11.

The grainsize distributions and mineralogical compositions of sieved kakirite samples are presented in Figure 5-12 and Figure 5-13. All samples show an extended grainsize distribution with in general low gravel (< 20%) and high silt/clay fraction (40-80%) content. Except of the very fine-grained sample Fom 5.1, the quartz content decreases with grain size.

The quartzite samples are characterised in thin sections by large polycrystalline quartz grains (up to 10mm) surrounded by small grained (< 0.2mm) quartz, feldspar, carbonate and white mica. Quartz aggregates show granoblastic structure with strong undulose extinction and evidence of

recrystallisation. The rough foliation is formed by irregularly anastomosing thin seams (pressure solution, graphite?), of dark material, sometimes together with white mica and chlorite. Quartz, crystallised in small veins, has equigranular, polygonal shape and shows no sign of intracrystalline strain. Evidence of cataclastic deformation is in clearly recognised only in fractures crosscutting these coarse grained veins.

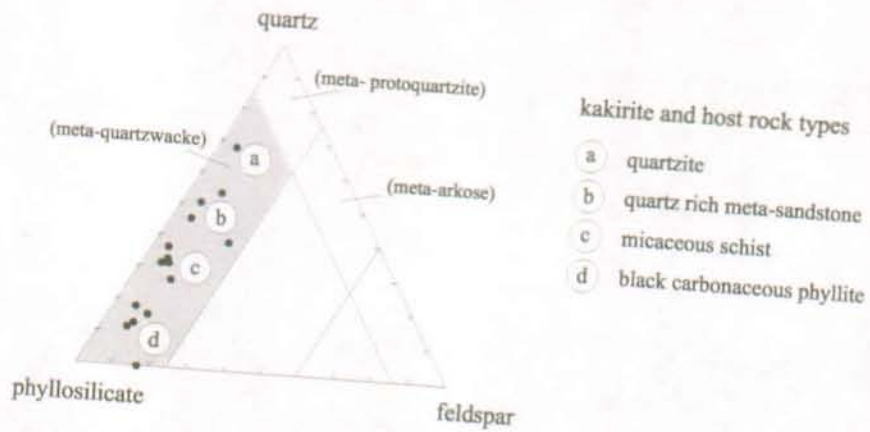


Figure 5-8: Gradual variation of mineralogical composition between quartzite and phyllite. Kikirite samples from Cleuson-Dixence, Zerjona. Adapted classification system for sandstones, after Selley (1982).

In comparison with the quartzite, the quartzitic meta-sandstones bear smaller and finer-grained quartz aggregates in a similar matrix. Fine grained white mica is more abundant, the schistosity is formed by irregular seams of dark material. Wide fracture zones have developed, characterised by a general grain comminution (Figure 5-9). Within the matrix, brittle deformation is observed in broken quartz aggregates.



Figure 5-9: Cataclastic fault zone crosscutting the (horizontal) foliation in micaceous schist. Thin section image, plane polarised light, width of view 7mm. (Sample Zr11, TM 9)

Micaceous schists distinguish from the former by their homogeneous fine grainsize and dark grey colour. Schistosity becomes more and more continuous and is strongly folded at the decimetric to millimetric scale. Discrete faulting is observed to take place in quartz and feldspar richer layers, the fractures rapidly die out in the adjacent mica-layers. In fine-grained shear bands crosscutting the foliation, deformation is accompanied by very small recrystallised grains of mica, quartz and carbonate. Shortening subparallel to the foliation is accommodated by folding, crude kinking and layer parallel slip of mica sheets.

In the black carbonaceous phyllites only a few small, spherical to eye-shaped grains are visible to the naked eye. In thin sections, they are identified as intensely fractured quartz and carbonate aggregates, surrounded by a submicroscopic brownish to black coloured matrix. By continued comminution, the development of fine-grained cataclastic rims and clast trails is observed (Figure 5-10). The genesis of cataclastic trails in fault gouges has been described recently by Keller et al. (1997).



Figure 5-10: Cataclastic trail around an eye-shaped, intensely fractured quartz aggregate. Thin section image, crossed polarised light, width of view 10mm. (Sample Zr21.4b, TM 14)

The rock fabrics of 9 kakirite samples are presented in Figure 5-14 to Figure 5-16. It is noted that in parallel to the quartz content, the clast density decreases from 30% (quartzite and meta-sandstone) to about 15, respectively 10% in the micaceous schist and phyllite. The spatial distribution of the clasts in the matrix is homogeneous or in layers, as shown in the examples of Zr9 and Zr43. The AF_1 does not consider such spatial distributions but only the orientation of the elongated clasts. It is varying between 0.7 and 1.0 for the analysed samples, reflecting the visual impression given by the rose diagrams. The TC's are ranging from 0.13 to 0.46.

In most of the samples 1 or 2 discontinuity sets with low angles in-between have been visually identified. The largest angle difference (40°) is measured in the cataclasite sample Zrbloc, the corresponding orientation factor δ is 2.9. Three discontinuity sets have been determined in the samples Zr13 and Zr30 with $\delta = 3.7$ respectively $\delta = 3.9$. Discontinuity roughness is observed to decrease from quartzite to phyllite samples, whereas in parallel the discontinuity density increases. The calculated MC's of the nine samples range between 0.12 and 0.48.

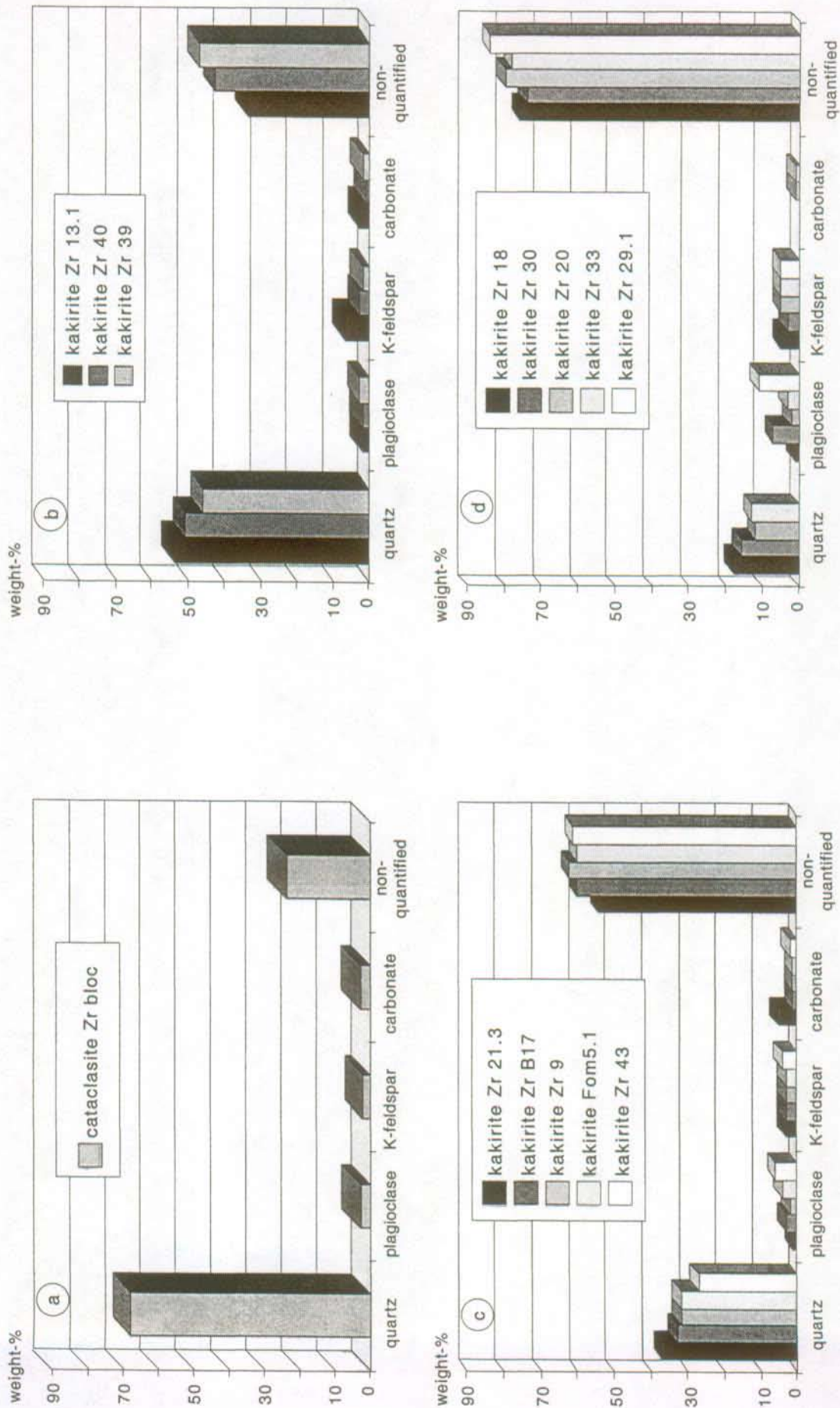


Figure 5-11: Mineralogical composition of fault rock samples from Cleuson-Dixence, Zerjona. a): quartzite, b): quartz rich metasandstone, c): micaceous schist, d): black phyllite.

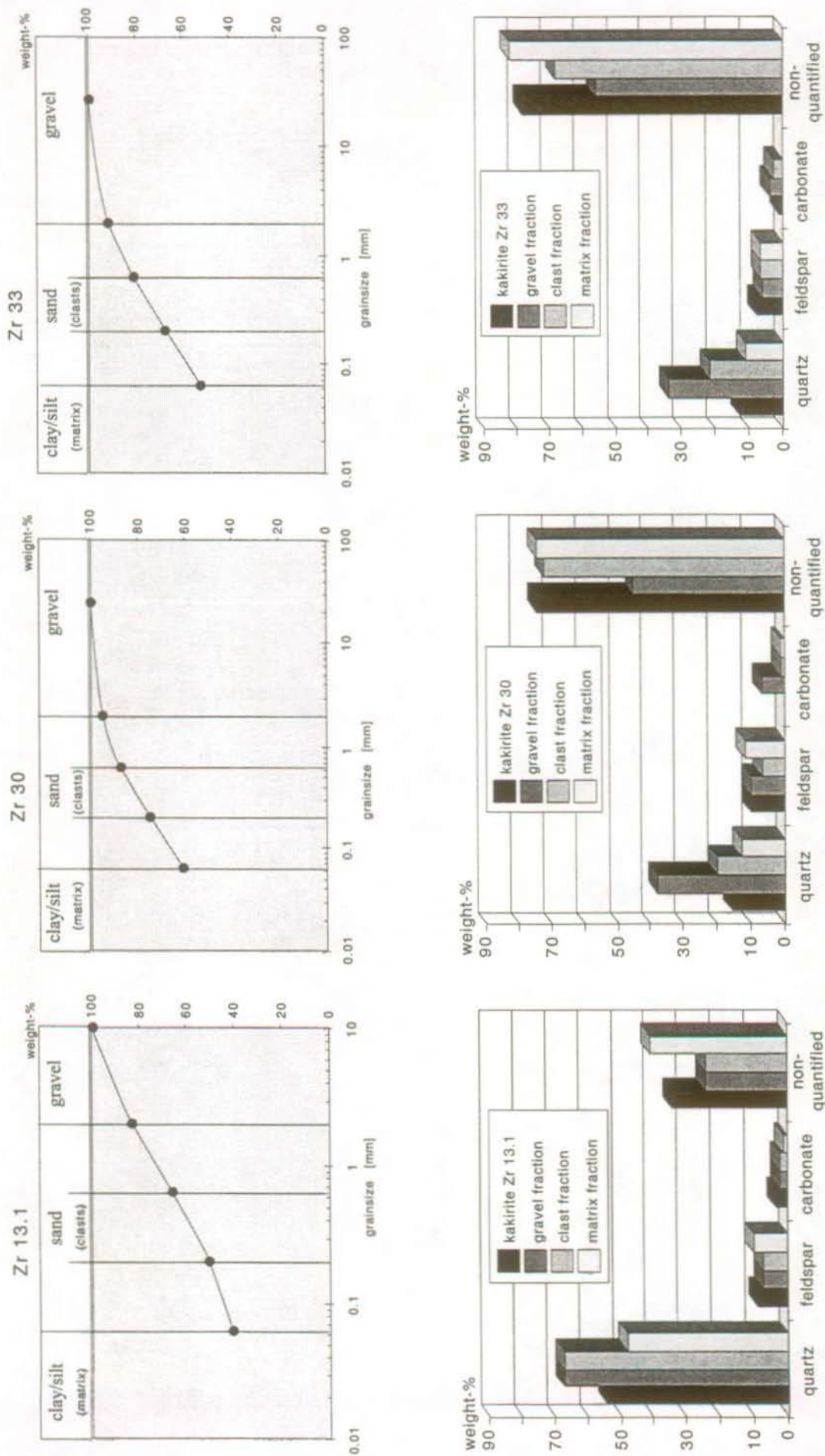


Figure 5-12: Granulometry and mineralogy of sieved kakirite samples from Cleuson-Dixence, unit D Zerjona.

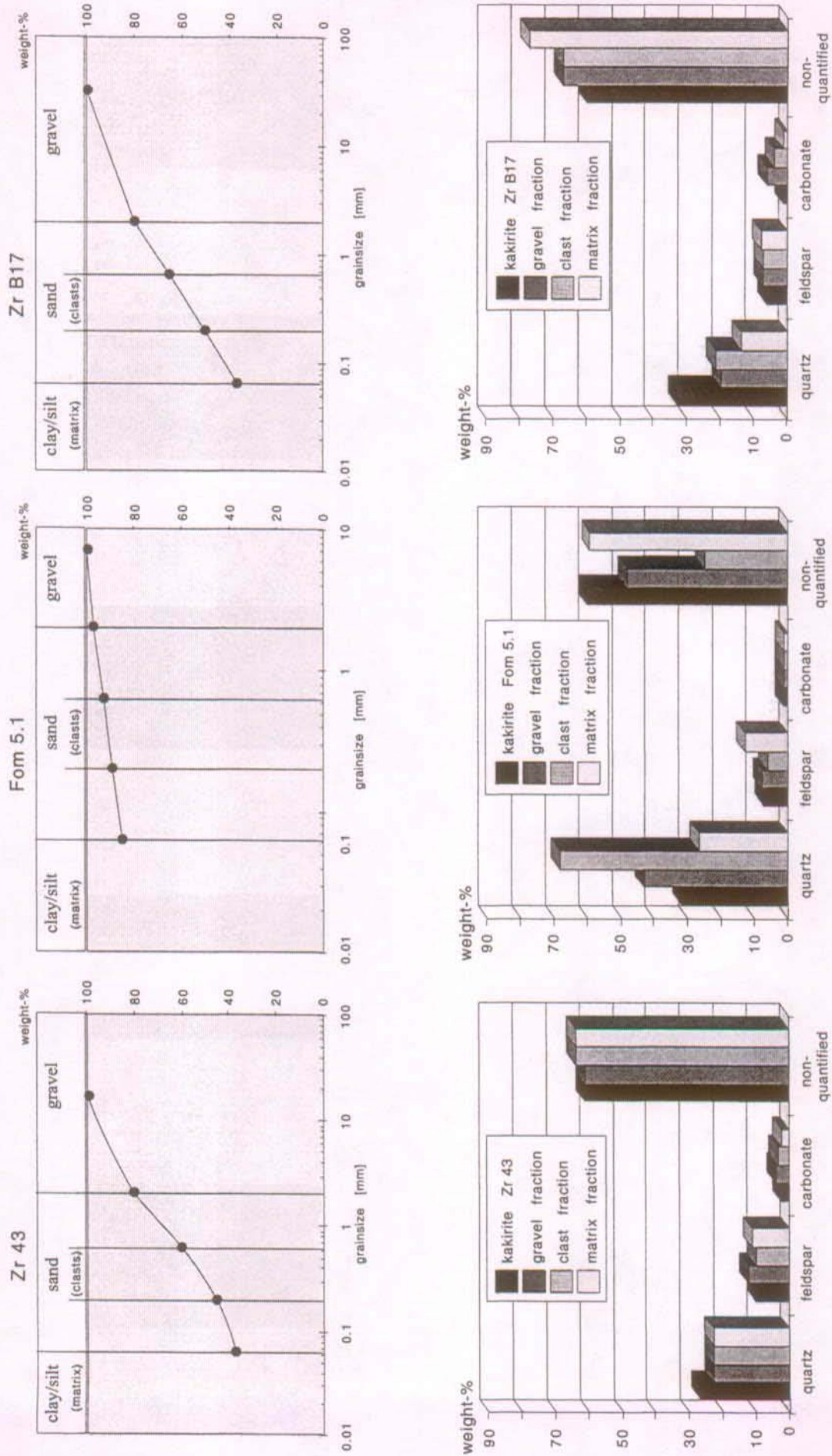


Figure 5-13: Granulometry and mineralogy of sieved kakirite samples from Cleuson-Dixence, unit D Zerjona.

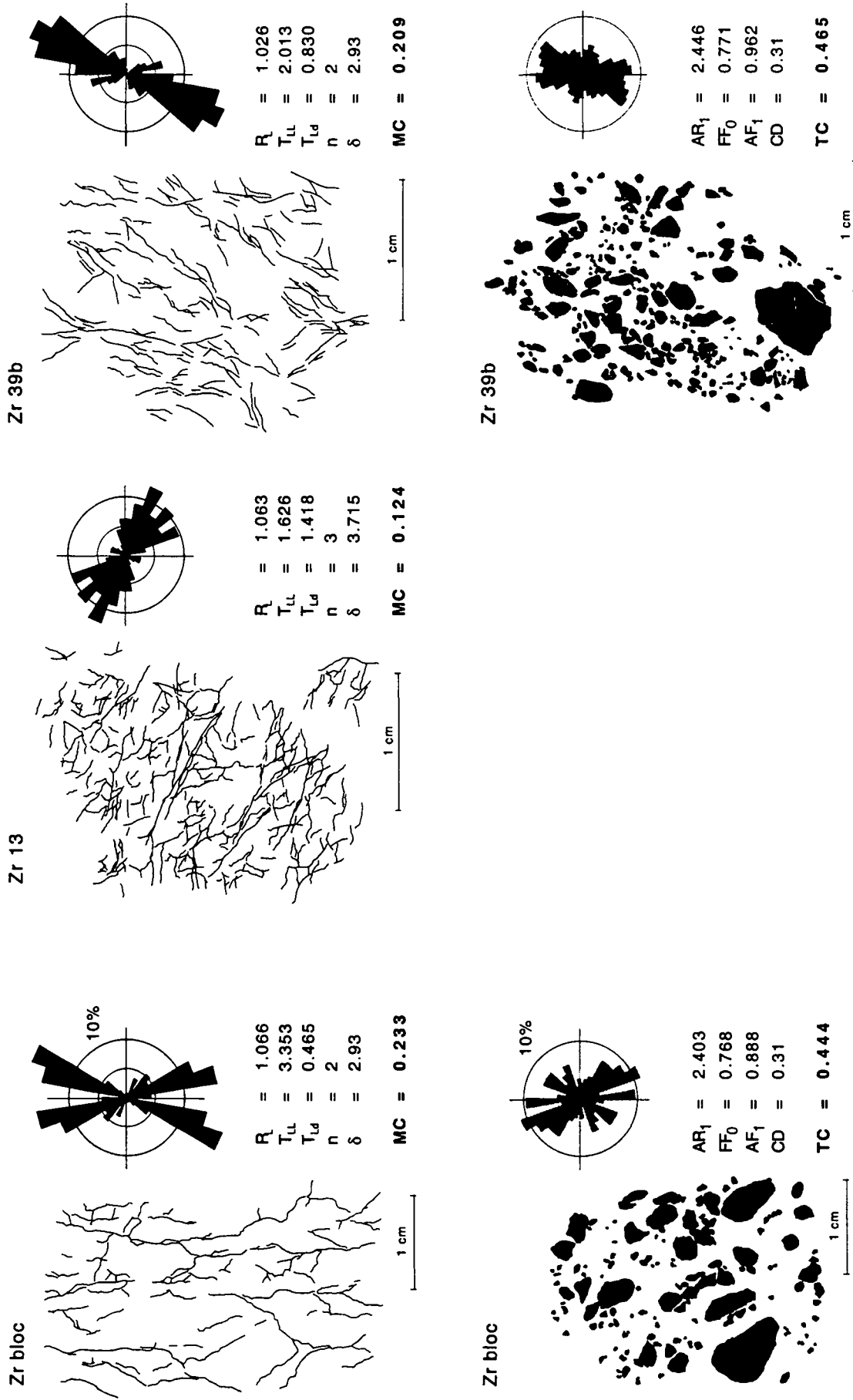


Figure 5-14: Quantified rock fabric of kakirites from quartzite (Zr bloc) and quartzitic meta-sandstone (Zr 13 , Zr 39b). Cleuson-Dixence, unit D - Zerjona.

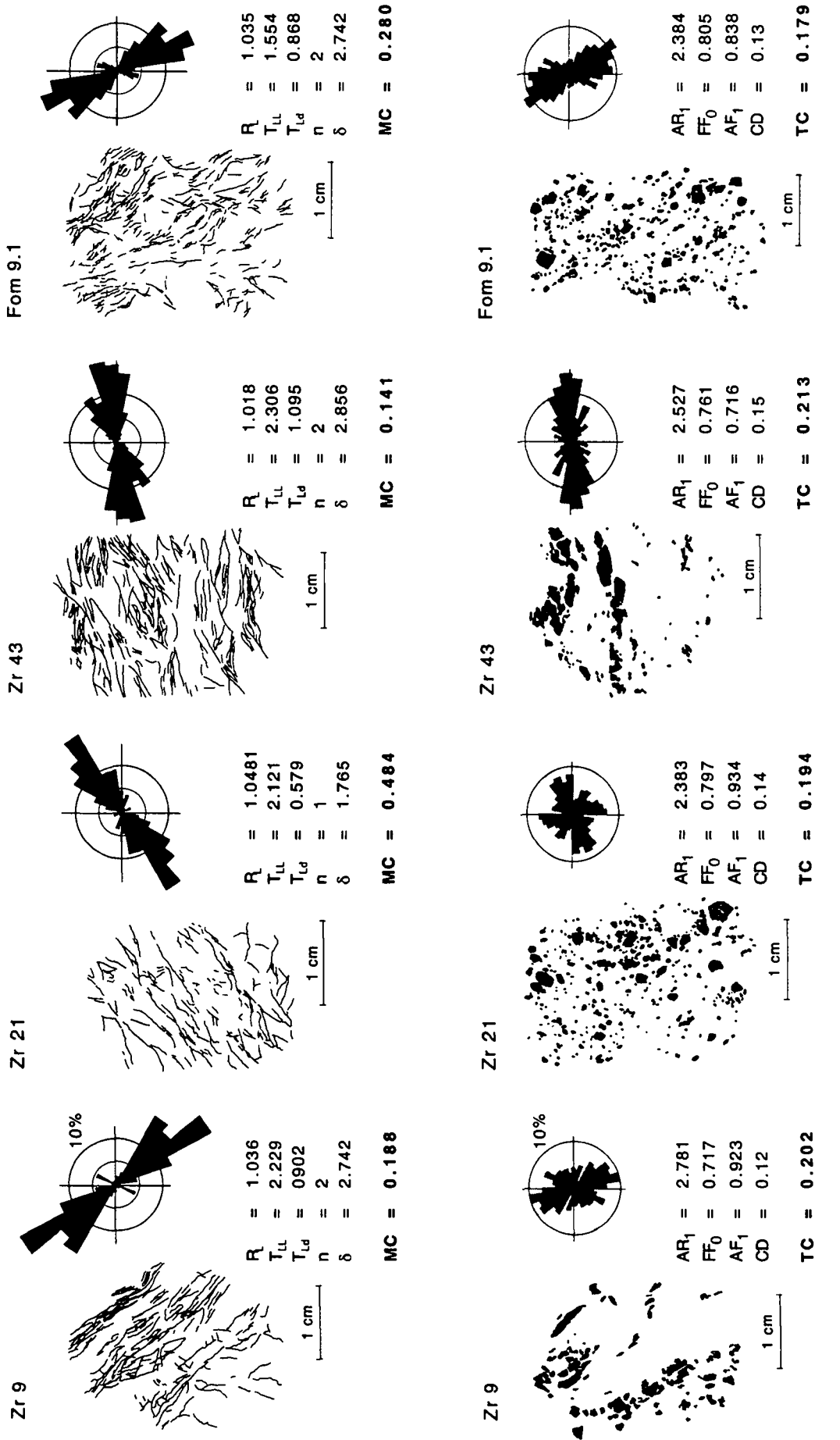


Figure 5-15: Quantified rock fabric of kakirite samples issue of micaceous schists. Cleuson-Dixence, unit D - Zerjona.

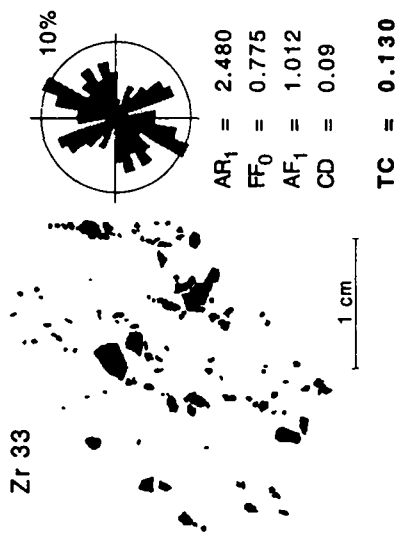
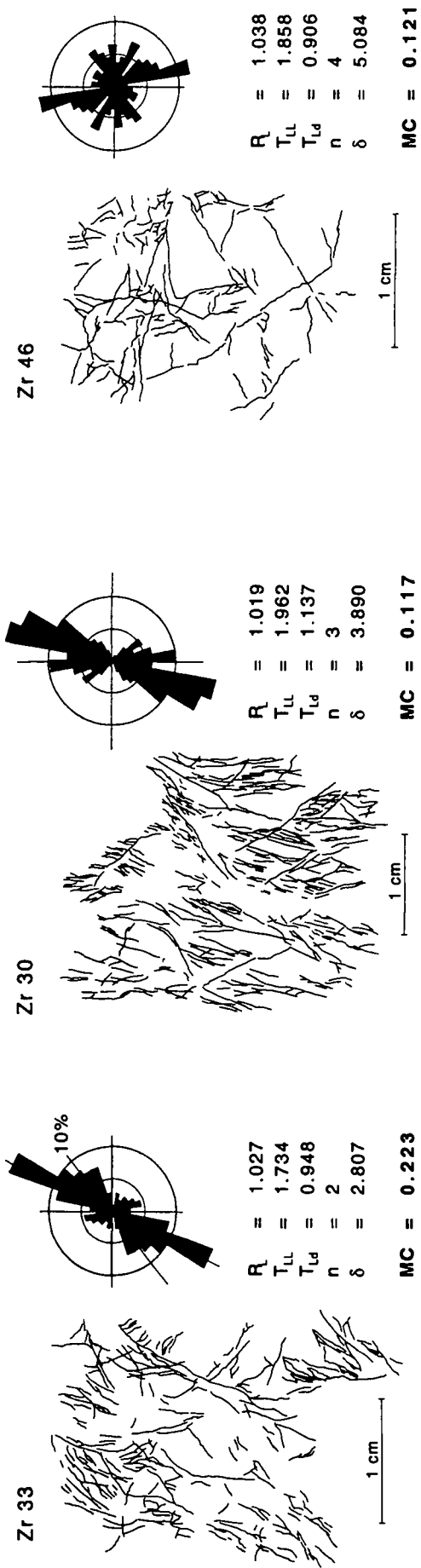


Figure 5-16: Quantified rock fabric of kakirites issue of black phyllite. Cleuson-Dixence, unit D - Zerjona.

5.1.4 Borehole Goltschried

Thin sections have been made only of samples taken in the Dornbach Zone. At the microscopic scale, the host rock shows a spaced foliation with discrete transition between quartz-plagioclase rich microlithons and fine-grained cleavage domains composed mainly of extremely small, flaky white mica, coarser grained chlorite and black (graphitic ?) material. Quartz has an extended grainsize distribution, but is found mostly as small grains (~0.1mm) in elongated aggregates showing a dynamic recrystallisation fabric. Larger grains rarely exceed 1.5mm in length. All quartz grains show undulose extinction, larger ones are often fractured perpendicular to the schistosity planes. Plagioclase is together with quartz (\pm calcite) the main component of the microlithons. It is forming relatively large, elongated crystals (0.5 - 2mm) and is extensively altered and clouded with sericite. Fractures in plagioclase and quartz are healed with coarsely crystallised calcite.

The mineralogical composition of host rock and kakirite samples from the Dornbach zone show important differences in phyllosilicate and feldspar content (Figure 5-19). Based on thin section analyses these differences are identified to be due mainly to small scale lithological heterogeneities. Cleavage domains are clearly more abundant and better developed in the kakirites. Alteration of feldspar may further accentuate the observed differences, however it is not recognised in thin sections to be notably higher in the kakirites than in the host rock. The mechanical weakness due to a high phyllosilicate content in the Dornbach zone has certainly favoured the cataclastic faulting exactly in this zone.

The host rock samples from the Aar massif basement show very high feldspar (plagioclase) content of 70%. As shown in Figure 5-19 it is strikingly lower in the clast and matrix fraction of the kakirite. In contrast to the other analysed kakirite samples an extended grainsize distribution with high gravel and only small silt/clay proportions has been found.

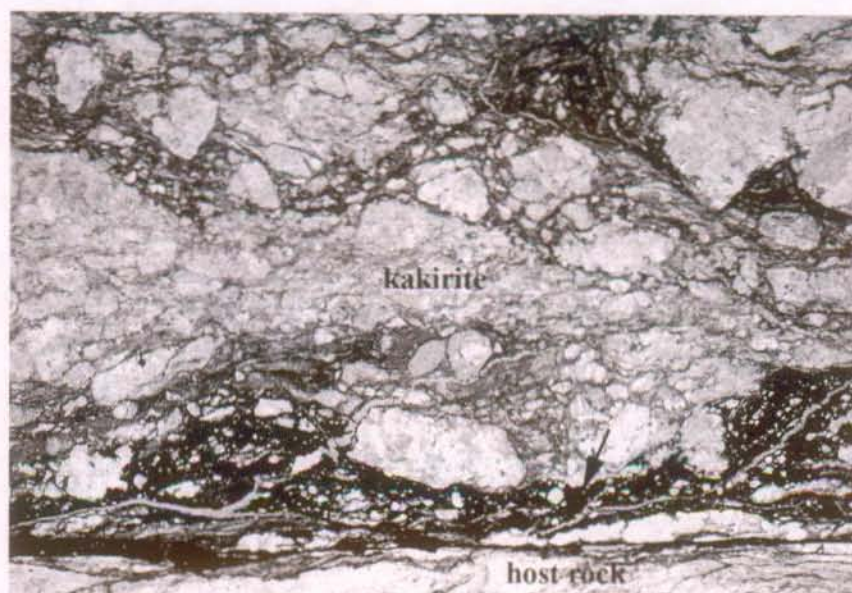


Figure 5-17: Black fringe at the sharp contact between kakirite and schistose host rock. Thin section image, plane polarised light, width of view 20mm. (Sample G-3, Dornbach Zone, borehole Goltschried)

The contacts between kakirites and host rock are very sharp and often characterised by black to dark brownish fringes (Figure 5-17). The kakirite samples show a cataclastic fabric composed of angular rock fragments floating in a medium to fine-grained matrix. A gradual grainsize transition between clasts and matrix is observed. Most of the clasts are polymineralic and polycrystalline composed of quartz, feldspar and mica. Larger clasts often bear calcite veins perpendicular to the preserved surrounding schistosity. The old schistosity is only partially and locally erased, namely

near the contact to the adjacent host rock. Smaller elongated grains in the matrix are randomly orientated whereas large clasts and preserved microlithons are still parallel to the original foliation. Clast boundaries are marked by a weathered-brownish rim.

The quantified rock fabrics of five samples are presented in Figure 5-20 and Figure 5-21. On three samples the texture and matrix coefficient were determined, whereas in two samples only the MC was determined. Two, respectively three discontinuity sets with low angles in-between have been identified. The mean discontinuity length is varying between 1.8 and 2.6mm, the discontinuity density lies between 0.65 and 0.98mm/mm². The calculated MC range from 0.13 to 0.24. The quite low MC are explained for the sample G4a by the presence of three discontinuity sets together with a relatively high mean discontinuity length. In the case of the samples G6-2 the low MC value is mainly due to the combined effect of a high discontinuity density and a long mean trace line length ($\bar{\phi}_{T_{LL}} = 2.6\text{mm}$).

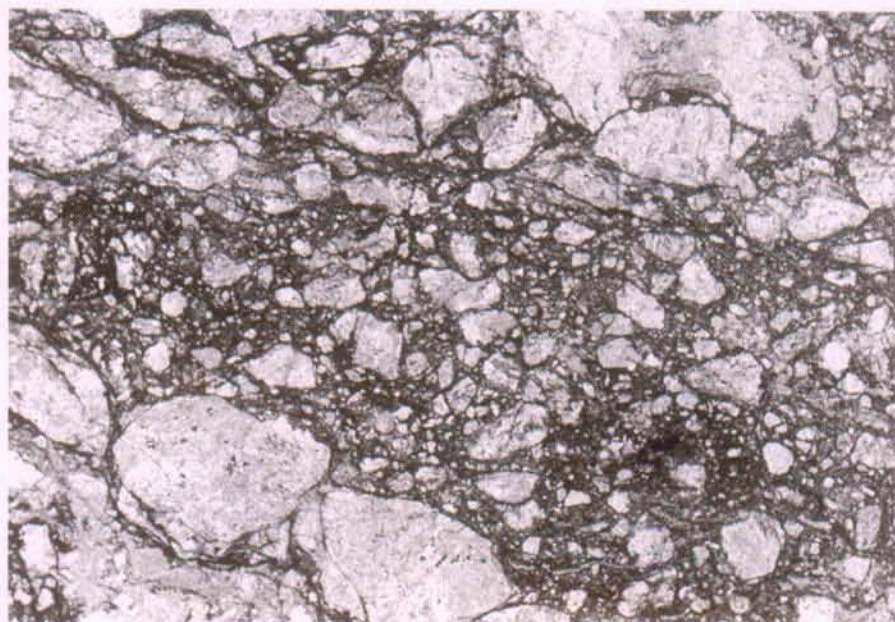
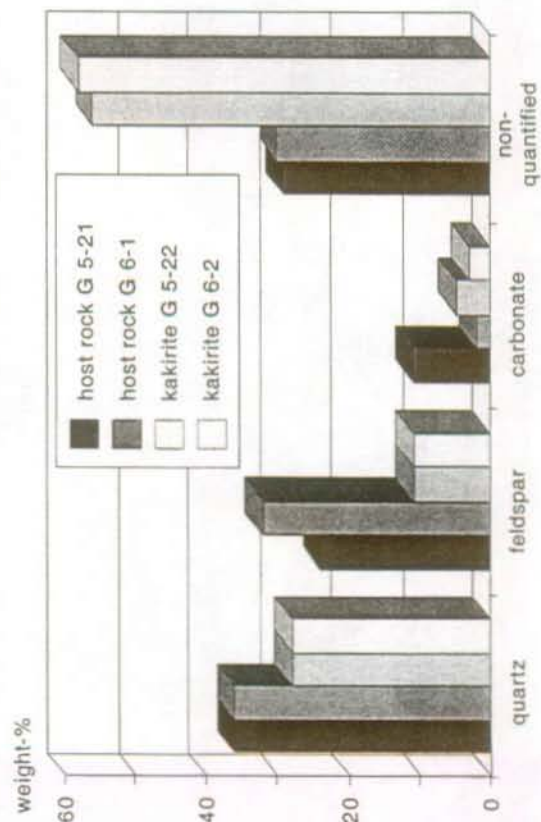
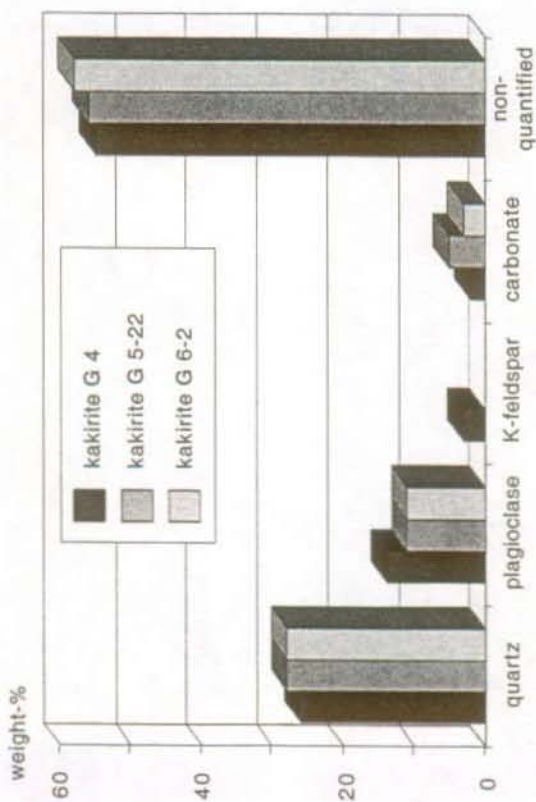
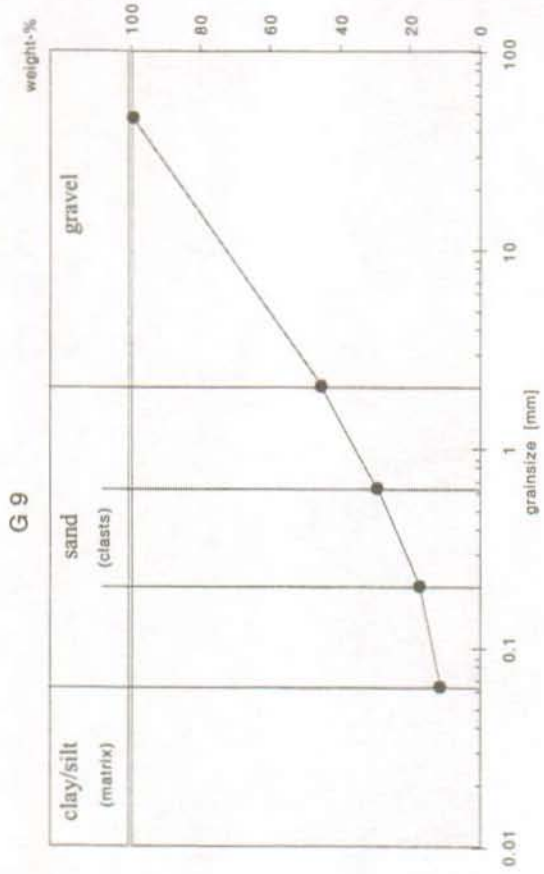


Figure 5-18: Cataclastic fabric adjacent to the host rock contact. Thin section image, plane polarised light, width of view 20mm. (Sample G-3, Dornbach Zone, borehole Goltschried)

With exception of the sample G10, the clast distribution reflects the disturbed old foliation and mineralogical layering. Clast orientation is clearly anisotropic with AF_1 of 0.41 and 0.87. In the sample G10 the old rock fabric is more disturbed and clast orientation homogeneous ($AF_1 = 0.98$). Clast density is found to be relatively high (max. 0.64) and the resulting TC's range between 0.43 and 0.98.



Figur 5-19: Mineralogical composition of host rock and kakirites samples from the Dornbach zone and Aar massif basement (G9), borehole Gollischried.

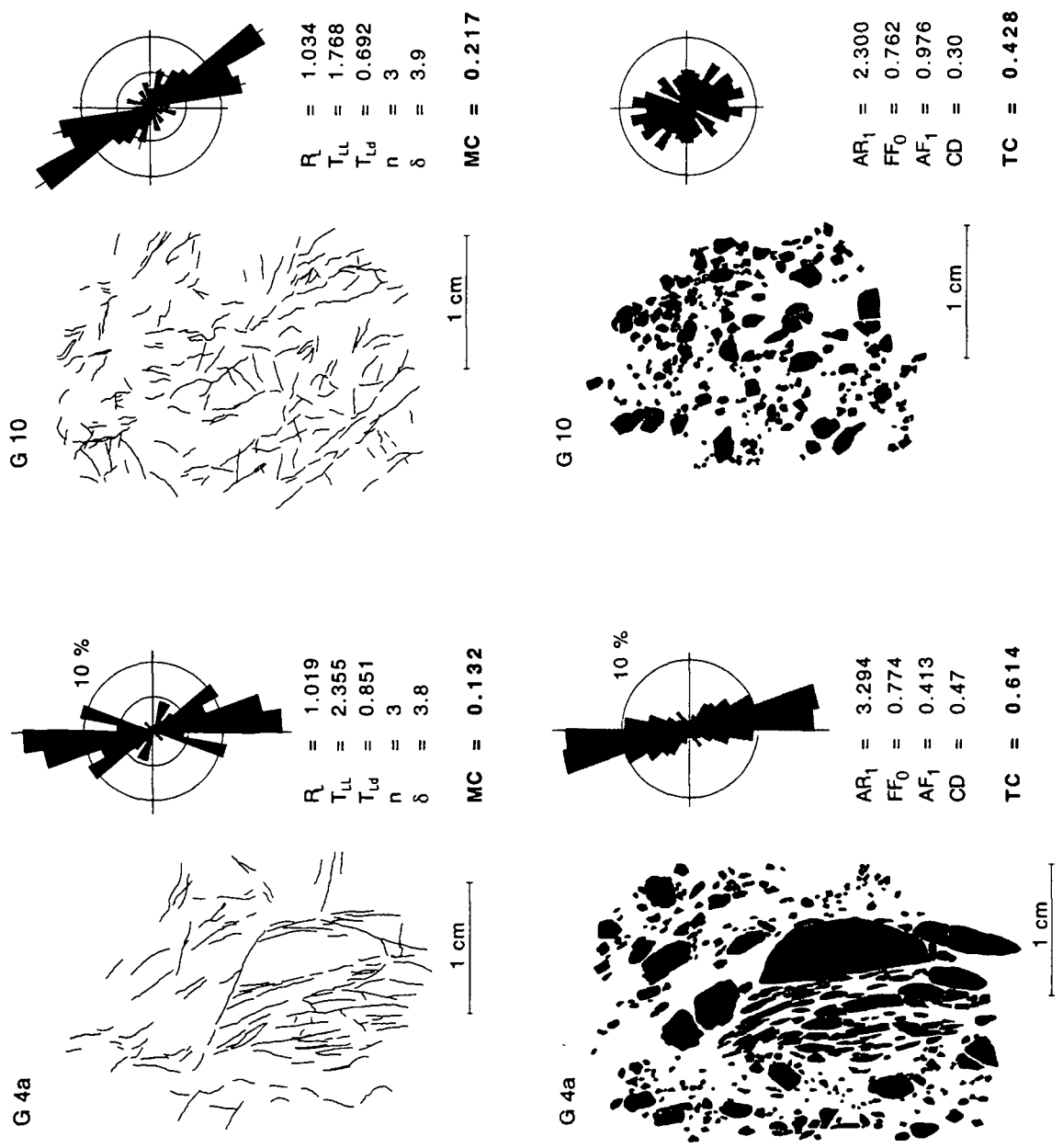


Figure 5-20: Quantified rock fabrics of kakirite samples from the southern branch of Dornbach zone, borehole Goltschried.

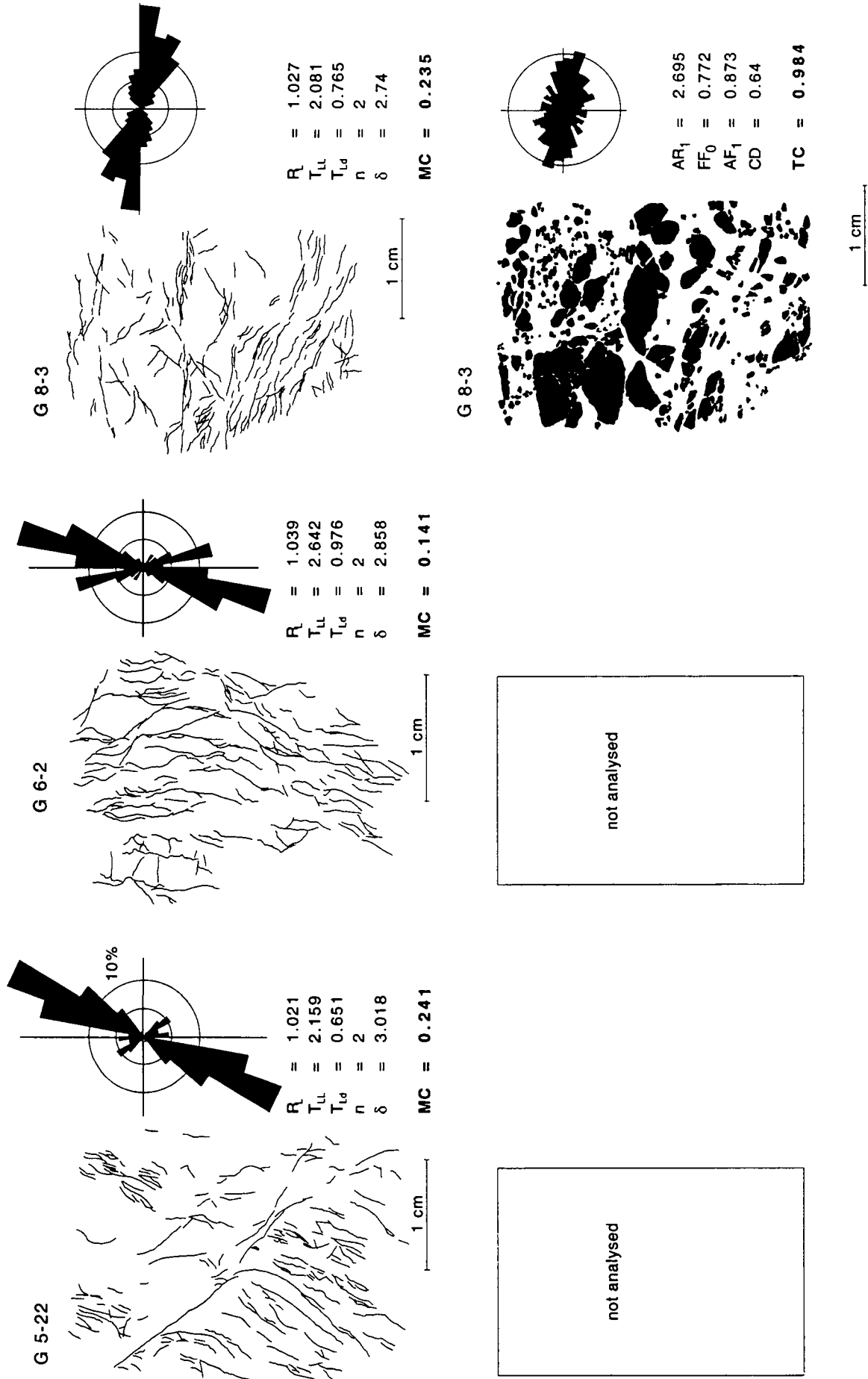


Figure 5-21: Quantified rock fabric of kakirite samples from the northern branch of Dornbach zone, borehole Goltschried.

5.1.5 Gallery Varzo

The gneiss of Antigorio nappe is composed of K-feldspar, plagioclase, quartz, biotite, muscovite and accessory minerals such as zircon, apatite, sphene, etc.. It shows a typical gneissic, crystalloblastic fabric with a spaced, more or less anastomosing foliation made of muscovite and biotite. With higher tectonic strain, quartz and plagioclase start to show brittle fracturing normal to the schistosity and alteration of biotite and plagioclase becomes more and more abundant.

In the studied kakirite samples from Varzo the original host rock fabric is still partially discernible. It has not so much been obliterated by cataclastic deformation but rather by important (hydrothermal) alteration processes. These processes are initiated by brittle cataclastic deformation which increases (initially) the permeability of the massif. Alteration is observed to affect the rock starting from open fractures in which large idiomorph carbonate has crystallised (Figure 5-22).



Figure 5-22: Rock fabric of hydrothermally altered kakirite sample. Note the idiomorph shape of carbonate crystals in the centre and upper right of the image. Original foliation from upper right to lower left. Thin section image, plane polarised light, width of view 30mm. (Sample Vz14, Varzo, TM 750)

XRD analyses have been performed on samples taken from the centre of the fault zone (Vz14a) and of the small clay-like layer (Vz2) at the contact to the host rock (chap. 3). The kakirite Vz14a contains about 40% quartz and phyllosilicate and relatively high content of carbonate (15%). Small amount of K-feldspar but no plagioclase has been detected in the XRD-pattern. The sample Vz2 is made up of mainly phyllosilicate with minor proportions of quartz, plagioclase and K-feldspar and very low carbonate content.

The sample Vz14a has an extended grainsize distribution with high gravel and relatively low silt/clay fraction proportions. The coarse grainsize fractions contain mainly quartz, phyllosilicate and carbonate, whereas the matrix fraction is composed principally of kaolinite (Append. II-e), an alteration product of plagioclase. In contrast to the kakirite samples from Cleuson-Dixence, quartz content does not show to decrease with grainsize, but is highest in the clast fraction. Supposed, as mentioned above, mechanical comminution to be less important than alteration processes, quartz grainsize would remain almost unchanged and hence a priori no decrease of quartz content with grainsize would have to be expected. In fact, the observed quartz - grainsize relation is thought to reflect more the original quartz grainsize distribution in the host rock than the effect of cataclasis. Alteration (fine-grained kaolinite) explains the high content of phyllosilicate in the matrix.

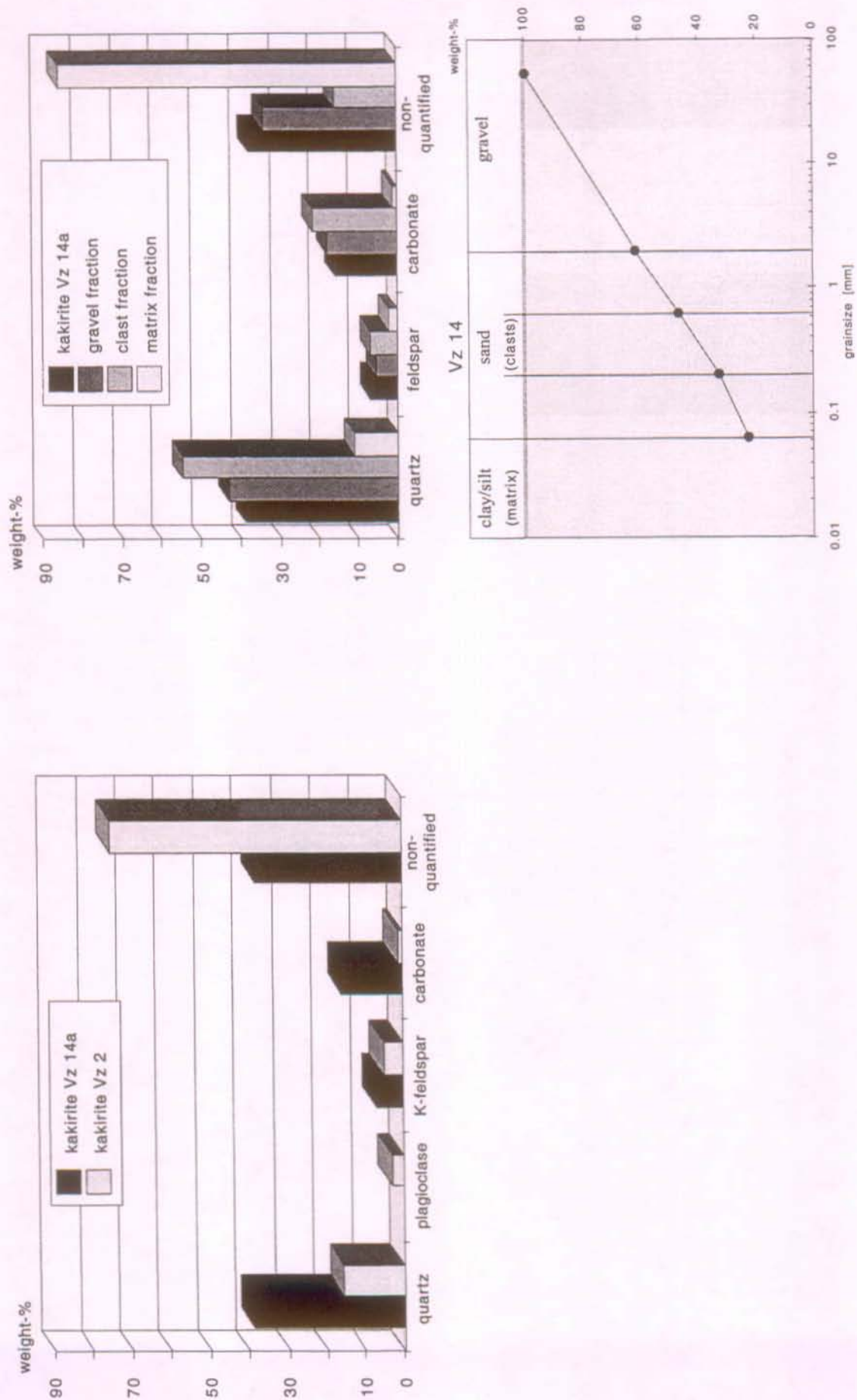


Figure 5-23: Mineralogical composition of kakirite samples from Varzo. Vz 2: clay-like layer at the contact to the host rock, Vz 14a: kakirite from the centre of the fault zone. (Varzo, TM 755).

5.2 Fault rocks in greenstones (Cleuson-Dixence, unit B)

At the microscopic scale the greenstone host rock samples are characterised by roundly shaped albite blasts superposed on a green coloured chlorite matrix. Albite commonly shows inclusion of sphene, chlorite and white mica tracing the underlying schistosity. Calcite is observed to have crystallised in proximity of albite crystals. The weakly developed continuous foliation is defined by lepidoblastic chlorite. In slightly deformed greenstones, thin carbonate veins crosscutting the foliation and albite blasts are observed.

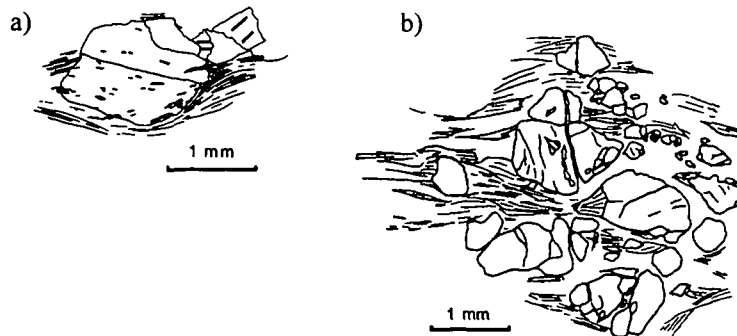


Figure 5-24: Sketch showing the microfabric of greenstone host rock: a) Inclusions of white mica and sphene in albite are arranged concordant to the underlying schistosity. b) Brittle fracture crosscutting albite crystals. (Samples CD4, CD14, Cleuson-Dixence, unit B, TM 3017, 3038)

The microfabrics of the greenstone kakirite samples are similar to the one of the undeformed host rock inasmuch as they show feldspar eyes (clasts) surrounded by a chlorite rich matrix. Old schistosity in contrast is intensely disordered and only locally preserved. Fractures and shearzones, often marked by a small flaky chlorite crystals, have developed principally in the cleavage domains but as shown in Figure 5-24 they also crosscut "hard" albite grains.

Polymineralic clasts composed mainly of albite, carbonate and chlorite are dominant. In up to 10mm large aggregates the original schistose rock fabric can be recognised. A few large monomineralic chlorite clasts of former cleavage domains have been observed. Monomineralic clasts of albite and/or carbonate measure in general only a few millimetres. Carbonate veins truncated at the clast boundaries and discordant foliation between clasts and surrounding matrix show evidence of rigid body rotation to have occurred.

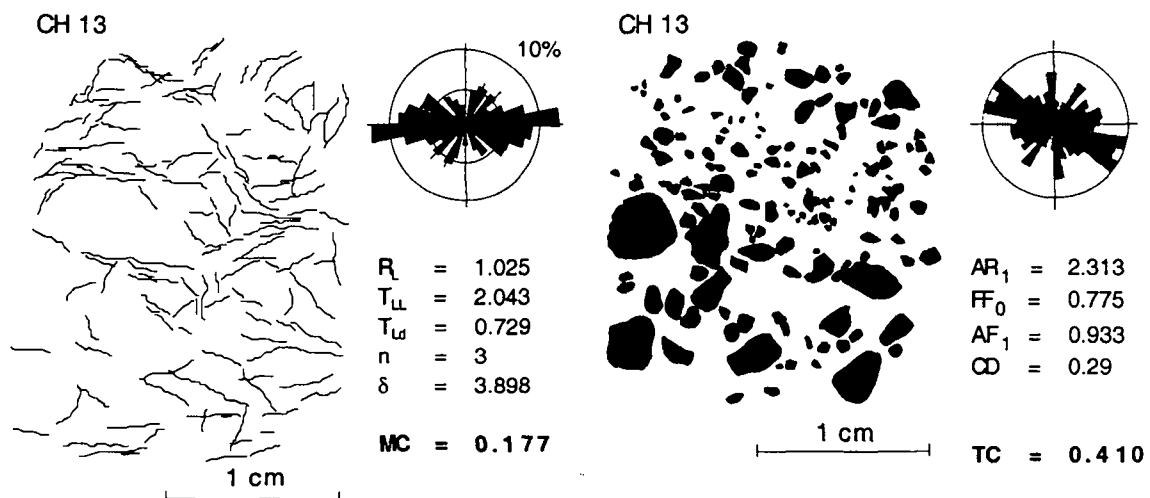


Figure 5-25: Quantified rock fabric of greenstone kakirite. (Cleuson-Dixence, TM 4290)

The studied sample CH13 shows a relatively low MC 0.18 due to the presence of three discontinuity sets forming angles of 20 and 40°. The determined TC is average (0.41).

The mineralogical composition of host rock and kakirites is quite similar, minor differences exist in quartz, amphibole and carbonate content. Quartz, the clast forming competent mineral phase in the kakirites of the quartzo-phyllitic series, is replaced by feldspar, which makes up about 30% of the rock. The non-quantified proportion is composed principally of chlorite

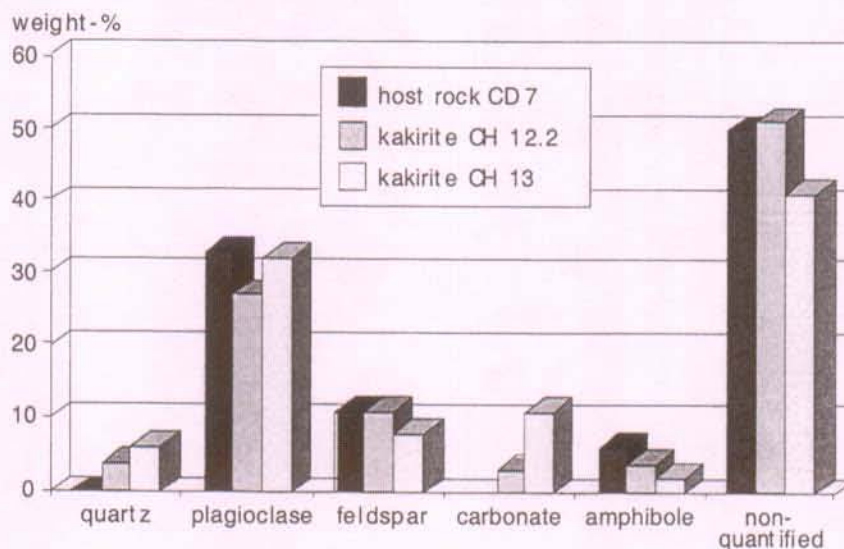


Figure 5-26: Mineralogical composition of greenstone kakirite and host rock samples from Cleuson-Dixence, unit B.

Thin section analyses show that carbonate in the analysed kakirites samples has crystallised in fractures and veins. It can be related to the effect of tectonic deformation involving extensional fracturing.

5.3 Fault rocks in serpentinite (Genoa, Italy)

5.3.1 Massif serpentinite

In the kakirites formed in massif serpentinite (Borzoli Cavern) no distinction of clasts and matrix is possible at the microscopic and mesoscopic scale of handspecimens. In fact, they are made up only of clasts separated from each other by thin discontinuities, along which only very limited differential movements seem to have occurred.

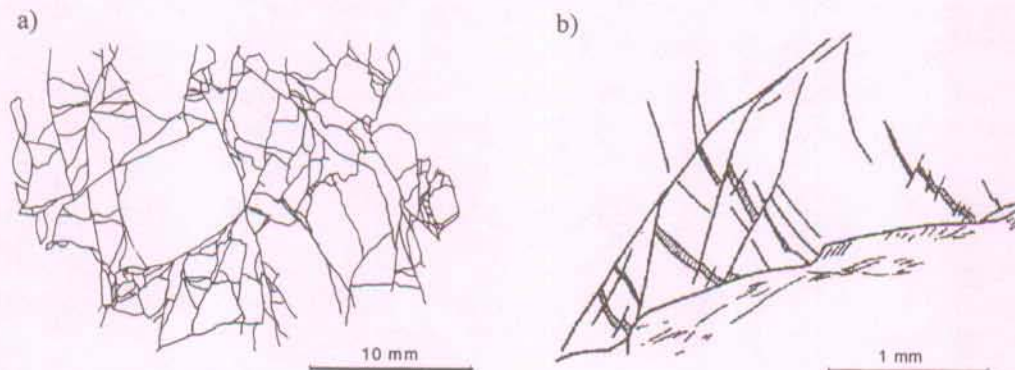


Figure 5-27: Microfabric of kakirite from massif serpentinite. a): The very angular clast shape is determined by the fracture network. b): Discontinuities crosscutting older tension veins showing small differential movements. (Sample MG20.1, Borzoli Cavern)

The very angular clast shape is principally determined by the geometry of the fracture network (Figure 5-27). Microfractures often show evidence of extension with crystallisation of fibrous serpentine normal to the fractures.

For one kakirite sample (MG20.1b) the matrix coefficient has been determined (Figure 5-29). Three discontinuity sets were identified with high angle differences of 30°, 60° and 90° and a resulting orientation factor of $\delta = 4.1$. The calculated MC is 0.14.

The kakirite samples are composed almost entirely of serpentine with only some accessory contents of relictic amphiboles, feldspar, opaque minerals and carbonate crystallised in small veins (Append. II-f). Serpentine has been identified to be lizardite. The grainsize distribution is dominated by the fine to coarse sand fraction (65%). No mineralogical differences have been identified between the different grainsize fractions.

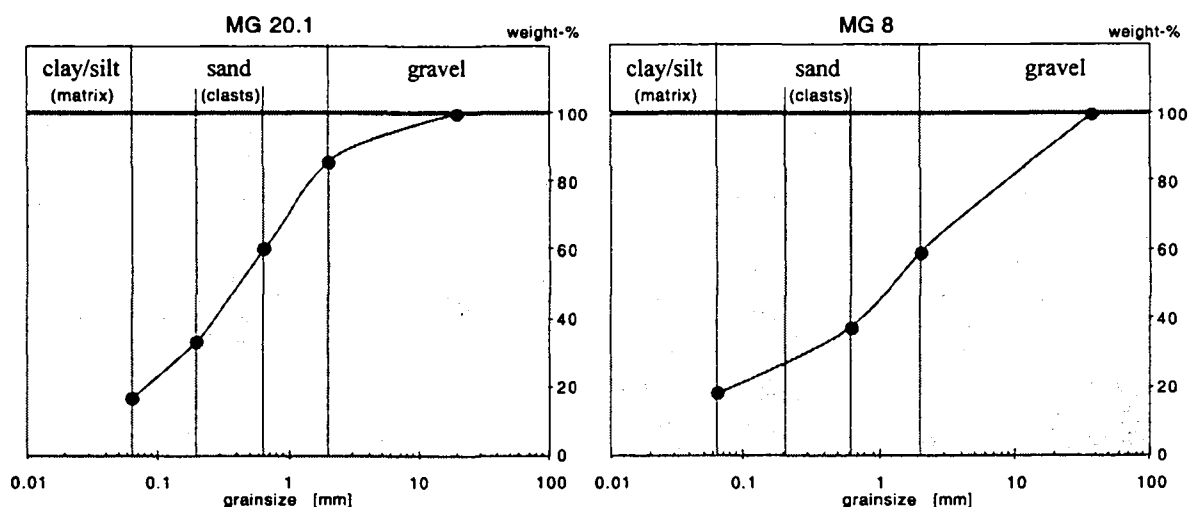


Figure 5-28: Granulometry of kakirite samples from massif (MG20.1) and schistose serpentinite (MG8) Borzoli cavern.

5.3.2 Schistose serpentinite

At the microscopic scale the kakirites of serpentinoschist (MG24.1) show to be composed mainly of flaky serpentine (lizardite) and variable proportions of chlorite and hydroxide forming a rough schistosity. Lenticular grains are composed of very fine-grained serpentine and high content of magnetite. Clasts are intensely fractured. In the fine-grained, often strongly weathered matrix small shear zones are discernible. The rock fabrics of two samples have been quantified (Figure 5-29). Schistosity is defined by rather short trace lines with a mean length of 1.3, respectively 1.4 millimetres and a low discontinuity roughness. One, respectively two discontinuity sets have been identified with resulting MC of 0.58 and 0.32.

The texture coefficient has been determined only for the sample MG24.1b. It bears dominantly small clasts at the limit of resolution of the chosen magnification scale. Clast are very angular and show a clear preferred orientation ($AF_0 = 0.72$). The calculated TC is 0.23.

Determined grainsize distribution (Figure 5-28) is extended with 40% gravel, consisting of irregular, extremely blade-shaped to lenticular clasts. Performed XRD analyses of entire kakirite samples show principally serpentinite of lizardite type with some minor amount of chlorite and accessory some amphibole, feldspar and calcite (Append II-f). The different grainsize fractions have not been analysed separately.

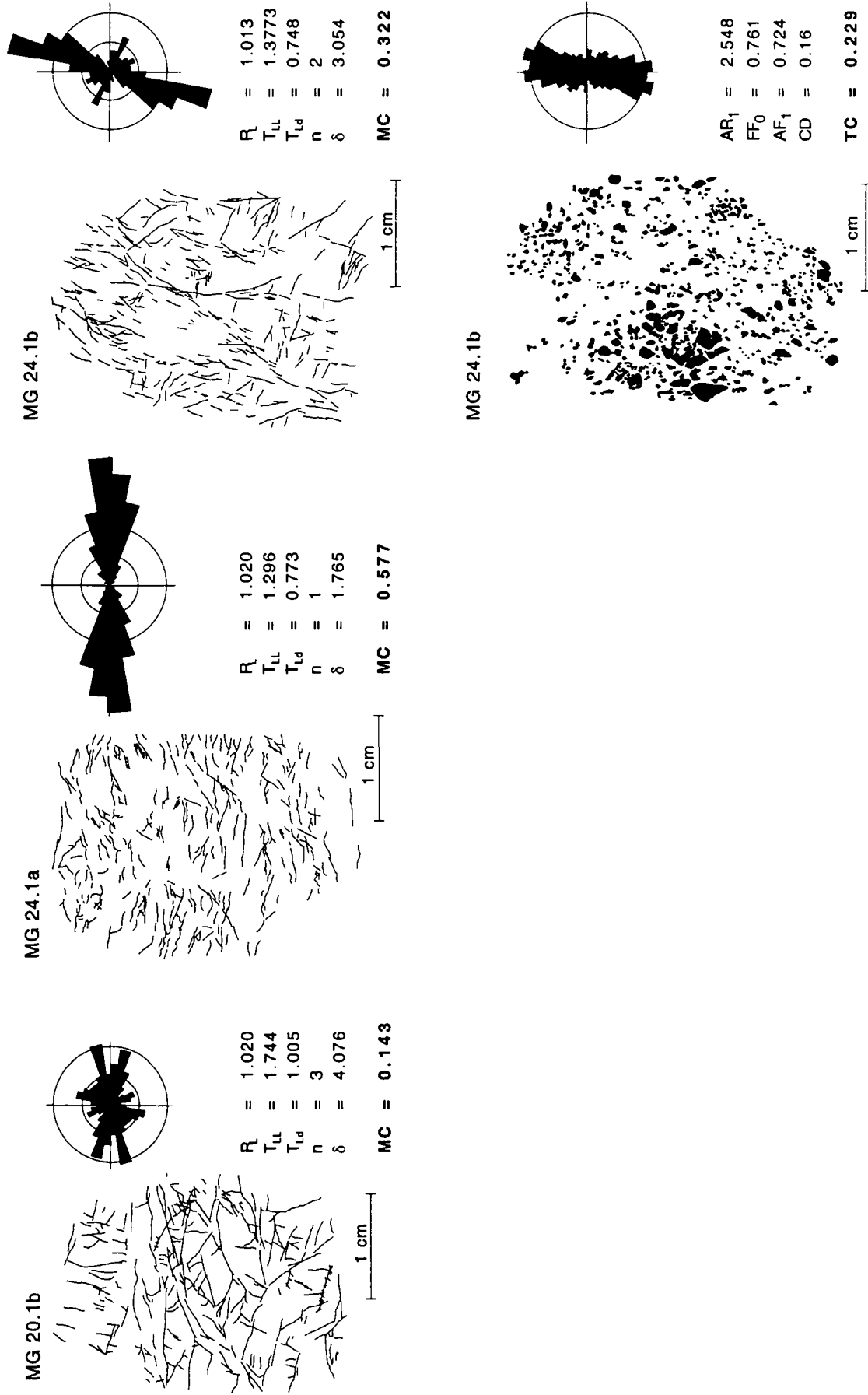


Figure 5-29: Quantified rock fabric of kikirite samples from massif (MG 20.1) and schistose serpentinite (MG24.1). Genoa, cavern Borzoli.

5.4 Fault rocks in carbonate rocks (Cleuson-Dixence, unit D)

The sampled breccia of the "Verrucano" unit is composed mainly of light greyish, commonly rounded clasts (up to 2cm large) taken in a characteristic yellow to orange coloured matrix. Based on this macroscopic observation, it is often called "dolomitic breccia". In the studied samples however only minor proportions of dolomite have been identified (about 1%, Figure 5-30). It is found mainly in the clast fraction (0.2 - 0.6mm), in which it makes up 25 weight-%. High contents of phyllosilicate are noted.

In thin sections an isotropic, loosely packed granular rock fabric with striking high porosity is observed. Clasts are light brownish, completely altered and composed of microcrystalline phyllosilicate and hydroxide together some scarce polycrystalline quartz grains. Idiomorph carbonate (dolomite) has crystallised in the matrix pores. This is thought to be the dolomite detected in the clast grainsize fraction.

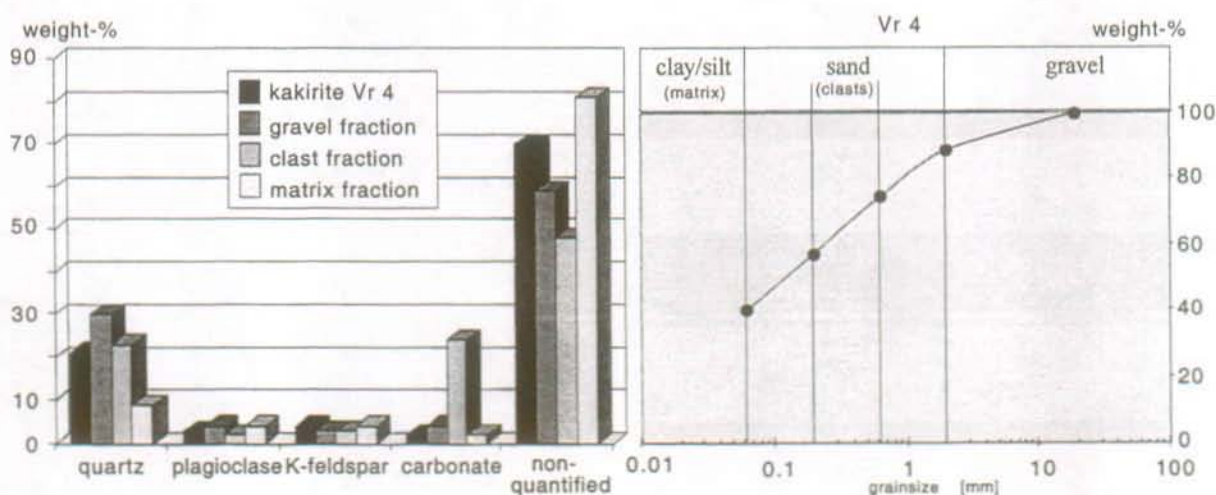


Figure 5-30: Mineralogical composition and granulometry of the "dolomitic breccia". Cleuson-Dixence, unit D, "Verrucano".

For two breccia samples the granular rock fabrics have been quantified. No discontinuities were discernible in the matrix. Quite similar clast parameters have been found. The clast orientations are nearly isotropic with $AF = 1.0$, respectively 0.93 . The determined TC are 0.31 and 0.35 .

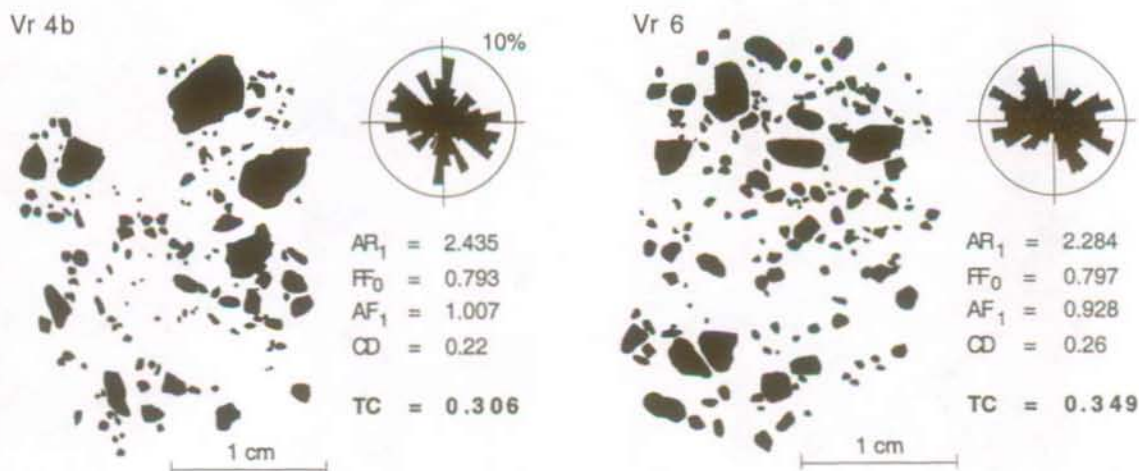


Figure 5-31: Quantified rock fabric of breccia. Cleuson-Dixence, unit D "Verrucano", TM 450.

5.5 Synthesis

Within the quartzo-phyllitic series the observed range of mineralogical proportions is quite large. For comparison between the kakirite samples from the different underground sites, the mineralogical composition is expressed by means of the calculated mean weighted Vickers hardness (mwVh).

In Figure 5-32, the samples from Cleuson-Dixence unit C and Goltschried show a relatively narrow range of Vickers hardness. The samples from unit B in contrast show a more heterogeneous mineralogy at the meso- to microscopic scale.

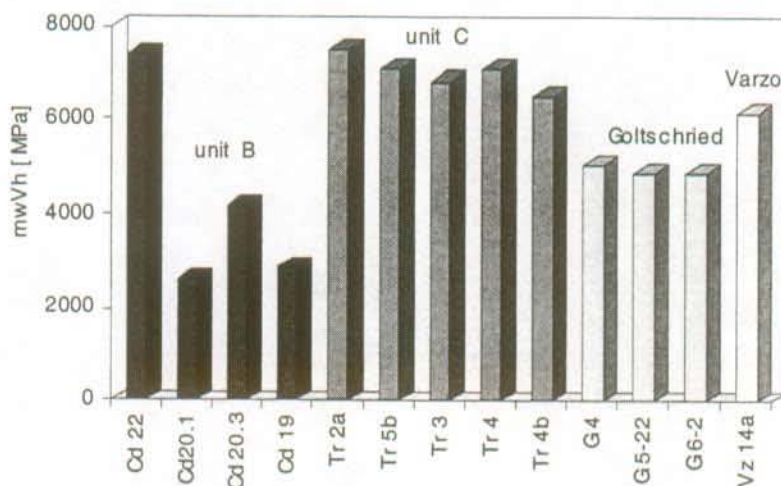


Figure 5-32: MwVh of kakirite from the quartzo-phyllitic series of Cleuson-Dixence unit B and C, Goltschried and Varzo.

A continuous series between the two end-members quartz and phyllosilicate has been noted amongst the kakirites from Cleuson-Dixence unit D, Zerjona. The quartz content varies between 10 and 70%, the one of phyllosilicate between 20 and 80%. Feldspar and carbonate play a minor role, varying in general between 5 and 10 weight-%. The determined mwVh are presented in Figure 5-33. The four macroscopically and mineralogically defined sub-groups are distinguished from each other by steps of Δ -mwVh of about 1 GPa.

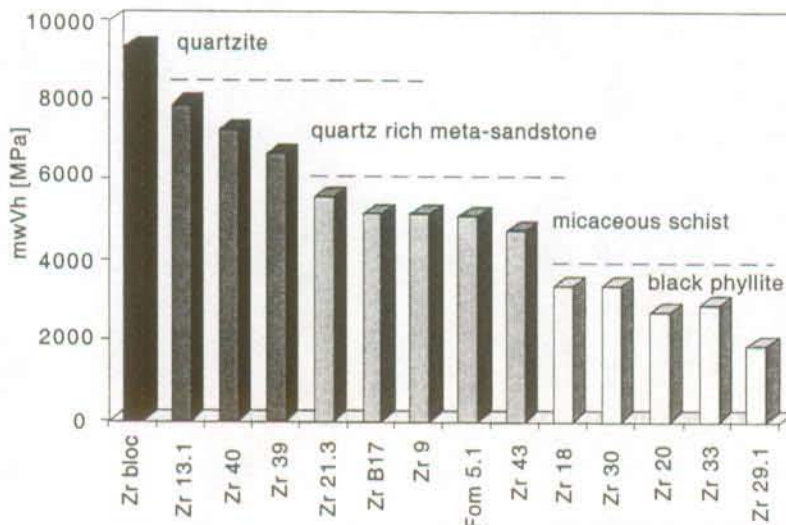


Figure 5-33: MwVh of kakirites from the quartzo-phyllitic series. Cleuson-Dixence, Zerjona.

The mineralogical series from Zerjona (Figure 5-33) has been observed on a rather limited number of analysed samples. The presented mineralogical, respectively Vickers hardness limits between the sub-groups have to be considered therefore with caution and are not intended to be generalised.

The mwVh of both, the greenstone kakirites and "dolomitic breccia" is close to 4GPa. The first is composed mainly of feldspar and chlorite, the second one of quartz and white mica. No data concerning the Vickers hardness of serpentine minerals have been found in literature.

The analysed kakirites samples have been regrouped in function of their mwVh as follows:

mwVh [GPa]	kakirite/rock type	site
< 4	- chlorito-sericitic schist	Cleuson-Dixence unit B
	- black phyllite	Cleuson-Dixence unit D, Zerjona
	- "dolomitic breccia"	Cleuson-Dixence unit D, "Verrucano"
4 - 6	- greenstone	Cleuson-Dixence unit B
	- micaceous schist	Cleuson-Dixence unit D, Zerjona
	- mica schist Dornbach Z.	Goltschried
6 - 8	- quartzo-sericitic schist	Cleuson-Dixence unit B and C
	- quartz rich metasandstone	Cleuson-Dixence unit D, Zerjona
	- gneiss Antigorio nappe	Varzo
	- gneiss Aar massif	Goltschried
> 8	- quartzite	Cleuson-Dixence unit D, Zerjona

Table 5-1: Grouping of the analysed rocks in function of their mineralogical composition expressed by the mean weighted Vickers hardness (mwVh).

Comparison between the mineralogical composition of kakirite and adjacent host rock samples has shown higher phyllosilicate and lower quartz proportions in the kakirites of mica schist. In terms of mwVh the difference is on the order of 2GPa. Based on thin section analyses these differences can be identified to be due to original mineralogical varieties between the host rock and the zone where faulting has occurred. Alteration of feldspar additionally increases the phyllosilicate proportion in the kakirite, this can however hardly be quantified by the performed analyses. With exception of the samples from Varzo, in fact only minor proportions of alteration mineral phases (kaolinite) have been detected.

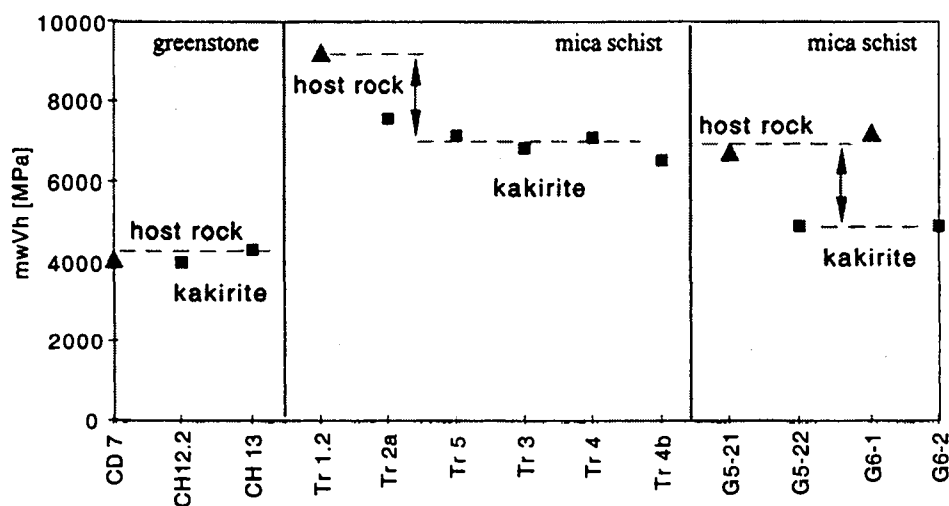


Figure 5-34: Comparison of the mwVh of kakirites and adjacent host rock.

In the case of the analysed greenstones no significant mineralogical differences between kakirites and host rock are discernible.

All sieved kakirite samples show extended grainsize distributions with in general high silt/clay grainsize proportions (mean 44%, min. 11%, max. 85% for analysed kakirites of the quartzo-phyllitic series). The quartz/phyllsilicate ratio is considerably higher in the coarser grained clast fractions than in the matrix fraction. The ratio of mwVh (clast fraction) to mwVh (matrix) is varying between 1.0 and 3.5, with an average value of 1.7.

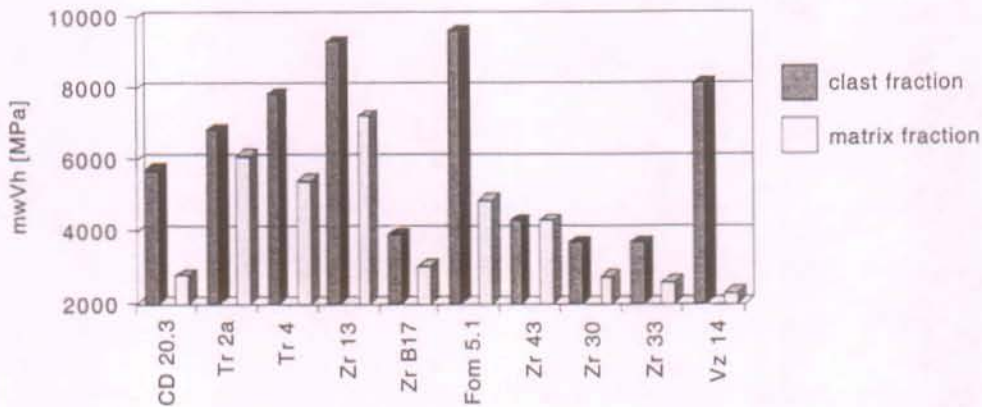


Figure 5-35: Comparison of mwVh of kakirite-clast and -matrix grainsize fractions.

Analysed kakirite fabrics can be separated in two major types. First, granular fabrics, bearing angular clasts in a homogeneously fine-grained, isotropic matrix. Second, discontinuity dominant fabrics, characterised by (dense) discontinuity patterns but without discernible clasts. For these end-member fabrics only one of the two parameters TC, respectively MC can be determined: The missing one is set equal to zero. Transition between granular and discontinuity dominant fabric is observed to be gradual.

The development of the type of cataclastic rock fabrics is observed to depend largely on the mineralogical composition, namely on the competence contrast between hard and weak mineral phases and on their spatial distribution in the host rock. In the case of a spaced original schistosity, discrete faulting and the development of competent clasts and incompetent matrix has been observed. In phyllosilicate rich rocks with a continuous cleavage however, strain is accommodated mainly by differential slip along discrete, anastomosing discontinuity planes controlled by the cleavage orientation. In these rocks it is often difficult, or even impossible to clearly determine clast boundaries. If clasts can be identified, they involve often deformed quartz veins. This observation is confirmed by the decreasing clast density in the quartzo-phyllitic series of Zerjona. The found CD is ~ 0.30 in the quartzite, ~ 0.15 in the metasandstone and ~ 0.10 in the kakirites of black phyllite. Another striking evidence for the influence of the original host rock structure on the kakirite fabric has been discussed considering the kakirites samples from Cleuson-Dixence unit C.

5.5.1 Conceptual rock fabric - mineralogy diagram

The MC and TC parameters have been assembled in a single diagram, called the *MC-TC fabric diagram*. The two extreme rock fabrics are plotting along the x- and y-axis respectively, the intermediate ones plot inside the diagram area. In a general way, and in correspondence to the definitions of the fabric parameters, samples of low (structural) rock strength plot towards the lower left corner of the MC-TC diagram. Samples of higher strength, and higher MC- and/or TC-values, tend to plot towards one of the three opposite corners. The range of the MC and TC values of all analysed kakirite samples is presented in Figure 5-36.

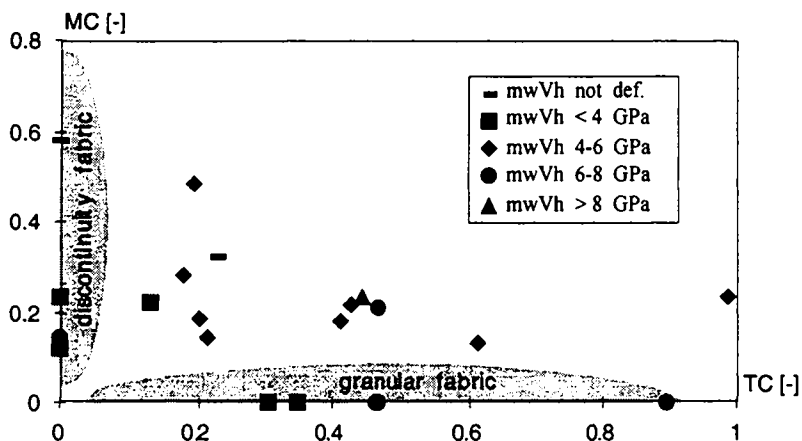


Figure 5-36: MC-TC fabric diagram presenting the range of variability of all quantified kakirite rock fabrics. Symbols correspond to different values of mwVh.

The third axis of the presented MC-TC fabric diagram is the mineralogical composition, considered to be the other rock strength controlling factor (chap. 4.4). The general formulation of p. 37 has been redefined in a first approach as follows:

$$\text{geomechanical properties} = f(\text{mwVh}(\text{MC}+\text{TC})) \tag{Eq. 5-1}$$

This definition reflects the idea that rock strength is controlled at first by the mineralogical composition (mwVh) and that the MC and TC parameters are rock fabric "correction factors". They adjust the theoretically possible, mineralogical rock strength by taking into account the structural characteristics. As shown in Figure 5-36, MC and TC are of similar scale and both vary between 0.0 and 1.0 for the analysed kakirites. Supposed to control rock strength with equivalent weights, they have been summed up and multiplied by the Vickers hardness. MC and TC are dimensionless parameters, the product $\text{mwVh}(\text{MC}+\text{TC})$ of Eq. 5-1 is expressed in [GPa].

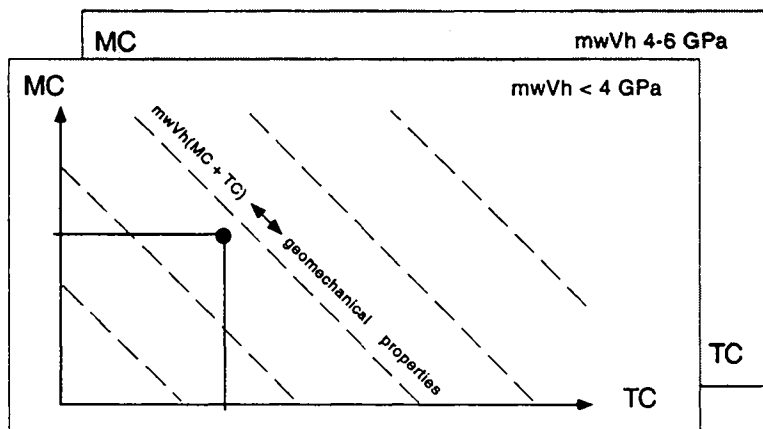


Figure 5-37: Conceptual method for the characterisation of weak cataclastic fault rocks taking into account their mineralogical composition (mwVh) and rock fabric (MC, TC).

The presented definition of Eq. 5-1 is only a conceptual approach. In the future the relationship between MC, TC and mwVh, respectively between the three geological factors and chosen geomechanical parameters (e.g. compressive strength, Young modulus) will have to be identified more in detail.

In its final stage, the concept of the MC-TC diagram is thought to enable the assessment of the geomechanical properties of fault rocks by entering the determined MC, TC fabric parameters in the chart (Figure 5-37) of the corresponding mineralogical composition (mwVh).

5.5.2 Critical discussion of the proposed characterisation method

The geological characterisation of above can only be validated if the resulting data can be put into correlation with the corresponding geomechanical behaviour. In the limited time of the study it was not possible to identify separately the influence and/or accuracy of the involved microstructural parameters, respectively the MC and TC. A few fundamental aspects and observations made during the application of the method are discussed below. A first attempt to evaluate the validity of the proposed method is presented in chap. 6.

The accuracy of the TC and the involved parameters has been tested on samples of intact rocks with varying success by different authors (Ersoy & Waller, 1995, Azzoni et al., 1992, Howarth & Rowlands, 1986, 1987). The rock fabric of weak cataclastic fault rocks differs from that of ordinary intact rocks by a generally lower grain, respectively clast density (CD) and a high proportion of weak, often phyllosilicate rich matrix. It is the great strength contrast between clasts and matrix which makes the TC especially adapted to weak cataclastic fault rocks. In fact, as shown by Azzoni et al. (1992), the concept of the TC is not appropriate for rocks with a low strength contrast between grains (clasts) and matrix, as e.g. in the case of igneous rocks with porphyritic texture.

The CD of the analysed kakirite samples varies between 0.09 and 0.64 with a mean density of 0.28. At first glance this would suggest that clasts behave passively during deformation and that rock strength is controlled principally by the matrix properties (Figure 2.6, p. 11). Thin section analyses show however, that clasts accommodate considerable cataclastic strain by fracturing and comminution, and this even when they are dispersed in the weak matrix (Figure 5-10, Keller et al., 1997). The decreasing influence of clasts on rock strength with decreasing CD is furthermore taken into account by the weighting of the TC (chap. 4.4.2.1, Eq. 4.5).

The TC and MC are deficient inasmuch as neither of them takes into account the spatial distribution of the clasts, respectively of the discontinuities, which are not necessarily homogeneous at the considered scale (e.g. Zr9, Zr43).

The most complex parameter of the developed MC is the orientation factor δ . By the involved parameters (chap. 4.4.2.2), δ increasing stepwise with the number of discontinuity sets (n) but much less in function of the increasing angles $\Delta\beta_i$ in-between. The influence of $\Delta\beta_i$ is hence supposed to be slightly underestimated in the present form of δ .

With reference to the rock fabrics of the samples G4a and G5-22 (Figure 5-20 and Figure 5-21), it is furthermore observed, that the number of discontinuity sets (n) determined simply by counting rose diagram petals exceeding a pre-defined level (e.g. 5%) is not always justified. In the case of G4a the secondary discontinuity set (orientated from upper left to lower right) is not taken into account as its cumulative length is just below this critical level. In sample G5-22 in contrast, it is just above it and its orientation contributes to the determination of the MC. From the geomechanical point of view and depending on the relative orientation of the applied load, both of these minor discontinuity sets may however control the rock strength. Whether a discontinuity set has to be taken into account or not has therefore to be decided considering the rose diagram *and* the observed spatial distribution of the discontinuities.

The developed characterisation method is based on a simplified approach, taking into account only mineralogical and structural properties of cataclastic fault rocks (chap. 4.4). The author is however conscious that many other factors (e.g. water content, presence of graphite, swelling clay minerals, etc.) may influence the geomechanical properties of these rocks. The presence of water, for example has shown to decrease importantly the geomechanical strength of kakirites. They often slake rapidly and turn into mud when they get in contact with it (see disaggregation of kakirite samples for grain size analyses). Water content (pore water pressure) will certainly have to be taken into account in the future for a more complete geological and geomechanical characterisation of weak cataclastic fault rocks.

6 CORRELATION OF GEOLOGICAL AND GEOMECHANICAL PROPERTIES

In this research on cataclastic fault rocks, a concept has been developed by which a more objective and quantitative geological characterisation of weak cataclastic fault rocks is possible. For the validation of the proposed method, finally only a few samples and very little time remained. The presented attempt to correlate geological and geomechanical properties has therefore to be regarded with great caution. Much more work will have to be done to confirm and improve the developed parameters.

The geomechanical properties of the analysed cataclastic fault rocks have been identified by Habimana (1999). A large number of different laboratory tests (mainly triaxial tests) have been performed in order to determine their stress-strain behaviour and to define an accurate failure criterion. For practical reasons, as mentioned initially, it was in general not possible to analyse exactly the tested samples. Furthermore, the equality of "corresponding" geological and geomechanical samples has often shown to be questionable due to frequently observed structural heterogeneities at the mesoscopic scale (e.g. strongly folded schistosity, presence of quartz veins, etc.). Only 12 samples could finally be retained for the correlation of the geological and geomechanical properties of kakirites.

As most of the analysed fault rock samples show macroscopically structural anisotropy (schistosity), correlation was only possible amongst samples tested and analysed with the same orientation relative to the applied load. Attention has been paid to this during sampling in the gallery and during sample preparation in the laboratory (chap. 4). However, due to the specific sampling and preparation techniques and the poor mechanical properties of kakirites, it was in general not possible to verify in detail the orientation of the schistosity after the geomechanical tests. This is one of the insufficiencies of the study which will have to be improved in a future work.

The most popular geomechanical parameter used for correlation purposes between different rock types is uniaxial compressive strength (σ_c). For evident reasons, this parameter can however hardly be determined in the case of weak cataclastic fault rocks. The geomechanical characterisation developed by Habimana (1999) is hence mainly based on triaxial test. In a simplified approach, the major principal stress at failure (σ_1) for a given confining pressure (σ_3) has been retained for correlation purposes. In order to take into account the non-linearity of the strength criterion of Habimana (1999), two principal stresses, namely $\sigma_1(5)$ and $\sigma_1(10)$, with $\sigma_3 = 5\text{MPa}$, respectively $\sigma_3 = 10\text{MPa}$ have been chosen. As the triaxial tests have not necessarily been performed exactly at these confining pressures, interpolation was necessary. The proceeding is illustrated in below.

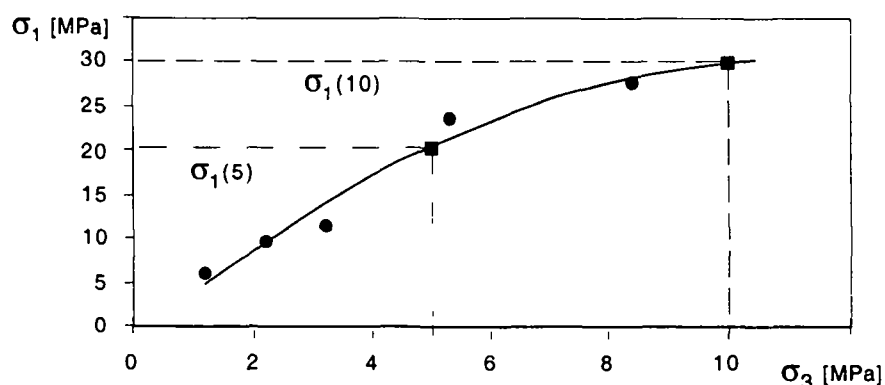


Figure 6-1: Concept for the determination of $\sigma_1(5)$, respectively $\sigma_1(10)$ by best fit regression using data from Habimana (1999).

The geological and geomechanical parameters of the kakirite samples which could be put into correlation are presented in Table 6-1.

sample	host rock	mwVh [GPa]	MC [-]	TC [-]	corresp. sample	$\sigma_1(5)$ [MPa]	$\sigma_1(10)$ [MPa]
Zr bloc	quartzite	9.3	0.233	0.444	A7 - A9	56	78
Zr 39b	quartzitic metasandstone	6.7	0.209	0.465	Zr39	22	38
Zr 9	micaceous schist	5.2	0.188	0.202	Zr9	21	30
Zr 43	micaceous schist	4.7	0.141	0.213	Zr40	22	38
Zr 30	black phyllite	3.4	0.117	0.0	Zr30, ZrX	14	25
Zr 33	black phyllite	2.9	0.223	0.130	Zr33	15	25
Zr 46	black phyllite	2.7	0.121	0.0	Zr46	16	28
G 4	schist	5.0	0.132	0.614	G95/23	26	43
G 10	schist	5.0	0.217	0.428	G95/23	26	43
Vr 4b	"dolomitic breccia"	3.8	0.0	0.306	Vr20 - 25	15	20
Vr 6	"dolomitic breccia"	3.8	0.0	0.349	Vr20 - 25	15	20
CH 13	greenstone	4.3	0.177	0.410	CH 3, 20, 21, 23	24	44

Table 6-1: Summary table of corresponding kakirite samples and fabric parameters.

Only a few samples with the same mineralogical composition were available, therefore no attempt has been made to correlate the MC or TC directly with the rock strength. However, taking all samples of different mineralogy together, no evident relationship between rock fabric and rock strength can a priori be expected to exist. In fact, kakirites with the same rock fabric (and same MC and TC values) can be formed in very different lithologies. With the available samples, the rock fabric parameters can hence only be correlated with $\sigma_1(5)$ and $\sigma_1(10)$ when the mineralogical composition is taken into account. An attempt of correlation has been made with the product $mwVh \cdot (MC+TC)$ as proposed in Eq. 5-1 of chap. 5.

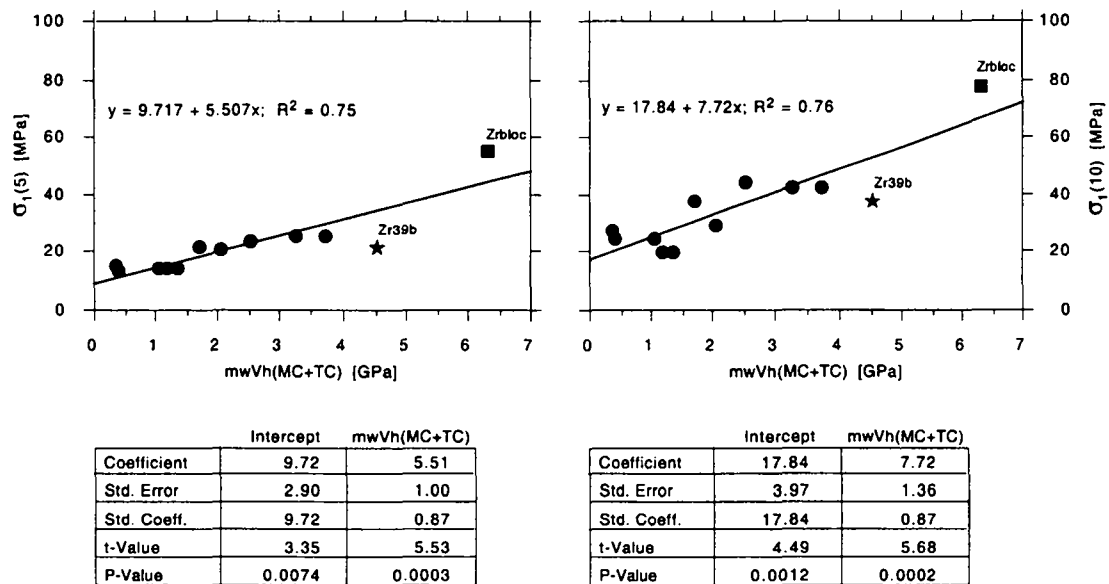


Figure 6-2: Correlation of geological and geomechanical properties of the kakirites of Table 6-1.

Relatively good correlation coefficients of $R=0.87$ have been found to exist between the rock strength and the geological parameters (Figure 6-2). The performed t-tests confirm both correlations to be significant at the level 0.05. The above correlation coefficients are however biased by the overestimated weight of the distant point in the upper right corner of the diagrams. The point is representing the quartzite-cataclasite sample *Zrbloc*, which in fact has shown a considerably higher rock strength than the other samples. In order to verify if the correlations are

still significant without this sample, it has been removed from the list and the coefficients recalculated. They drop in fact from $R=0.87$ to 0.82 respectively to 0.75 . They statistically still significant.

As mentioned above, the rock fabric parameters could not be correlated with the rock strength without involving the mineralogical composition. The validity and weight of the term (MC+TC) can in contrast be assessed indirectly by comparison with the correlation of the mwVh vs. rock strength (see also Calamebert et al. 1980a,b, 1982). As shown in Figure 6-3, a relatively good correlation is found. Without the sample Zrbloc however, the correlation coefficients drop from $R=0.90$ to 0.71 , respectively from 0.86 to 0.60 . They are clearly lower than the ones found for mwVh(MC+TC) vs. $\sigma_1(5)$.

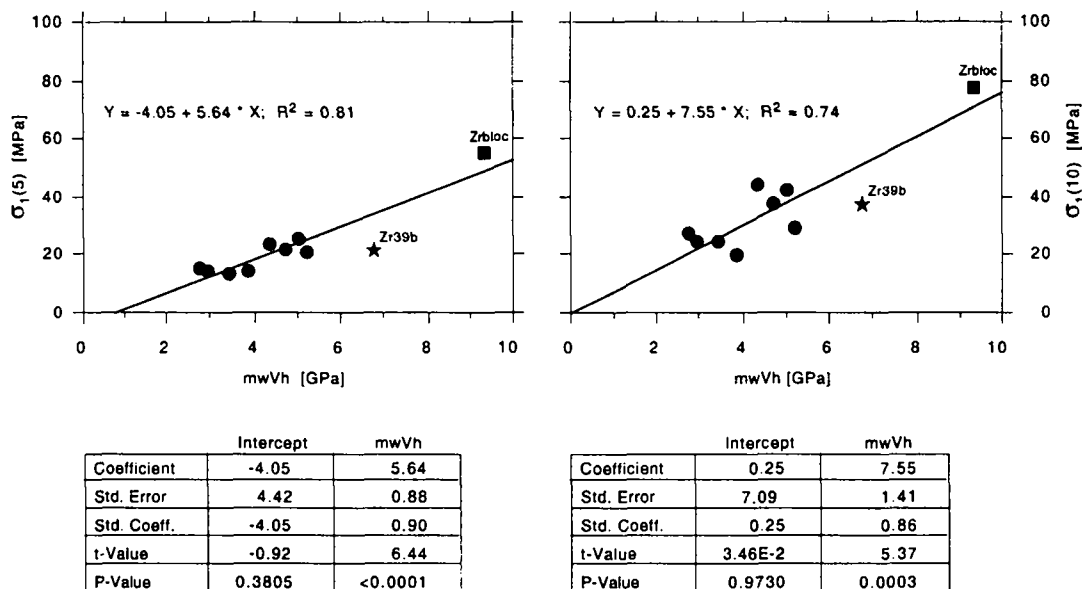


Figure 6-3: Correlation between mineralogical composition (mwVh) and triaxial rock strength.

The higher R found for the correlation of mwVh(MC+TC) vs. $\sigma_1(5)$, respectively $\sigma_1(10)$ is taken as an indication for the accuracy and adjusting effect of the MC and TC parameters.

Based on the preceding, a tendency of a positive correlation between the developed geological parameters and the geomechanical strength can be deduced. However, it is repeated again, due to the small number of samples and the reasons mentioned above this correlation can not pretend to validate the proposed characterisation method for kakirites. It can only be taken as a strong motivation to continue research on cataclastic fault rocks with the chosen mineralo-structural approach.

For this first rough evaluation of the proposed characterisation method only a linear correlation has been tested. More abundant data will enable to verify and test non-linear relations in the future. It is suggested to analyse a possible correlation between the geological (MC, TC, mwVh) and the geomechanical parameters involved in the failure criterion of Habimana (1999). For this purpose his new parameter σ_{ci} , introduced in order to take into account the "degree of tectonisation", is of special interest.

Annotations to the sample Zr39

The sample Zr39 (Cleuson-Dixence, Zerjona) shows quite a heterogeneous petrographic composition at the centimetric scale (quartz rich meta-sandstone and micaceous schist). As can be observed in the rest of the drilled block (Figure 6-4), it is furthermore crosscut by a persistent shear zone orientated at $\alpha \approx 45^\circ$ to the main schistosity, respectively to the applied load. Such shear zones are quite common in micaceous schists and black phyllites of the Zone Houillère

(chap. 3.1.2). The presence of a dominant, single discontinuity in a kakirite sample may however completely control its strength. In the case of Zr39, it is truly lower than expected with regard to the found structural and mineralogical properties. Since the sample could not be analysed after the test, the exact mode of failure is however unknown. Two interpretations are hence possible: first, failure has occurred across the kakirite sample without involving the shear zone, and second, it has occurred along the pre-existing shear zone.

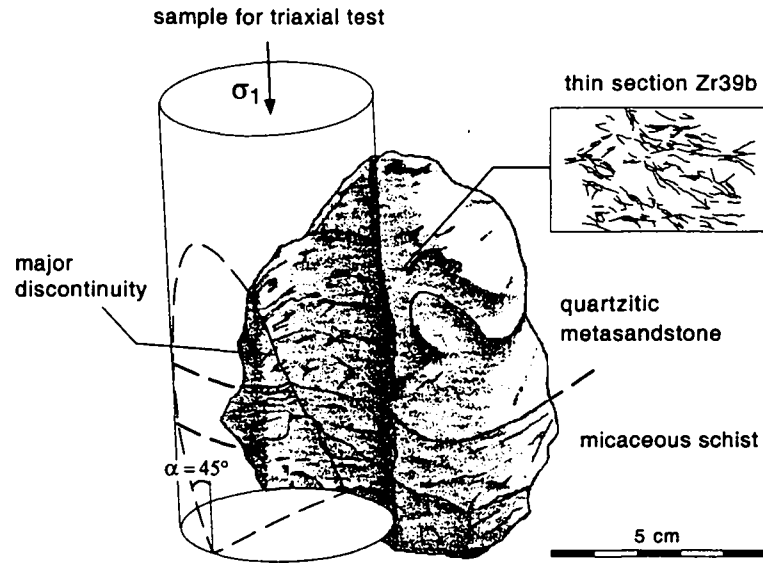


Figure 6-4: Schematic sketch of the rest of the block wherein the kakirite sample Zr39 has been drilled. A persistent and dominant shear zone is crosscutting the sample from upper left to lower right. Note the heterogeneous petrographic composition at the scale of the sample.

For the first case to be true, the shear strength of the discontinuity ($\alpha = 45^\circ$) would have to exceed the rock strength of the kakirite sample. Supposed the found relation between $\sigma_1(5)$ and $mwVh(MC+TC)$ for the other samples is correct, the mismatch of Zr39 (Figure 6-2 and 6-3) can not be explained further on the basis of the available data. It could be due in fact to many other, not considered factors (e.g. a higher water content).

In the second case, the low triaxial strength ($\sigma_1(5) = 22\text{MPa}$) is considered to be controlled by the characteristics of the dominant, single discontinuity. Based on this hypothesis, the theoretical

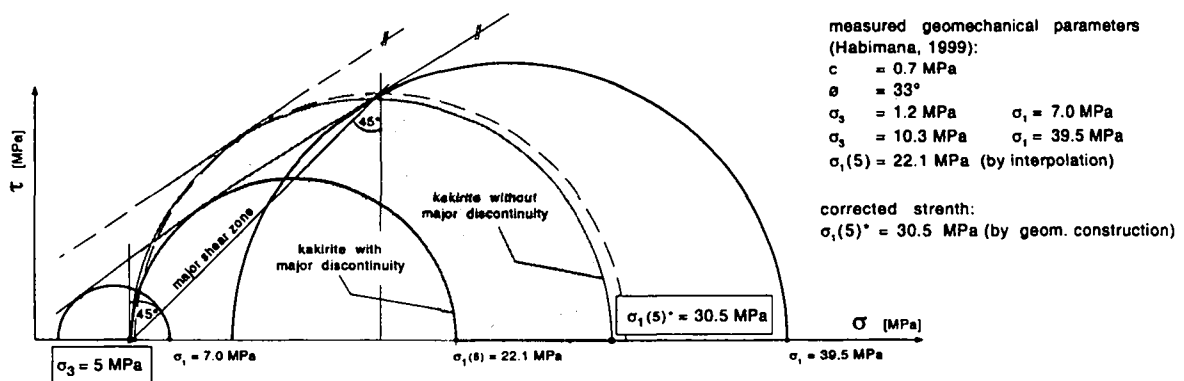


Figure 6-5: Reconstruction of the theoretical triaxial strength $\sigma_1(5)^*$ for the sample Zr39 without the observed major discontinuity. Based on data of Habimana (1999), after Zenhäusern & Bürgi (1999).

triaxial strength of the sample Zr39 without a dominant discontinuity can be determined geometrically by means of Mohr circles (Figure 6-5). The resulting, "rectified" $\sigma_1(5)^* = 30\text{MPa}$ is in quite good correspondence with the tendency observed in Figure 6-2.

Petrographic heterogeneities and shear zones are common in micaceous schists and black phyllites of the Zone Houillère (chap. 3.1.2). Because of their black metallic glance and extremely smooth surfaces, shear zones are often thought to bear high contents of graphite. Photospectrometric analyses¹ however have shown the carbon contents in such shear zones to be very low (≤ 1 weight-%). In fact, it is supposed to be the spatial distribution rather than the total content of graphite that controls shear strength. Even a thin graphite layer on a discontinuity surface can make its shear strength to drop considerably. In order to determine the influence of graphite coatings on discontinuities, future studies will have to consider in detail the discontinuity surface compositions (mineralogy, microstructure, coating thickness, genesis, etc.).

The example from above illustrates the limits of the chosen approach and the presented characterisation method. It is based on "mean weighted" parameters, quantifying the overall structural and mineralogical properties of kakirites. However, if failure occurs along a pre-existent, dominant discontinuity, a priori no physical relation can be expected to exist between σ_1 and MC, TC and mwVh. The application of the proposed characterisation method is hence restricted to kakirites with a certain structural and mineralogical homogeneity at the scale of thin sections and triaxial tests. For correlation purposes, the studied geological and geomechanical samples have to represent accurately the (same) properties of interest: shear strength of a single discontinuity, triaxial strength of an entire kakirite sample, etc. The example makes evident the crucial moment of taking representative kakirite samples. It furthermore shows the absolute necessity of detailed structural analyses of both, the "geomechanical" *and* "geological" samples in order to control their equivalence and the mode of failure.

¹ Performed on a CarloErba Elemental Analyzor EA1108. Institute of Geology, University of Neuchâtel.

7 THE HYDROGEOLOGICAL ROLE OF CATACLASTIC FAULT ZONES

Based on hydrogeological observations and indirectly by analyses of groundwater chemistry, the hydrogeological impacts of crossing kakirite zones by underground excavations has been analysed.

Field observations have shown that most of the crossed kakirite zones are almost impermeable, natural flow barriers, separating the massif in different hydrogeological compartments. Depending on if the gallery is driven through a saturated massif or not, on the relative orientation, dip and extension of kakirite zones and on the size of the separated hydrogeological compartments, crossing such flow barriers may have important impacts on the local or even regional hydrogeological environment. Short-circuiting of different groundwater compartment, important lowering of the groundwater table, dry up of springs, mixing of previously separated groundwater aquifers may have its impacts on the groundwater chemistry and regional resources.

During the study of this project the crossing of several kakirite zones was observed. However, in the most cases the available hydrogeological data did not permit a more detailed identification of the geological and hydrogeological situation. The case history of a well documented, 8 meter thick kakirite zone in the gallery of Cleuson-Dixence (chap. 3.1) is treated more in detail as an example.

7.1 Case history: Cleuson-Dixence lot C (PM 5597)

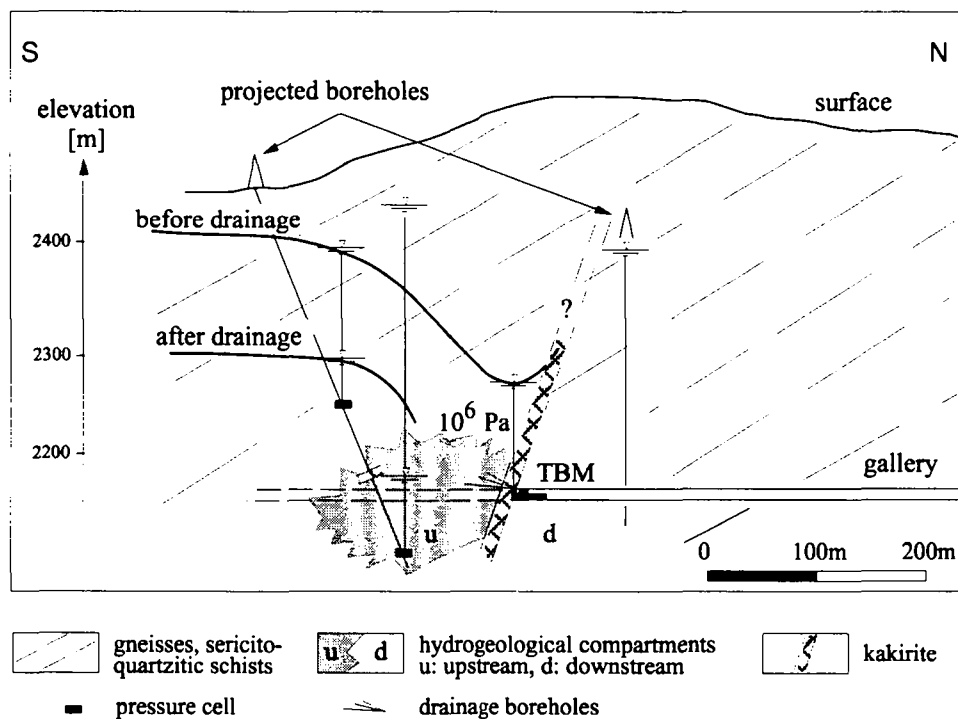


Figure 7-1: Schematic sketch of the hydrogeological situation crossed by the gallery of Cleuson-Dixence. The massif is split up in two distinct hydrogeological compartments by an impermeable, 8m thick kakirite zone.

After advancing for more than 500 meters in poorly fissured and dry schistose gneisses (no water inflows were detected in drilled pilot boreholes), the TBM penetrated in a subvertical plunging and perpendicular to the gallery orientated kakirite zone of 8 to 12 meters large. A very high initial water pressure of 14 bars inside this zone caused a sudden inflow of water and fine grained material

into the gallery. To pass this zone, a great number of boreholes were drilled across the kakirite zone to drain the upstream compartment. The draining effect could be observed in a near borehole, drilled earlier from the surface and equipped with pressure gauges. The macro- and micro-structural and mineralogical characteristics of this zone have been described more in detail in chap. 3.1 and 5.1.2.

As shown in Figure 7-2, the upstream compartment is limited on the downstream side by the kakirite zone and on the upstream side by the Synclinal des Chèques (see chap. 3.1). The latter is a major tectonic contact between the series of Mont Gond and the serie of Creppon Blanc and composed mainly of quartzites and some calcareous components. It is supposed to as natural flow barrier as well, closing the compartment to the upper side.

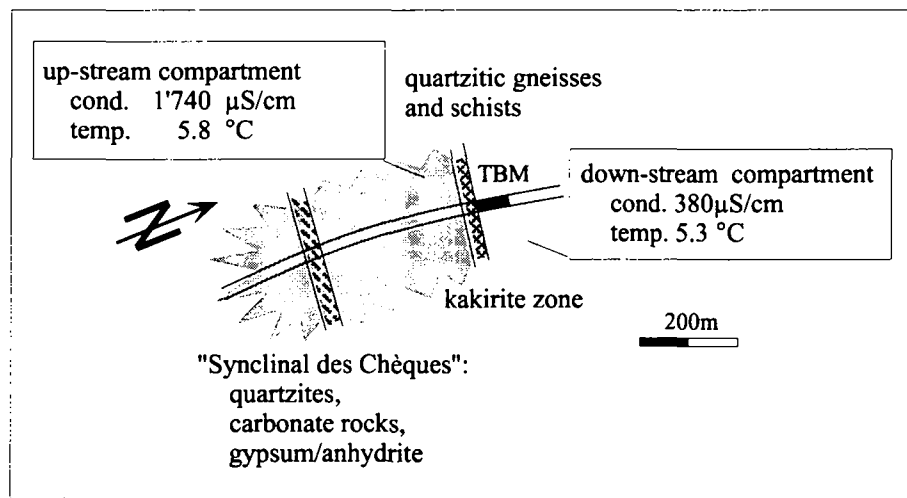


Figure 7-2: Profile through the hydrogeological compartments formed by a subvertical kakirite zones. Crossing the natural flow barrier, the water table in the upstream compartment was lowered by 300m (Cleuson-Dixence, lot C, PM 5997).

To pass through the kakirite zone, the upstream compartment had to be drained by numerous boreholes drilled from the front of the gallery. Although the quantitative water-inflow in these drains was not very high, it caused an important lowering of the ground water table of almost 300 m. The drainage of the compartment was observed in a subvertical borehole situated 130 m in front of the tunnel face. After lowering the water table to the gallery level and the injection of a consolidation vault, the kakirite zone could finally be passed through by the TBM.

As the kakirite zone cuts through quartzitic gneisses and schists, one would expect to find a similar groundwater chemistry, characteristic of a crystalline aquifer, up- and downstream the panel. Groundwaters from crystalline aquifers in the Mont Blanc and the Aiguilles Rouges Massif have been characterised by Dubois (1992). They usually show a very low mineralization with total dissolved solids (TDS) of about 100 mg/l (electric conductivity $\sim 100 \mu\text{S}/\text{cm}$ at 20°C). Compared to other types of groundwater in Switzerland, e.g. from carbonate aquifers or from detrital rocks, they are characterised by a low total mineralization but distinctively higher contents of As, Mo and U. According to the classification of Jäckli (1970), they belong to the Ca - (Si) - HCO₃ - SO₄ type of groundwater.

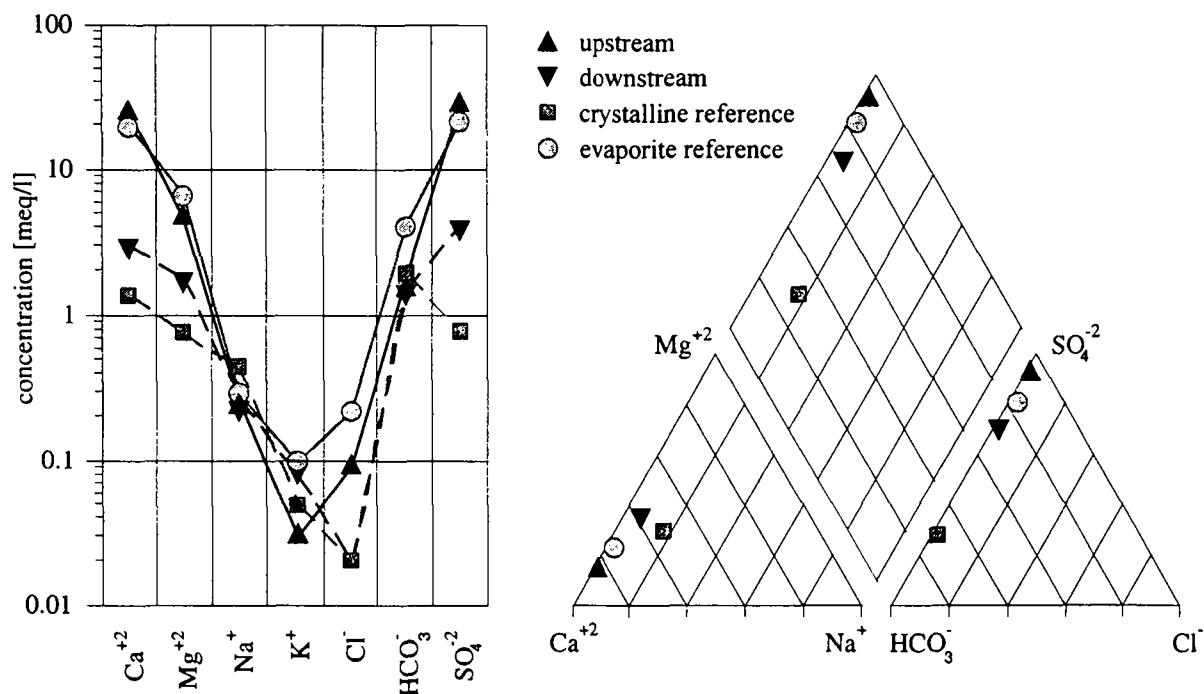


Figure 7-3: Comparison of major elements from the up- and downstream watersamples with the reference analyses. Note the composition of the downstream watersample situated intermediate between the "evaporite" and "crystalline reference".

In the present example, the groundwater upstream the kakirite zone shows a rather high mineralization (TDS: 2'000 mg/l, electric conductivity : 1'740 μ S/cm at 20°C). The conspicuous content of SO₄, Ca, Mg, Sr, and Mn makes it of a Ca - (Mg) - SO₄ type (Jäckli, 1970). After Mandia (1991), high concentrations of SO₄, Ca and Sr are characteristic of the evaporite aquifers in this region. In fact, some 300 m upstream the kakirite zone, there is the Triassic "Synclinal des Chèques" composed of quartzite, gypsum, anhydrite and carbonate rocks. Apparently these Triassic rocks have strongly marked the groundwater composition in the upstream compartment.

The hydrochemistry in the downstream compartment in contrast is quite different. Compared to the groundwater from the upstream compartment, its mineralization is less important (TDS: 379 mg/l, conductivity: 380 μ S/cm at 20°C). Also chemically, this groundwater is different, being of the Ca - Mg - SO₄ - HCO₃ type. For comparison, a water sample taken from upstream the Triassic syncline, but from the same type of aquifer (quartzitic schists and gneisses), has been chosen as a reference. In the downstream compartment, the concentrations of the major elements SO₄, Ca, Mg are slightly higher than in this reference. In fact, the hydrochemistry appears to be intermediate between a "crystalline" and an "evaporite" type of groundwater.

In both compartments the specific "crystalline" mineralization is overprinted by the mineralization from the evaporite rocks of the Triassic syncline. Taking into account only the major elements, one would consider the upstream groundwater to be of an almost pure evaporite type. Whereas downstream the composition would simply be the effect of mixing 80% "crystalline" and 20% "evaporite" groundwater. The analysed trace elements show, however, that hydrochemical processes are not as simple. Sr, for example, is a very typical trace element for evaporite groundwater (Mandia, 1991) and fits, like the major elements, the theory of mixing two groundwater types. The concentration of other elements, such as Rb, a typical trace element for evaporite groundwater as well, As, Br, Li and Mn, can however not easily be explained. Various interactions between mineral phases and dissolved compounds can occur. Analysing trace elements helps to avoid oversimplifications of conclusions based only on the analyses of major elements.

	upstream	downstream	evaporite ref. ^{*)}	crystalline ref. ^{*)}
Temp. [°C]	5.8	5.3	8.6	15.0
TDS [mg/l]	2'000	379	1'780	209
Cond. at 20°C [µS/cm]	1'740	380	1'570	
major elements	[mg/l]	[mg/l]	[mg/l]	[mg/l]
Ca	488.90	58.80	389.79	27.60
Mg	56.40	22.00	80.97	9.30
Na	5.64	5.93	6.44	9.90
K	1.18	3.22	4.05	1.95
Cl	3.20	< 1.00	7.64	< 1.00
HCO ₃	112.90	90.30	251.96	120.20
SO ₄	1'314.00	192.00	1'025.26	38.40
Si	7.50	3.70	3.69	-
trace elements	[µg/l]	[µg/l]	[µg/l]	[µg/l]
Al	3.89	45.09	19.30	-
As	27.86	7.31	0.80	-
B	5.54	3.57	15.10	4.30
Ba	4.36	20.81	8.80	96.80
Br	5.47	5.02	12.40	21.00
Cd	< 0.20	< 0.20	< 0.20	-
Cr	< 0.20	1.84	0.20	0.90
Cu	0.72	0.55	2.90	2.10
Fe	37.68	56.82	-	19.20
I	2.04	1.49	5.40	45.20
Li	6.91	8.78	28.60	4.60
Mn	105.46	6.50	10.80	30.80
Mo	15.81	25.94	-	-
Ni	5.19	1.78	3.20	1.00
Rb	1.99	10.06	18.40	3.20
Sr	9'700.80	1'373.10	7'040.00	450.00
U	19.99	36.56	18.40	0.30
V	0.21	0.23	0.50	0.30
Zn	13.82	9.56	7.00	6.40

Table 7-1: Groundwater composition in the hydrogeological compartments up- and downstream the kakirite zone and reference analyses: ^{*)} Mandia (1991), evaporite aquifers in the western Penninic Alps of Switzerland, ^{*)} water sample form upstream the Triassic syncline.

The observed difference in hydraulic charge and groundwater composition up- and downstream the kakirite zone is a strong indication for this zone to be of a very low permeability and to have a quit important extension and continuity. It clearly separates two distinct hydrogeological compartments. Permeability tests on a kakirite sample in a triaxial cell lead to a permeability coefficient in the order of 10^{-9} m/s.

8 SUMMARY AND CONCLUSIONS

Weak cataclastic fault rocks regrouped under the general term of "crushed rocks" show a large scatter of geological and geomechanical properties. The purpose of this study was to develop a more detailed and objective differentiation and characterisation method for these rocks.

8.1 Geological characterisation

In a simplified approach, the mechanical behaviour of (fault) rocks is supposed to be controlled mainly by mineralogical composition and rock fabric. For correlation purposes the proposed geological characterisation of kakirites is referring to a similar scale as common geomechanical laboratory tests, respectively to the meso- to microscopic scale of handspecimens and thin sections.

The developed characterisation method is based on a two-phase "clast-matrix" model, considering kakirites to be composed of varying proportions of "hard" clasts and "weak", fine-grained matrix. The quantitative method involves the overall kakirite mineralogy and rock fabric, respectively clast and matrix (discontinuity) properties.

considered factor	quantified by:
mineralogy	Vickers hardness, mwVh [GPa]
rock fabric	
- clast properties	texture coefficient, TC [-] $TC = CD \left[\left(\frac{N_0}{N_0 + N_1} \cdot \frac{1}{FF_0} \right) + \left(\frac{N_1}{N_0 + N_1} \cdot AR_1 \cdot AF_1 \right) \right]$
- discontinuity properties	matrix coefficient, MC [-] $MC = \frac{R_L}{T_{Ld} \cdot T_{Ll}} \cdot \frac{1}{\delta}$

8.1.1 Mineralogy

The concept of the *mean weighted Vickers hardness* (mwVh) proposed by Calembert et al. (1980a) has been adopted. It consists of the Vickers hardness of the rock forming mineral phases weighted by their relative proportions. It has been determined for the studied kakirites on the basis of semi-quantitative XRD-analyses.

By thin section and XRD-analyses the mineralogical compositions of kakirites, adjacent host rock samples and sieved kakirite grainsize fractions have been determined. Quartz content is observed to be considerably higher in the clast (0.2-0.6mm) and gravel fractions than in the fine-grained matrix fraction (< 0.063mm). The later is in fact primarily composed of phyllosilicates. This mineralogical grainsize fractionation is interpreted to have three origins. First, the influence of the original host rock fabric: in the case of a spaced foliation (e.g. Cleuson-Dixence, unit C) the "hard" quartz and feldspar rich microlithons form obviously rather clasts, whereas the phyllosilicate rich cleavage domains are split up in the matrix. The two other reasons are related to the cataclastic deformation, namely the strength contrast between the involved mineral phases (e.g. quartz - mica), and alteration processes, which further increase the fine-grained phyllosilicate content in the matrix.

Sieved kakirite samples show extended grainsize distributions with in general high proportions of silt/clay grainsize fraction (mean 44%). These high proportions of fine-grained, phyllosilicate rich matrix explains the often observed very low permeability of kakirite zones (chap. 6).

Minor mineralogical differences have been found between kakirite and adjacent host rock samples. They are interpreted to be due to: first, original mineralogical heterogeneities between

the host rock and the zone where cataclastic faulting exactly has occurred (e.g. Dornbach Zone, Goltschried) and second, alteration processes (e.g. feldspar), accentuated by the (initially) increased rock mass permeability due to brittle faulting (samples G5-21/G5-22, G6-1/G6-2, Vz14). Extensional fracturing in fault zones accompanied by the crystallisation of carbonate further increases the differences between the bulk rock mineralogy of kakirites and host rocks (e.g. Vz14).

Except of the quantitative mineralogical differences between host rocks and kakirites, the only newly formed mineral phase which has been identified in kakirites is kaolinite, issue of the alteration of plagioclase (Vz14, CD20.3). No specific mineralogical analyses have been made in consequence. The formation and presence of very small amounts of (swelling) clay-minerals, which can not be detected by the performed whole rock XRD-analyses, can however not be excluded completely.

8.1.2 Rock fabric

The *texture coefficient* (TC), developed by Howarth & Rowlands (1985), has been adapted to the specific fabric properties of kakirites. It involves the clast density, shape and relative orientation of elongated clasts.

As shown in the present study, the clast density in kakirites is often very low (mean CD ~ 0.3) and clast supported rock fabrics are the exception (e.g. G8-3). The specific properties of the fine-grained matrix, namely mineralogy and structural and/or mineralogical discontinuities, therefore become rock strength controlling factors. To take into account the influence of pre-existing discontinuities, a new parameter, the *matrix coefficient* (MC) has been developed. It involves the discontinuity density, roughness, mean length and relative orientation.

Combining the MC and TC, a new quantitative method has been presented to characterise and differentiate appropriately a wide range of weak cataclastic fault rocks by their microscopic fabric. Two opposite fabric types can be distinguished: first, a granular fabric, characterised by clasts in a homogeneously fine-grained, isotropic matrix (e.g. sample Tr5, Figure 5-4) and second, a discontinuity dominated, fine-grained and often schistose fabric wherein no clasts can be distinguished (e.g. sample Zr30). In-between these two end-members a gradual transition of rock fabrics bearing clasts and matrix-discontinuities is observed (e.g. sample CH13, Figure 5-25). The type of cataclastic rock fabric developed during faulting depends, except of faulting conditions, strongly on the structure, and texture of the host rock and on the strength contrast of involved mineral phases.

Based on the mineralogical-structural approach, a conceptual method (MC-TC-diagram) is proposed which could enable the future assessment of the geomechanical properties of weak cataclastic fault rocks. The validity of the proposed method has been evaluated in a first attempt by the correlation with rock strength $\sigma_1(5)$ of the analysed kakirites (Habimana, 1999). Although only a small number of corresponding samples were finally to disposal, an encouraging correlation has been found. Much more work is however obviously necessary to improve and positively confirm the validity of the proposed geological characterisation method.

The main purposes of this work has been achieved by the development of the presented new characterisation method enabling an objective differentiation of weak cataclastic fault rocks. The method contributes to the geomechanical characterisation of kakirites by the introduction of quantitative geological parameters, intended to replace in the future currently used visual appreciation indexes (e.g. GSI).

The proposed mineralo-structural characterisation is referring to a scale comparable with common geomechanical laboratory test. It needs only very little undisturbed kakirite material and can be applied even when no geomechanical tests can be performed (e.g. in the case of low core recovery). It is an additional tool amongst all the other, conventional investigation methods making part of a complete geological-geomechanical study. It has to be integrated in a general approach characterising fault zones at different scales and of course a transition from thin section to the underground construction and to the scale of the rock massif is needed.

8.2 Hydrogeological aspect

The hydrogeological role of weak cataclastic fault zones has been treated only marginally in this work. It is illustrated by means of a case history of a crossed fault zone in the gallery of Cleuson-Dixence, demonstrating the often observed groundwater flow barrier-effect of cataclastic fault zones and their impact on the excavation work and the local groundwater regime.

8.3 Suggested further research

The validity of the proposed characterisation method will have to be confirmed by more geological and geomechanical data. In the present work only kakirites mostly from quartzo-phyllitic host rocks have been analysed. It is suggested to apply the method to fault rocks from other lithologies, e.g. sedimentary and isotropic igneous rocks (e.g. granites).

The accuracy of the MC can be improved by taking into account more properly the anisotropy and spatial distribution of discontinuities. By the developed orientation factor δ (chap. 4.4.2.2), an attempt has been made to introduce a parameter taking into account the rock fabric anisotropy on the basis of measured angles between sets discontinuities. Much information is however lost by this transformation of a 2D-, respectively 3D-feature in a scalar parameter. It is suggested to try to redefine the MC as a tensor, which will make correlations with geomechanical properties more expressive.

The hydrogeological aspects of cataclastic fault rocks, as well as the observed alteration phenomena have been touched only marginally. They will have to be examined by more specific investigation methods. An other key in understanding the geological and geomechanical properties of cataclastic fault rocks is the study of the "post-tectonic" evolution of cataclastic fault zones (e.g. alteration, porosity, re-cimentation, groundwater circulation, etc.) and water content.

8.3.1 Practical recommendations

Based on the experiences made during the present work, the following practical recommendations can be made in regard to a potential continuation of the research project.

Sampling, transport and preparation of undisturbed kakirite samples has been a major difficulty. Amongst the tested sampling techniques two methods can be recommended, namely the U-shaped sampler (chap. 4.2) and, with some restriction, the hydraulic sampler (Habimana, 1999). Both techniques enable to take orientated samples and offer an excellent protection during transport. The methods are especially suitable for fine to medium grained kakirites. Great attention is required however when kakirites bear relatively coarse clasts with respect to the size of the sampler. If the cutting blade of the metallic tube or the U-shaped sampler hits upon larger clasts or more competent layer, samples unavoidably will be disturbed. It is hence recommended to take samplers of different size and diameter in order to adapt the sample size to the characteristics of the fault zone.

The major disadvantage of the hydraulic sampler is that no visual control of the structural features is possible prior to the triaxial test. As mentioned above, detailed geological analyses of the tested samples are however crucial for the success of the sought correlation between geological and geomechanical properties. The chosen approach of separately taken "corresponding" samples for geological and geomechanical studies has shown to be difficult. It perfectly works in the case of relatively fine-grained, granular and homogeneous kakirites at the scale of handspecimens, but it becomes deficient in the case of strongly folded schistose kakirites. For the future it is therefore imperative to enable a detailed structural study of the tested samples. We suggest to leave the tested samples in the rubber sleeve of the triaxial test cell for impregnation. By means of polished sections it will then be possible to control the relative orientation of the foliation with respect to the applied load, to identify more precisely the mode of failure and to make out eventually present structural heterogeneities. It will enable as well to confirm, respectively reject the "correspondence" between geological and geomechanical samples.

The possibility of non-destructive tests (e.g. wave velocity) prior to the triaxial testing should be evaluated.

REFERENCES

- Aleksandrov, K. S., Belikov, B. P., Ryzova, T. V. (1967): Calcul des constantes élastiques des roches d'après leur composition minéralogique. *Izv. Akad. Nauk SSSR. Serija Geologiceskaja URSS*, No. 2. Traduction du Lab. Centrale Ponts et Chaussées, No. 67.T.90, Paris.
- Al-Harhi, A. A. (1998): Effects of planar structures on the anisotropy of Ranyah sandstone, Saudi Arabia. *Eng. Geology*, Vol. 50, 49-57.
- Azzoni, A., Bailo, F., Rondena, E., Zaninetti, A. (1992): Valutazione quantitativa della tessitura delle rocce e correlazione con la resistenza a compressione monoassiale. *Bollettino Assoc. Mineraria Subalpina*, Anno XXIX, No. 4, 347-352.
- Barton, N. (1973): Review of a new shear strength criterion for rock joints. *Eng. Geology*, Vol. 7.
- Barton, N., Lien, R., Lunde, J. (1974): Engineering classification of rock masses for the design of tunnel support. *Rock Mech.*, Vol. 6, 183-236.
- Beddow, J. K. et al. (1980): *Advanced particulate morphology*. Ed. by J. K. Beddow & T. P. Meloy. CRC Press, Boca Raton, Florida.
- Bell, F. G. (1978): The physical and mechanical properties of the Fell Sandstones, Northumberland. *Eng. Geology*, Vol. 12, 1-29.
- Bell, T. H. & Etheridge, M. A. (1973): Microstructures of mylonites and their descriptive terminology. *Lithos*, Vol. 6, 337-348.
- Bieniawski, Z. T. (1989): *Engineering rock mass classifications*. Wiley & Sons, New York.
- Bieniawski, Z. T. (1979): The geomechanics classification in rock engineering application. *Proc. 4th Int. Congr. Rock Mech.*, ISRM, Montreux, Vol. 2, 41-48.
- Bieniawski, Z. T. (1967): Mechanism of brittle fracture. *Int. Journal Rock Mech. Min. Sci.*, Vol. 4, 395-430.
- Botte, J., Méan, Ph., Tournery, J.-F. (1997): Le puits incliné de l'aménagement Cleuson-Dixence. *Tunnels et ouvrages souterrains*, No. 142, 205-231.
- Botte, J., Méan, Ph., Tournery, J.-F. (1996): Galerie d'amenée de l'aménagement Cleuson-Dixence. *Traitement des accidents géologiques*. *Tunnels et ouvrages souterrains*, No. 138, 329-338.
- Bürgi, C. (1995): *Comportement des roches cataclastiques dans les ouvrages souterrains - volet géologique*. Unpublished thesis, EPF-Lausanne.
- Bürgi, C., Parriaux, A., Rey, J.-Ph., Franciosi, G. (1999): Cataclastic rocks in underground structures - terminology and impact on the feasibility of projects (initial results). *Eng. Geology*, Vol. 51/3, 225-235.
- Burkhard, M. (1988): L'Helvétique de la bordure occidentale du massif de l'Aar (évolution tectonique et métamorphique). *Eclogae geol. Helv.*, Vol. 81, No. 1, 63-114.
- Burri, M. (1983a): Le front du Grand St-Bernard du val d'Hérens au val d'Aoste. *Eclogae geol. Helv.*, Vol. 76, No. 3, 469-490.
- Burri, M. (1983b): Description géologique du front du St-Bernard dans les vallées de Bagnes et d'Entremont (Valais). *Bulletin Lab. Géol. Univ. Lausanne*, No. 270, 1-88.
- Calembert, T., Popescu, C., Popescu, M., Schroeder, C. (1980a): Relationships between the petrographic and mineralogical properties of soils and rocks and their mechanical properties. *Bulletin Int. Assoc. Eng. Geol.*, No. 22, 167-172.
- Calembert, L., Monjoie, A., Polo-Chiapolini, C., Schroeder, C. (1980b): *Géologie de l'ingénieur et mécanique des roches*. Ministère des Travaux Publics, Bruxelles.

- Calembert, L., Monjoie, A., Polo-Chiapolini, C., Schroeder, C. (1982): Géologie de l'ingénieur et mécanique des roches - suite. Extrait des Annales des Travaux Publiques de Belgique, No. 6, 1981, Bruxelles.
- Chester, F. M. & Logan, J. M. (1986): Implications for mechanical properties of brittle faults from observations of the Punchbowl fault zone, California. *Pure and Applied Geophysics*, Vol. 124, No. 1/2, 79-106.
- Chester, F. M., Friedmann, M., Logan, J. M. (1985): Foliated cataclasites. *Tectonophysics*, Vol. 111, 139-146.
- Christie, J. M. (1960): Mylonitic rocks of the Moine Thrust-Zones in the Assynt region, North-West Scotland. *Trans. geol. Soc. Edinburgh*, Vol. 111, 79-93.
- Clerici, A. (1992): Engineering geological characterization of weak rocks: classification, sampling and testing. *In Rock characterization, ISRM Symposium: Eurock '92*, Chester, UK. Ed. by J. A. Hudson, British geotechn. Soc., London, 179-184.
- Cording, E. J. & Deere, D. U. (1972): Rock tunnel supports and field measurements. *Proc. Rapid. Excav. Tunnelling Conf. AIME*, New York, 601-622.
- Cortesogno, L. & Haccard, D. (1985): Carta geologica della zona Sestri-Voltaggio, 1:25'000. Selca, Firenze.
- Cortesogno, L. & Haccard, D. (1979): Présentation des principales unités constitutives de la zone de Sestri Voltaggio et de leurs relations structurales. *Bulletin Soc. géol. France*, No. 4, 379-388.
- Detraz, H. & Monthonnex, F. (1996): Reconnaissances à l'avancement dans un puits incliné excavé au tunnelier. L'exemple de l'aménagement Cleuson-Dixence (Valais, Suisse). *Travaux*, No. 724, 52-60.
- Dubois, J.-D. (1991): Typologie des aquifères du cristallin: exemple des massifs des Aiguilles Rouges et du Mont-Blanc (France, Italie, Suisse). PhD thesis No. 950, EPF-Lausanne.
- ENEL S.p.A. (1991): Utilizzazione idroelettrica del medio torrente Diveria. Unpublished report.
- Ersoy, A. & Waller, M. D. (1995): Textural characterisation of rocks. *Eng. Geology*, Vol. 39, 123-136.
- Escher, A., Masson, H., Steck, A. (1992): Nappe geometry in the Western Alps. *Journal Struct. Geology*, Vol. 15. No. 3/5, 501-509.
- Evans, J. P. (1988): Deformation mechanisms in granitic rocks at shallow crustal levels. *Journal Struct. Geology*, Vol. 10. No. 5, 437-443.
- Evans, J. P. (1997): Permeability of fault-related rocks, and implications for hydraulic structure of fault zones. *Journal Struct. Geology*, Vol. 19. No. 11, 1393-1404.
- Escher, A. (1988): Structure de la nappe du Grand Saint-Bernard entre le Val de Bagnes et les Mischabel. *Rapport géol. No. 7. Service hydrogéol. et géol. nat.*
- Fairbridge, R. W. & Bourgeois, J. (eds.) (1978): *The Encyclopedia of Sedimentology*. *In Encyclopedia of Earth Sciences series*, Vol. VI. Dowden, Hutchinson & Ross, Inc., Stroudsburg, Pennsylvania.
- Fernlund, J. M. R. (1997): The effect of particle form on sieve analysis: a test by image analysis. *Eng. Geology*, Vol. 50, 111-124.
- Galli, M., Messiga, B., Piccardo, G. B. (1979): Caractères pétrographiques du massif cristallin de Savone et du groupe de Voltri. *Bulletin Soc. géol. France*, No. 4, 389-400.
- Gehriger, W. (1992): Projektübersicht Gotthard-Basistunnel. *In SIA D 085, Die AlpTransit-Basistunnel Gotthard und Lötschberg*, 25-33.
- Gouffon, Y. & Burri, M. (1997): Les nappes des Pontis, de Siviez-Mischabel et du Mont Fort dans les vallées de Bagnes, d'Entremont (Valais, Suisse) et d'Aoste (Italie). *Eclogae geol. Helv.*, Vol. 90, No. 1, 29-41.

- Grasso, P., Brino, L., Rabajoli, G., Astore, G., Pelizza, S. (1994): Methodology for the prevision of subsidence. A case-history - Bretella di Voltri. *Gallerie e grandi opere sotterranee*, No. 43, 12-24.
- Groshong, R. H. jr. (1988): Low-temperature deformation mechanisms and their interpretation. *Bulletin Geol. Soc. Am.*, Vol. 100, 1329-1360.
- Grubenmann, U. & Niggli, P. (1924): *Die Gesteinsmetamorphose*. Bornträger, Berlin.
- Gunsallus, K. L. & Kulhawy, F. N. (1984): A comparative evaluation of rock strength measures. *Int. Journal Rock Mech. Min. Sci.*, Vol. 21, 233-248.
- Habimana, J. (1999): Caractérisation géomécanique des roches cataclastiques rencontrées dans des ouvrages souterrains alpins. PhD thesis No. 1945, EPF-Lausanne.
- Habimana, J., Labiouse, V., Descouedres, F. (1998): Influence of the tectonisation on geomechanical parameters of cataclastic rocks: Experience from Cleuson-Dixence project. *In The Geotechnics of hard soils - soft rocks*. Ed. by Evangelista & Picarelli. Vol. 1, 529-536. Balkema, Rotterdam.
- Haccard, D. & Lorenz, C. (1979): Les déformations de l'Éocène supérieur au Stampien de la terminaison septentrionale de la zone de Sestri-Voltaggio. *Bulletin Soc. géol. France*, No. 4, 401-413.
- Handy, M. R. (1990): The solid-state flow of polymineralic rocks. *Journal Geophys. Res.*, Vol. 95, No. B6, 8647-8661.
- Head, K. H. (1980): *Manual of soil laboratory testing. Volume 1: Soil classification and compaction tests*. Pentech Press, Plymouth.
- Heitzmann, P. (1985): Kakirite, Kataklasite, Mylonite - Zur Nomenklatur der Metamorphite mit Verformungsgefüge. *Eclogae geol. Helv.*, Vol. 78, No. 2, 273-286.
- Higgins, M. W. (1971): Cataclastic rocks. *U. S. Geol. Survey Prof. Paper*, No. 687.
- Hippler, S. J., Knipe, R. J. (1990): The evolution of cataclastic fault rocks from a pre-existing mylonite. *In Deformation Mechanisms, Rheology and Tectonics*. Ed. by R. J. Knipe & E. H. Rutter. *Geol. Soc. Spec. Paper*, No 54, 71-79.
- Hobbs, B. E., Means, W. D., Williams, P. F. (1976): *An outline of structural geology*. Wiley, New York.
- Hoek, E., Marinos, P., Benissi, M. (1998): Applicability of the geological strength index (GSI) classification for very weak and sheared rock masses. The case of the Athens schist formation. *Bulletin Eng. Geol. Env.*, No. 57, 151-160.
- Hoek, E., Brown, E. T. (1997a): *Underground excavation in rock*. E & FN Spon, London.
- Hoek, E., Brown, E. T. (1997b): Practical estimates of rock mass strength. *Int. Journal Rock Mech. Min. Sci.*, Vol 34, No. 8, 1165-1186.
- Hoek, E. (1994): Strength of rock and rock masses. *ISRM News J* 2, 4-16.
- Howarth, D. F., Rowlands, J. C. (1986): Development of an index to quantify rock texture for qualitative assessment of intact rock properties. *Geotechnical Testing Journal*, Vol. 9, No. 4, 169-179.
- Howarth, D. F., Rowlands, J. C. (1987): Quantitative assessment of rock texture and correlation with drillability and strength properties. *Rock Mech. and Rock Eng.*, Vol. 20, 57-85.
- Hugman, R. H., Friedman, M. (1979): Effects of texture and composition on mechanical behaviour of experimentally deformed carbonate rocks. *Am. Assoc. Pet. Geol. Bulletin*, No. 63, 1478-1489.
- International Society for Rock Mechanics (1981): Basic geotechnical description of rock masses. *Int. Journal Rock Mech. Min. Sci.*, Vol. 18, 85-110.

- Jäckli, H. (1970): Kriterien zur Klassifikation von Grundwasservorkommen. *Eclogae geol. Helv.* Vol. 63, No. 2, 389-434.
- Keller, J. V. A., Hall, S. H., McClay, K. R. (1997): Shear fracture pattern and microstructural evolution in transpressional fault zones from field and laboratory studies. *Journal Struct. Geology*, Vol. 19, No. 9, 1173-1187.
- Kellerhals, P. (1992): Geologie des Lötschberg-Basistunnel. *In* SIA D 085, Die AlpTransit-Basistunnel Gotthard und Lötschberg, 35-43.
- Kellerhals, P., Isler, A. (1998): Lötschberg-Basistunnel: Geologische Voruntersuchungen und Prognose. *Landeshydrologie und -geologie, Geologische Berichte*, Nr. 22, Bern.
- Klug, H. P., Alexander, L. E. (1974): X-Ray diffraction procedures. Wiley, New York.
- Knipe, R. J. (1986): Deformation mechanism path diagrams for sediments undergoing lithification. *Memoir Geol. Soc. Am.*, No. 166, 151-160.
- Knipe, R. J. (1989): Deformation mechanisms - recognition from natural tectonites. *Journal Struct. Geology*, Vol. 11, No. 1/2, 127-146.
- Krumbein, W. C. (1941): Measurement and geological signification of shape and roundness of sedimentary particles. *Journal Sed. Petrology*, Vol. 11, No. 2, 64-72.
- Lapworth, C. (1885): The Highland Controversy in British Geology: its causes, course, and consequences. *Nature*, Vol. 32, 558-559.
- Laubscher, H. & Bernoulli, D. (1980): Cross-section from the Rhine Graben to the Po Plain. *In* *Geology of Switzerland - a guide book*, Part B. Ed. by Schw. Geol. Kommission. Wepf & Co., Basel.
- Lauffer, H. (1958): Gebirgsklassifizierung für den Stollenbau. *Geol. Bauwesen*, Vol. 74, 46-51.
- Lin, A. (1996): Injection veins of crushing-originated pseudotachylyte and fault gouge formed during seismic faulting. *Eng. Geology*, Vol. 43, 213-224.
- Manatschal, G. (1995): Jurassic rifting and formation of a passive continental margin (Platta and Err nappes, Eastern Switzerland): geometry, kinematics and geochemistry of fault rocks and a comparison with the Galicia margin. PhD thesis No. 11188, ETH-Zürich.
- Mancktelow, N. (1990): The Simplon Fault Zone. *Beitr. Geol. Schweiz*, No. 163.
- Mancktelow, N. (1985): The Simplon line: a major displacement zone in the western Lepontine Alps. *Eclogae geol. Helv.*, Vol. 78, No. 1, 73-96.
- Mandia, Y. (1991): Typologie des aquifères évaporitiques du Trias dans le Bassin lémanique du Rhône (Alpes occidentales). PhD thesis No. 948, EPF-Lausanne.
- Mandl, G. (1988): *Mechanics of tectonic faulting - models and basic concepts*. Ed. by H. J. Zwart. Elsevier, Amsterdam.
- Maréchal, J.-C. (1998): Les circulations d'eau dans les massifs cristallins alpins et leurs relations avec les ouvrages souterrains. PhD thesis No. 1769, EPF-Lausanne.
- Marone, C. & Scholz, C. H. (1989): Particle-size distribution and microstructures within simulated fault gouge. *Journal Struct. Geology*, Vol. 11, No. 7, 799-814.
- Marthaler, M. (1984): Géologie des unités penniques entre le Val d'Anniviers et le Val de Tourmagne (Valais, Suisse). *Eclogae geol. Helv.*, Vol. 77, No. 2, 395-448.
- Maurer, H. R., Burkhard, M., Deichmann, N., Green, A. G. (1997): Active tectonism in the central Alps: contrasting stress regimes north and south of the Rhone Valley. *Terra Nova*, Vol. 9, No. 2, 91-94.
- McCreery, G. L. (1949): Improved mount for powdered specimens used on the Geiger-counter X-ray spectrometer. *Journal Am. Ceramic Soc.*, Vol. 32, No. 4, 141-146.
- Méan, Ph. (1994): Le projet Cleuson-Dixence. *In* SIA D 0119, Cleuson-Dixence, 7-14.

- Medalia, A. I. (1970): Dynamic shape factors of particles. *Powder Technology*, Vol. 4, 117-138.
- Norbert, J. Schaeren, G. (1995): *Projet Cleuson-Dixence - Lot D: T-Sup - Rapport géologique*. Unpublished report, No. 1097, Bureau Norbert SA, Lausanne.
- Norbert, J. Schaeren, G. (1996): *Projet Cleuson-Dixence - Lot D: T-Sup - Rapport géologique*. Unpublished report, No. 1102, Bureau Norbert SA, Lausanne.
- Olsson, W. A. (1974): Grain size dependence of yield stress in marble. *Journal Geophys. Res.*, Vol. 79, 4859-4861.
- Onodera, T. F. & Kumara, A. H. M. (1980): Relation between texture and mechanical properties of crystalline rocks. *Bulletin Int. Assoc. Eng. Geol.*, No. 22, 173-177.
- Parriaux, A., Dubois, J. D., Mandia, Y., Basabe, P., Bensimon, M. (1990): The AQUITYP project: towards an aquifer typology in the alpine orogen. *Memoires XXIIInd Congress IAH, EPF-Lausanne, Part I*, 254-262.
- Passchier, C. W., Trouw, R. A. J. (1996): *Microtectonics*. Springer Verlag, Berlin.
- Pelizza, S., Peila, D., Grasso, P., Rabajoli, G. (1994): Ground reinforcing in tunnelling. 2nd Int. Symposium Tunnel construction & Underground structures. Ljubliana, 28. - 30. sept. 1994, 15-26.
- Pickens, J. R. & Gurland, J. (1976): *Proceedings of the 4th Int. Congress of Stereology*. Ed. by E. E. Underwood, R. de Wit and G. A. Moore. National Bureau of Standards Special Publication No. 431. U.S. National Bureau of Standards Gaithersburg.
- Pirard, E. (1994): Analyse morphologique des poudres: une approche systématique et robuste par la morphologie mathématique. *Revue de Métallurgie - CIT/Science et Génie des Matériaux*. Fév., 295-303.
- Quensel, P. (1916): Zur Kenntnis der Mylonitbildung, erläutert an Material aus dem Kebnekaisegebiet. *Bull. Geol. Inst. Univ. Upsala*, Vol. 15, 91-116.
- Rand, M. C., Greenberg, A. E., Taras, M. J. (1975): Standard methods for the examination of wear and wastewater. Am. Public Health Association, Washington.
- Russo, G., Scotti, G., Habimana, J. (1998): On the use of direct and indirect methods in defining geomechanical properties of weak and complex rock masses - Application: Borzoli Cavern. *The Geotechnics of Hard Soils - Soft Rocks*, Vol. 2. Ed. by Evangelista & Picarelli. Balkema, Rotterdam, 825-831.
- Russo, G. (1994): Some considerations on the applicability of major geomechanical classifications to weak and complex rocks in tunnelling. *Bollettino Assoc. Mineraria Subalpina*, Anno XXIX, No. 4, 63-70.
- Rutter, E. H. (1986): On the nomenclature of mode of failure transitions in rocks. *Tectonophysics*, Vol. 122, 381-387.
- Sammis, C. G., Osborne, R. H., Anderson, J. L., Banerdt, M., White, P. (1986): Self similar cataclasis in the formation of fault gouge. *Pure and Applied Geophysics*, Vol. 124, No. 1/2, 53-78.
- Sartori, M. (1990): *L'unité du Barrhorn (Zone pennique, Valais, Suisse)*. PhD thesis Univ. Lausanne. *Mem. Géologie (Lausanne)*, No. 6.
- Schaer, J.-P. (1959): Géologie de la partie septentrionale de l'Eventail de Bagnes. *Arch. Sci. Genève*, Vol. 12, fasc. 4, 473-620.
- Schaeren, G. (1998): Description du massif - géologie et hydrogéologie. *In Erfassen des Gebirges im Untertagebau - Einführungstagung zur Empfehlung SIA 199 (1998)*, FGU. 26. Nov. 1998, Fribourg.
- Schaeren, G. (1994): Les conditions géologiques et les travaux de reconnaissance. *In SIA D 0119, Cleuson-Dixence*, 15-22.

- Schaeren, G. & Cervera, G. (1995): *Projet Cleuson-Dixence - Lot C: Difficultés géologiques C0 à C5*. Unpublished report, No. 1096, Bureau Norbert SA, Lausanne.
- Schaeren, G. & Cervera, G. (1998): *Aménagement Cleuson-Dixence: Géologie après exécution-Lot C*. Unpublished report, Bureau Norbert SA, Lausanne.
- Schmid, S. M., Handy, M. R. (1991): Towards a genetic classification of fault rocks: geological usage and tectonophysical implications. *In Controversies in modern geology*. Ed. by D. W. Müller et al.. Academic Press Limited, London, 339-361.
- Schneider, T. (1992): Einige geologische und geotechnische Probleme des Gotthard-Basistunnels. *Felsbau*, Vol. 10, No. 1, 20-26
- Schroeder, C. (1972): Influence de la lithologie sur le comportement mécanique des roches soumises à essais de compression simple et brésiliens. *Eng. Geology*, Vol. 6, No. 1, 32-43.
- Selley, R. C. (1982): *An introduction to sedimentology*. Academic Press, London.
- SIA Norm 198 (1993): *Travaux souterrains*. Ed. by Société Suisse des Ingénieurs et Architectes. SIA, Zürich.
- SIA Norm 199 (1998): *Erfassung des Gebirges im Untertagebau*. Ed. by Société Suisse des Ingénieurs et Architectes. SIA, Zürich.
- SIA Norm 199 (1975): *Etude du massif rocheux pour les travaux souterrains*. Ed. by Société Suisse des Ingénieurs et Architectes. SIA, Zürich.
- Sibson, R. H., White, S. H., Atkinson, B. K. (1979): Fault rock distribution and structure within the Alpine fault zone: a preliminary account. The origin of the southern Alps, *Royal Soc. New Zealand, Bulletin No 18*, 55-65.
- Sibson, R. H. (1990): Conditions for fault-valve behaviour. *In Deformation Mechanisms, Rheology and Tectonics*. Ed. by R. J. Knipe & E. H. Rutter. *Geol. Soc. Spec. Paper*, No 54, 16-28.
- Sibson, R. H. (1986): Brecciation processes in fault zones: inferences from earthquake rupturing. *Pure and Applied Geophysics*, Vol. 124, No. 1/2, 159-175.
- Sibson, R. H. (1977): Fault rocks and fault mechanisms. *Journal geol. Soc. London*, Vol. 133, 191-213.
- Snoke, A. W., Tullis, J., Todd, V. R. (1998): *Fault-related rocks - a photographic atlas*. Princeton Univ. Press, New Jersey.
- Staub, R. (1915): Petrographische Untersuchungen im Westlichen Berninagebirge. *Vjschr. natf. Ges. Zürich*, Vol. 60, 55-336.
- Swensson, E. (1990): Cataclastic rocks along the Nesodden fault, Oslo region, Norway: a reactivated Precambrian shear zone. *Tectonophysics*, Vol. 178, 51-65.
- Takacs, A. P. & Clay, R. B. (1997): Rock mass classification - practical application under site conditions. *Int. Conf. Tunnelling under difficult conditions & rock mass classification*, Basel, Oct. 1997. ITC Ltd Kempston, Belford, 57-73.
- Tektonische Karte der Schweiz, 1:500'000. Ed. by Schweiz. Geol. Kommission.
- Teuscher, P. (1992): Projektübersicht Lötschberg-Basistunnel. *In SIA D 085, Die AlpTransit-Basistunnel Gotthard und Lötschberg*, 45-53.
- Teuscher, P. (1997): Sondierstollen Kandertal. *In SIA D 0143, AlpTransit: Das Bauprojekt - Schlüsselfragen und erste Erfahrungen*, 95-101.
- Teuscher, P., Keller, M., Ziegler, H.-J. (1998): The Lötschberg base-tunnel: Findings from the preliminary investigations. *Tunnel*, Nr. 4, 32-38.
- Thélin, P., Gouffon, Y., Allimann, M. (1994): Caractéristiques et métamorphisme des phyllosilicates dans la partie occidentale de la "super" nappe du Grand St-Bernard (Val d'Aosta et Valais). *Bulletin Lab. Géol. Univ. Lausanne*, No. 327, 93-145.

- Thélin, P. (1987): Nature originelle des gneiss ocellées de Randa (Nappe de Siviez-Mischabel, Valais). *Bulletin Lab. Géol. Univ. Lausanne*, No. 290, 1-75.
- Termier, P. & Maury, E. (1928): Nouvelles observations géologiques dans la Corse orientale; phénomènes d'écrasement et de laminage; mylonites et brèches tectoniques. *Comptes rendu*, Tome 186, 1247-1251.
- Therry, R. D., Chilingarian, G. V. (1955): Summary of "Concerning some additional aids in studying sedimentary formations" by M. S. Shvetsov. *Journal Sed. Petrology*, Vol. 25, 229-234.
- Trümpy, R. (1980): *Geology of Switzerland - a guide book*, Part A. Ed. by Schw. Geol. Kommission. Wepf & Co., Basel.
- Tourenq, C. (1966): La dureté Vickers des minéraux et des roches, quelques applications. *Bulletin Liaison Lab. Ponts et Chaussées*, No. 19, 1-12.
- Tugrul, A. & Zarif, I. H. (1999): Correlation of mineralogical and textural characteristics with engineering properties of selected granitic rocks from Turkey. *Eng. Geology*, Vol. 51, 303-317.
- Ünal, E., Özkan, I., Ulusay, R. (1992): Characterization of weak, stratified and clay-bearing rock masses. *In Rock characterization, ISRM Symposium: Eurock '92*, Chester, UK. Ed. by J. A. Hudson, British geotechn. Soc., London, 330-335.
- Vanossi, M., Cortesogno, L., Galbiati, B., Messiga, B., Piccardo, G., Vannucci, R. (1984): *Geologia delle Alpi Liguri: Dati, problemi, ipotesi*. *Memorie Soc. Geol. Italiana*, No. 28, 5-75.
- Wallace, R. E. & Morris, H. T. (1986): Characteristics of faults and shear zones in deep mines. *Pure and Applied Geophysics*, Vol. 124, No. 1/2, 107-125.
- Waters, A. C. & Campbell, C. D. (1935): Mylonites from the San Andreas fault zone. *Am. Journal Science*, Vol. 29, No. 174, 473-503.
- Watterson, J. (1986): Fault dimensions, displacements and growth. *Pure and Applied Geophysics*, Vol. 124, No. 1/2, 365-373.
- White, S. (1982): Fault rocks of the Moine Thrust Zone: A guide of their nomenclature. *Textures & Microstructures*, Vol. 4, 211-221.
- Wise, D. U., Dunn, D. E., Engelder, J. T., Geiser, P. A., Hatcher, R. D., Kish, S. A., Odom, A. L., Schamel, S. (1984): Fault-related rocks: Suggestions for terminology. *Geology*, Vol. 12, 391-394.
- Wyder, R. F. (1997): Die Kakirite des Tavetscher Zwischenmassivs aus den NEAT Sondierbohrungen. PhD thesis, Univ. Basel.
- Wyder, R. F. & Mullis, J. (1998a): Geologische Resultate der NEAT Sondierbohrung SB3 - Tujetsch (Sedrun/GR). *Bulletin angew. Geol.*, Vol. 3, No. 2, 205-228.
- Wyder, R. F. & Mullis, J. (1998b): Fluid impregnation and development of fault breccia in the Tavetsch basement rocks / Sedrun, Central Swiss Alps. *Tectonophysics*, Vol. 294, No. 1/2, 89-107.
- Zenhäusern, S. & Bürgi, C. (1999): Annotations concernant le projet de recherche "Cataclasites". Unpublished report, GEOLEP - EPF-Lausanne
- Zhang, X. & Sanderson, D. J. (1995): Anisotropic features of geometry and permeability in fractured rock masses. *Eng. Geology*, Vol. 40, 65-75.
- Zhao, Z. Y., Wang, Y., Liu, X. H. (1990): Fractal analysis applied to cataclastic rocks *Tectonophysics*, Vol. 178, 373-377.
- Ziegler, H.-J. (1997): Lötschberg-Basistunnel: Neue geologische Erkenntnisse aus den Sondierarbeiten. *In SIA D 0143, AlpTransit: Das Bauprojekt - Schlüsselfragen und erste Erfahrungen*, 33-39.

APPENDIX

Append. I: list of samples and performed analyses

Append. II: semi-quantitative XRD-analyses

- II-a: Cleuson-Dixence, unit B
- II-b: Cleuson-Dixence, unit C
- II-c: Cleuson-Dixence, unit D
- II-d: borehole Goltschried
- II-e: Varzo
- II-f: Genoa

Symbols of identified mineral phases in XRD-patterns

Ak: ankerite [104]	LiF: griceite (internal standard)
Ant antigorite	Liz lizardite
Ar aragonite	M: mica group
Cc: calcite [104]	Mgt magnetite
Chl: chlorite group	Pa: paragonite
Dol: dolomite [104]	Pl: Na-plagioclase [201]
Gibs: gibbsite	Py: pyrite
Go: goethite	Qz: quartz [101]
Ka: kaolinite group	Tr: tremolite-actinolite group [110]
Kf: K-feldspar [002]	

Miller Index [hkl] used for quantification.

Cleuson-Dixence Unit B, le Chargeur - Tortin

sample	TM	host rock	sample type	analyses
CD 19	2837	chlorito-sericitic schist	kakirite	TS XRD
CD 20.1	2830		"	TS, XRD
CD 20.3	2830		"	TS gr XRD
CD 22	2780		"	TS XRD
CD 23	2874		"	TS XRD
CD 7	3000	greenstone	host rock	TS XRD
CH 12.2	4290		"	TS XRD
CH 13	4290		"	TS XRD

Cleuson-Dixence Unit C, Tracouet - Tortin

sample	TM	host rock	sample type	analyses
Tr 1.2	5180	sericitic quartz schist	host rock	TS XRD
Tr 1c	5180		kakirite	TS
Tr 2a	5180		"	gr XRD
Tr 5b	5180		"	TS XRD
Tr 3	5597		"	TS XRD
Tr 4	5597		"	TS gr XRD

Cleuson-Dixence Unit D, Zerjona

sample	TM	host rock	sample type	analyses
Zr bloc	4	quartzite	cataclasite	TS XRD
Zr 13.1	9	quartzitic meta-sandstone	kakirite	TS gr XRD
Zr 21.2	14		"	TS XRD
Zr 39	9		"	TS XRD
Zr 40	9		"	XRD
Zr 9	7		micaceous schist	kakirite
Zr 18	13	"		XRD
Zr 20	13	"		XRD
Zr 21.3	14	"		XRD
Zr 29.1	21	"		TS XRD
Zr 30	1	"		TS gr XDR
Zr 33	4	"		TS gr XRD
Zr 43	1	"		TS gr XRD
Zr 46	1	"		TS
Zr B17	13	black carbonaceous phyllite		"
Zr 21.4	14		kakirite	TS
Fom 9.1 ^{*)}	118m		"	TS gr XRD

^{*)} Sample from borehole DZ2.

Unit D, "Verrucano"

sample	TM	host rock	sample type	analyses
Vr 4	450	carbonate breccia	kakirite	TS gr XRD
Vr 6	450		"	TS XRD

TS: thin section, gr: granulometry, XRD: X-ray diffraction analyse

Borehole Goltschried (95/23), Aar massif

sample	depth	host rock	sample type	analyses
G 4a	626 m	phyllite of S-DZ	kakirite	TS XRD
G 5-21	703.5	phyllite of N-DZ	host rock	TS XRD
G 5-22			kakirite	TS XRD
G 6-1	713.8	phyllite of N-DZ	host rock	TS XRD
G 6-2			kakirite	TS XRD
G 8	727.7	phyllite of N-DZ	kakirite	TS XRD
G 9-1	731.7	schistose gneiss of AM	host rock	XRD
G 9-2			kakirite	gr XRD

DZ: Dornbachzone, N: northern, S: southern, AM: Aar massif basement

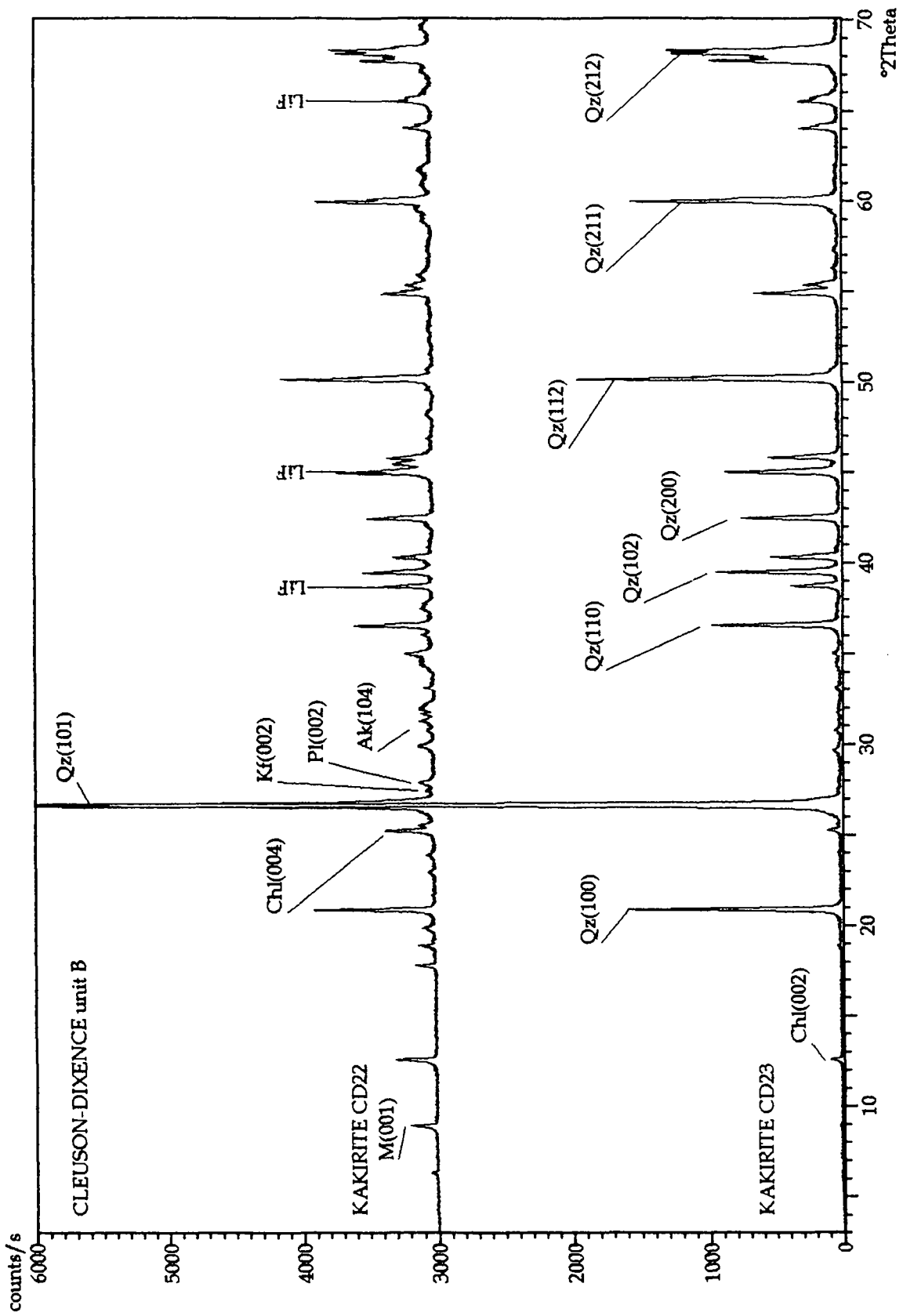
Varzo

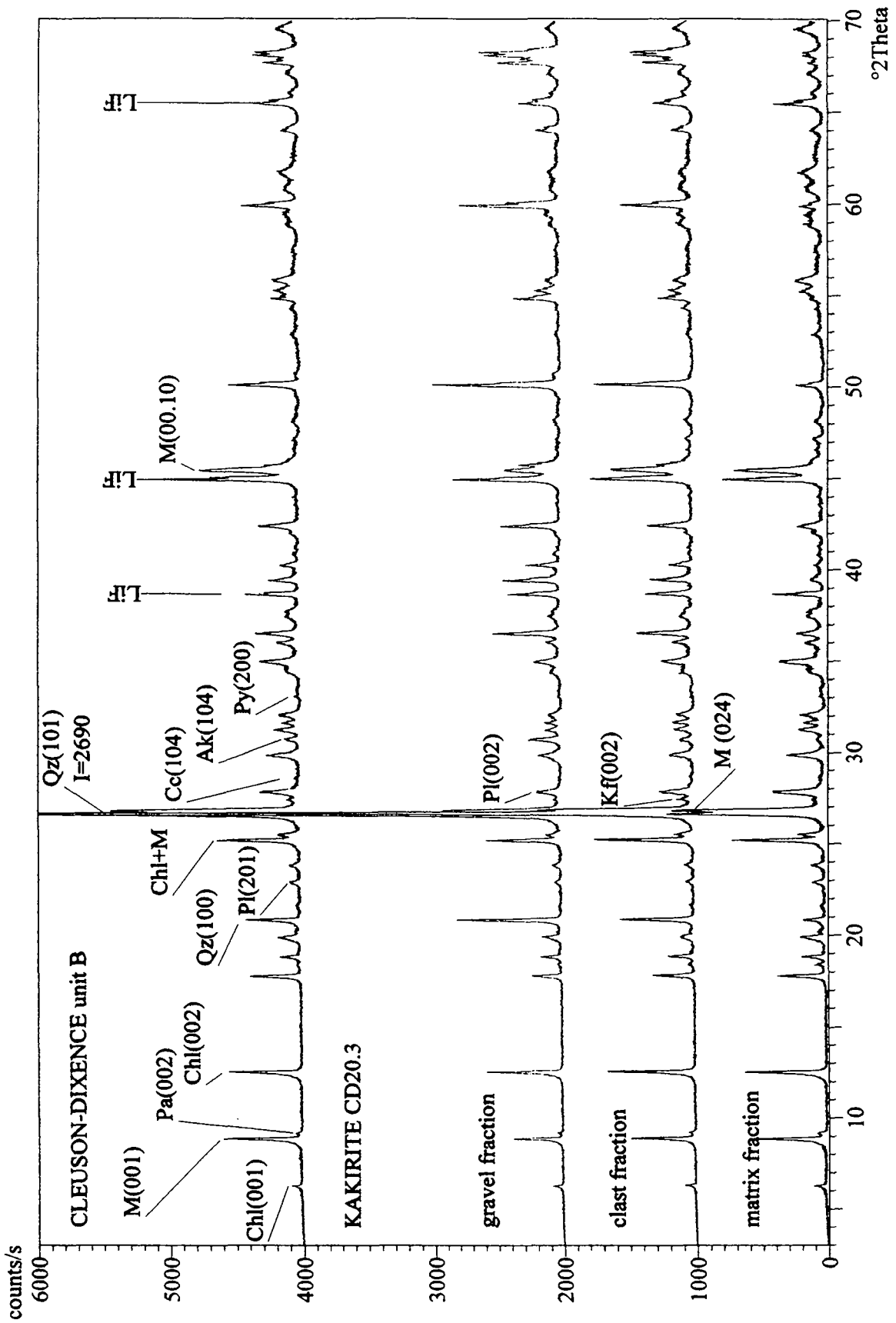
sample	depth	host rock	sample type	analyses
Vz 2	755	gneiss	kakirite	TS XRD
VZ 14	755		kakirite	TS gr XRD

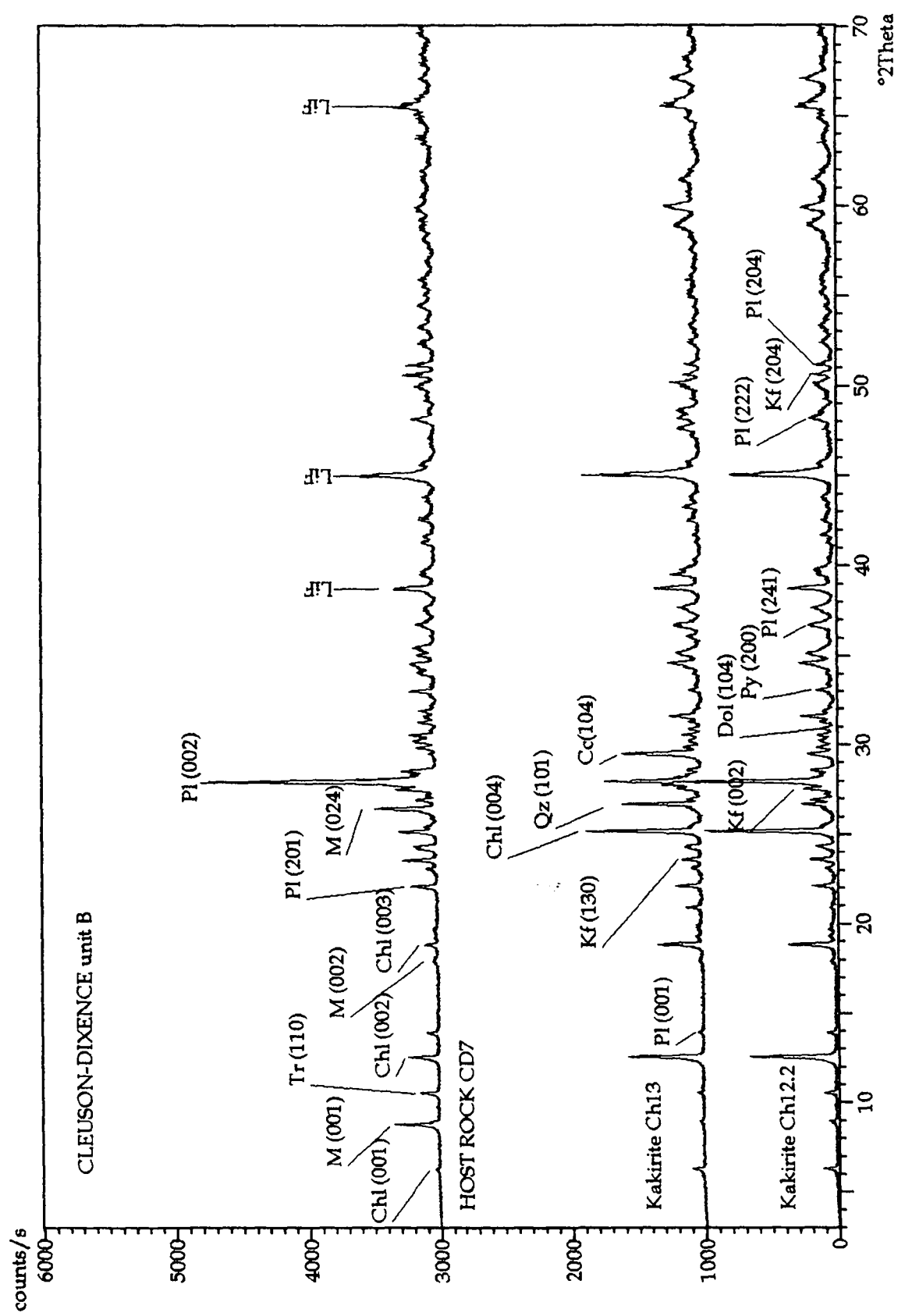
Genoa

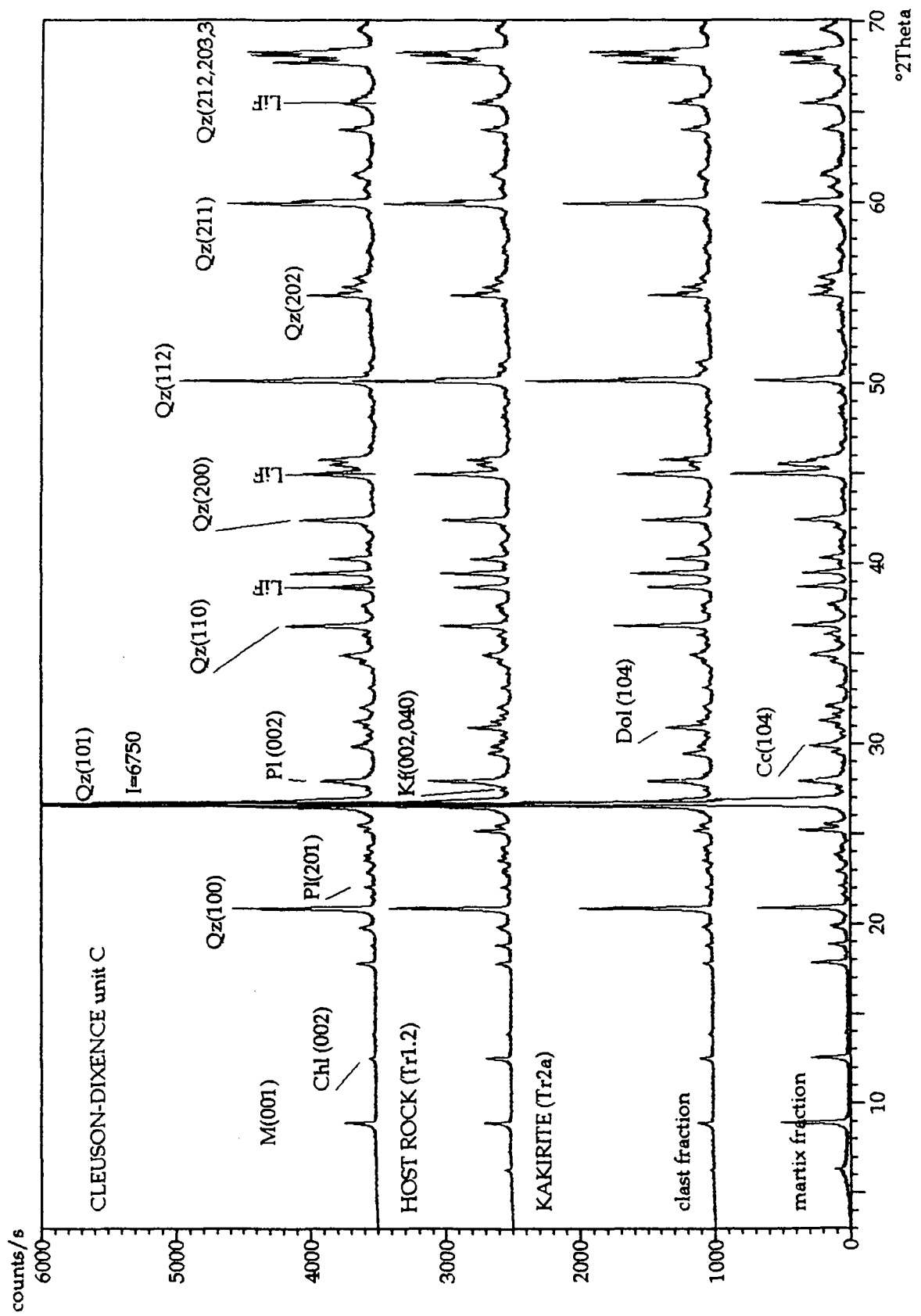
sample		host rock	sample type	analyses
MG 3.1	Mt Gazzo	serpentin schist	kakirite	TS XRD
MG 8	Borzoli Cavern	serpentinite	"	TS gr XRD
MG 11-1	Mt Gazzo	serpentinite	serp. lense	XRD
MG 20.1			"	TS gr XRD
MG 20.1a/b			"	TS XRD
MG 24.1a/b	Mt Gazzo	serpentin schist	"	TS XRD

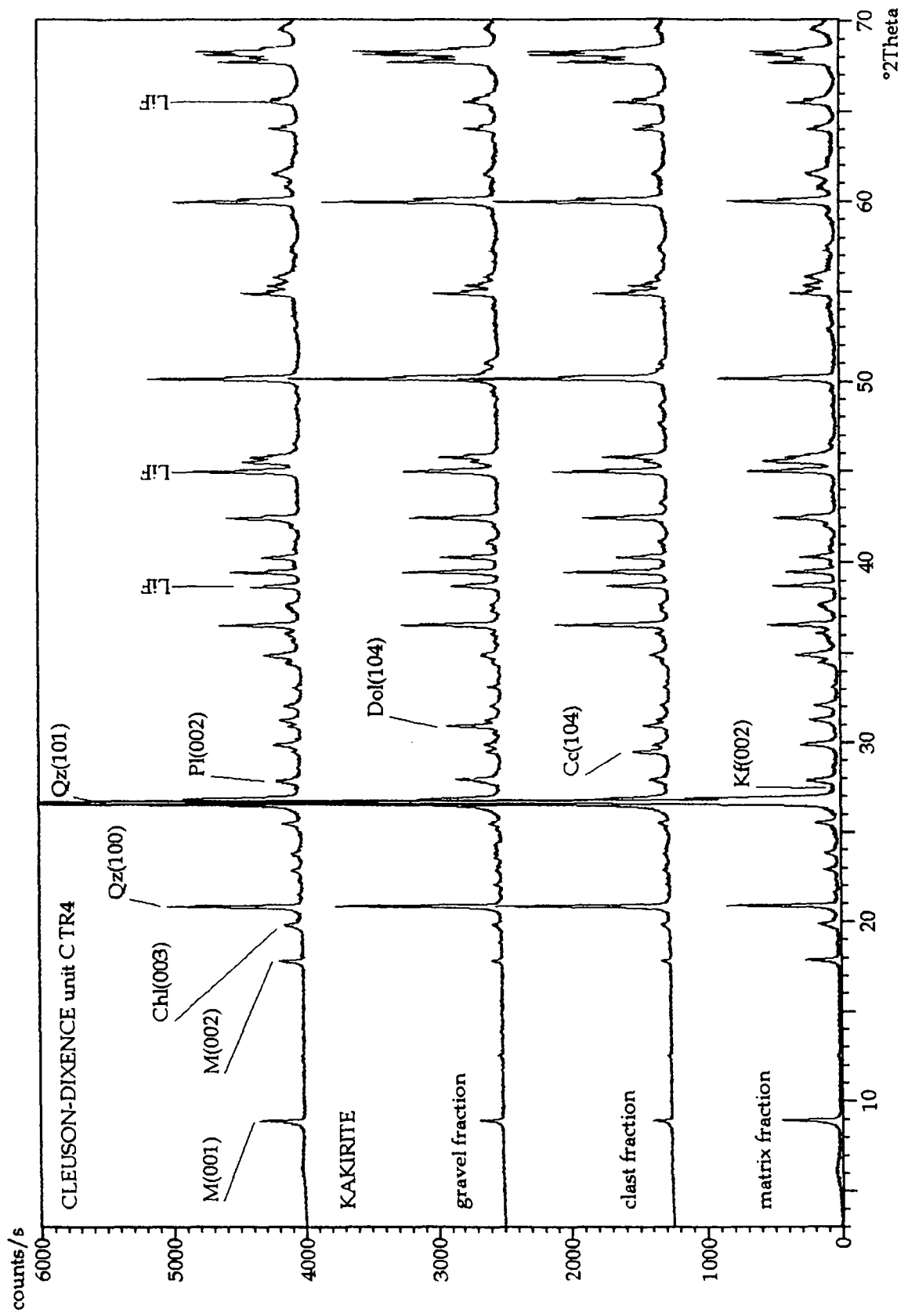
TS: thin section, gr: granulometry, XRD: X-ray diffraction analyse









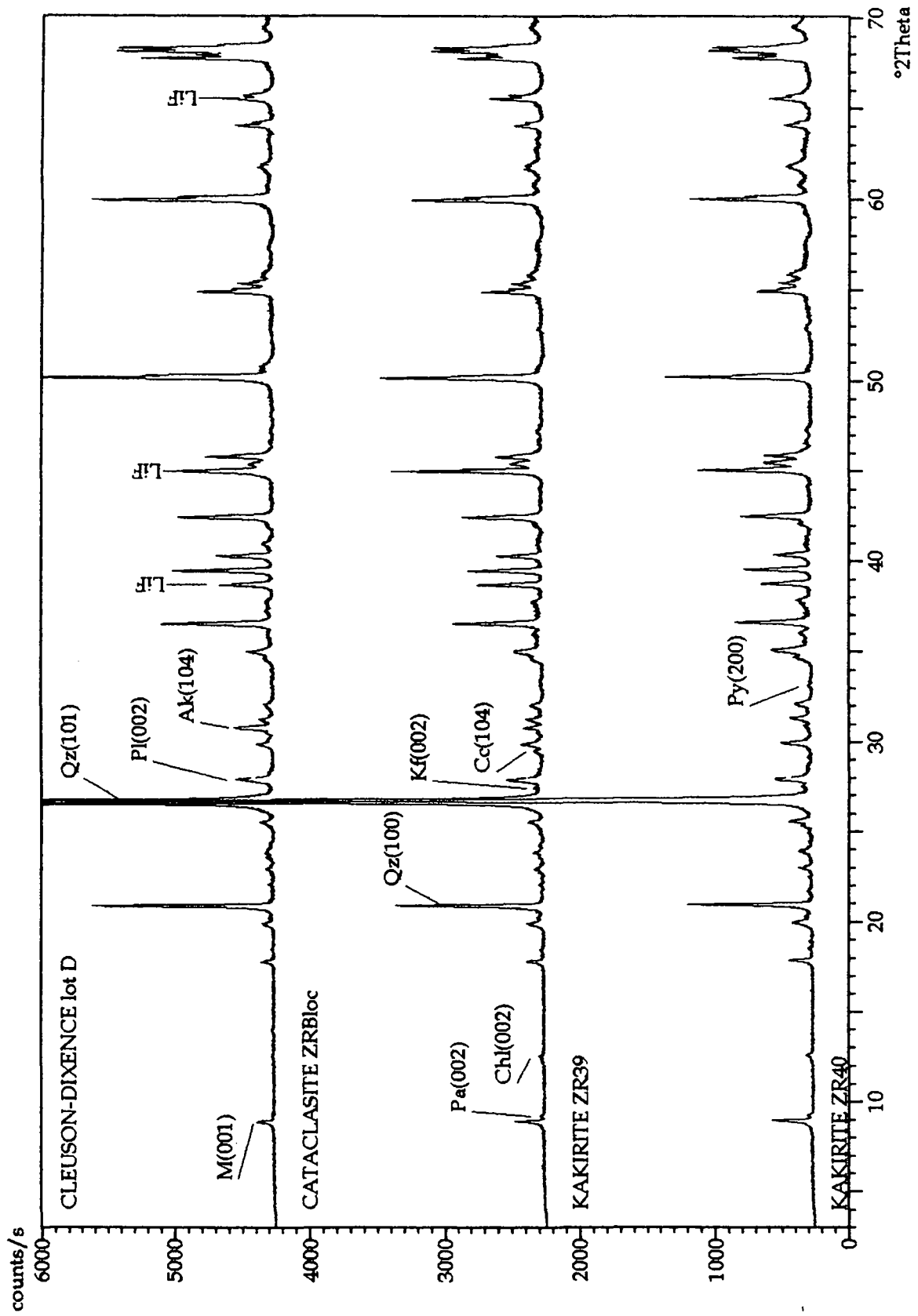


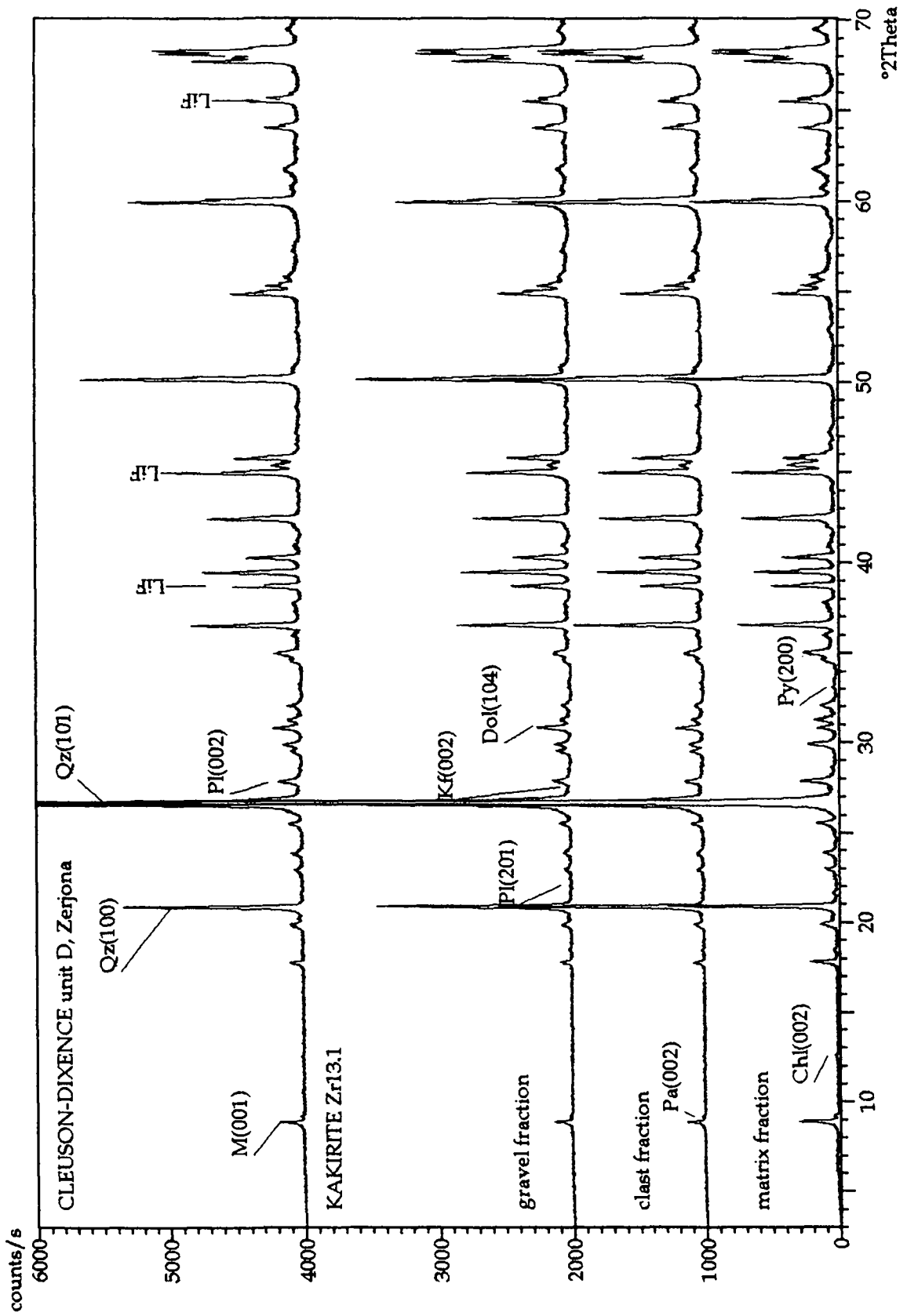
sample rock type	Zr 18				Zr 20				Zr 29.1				Zr 30			
	kakirite	gravel fract.	clast fract.	matrix fract.	kakirite	gravel fract.	clast fract.	matrix fract.	kakirite	gravel fract.	clast fract.	matrix fract.	kakirite	gravel fract.	clast fract.	matrix fract.
quartz	18				12				16				16			
plagioclase	1				2				11				7			
K-feldspar	5				5				5				3			
calcite													2			
dolomite																
ankerite					1								5			
amphibole																
non-quantified	76				80				68				74			
chlorite	x				x				xx				x			
white mica	x				x				xx				x			
paragonite					x				x							
kaolinite																
iron oxyde																
magnetite																
sphene																
epidote																

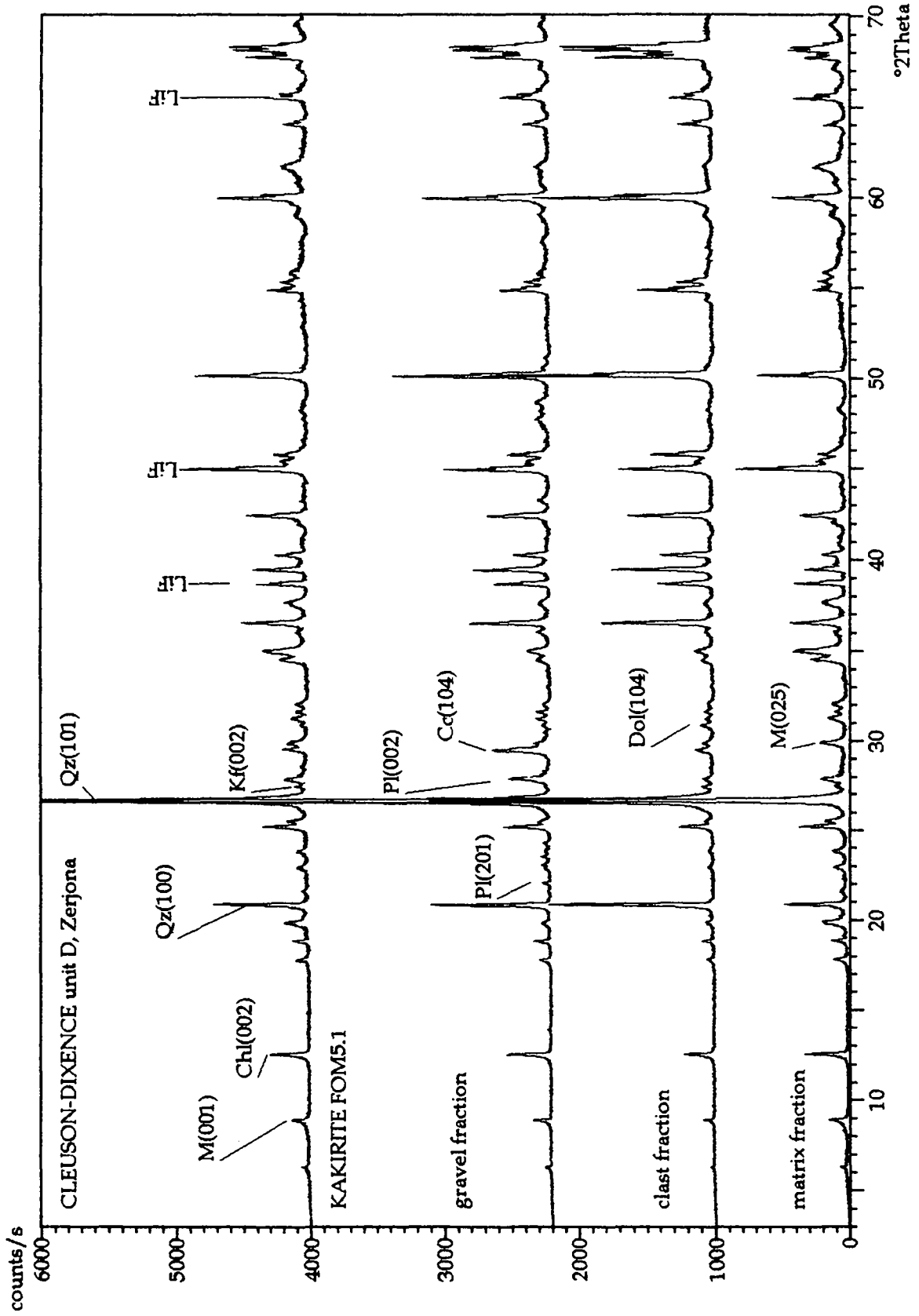
sample rock type	Zr 43				Zr 30			
	kakirite	gravel fract.	clast fract.	matrix fract.	kakirite	gravel fract.	clast fract.	matrix fract.
quartz	27	23	23	23	12			
plagioclase	6	9	7	8	2			
K-feldspar	4	3	3	3	5			
calcite	1							
dolomite								
ankerite	1	4	3	2				
amphibole								
non-quantified	61	61	64	64	80			
chlorite	x	x			x			
white mica	x	x			x			
paragonite								
kaolinite								
iron oxyde								
magnetite								
sphene								
epidote	x							

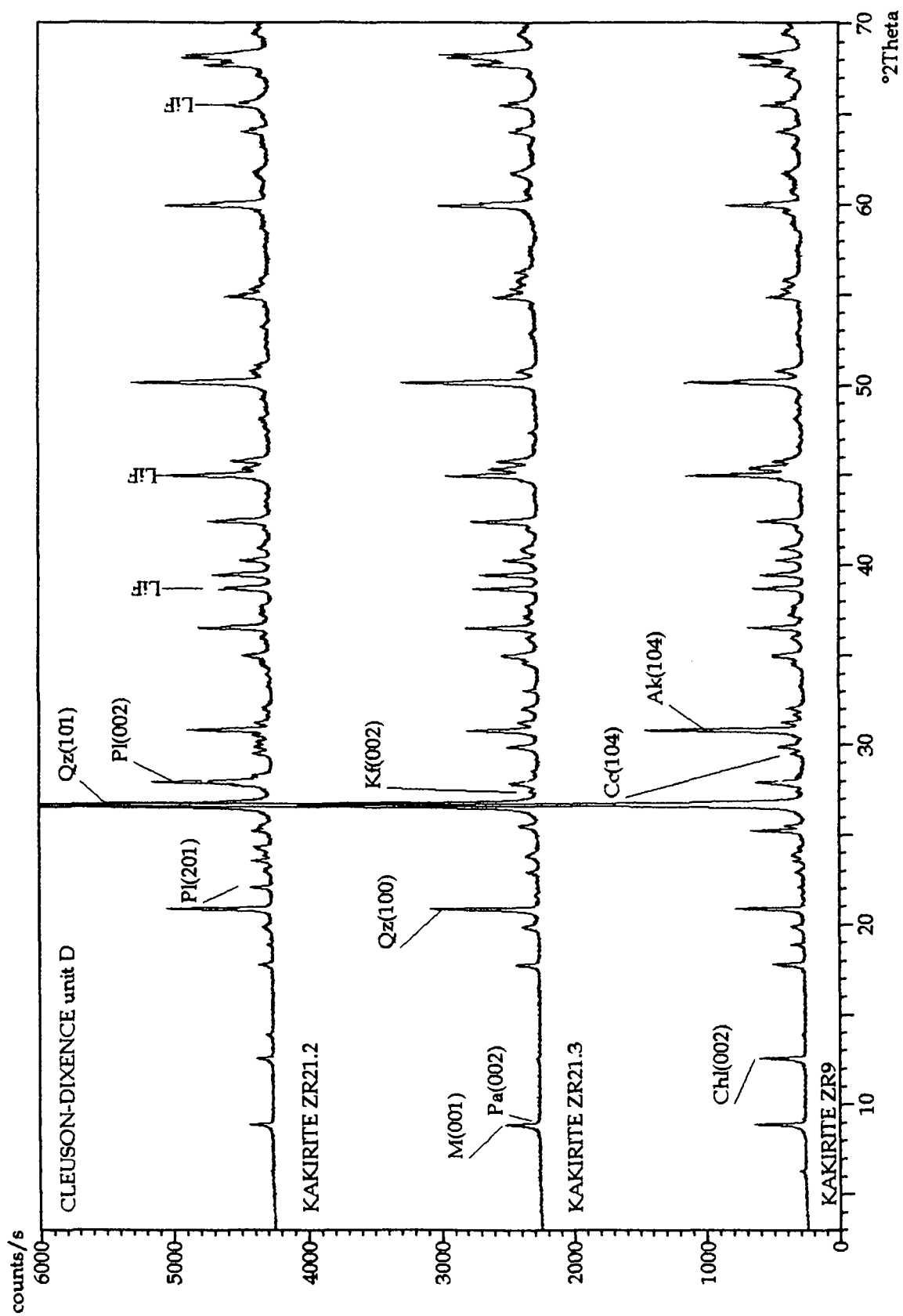
sample rock type	Zr 18				Zr 20				Zr 29.1				Zr 30			
	kakirite	gravel fract.	clast fract.	matrix fract.	kakirite	gravel fract.	clast fract.	matrix fract.	kakirite	gravel fract.	clast fract.	matrix fract.	kakirite	gravel fract.	clast fract.	matrix fract.
quartz	21				30				23				9			
plagioclase	3				4				2				4			
K-feldspar	4				3				3				4			
calcite	1				1				1				1			
dolomite	1				3				23				1			
ankerite																
amphibole																
non-quantified	70				59				48				81			
chlorite	x				x				x				x			
white mica	xx				x				x				xx			
paragonite																
kaolinite													x			
iron oxyde																
magnetite	x															
sphene																
epidote	x															

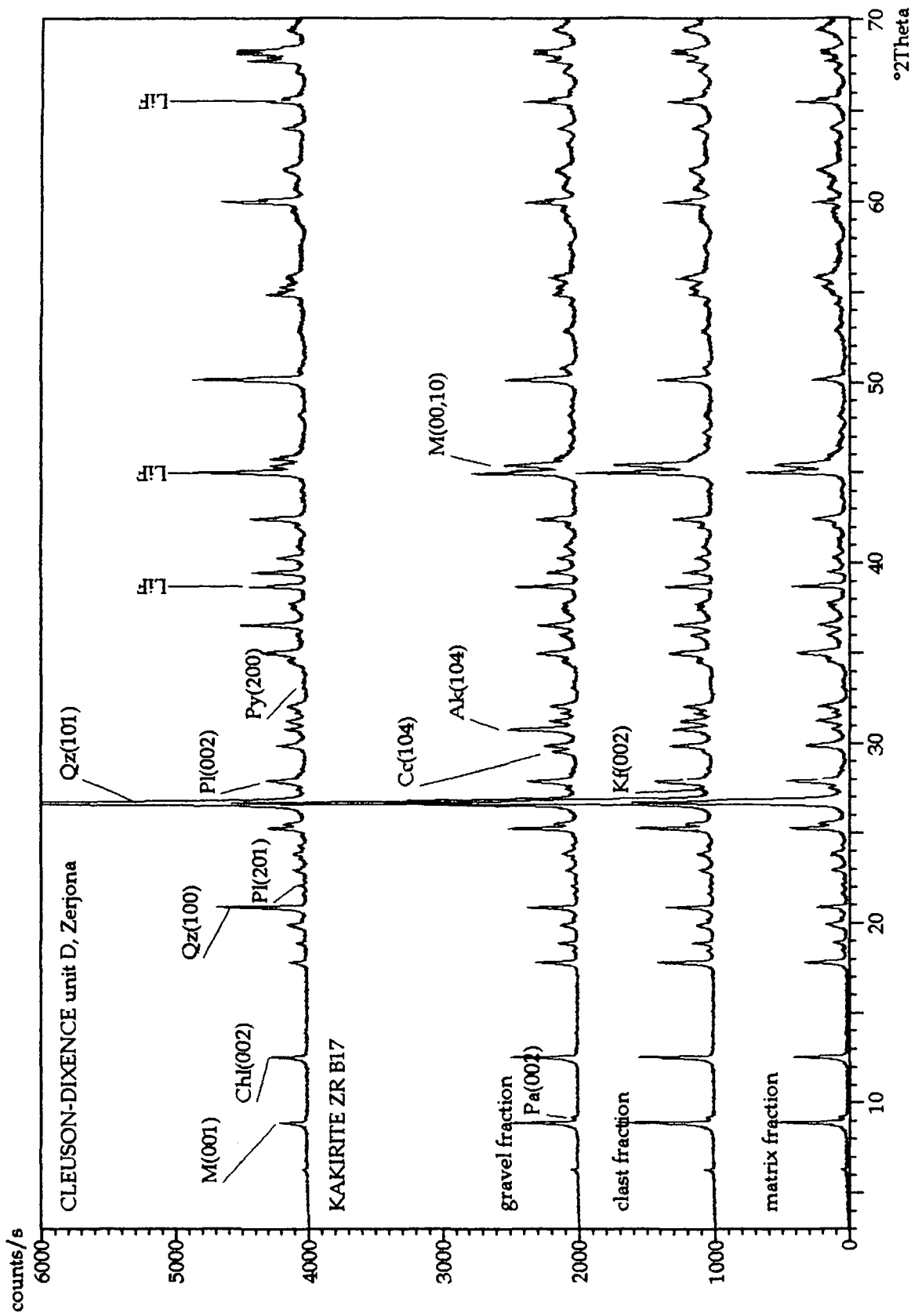
sample rock type	Zr 43				Zr 33			
	kakirite	gravel fract.	clast fract.	matrix fract.	kakirite	gravel fract.	clast fract.	matrix fract.
quartz	13	34	22	11	13	34	22	11
plagioclase	3	3	4	2	3	3	4	2
K-feldspar	5	3	3	5	5	3	3	5
calcite		1	1			1	1	
dolomite								
ankerite	1	3	2		1	3	2	
amphibole								
non-quantified	78	56	68	82	78	56	68	82
chlorite	x	x	x	xx	x	x	x	xx
white mica	x	x	x	xxx	x	x	x	xxx
paragonite				x				x
kaolinite								
iron oxyde								
magnetite	x	x	x		x	x	x	
sphene								
epidote					x		x	

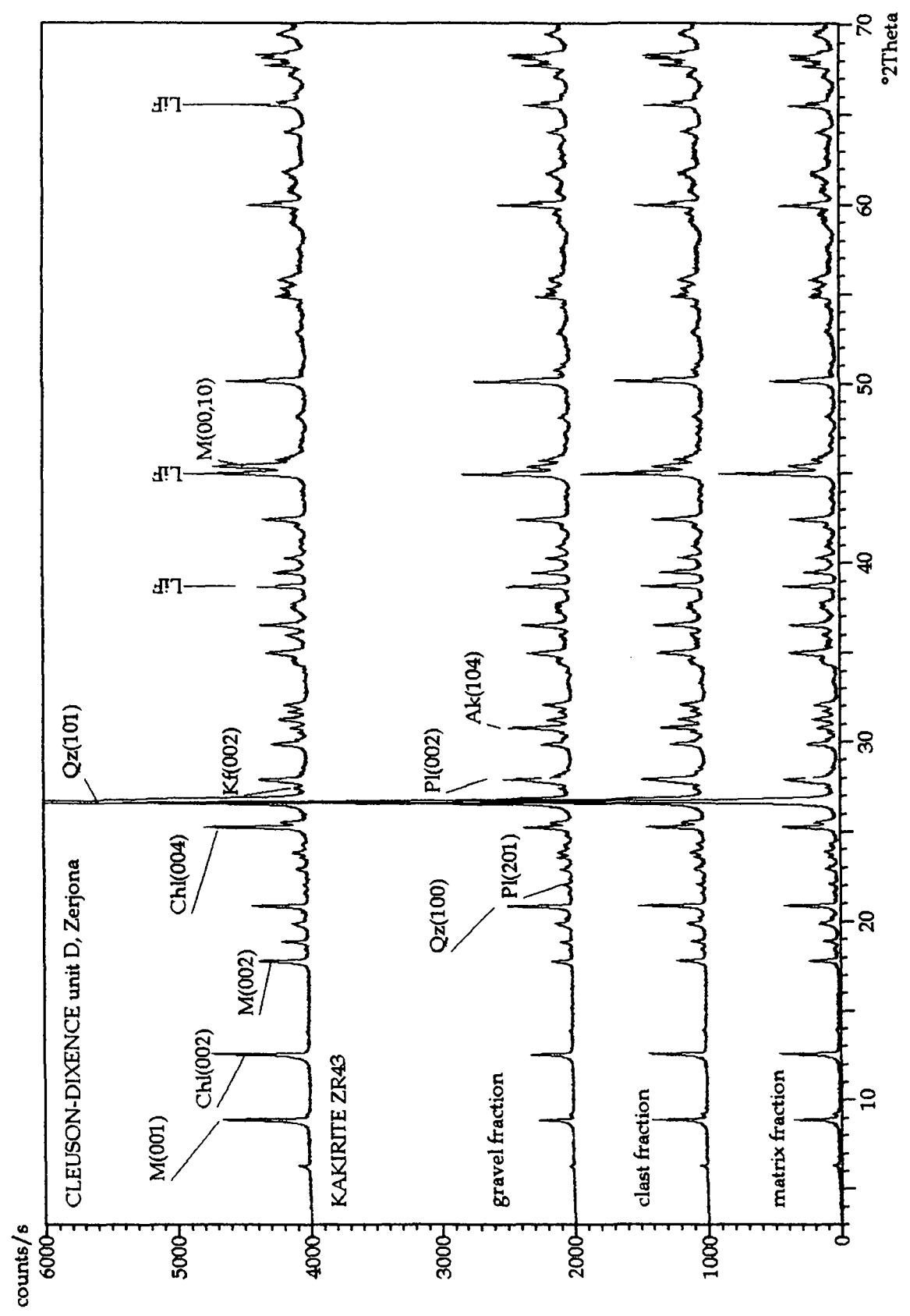


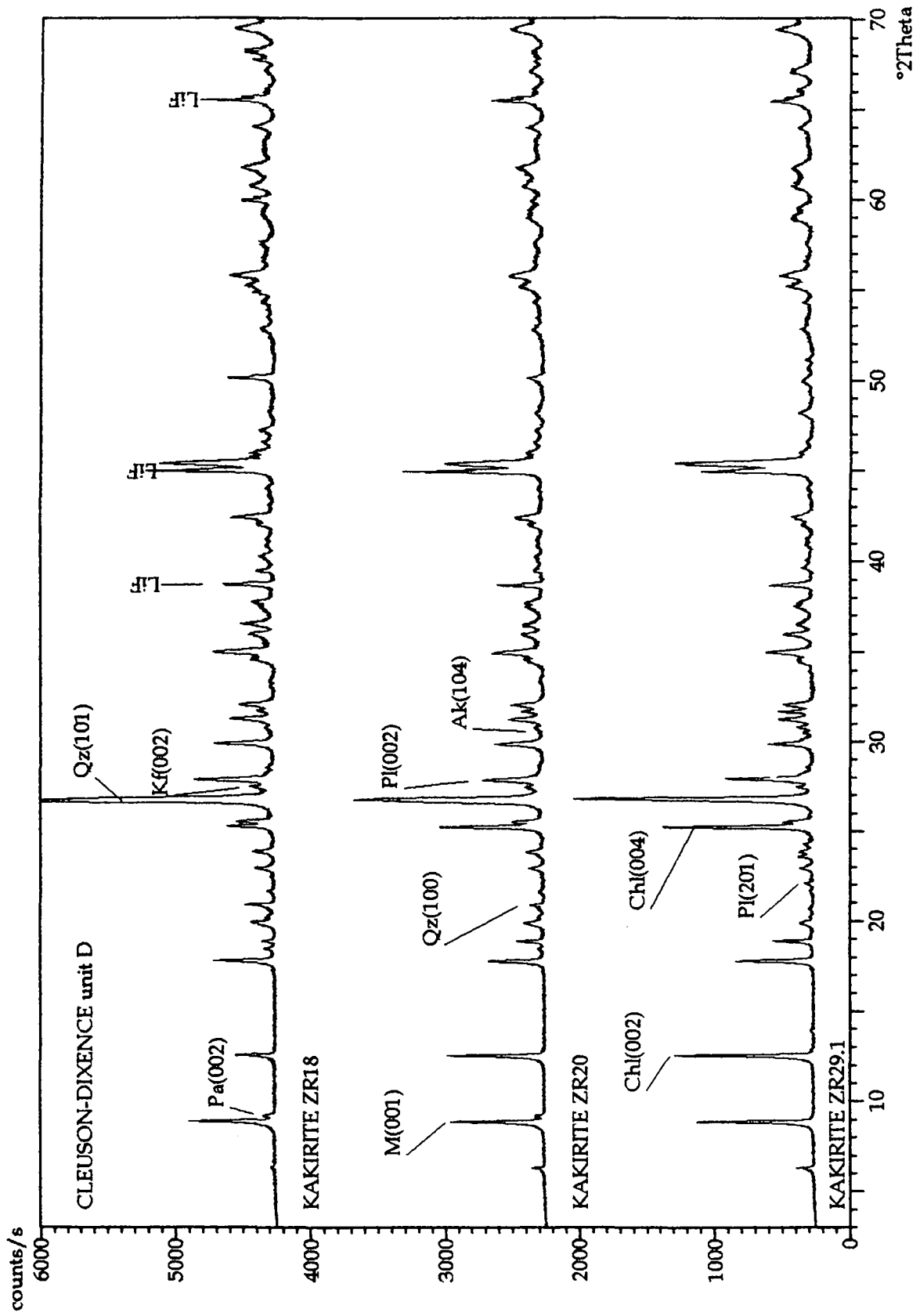


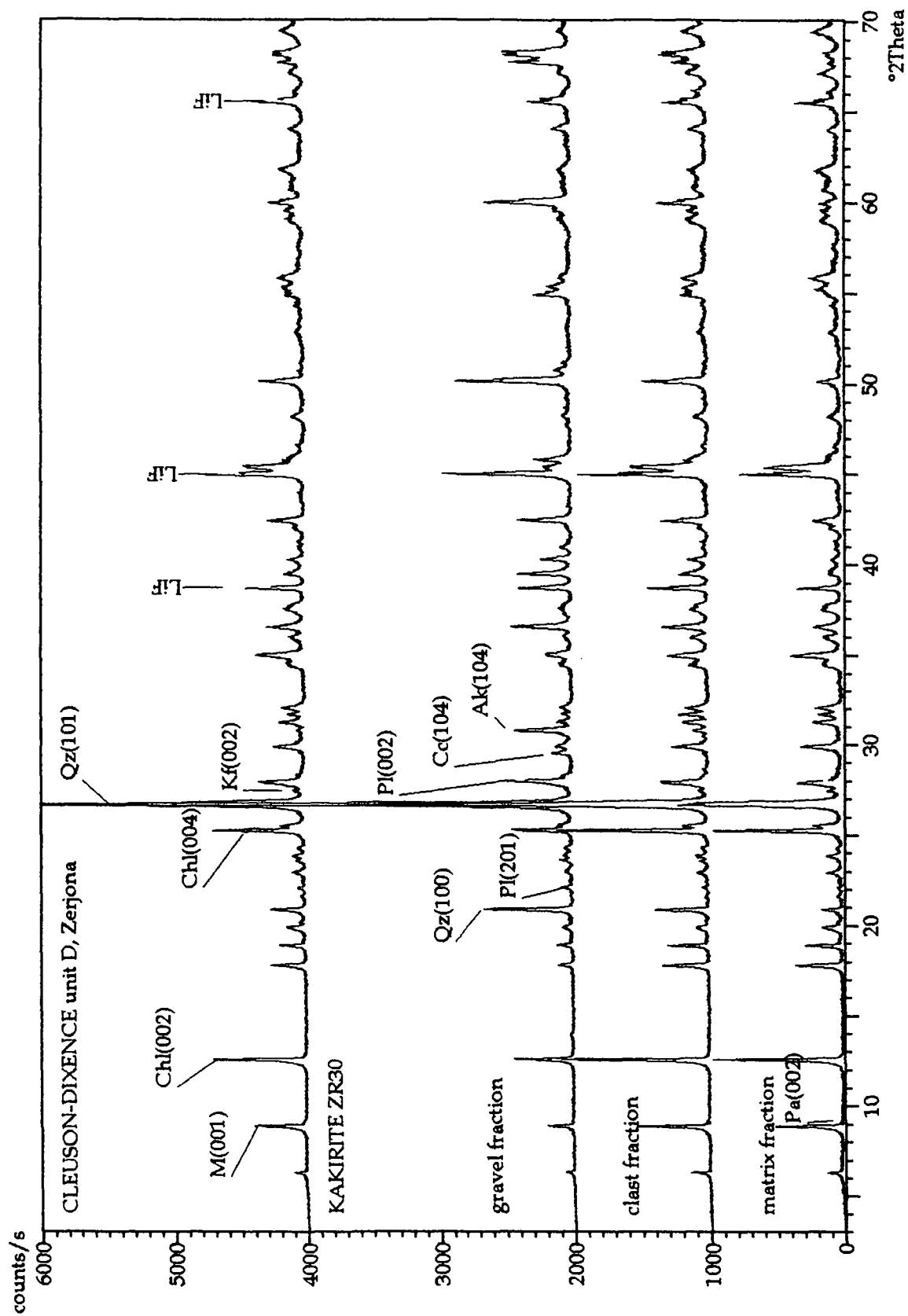


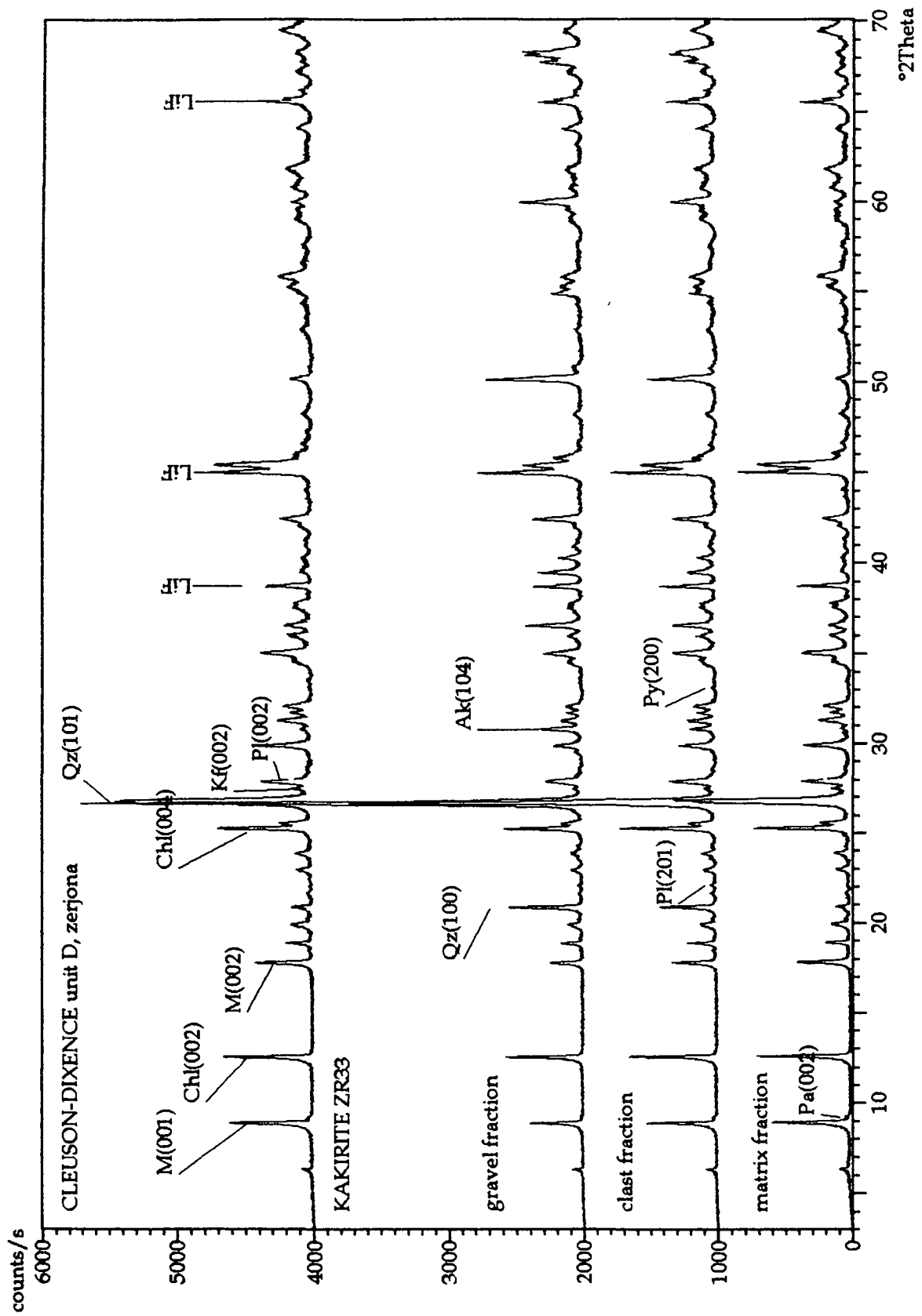


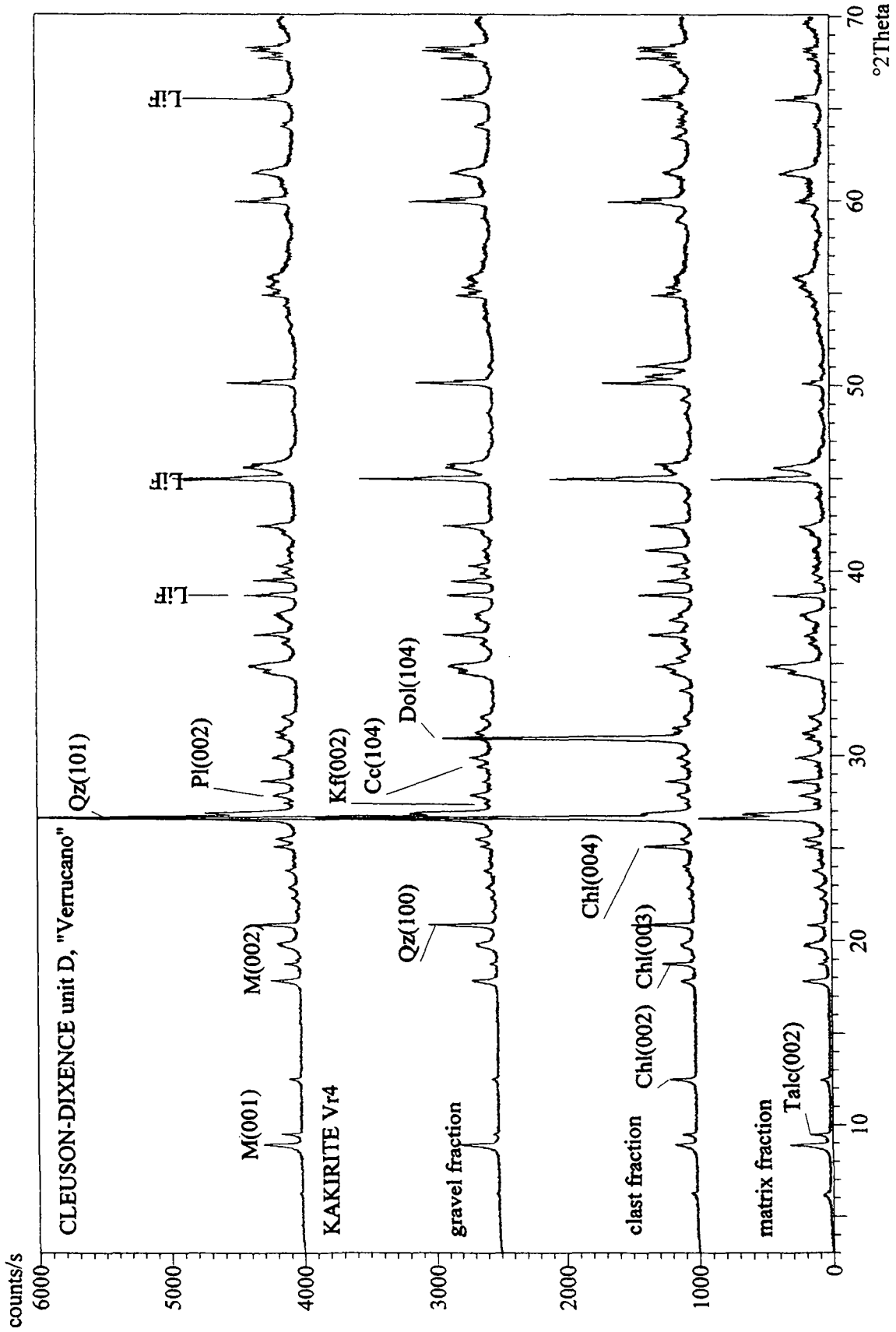






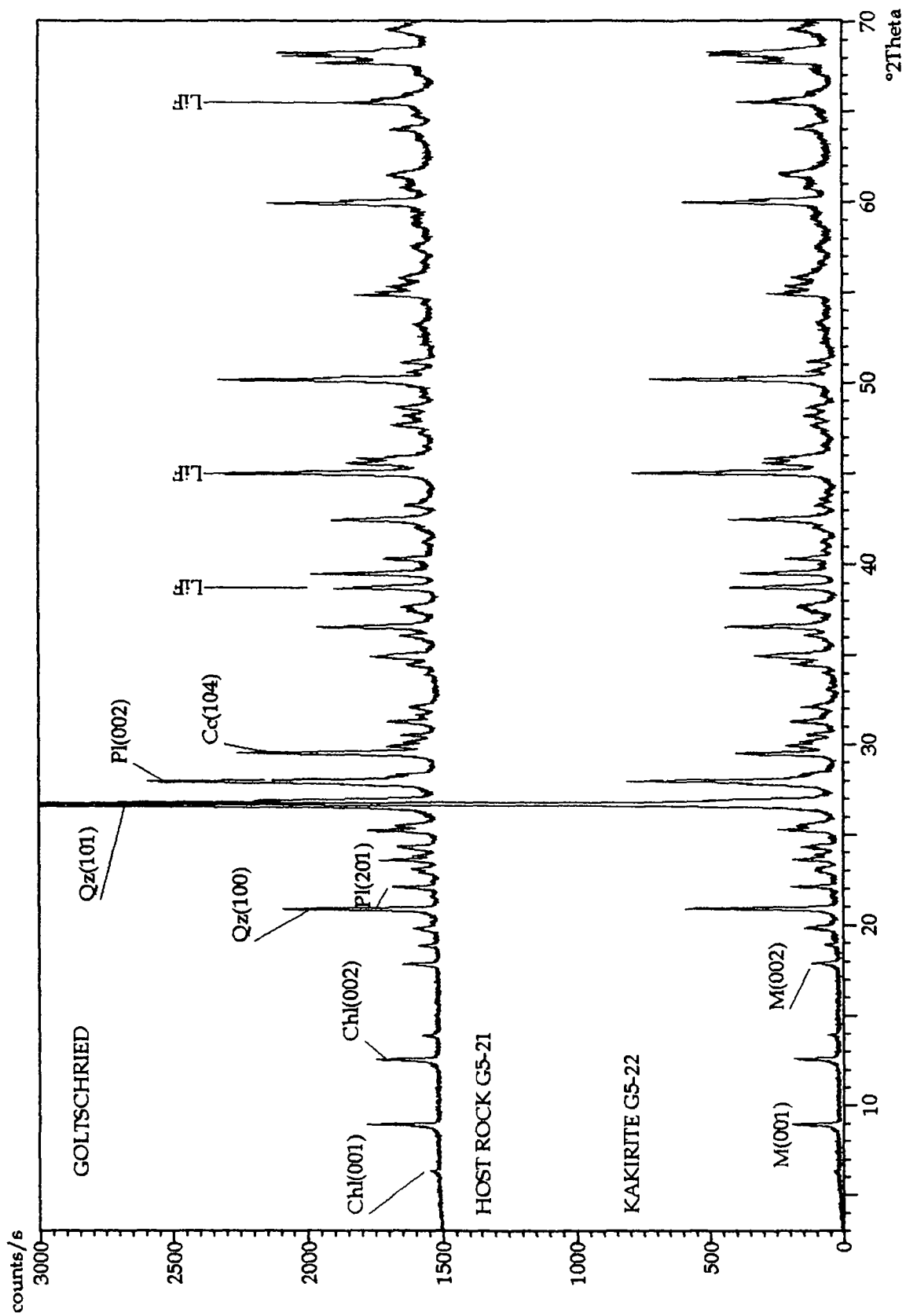


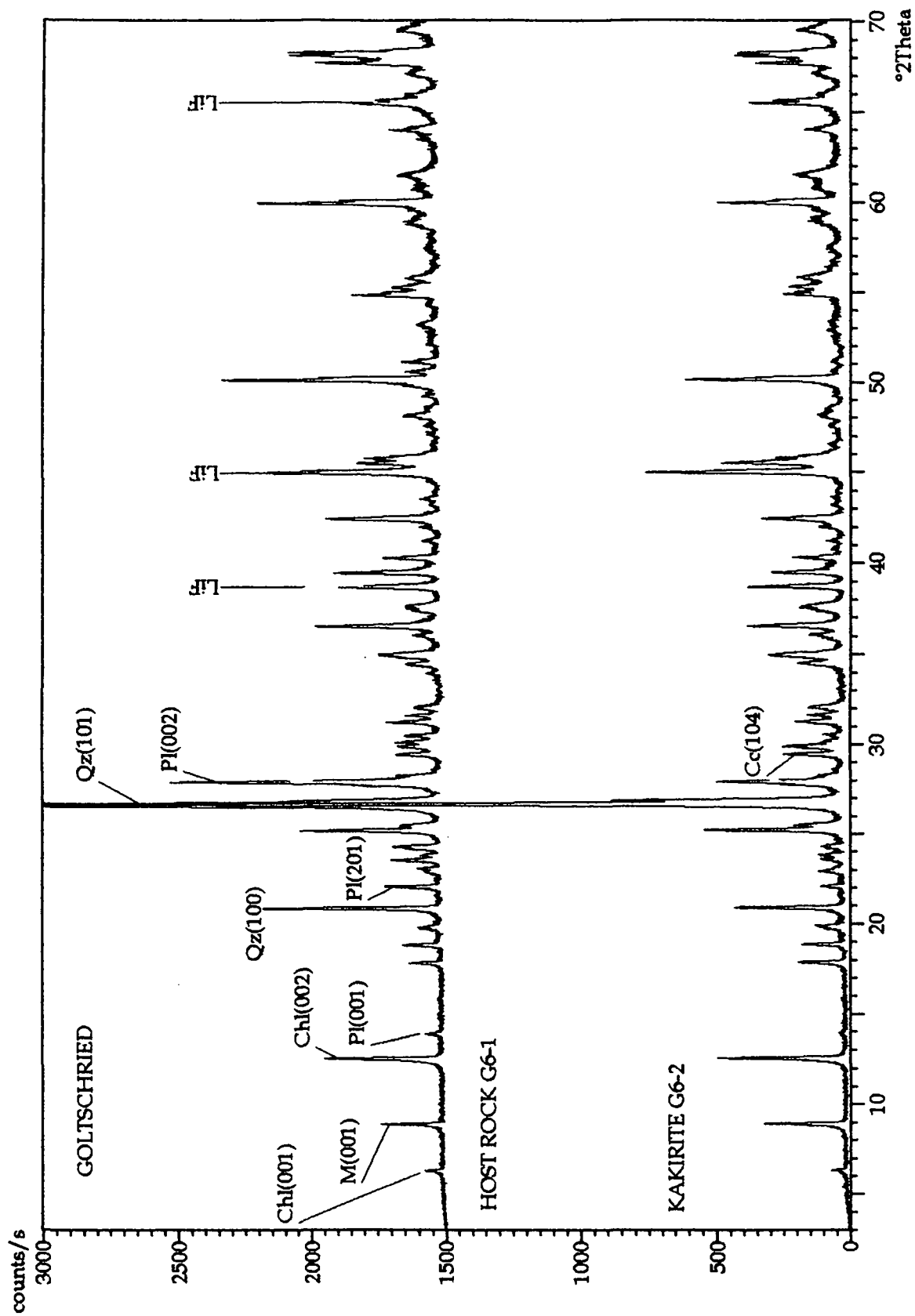


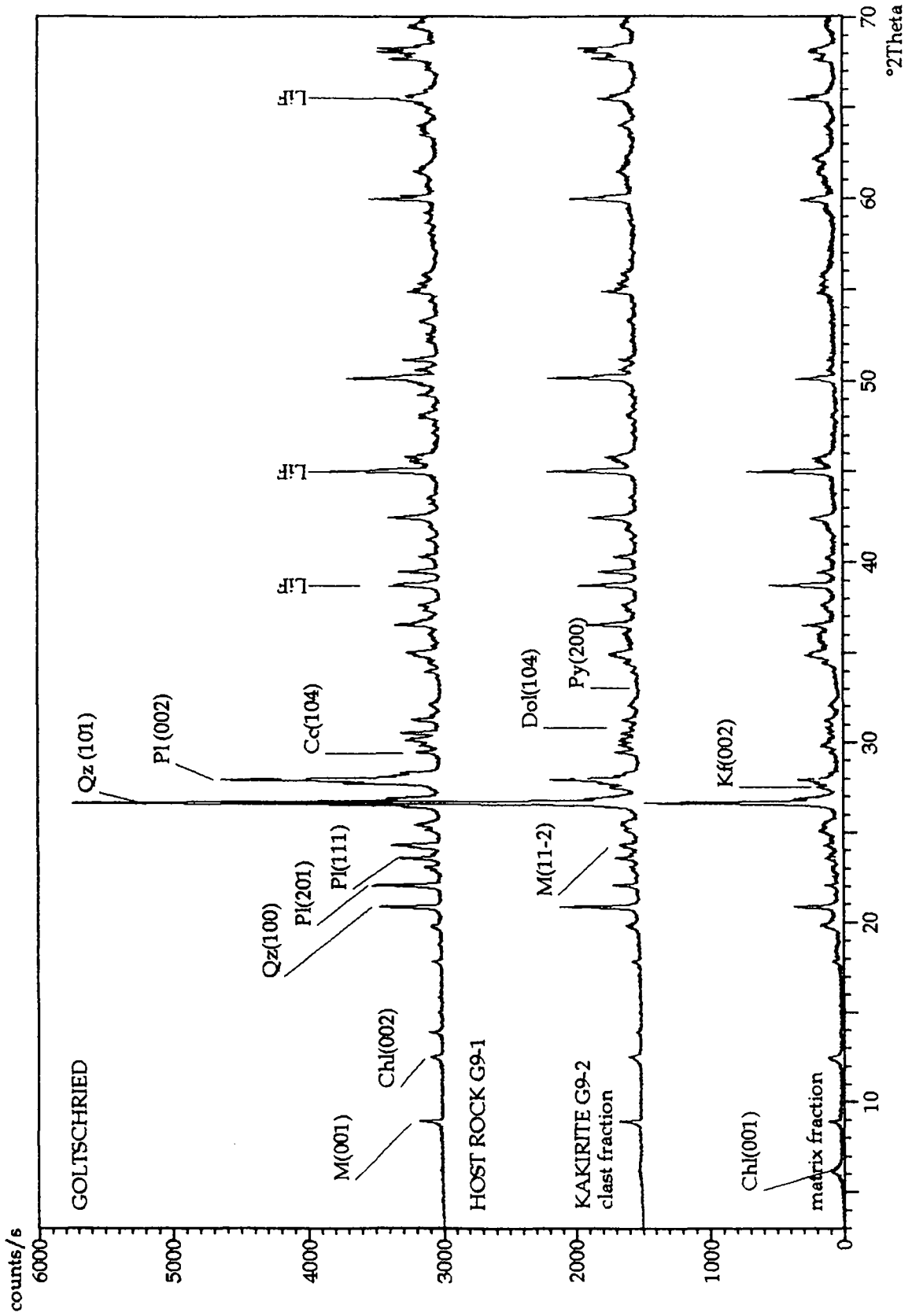


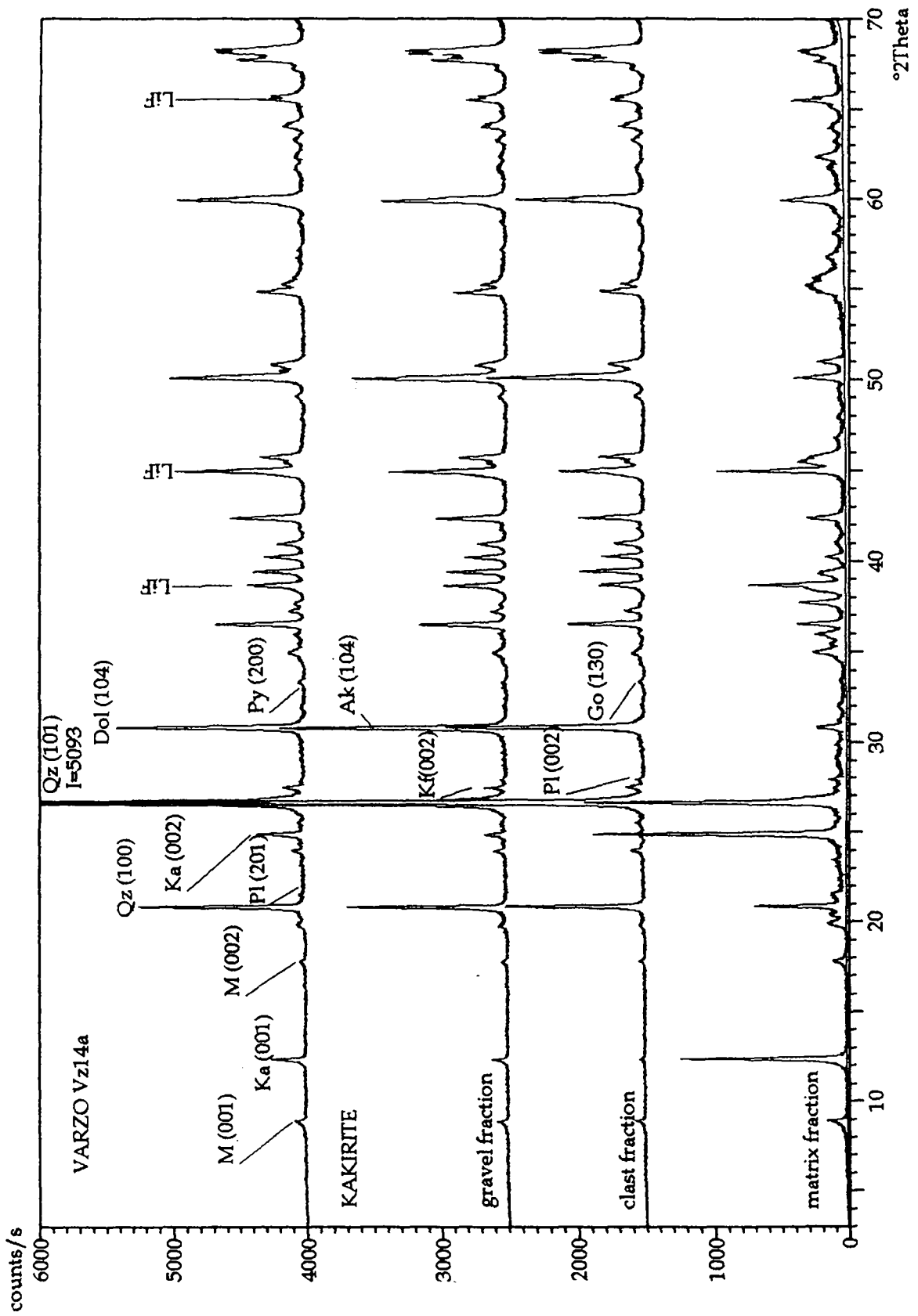
sample rock type	G 4 kikirite	G 5 - 21 host rock	G 5 - 22 kikirite	G 6 - 1 host rock	G 6 - 2 kikirite	G 9 - 1 host rock	G 9 - 2	
							clast fract.	matrix fract.
quartz	26	36	28	36	28	22	24	11
plagioclase	14	24	11	30	11	69	24	11
K-feldspar	3			2		2	2	5
calcite	2	11	5	2	3	2	2	1
dolomite							1	1
ankerite								
amphibole								
non-quantified	55	29	56	30	58	5	47	71
chlorite	x	x	x	x	x	x	x	x
white mica	x	x	x	x	x	x	x	x
paragonite								x
kaolinite								
iron oxyde			x	x	x	x	x	x
magnetite								
sphene								
epidote								

sample rock type	Vz 2 kikirite	Vz 14a			matrix fract.
		kikirite	gravel fract.	clast fract.	
quartz	16	39	43	55	11
plagioclase	3				
K-feldspar	5	7	5	7	2
calcite					
dolomite			18	22	1
ankerite	1	16			
amphibole					
non-quantified	75	38	34	16	86
chlorite	x			x	
white mica	x	x	x		x
paragonite					
kaolinite			x	x	xx
iron oxyde	x		x	x	x
magnetite					
sphene		x	x		
epidote	x	x			

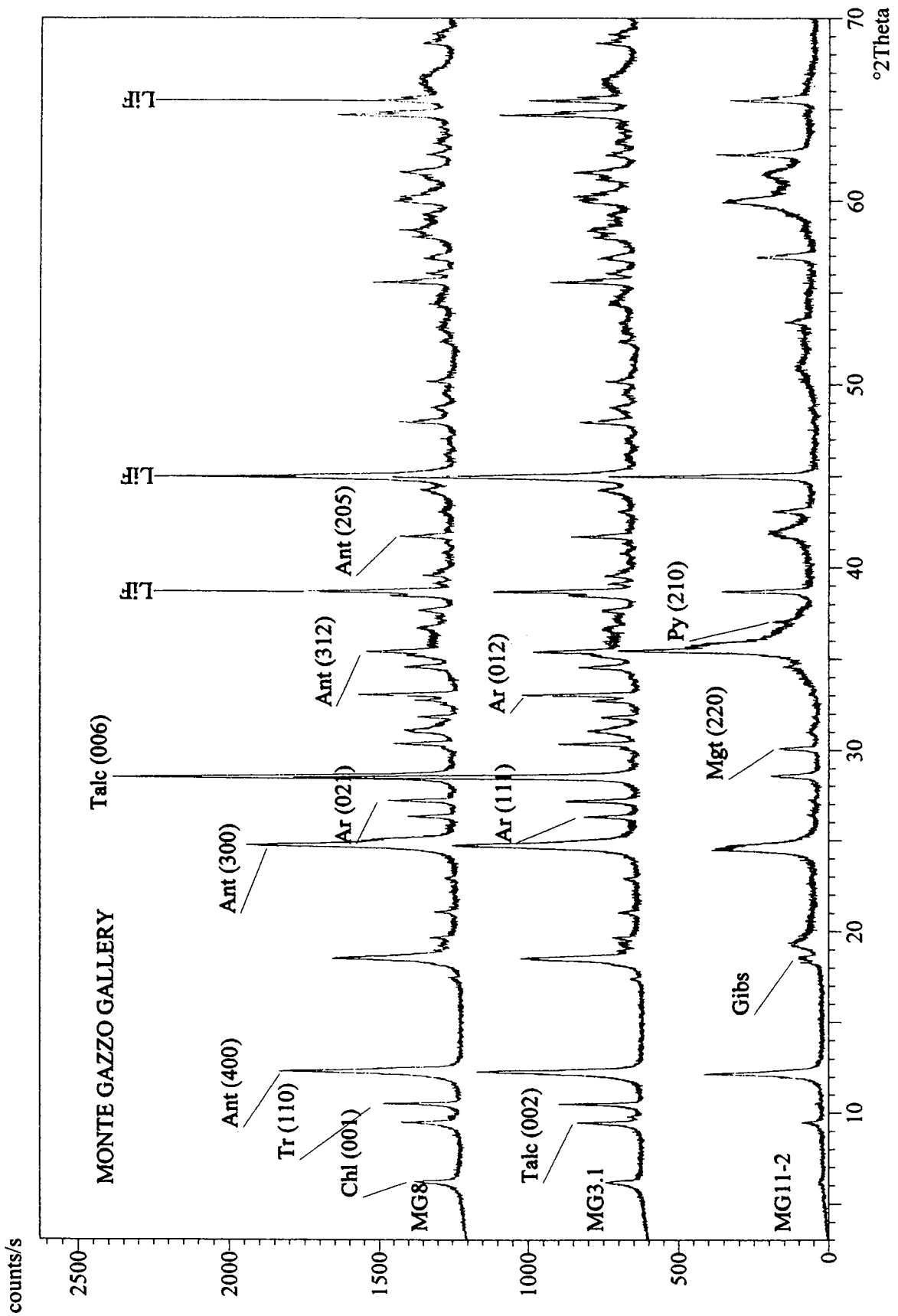


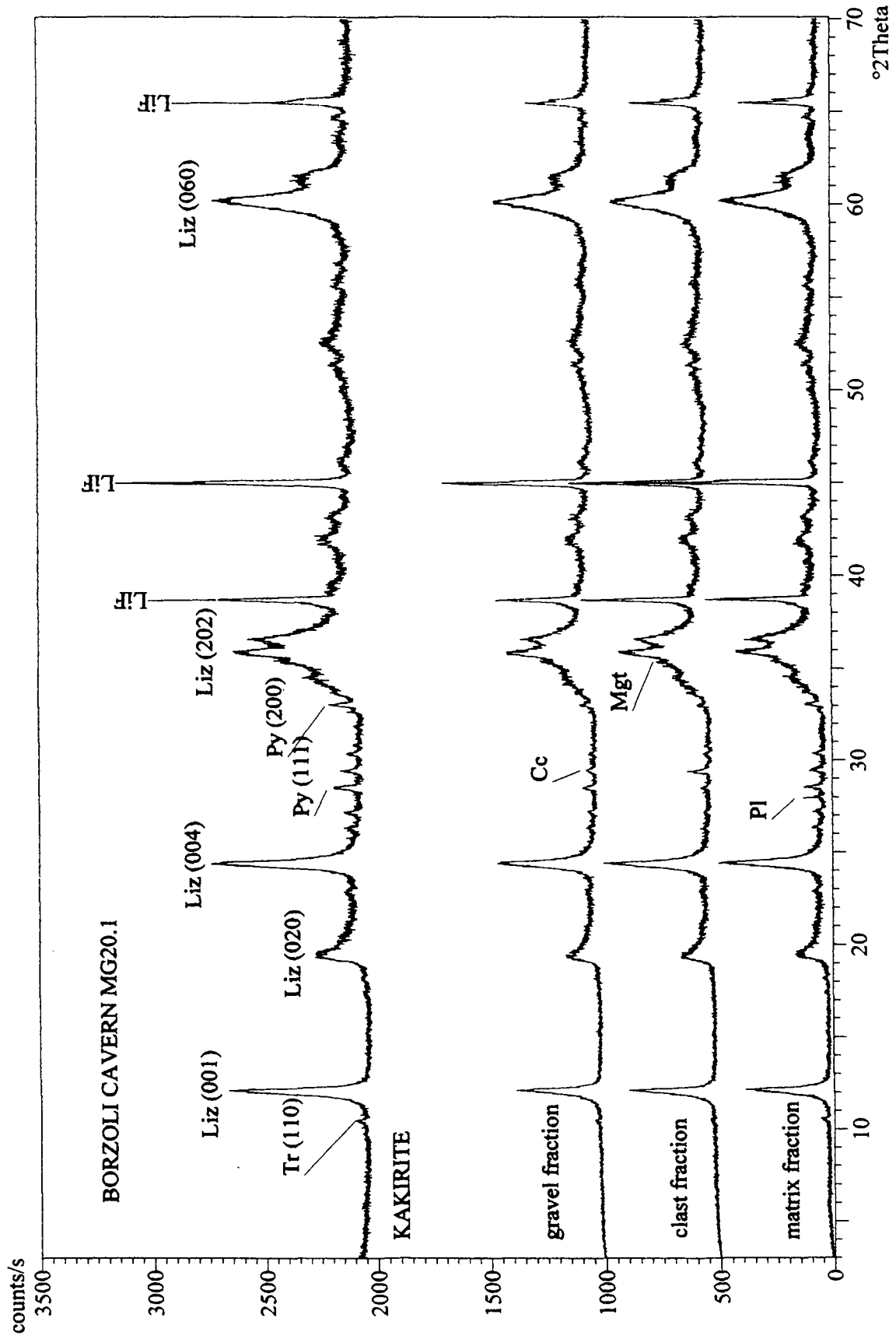






sample rock type	Mg 3.1 a	Mg 8	Mg 11 - 2		Mg 20.1			Mg 20.1 a
	kakirite	kakirite	kakirite	gravel fract.	clast fract.	matrix fract.	kakirite	
quartz								
plagioclase		1		2		1	1	
K-feldspar	2	1						
calcite		1		1	1	1	1	
dolomite								
ankerite								
amphibole	6	6	1	1	1	1	1	
non-quantified	92	91	99	96	98	97	97	
aragonite	xx	xx						
chlorite	x	x	x					
white mica								
paragonite								
kaolinite								
taic	xx	xx	x					
Al-hydroxide	x	x						
opaques	x	x	x	x	x	x	x	
iron oxyde								
magnetite		x	x					
sphene								
epidote								





CURRICULUM VITAE

Christoph Bürgi

born on 2nd July, 1967

Swiss citizen

Education

- 1982 - 1987 Städtisches Gymnasium Bern - Kirchenfeld
Swiss general Certificate of Education (A level)
- 1989 - 1994 Swiss Federal Institute of Technology - Zurich
Graduate studies in Earth Sciences (geology)
Dipl. Natw. ETH
- 1994 - 1995 Swiss Federal Institute of Technology - Lausanne
Postgraduate studies in engineering geology
Certificat de maîtrise de spécialisation en Géologie appliquée à l'ingénierie et à l'environnement
- 1995 - 1999 Swiss Federal Institute of Technology - Lausanne
PhD studies in engineering geology
Dr ès Sciences